

**The Response of *Cannabis sativa* L. to Three Novel Plant Growth-Promoting
Rhizobacteria: Yield and Cannabinoid and Terpene Profile**

Dongmei Lyu

Department of Plant Science

McGill University, Montreal

December 2022

A thesis submitted to McGill University in partial fulfillment of the requirements of the
degree of DOCTOR OF PHILOSOPHY

© Dongmei Lyu 2022

TABLE OF CONTENTS

TABLE OF CONTENTS	2
ABSTRACT.....	2
RÉSUMÉ	10
ACKNOWLEDGEMENTS	13
CONTRIBUTIONS TO ORIGINAL KNOWLEDGE	15
CONTRIBUTION OF AUTHORS	17
LIST OF FIGURES	18
LIST OF TABLES	20
LIST OF ABBREVIATIONS	22
CHAPTER 1 INTRODUCTION.....	26
1.1 CANNABIS.....	26
1.2 PLANT GROWTH-PROMOTING RHIZOBACTERIA (PGPR).....	27
1.3 OBJECTIVES	28
CHAPTER 2 LITERATURE REVIEW.....	30
2.1 ABSTRACT	30
2.2 INTRODUCTION	31
2.3 SECONDARY METABOLITES	32
2.3.1 <i>Cannabinoids</i>	32
2.3.1.1 Biosynthesis of Cannabinoids.....	33
2.3.1.2 Classification of Cannabis	34
2.3.2 <i>Terpenes</i>	36
2.3.2.1 Biosynthesis of terpenes	36

2.4	CASE STUDIES: <i>BACILLUS</i>, <i>PSEUDOMONAS</i>, AND <i>MUCILAGINIBACTER</i> AS PGPR	37
2.4.1	<i>Bacillus</i>	38
2.4.2	<i>Pseudomonas</i>	38
2.4.3	<i>Mucilaginibacter</i>	39
2.5	CONCLUSIONS	42
2.6	REFERENCES	43
CONNECTING TEXT		56
CHAPTER 3 THREE PLANT GROWTH-PROMOTING RHIZOBACTERIA ALTER MORPHOLOGICAL DEVELOPMENT, PHYSIOLOGY AND FLOWER YIELD OF CANNABIS SATIVA L.		
		57
3.1	ABSTRACT	57
3.2	INTRODUCTION	58
3.3	MATERIALS AND METHODS	61
3.3.1	<i>Bacterial strains, culture conditions, and inoculum preparation</i>	61
3.3.2	<i>Plant material and growth conditions</i>	61
3.3.3	<i>Root development of cannabis cuttings</i>	62
3.3.4	<i>Growth and yield of cannabis plants inoculated with PGPR</i>	63
3.3.4.1	<i>Physiological measurements and harvest</i>	65
3.3.5	<i>Calculations and statistical analysis</i>	65
3.4	RESULTS	66
3.4.1	<i>PGPR inoculation improves cannabis early root development</i>	66
3.4.2	<i>Photosynthetic rate</i>	69
3.4.3	<i>PGPR inoculation increases cannabis flower number</i>	70

3.5	DISCUSSION	74
3.5.1	<i>Bacterial inoculation enhances cannabis cutting root development</i>	74
3.5.2	<i>PGPR inoculation leads to cannabis yield improvement</i>	76
3.6	CONCLUSIONS	78
3.7	REFERENCES	80
	CONNECTING TEXT	87
	CHAPTER 4 EVALUATION OF PGPR ON CANNABINOIDS AND TERPENES	
	ACCUMULATION IN INFLORESCENCES OF CANNABIS SATIVA L.	88
4.1	ABSTRACT	88
4.2	INTRODUCTION	89
4.3	MATERIALS AND METHODS	93
4.3.1	<i>Plant materials</i>	93
4.3.2	<i>Cannabinoid and terpene analysis</i>	93
4.3.2.1	Chemical materials and reagents	93
4.3.2.2	Cannabinoid analysis	94
4.3.2.2.1	Sample extraction	94
4.3.2.2.2	UHPLC-UV	96
4.3.2.2.3	LC-MS/MS	96
4.3.2.3	Terpene analysis	98
4.3.2.3.1	Sample extraction	98
4.3.2.3.2	GC-MS	98
4.3.3	<i>Data analysis</i>	101
4.4	RESULTS	103

4.4.1	<i>Cannabinoid accumulation in cannabis flowers</i>	103
4.4.1.1	Abundance	103
4.4.1.2	Cannabinoid accumulation responds to PGPR inoculation	104
4.4.1.2.1	Major cannabinoids.....	104
4.4.1.2.2	Minor cannabinoids.....	108
4.4.1.2.3	Total cannabinoid accumulation	108
4.4.2	<i>Terpene accumulation in cannabis flowers</i>	109
4.4.2.1.1	Monoterpenes.....	109
4.4.2.1.2	Sesquiterpenes.....	110
4.4.2.1.3	Total terpene accumulation	112
4.4.3	<i>Correlation analysis among secondary metabolites</i>	114
4.5	DISCUSSION	117
4.5.1	<i>Selection of plant chemotype and reproductive period determination</i>	117
4.5.2	<i>Biochemical levels vary in response to PGPR inoculation</i>	118
4.5.3	<i>Influence of PGPR inoculation on metabolomics pathways</i>	120
4.6	CONCLUSIONS	122
4.7	REFERENCE	123
	CONNECTING TEXT	132
 CHAPTER 5 PROTEOMIC PROFILE OF CANNABIS FLOWERS PROVIDES		
INSIGHTS INTO PGPR PROMOTION OF CANNABIS GROWTH AND		
DEVELOPMENT		
5.1	ABSTRACT	133
5.2	INTRODUCTION	134

5.3	MATERIALS AND METHODS	135
5.3.1	<i>Maintenance of bacterial culture</i>	135
5.3.2	<i>Plant material</i>	136
5.3.2.1	Protein Extraction	136
5.3.2.2	Proteome profiling	137
5.3.3	<i>Data interpretation and analysis</i>	138
5.4	RESULTS	138
5.4.1	<i>Identification of expressed proteins among treatments</i>	138
5.4.2	<i>GO functional annotation and analysis</i>	139
5.4.3	<i>Differentially expressed proteins (DEPs)</i>	139
5.4.4	<i>Up-regulated differentially expressed proteins (DEPs)</i>	140
5.4.5	<i>Proteins involved in cannabis secondary metabolite biosynthesis</i>	150
5.5	DISCUSSION	154
5.5.1	<i>Protein synthesis</i>	156
5.5.2	<i>Photosynthesis</i>	156
5.5.3	<i>Carbohydrate metabolism</i>	157
5.5.3.1	Primary metabolism	157
5.5.3.2	The central carbohydrate metabolism pathways (glycolysis-, redox-, and tricarboxylic acid-related proteins)	158
5.5.3.3	Glycine cleavage (GCV) system	160
5.5.4	<i>Defense proteins</i>	163
5.5.5	<i>Other proteins</i>	164
5.5.5.1	Cell wall	164

5.5.5.2 Purple acid phosphatases	164
5.6 CONCLUSIONS	165
5.7 REFERENCE	167
CHAPTER 6 GENERAL DISCUSSION	176
CHAPTER 7 FINAL CONCLUSIONS AND FUTURE DIRECTIONS	182
BIBLIOGRAPHY	185
APPENDIX A	191
APPENDIX B	193
APPENDIX C	196
APPENDIX D	232

ABSTRACT

Cannabis has been experiencing a rapid increase in legal consumer demand and, at the same time, there is an increased demand for producers to develop varieties for a range of end-use applications, as a result of changing legislation in Canada and around the world. It is now critical to improve cannabis yield and quality (e.g., cannabinoid and terpene concentrations) for the medical and recreational markets. Members of phytomicrobiome, plant growth-promoting rhizobacteria (PGPR), are now recognized as playing a key role in plant productivity. This project is focused on examining the effects of novel strains of *Bacillus* sp., *Mucilaginibacter* sp. and *Pseudomonas* sp., on the growth of *Cannabis sativa* L.

In the first study, the three PGPR, in the form of pure cell suspension, were individually inoculated onto cuttings to determine effects on cannabis cutting rooting and subsequent plant growth. At propagation, *Pseudomonas* sp. significantly increased root growth on cuttings (32% greater than the control). At harvest, fresh flower weight was increased by 5.13, 6.94 and 11.45%, over the control, for plants inoculated with *Bacillus* sp., *Mucilaginibacter* sp. and *Pseudomonas* sp., respectively. Inoculation with *Pseudomonas* sp. resulted in the greatest increase in photosynthetic rate and harvest index; *Bacillus* sp., and *Mucilaginibacter* sp. increased flower number and axillary bud outgrowth rate at approximately equivalent amounts.

The second study utilized metabolomics analysis to identify and quantify 16 cannabinoids and 21 terpenes in cannabis flowers, using UHPLC-UV (Ultra High-Performance Liquid Chromatography with an ultraviolet detector), LC-MS/MS (Liquid Chromatograph coupled with a tandem Mass Spectrometer) and GC-MS (Gas Chromatography-Mass Spectrometry). Treatment with *Mucilaginibacter* sp. led to a 14% increase in total THC and CBD, and a 12% increase for terpenes. *Pseudomonas* sp. was less efficacious resulting in a 6% increase of total THC, and CBD.

The ratio of CBD/THC was constant across all PGPR treatments and the control.

In the third study, proteomic profiling of cannabis flowers provided insights into growth and development responses to PGPR inoculation. The three PGPR all increased production of key proteins involved in sucrose metabolism, glycolysis, the citrate cycle and other important metabolic pathways. *Mucilaginibacter* sp. upregulated the expression of proteins involved in cannabinoid biosynthesis. Among the three PGPR, *Pseudomonas* sp. led to the most abundant expression of proteins in cannabis flowers, following by *Mucilaginibacter* sp..

Overall, this project determined that (1) *Bacillus* sp., *Mucilaginibacter* sp. and *Pseudomonas* sp. all manifested beneficial effects on the growth of cannabis, from rooting speed to whole plant growth and flower yield, (2) two of selected pure PGPR (*Mucilaginibacter* sp. and *Pseudomonas* sp.) positively altered the cannabinoid and terpene profiles, (3) production of key proteins involved in cannabis plant growth and development were up-regulated by inoculation of PGPR. The benefits of this project include (1) demonstration that application of three PGPR strains improve crop productivity of cannabis, with the effect varying among PGPR, (2) insights into the molecular basis of plant-microbe interactions at the proteomic level, and (3) provision of new efficient methods for industrial production of cannabis through application of those beneficial bacteria.

RÉSUMÉ

Le cannabis connaît une augmentation rapide de la demande légale des consommateurs et, en même temps, il y a une demande accrue pour que les producteurs développent des variétés pour une gamme d'applications finales, résultant de la législation changeante au Canada et dans le monde. Il est maintenant crucial d'améliorer le rendement et la qualité du cannabis (par exemple, les concentrations de cannabinoïdes et de terpènes) pour les marchés médicaux et récréatifs. Les membres du phytomicrobiome, les rhizobactéries favorisant la croissance des plantes (PGPR), sont maintenant reconnus comme jouant un rôle clé dans la productivité des plantes. Ce projet vise à examiner les effets de nouvelles souches de *Bacillus* sp., *Mucilaginibacter* sp. et *Pseudomonas* sp. sur la croissance de *Cannabis sativa* L.

Dans la première étude, les trois PGPR, sous forme de suspension de cellules pures, ont été inoculés individuellement sur des boutures pour déterminer les effets sur l'enracinement des boutures de cannabis et la croissance ultérieure des plantes. Au moment de la propagation, *Pseudomonas* sp. a provoqué une croissance racinaire significativement plus importante sur les boutures (32% de plus que le témoin). À la récolte, le poids de fleurs fraîches a été augmenté de 5,13%, 6,94% et 11,45% par rapport au témoin, pour les plantes inoculées avec *Bacillus* sp., *Mucilaginibacter* sp. et *Pseudomonas* sp., respectivement. L'inoculation avec *Pseudomonas* sp. a entraîné la plus grande augmentation du taux de photosynthèse et de l'indice de récolte; *Bacillus* sp. et *Mucilaginibacter* sp. ont augmenté le nombre de fleurs et le taux de croissance des bourgeons axillaires à des quantités approximativement équivalentes.

La deuxième étude a utilisé une analyse de métabolomique pour identifier et quantifier 16 cannabinoïdes et 21 terpènes dans les fleurs de cannabis, en utilisant UHPLC-UV (chromatographie liquide ultra haute performance avec un détecteur ultraviolet), LC-MS/MS

(chromatographe liquide couplé à un spectromètre de masse en tandem) et GC-MS (chromatographie en phase gazeuse-spectrométrie de masse). Le traitement avec *Mucilaginibacter* sp. a conduit à une augmentation de 14% des taux totaux de THC et de CBD, ainsi qu'à une augmentation de 12% pour les terpènes. *Pseudomonas* sp. a été moins efficace, entraînant une augmentation de 6% des taux totaux de THC et de CBD. Le rapport CBD/THC était constant pour tous les traitements de PGPR ainsi que pour le témoin.

Dans la troisième étude, le profilage protéomique des fleurs de cannabis a fourni des informations sur les réponses de croissance et de développement à l'inoculation de PGPR. Les trois PGPR ont tous augmenté la production de protéines clés impliquées dans le métabolisme du saccharose, la glycolyse, le cycle de l'acide citrique et d'autres voies métaboliques importantes. *Mucilaginibacter* sp. a régulé à la hausse l'expression de protéines impliquées dans la biosynthèse des cannabinoïdes. Parmi les trois PGPR, *Pseudomonas* sp. a conduit à l'expression la plus abondante de protéines dans les fleurs de cannabis, suivie de *Mucilaginibacter* sp.

Dans l'ensemble, ce projet a démontré que (1) *Bacillus* sp., *Mucilaginibacter* sp. et *Pseudomonas* sp. ont tous manifesté des effets bénéfiques sur la croissance du cannabis, allant de la vitesse d'enracinement à la croissance de la plante entière et du rendement en fleurs, (2) deux des PGPR purs sélectionnés (*Mucilaginibacter* sp. et *Pseudomonas* sp.) ont positivement modifié les profils de cannabinoïdes et de terpènes, (3) l'inoculation de PGPR a régulé à la hausse la production de protéines clés impliquées dans la croissance et le développement des plantes de cannabis. Les avantages de ce projet incluent (1) la démonstration que l'application de trois souches de PGPR améliore la productivité de la culture de cannabis, l'effet variant selon les PGPR, (2) l'acquisition de connaissances sur les interactions moléculaires entre les plantes et les micro-

organismes au niveau protéomique, et (3) la mise à disposition de nouvelles méthodes efficaces pour la production industrielle de cannabis grâce à l'application de ces bactéries bénéfiques.

Acknowledgements

Time passes without our noticing. I think back to the moment when I was standing outside of the Raymond Building in Macdonald Campus, McGill University; it would have been difficult to realize how long it would take for me to get the final stages of my PhD program. I cannot imagine how difficult it would be without the support and guidance of the people I met during this PhD journey. It is impossible to express all my thanks to the people who provided their valuable assistance during this project. However, I will try to take this opportunity to acknowledge all of those who made larger contributions to this thesis.

First and foremost, I would like to thank my supervisor, Dr. Donald Smith, who always supported and encouraged me, in many ways. I truly thank him for his persistence in supporting me during my time in one of the best laboratories, in one of the best universities while I completed my research. I am grateful to the members of my supervisory committee, Drs. Jean-Benoit Charron and Pierre Dutilleul (both in the Department of Plant Science, McGill University) and Jennifer Ronholm (Department of Food Science and Agricultural Chemistry, McGill University) for their suggestions and guidance on my project. I was the one with a lot of anxiety during each committee meeting, but their smiles and encouragement always made me feel more relaxed. I really appreciated their valuable advice on my project.

This project could not have existed and been completed without Dr. Rachel Backer. I thank her very much for sharing her insights, for her positive and patient explanations in response to all my questions, and for her mentorship regarding the project. I also extend many thanks to Dr. Sowmyalakshmi Subramanian for teaching me proteomic techniques and associated data analysis and helping me to collect the cannabis flowers for analysis. I would also like to thank Dr. Alfred

Souleimanov, for his help when I needed it and for showing me the proper use of all the equipment in our laboratory.

I also gratefully acknowledge financial support from the Natural Sciences and Engineering Research Council (NSERC) of Canada during my Ph.D. studies. I sincerely appreciate Dr. Fabrice Berru  and his team at National Research Council, Halifax and Dr. Denis Faubert and his team at the Proteomics Discovery Platform, Institut de Recherches Cliniques de Montr al (IRCM) for both of metabolomics and proteomics analysis for my projects. I also greatly appreciate Dr. Eric Ruan and his team at Innotech Alberta, for training me on metabolomics analysis and providing the equipment for analysis of my samples and those of other members.

My special thanks to my dearest friend, Dr. Lianne Dwyer, a scientist at Agriculture and Agri-Food Canada, who encouraged me to come to Canada to do a PhD. I also thank my family for always being by my side and thinking of me.

Last, but not least, I deeply thank my Mother. She was the one who always supported my decisions and encouraged me to pursue my dreams. She was also the person who led me to decide to do PhD. I believe her love and support have always been and will be with me.

我爱你可能没有你爱我那么深沉伟大，但我永远记得。爱你，妈妈。

Contributions to Original Knowledge

Chapter 3

This is the first study to report the effects of beneficial rhizobacteria isolated from a location in Quebec, Canada by Dr. Fan (2018), and their interaction with cannabis plants. *Bacillus* sp., *Mucilaginibacter* sp., and *Pseudomonas* sp. were inoculated onto cannabis at the early vegetative stage. Agronomic traits, including root development, plant height, flower number, flower yield and total biomass, and a set of key physiological variables (related to photosynthetic activity) were determined in this experiment. The three isolates, improved cannabis plant growth. This is one of the few studies that monitored the impact of PGPR on cannabis from the vegetative stage to maturity. The study suggested that these rhizobacterial strains can be effectively utilized as bioinoculants to enhance cannabis growth and yield.

Chapter 4

Identification and quantification of the cannabinoid and terpene profiles in cannabis flowers helped us understand the biosynthesis pathway of key secondary metabolites and verify the effects of PGPR on those metabolites. This work was conducted using multiple techniques such as UHPLC, LC-MS/MS, GC-MS and indicated the potency of cannabinoids and terpenes. The three PGPR inoculants caused different levels of response among the key cannabinoids and terpenes with regard to accumulation in cannabis flowers. This is also first study to report the effects of PGPR on the accumulation of a large number (16 cannabinoid and 21 terpene) of secondary metabolite compounds in cannabis flowers.

Chapter 5

Analysis of the cannabis flower proteome revealed a vast network of signaling pathways related to plant growth and development modulated by inoculation with each of the three PGPR. The study

provided a comprehensive understanding of plant-microbe interactions between cannabis and the rhizobacterial strains *Bacillus* sp., *Mucilaginibacter* sp., and *Pseudomonas* sp. at the proteomic level, potentially leading to cannabis crop improvement. In addition, the proteins related to biosynthesis of cannabis secondary metabolites were also upregulated by the inoculation of PGPR. This is the first study to report the responses of whole proteome profiles in cannabis flowers to inoculation with specific rhizobacteria.

Contribution of Authors

Chapter 1 – The initial draft of the chapter was written entirely by Dongmei Lyu and was then reviewed by Dr. Smith

Chapter 2 – Dongmei Lyu gathered the relevant literature and prepared the manuscript. Dr. Backer and Dr. Smith provided feedback during the progression of manuscript development.

Chapter 3 – Dongmei Lyu conducted the research, collected the data and interpreted the results. Dr. Backer and Dr. Smith helped in editing the manuscript and provided feedback on its approach and structure. The initial draft of the chapter was written entirely by Dongmei Lyu.

Chapter 4 – Dongmei Lyu conducted the research, collected the data and interpreted the results. Dr. Ruan helped to analyze the cannabinoid and terpene profiles and provided the equipment at Innotech Alberta. Dr. Backer, Dr. Smith and Dr. Ruan reviewed the manuscript and provided feedback. The initial draft of the chapter was written entirely by Dongmei Lyu.

Chapter 5 – Dongmei Lyu conducted the research, collected the data and interpreted the results. Dr. Subramanian helped collect the flower samples, analyze the raw LC-MS/MS files and helped with the Scaffold and Omicsbox platforms used to analyze the proteomics data. Dr. Subramanian and Dr. Smith reviewed the manuscript and provided feedback. The initial draft of the chapter was written entirely by Dongmei Lyu.

List of Figures

Figure 3.1 Cannabis leaves are attached to the plant stem at nodes. The axillary buds emerged just above the nodes	66
Figure 3.2 Photosynthetic rates of <i>Cannabis sativa</i> cv. CBD Kush plants with and without bacterial inoculation	69
Figure 4.1 Main cannabinoids and terpenes biosynthesis pathway in cannabis flower	91
Figure 4.2 Typical chromatograph of 10 compounds by Ultra High-Performance Liquid Chromatography with UV detection at 220 nm	97
Figure 4.3 Typical chromatograph of the 21 terpenes measured by Gas Chromatography-Mass Spectrometry	99
Figure 4.4 The abundance of target cannabinoids in CBD Kush flowers.....	104
Figure 4.5 Box and whisker plots of the concentrations of the 4 neutral (cannabigerol (CBG), cannabidiol (CBD), tetrahydrocannabinol (THC), cannabichromene (CBC)) and the four acidic cannabinoids (cannabigerolic acid (CBGA), cannabidiolic acid (CBDA), tetrahydrocannabinolic acid (THCA), cannabichromenic acid (CBCA)) in flowers of CBD Kush	107
Figure 4.6 Total measured amount of 16 cannabinoids per gram of dry flower (C_{sum} , mg g^{-1} , blue) and per plant (CT_{sum} , mg, orange) treated with either of the three PGPR	109
Figure 4.7 Content of sesquiterpenes accumulated in CBD Kush flowers treated with each of the PGPR	112
Figure 4.8 The abundance of all 21 measured terpene compounds in CBD Kush treated with PGPR (mg g^{-1} DFW)	113

Figure 4.9	The total suite of 21 targeted terpene compounds per gram of dry flower (T_{sum}, $mg\ g^{-1}$, blue) and per plant (TT_{sum}, mg, orange) treated with each of the three PGPR.....	114
Figure 4.10	Correlation matrix of all analyzed secondary metabolites (13 cannabinoids and 21 terpenes) in cannabis flowers.....	115
Figure 4.11	Scatterplot and Component Plot (PC1 vs PC2) obtained via Principal Component Analysis (PCA) according to the concentrations of all analyzed compounds of cannabis flowers across the four treatments	116
Figure 5.1	Summary of up-regulated ($p \leq 0.05$, Fold change ≥ 1.2) of DEPs between the PGPR treatment groups (<i>Bacillus</i>, <i>Mucilaginibacter</i>, <i>Pseudomonas</i>) and the control.....	140
Figure 5.2	The quantitative spectra of proteins which respond to PGPR inoculation and are involved in cannabinoid and terpene biosynthesis in cannabis flowers. (a) The detailed cannabinoids and terpene biosynthesis pathway, (b) Quantitative spectra of proteins involved in cannabinoids and terpene biosynthesis.....	153
Figure 5.3	The metabolic pathways identified in cannabis flowers.....	155
Figure 5.4	The proteins up-regulated by PGPR in the central carbohydrate metabolism pathways of cannabis flowers (glycolysis, pyruvate oxidation, and the citrate cycle).....	162

List of Tables

Table 2.1 The determination of drug-, intermediate- and fiber phenotypes	33
Table 2.2 Growth-promoting substances released by PGPR (<i>Bacillus</i> sp., <i>Pseudomonas</i> sp. and <i>Mucilaginibacter</i> sp.).....	41
Table 3.1 The growth conditions for cannabis plants.....	64
Table 3.2 Root development as affected by inoculation of individual bacteria onto cannabis cv. CBD Kush	68
Table 3.3 Effects of PGPR treatments on agronomic characteristics of cannabis plants at 21, 42 and 70 days after transplanting.....	71
Table 3.4 The fresh and dry weight of leaves, stems, flowers and total aboveground biomass per cannabis plant as affected by inoculation with single bacterium cell suspensions.....	73
Table 3.5 Effects of PGPR treatments on flower yield characteristics of cannabis plants ..	74
Table 4.1 Target cannabinoids detection method and retention time.....	95
Table 4.2 The linear calibration parameters for quantification of target terpenes.....	100
Table 4.3 Accumulation of total main cannabinoids and CBD/THC ratio	106
Table 4.4 The concentration of minor cannabinoids	108
Table 4.5 Content of monoterpene (mg g⁻¹ DFW) accumulated in CBD Kush flowers of plants treated with one of the three PGPR.	111
Table 5.1 Total number of proteins identified at 99% protein probability and total spectra at 95% peptide probability, with two minimum peptides.....	139
Table 5.2 Proteins that were specifically up-regulated by treatment with <i>Bacillus</i>, <i>Mucilaginibacter</i>, or <i>Pseudomonas</i> relative to the control treatment (Fold change>1.2 (P<0.05; n=3)).....	142

Table 5.3 The identified proteins responding to PGPR inoculation and involved in cannabinoid and terpene biosynthesis in cannabis flowers.....	151
-------------------------------------------------------------------------------------------------------------------------------------------------------	------------

List of Abbreviations

ABA: Abscisic acid

ACC: Aminocyclopropane-1-carboxylate

BP: Biological processes

CBC: Cannabichromene

CBCA: Cannabichromenic acid

CBCAS: Cannabichromenic acid synthase

CBCVA: Cannabichromevarinic acid

CBCVAS: Cannabichromevarinic acid synthase

CBD: Cannabidiol

CBDA: Cannabidiolic acid

CBDAS: Cannabidiolic acid synthase

CBDV: Cannabidivarin

CBDVA: Cannabidivarinic acid

CBDVAS: Cannabidivarinic acid synthase

CBG: Cannabigerol

CBGA: Cannabigerolic acid

CBGV: Cannabigerovarin

CBGVA: Cannabigerovarinic acid

CBL: Cannabicyclol

CBN: Cannabinol

CBNA: Cannabinolic acid

CBNRA: Cannabinerolic acid

CC: Cellular components

CFU: Colony forming units

CH₂-THF: Methylene tetrahydrofolate

DEP: Differentially expressed protein

DFW: Dry flower weight

DMAPP: Dimethylallyl diphosphate

DOXP/MEP: 2-C-methyl-D-erythritol 4-phosphate/1-deoxy-D-xylulose 5-phosphate

DOXP: Deoxyxylulose phosphate

DW: Dry weight

DXR: 1-Deoxy-d-xylulose-5-phosphate reductoisomerase

EPS: Exopolysaccharides

FC: Fold change

FW: Fresh weight

GA: Gibberellins

GA₃: Gibberellic acid

GABA: γ -aminobutyric acid

GC-MS: Gas chromatography-mass spectrometry

GCV: Glycine cleavage

GO: Gene ontology

GPP: Geranyl diphosphate

HCN: Hydrogen cyanide

HDR: 1-hydroxy-2-methyl-2-(E)-butenyl-4-diphosphate reductase

HI: Harvest index

IAA: Indole-3-acetic acid

ISD: Internal standard

LC-MS/MS: Liquid chromatograph coupled with a tandem mass spectrometer

MEV: Mevalonate

MF: Molecular functions

NAD: Nicotinamide adenine dinucleotide

NADP+: Nicotinamide adenine dinucleotide phosphate

NPP: Neryl pyrophosphate

OD: Optical density

OGDH: 2-oxoglutarate dehydrogenase

OLA: Olivetolic acid

PAP: Purple acid phosphatase

PCA: Principal component analysis

PGPR: Plant growth-promoting rhizobacteria

PKS: Polyketides

SCL: Sub-canopy lighting

TCA: Citrate cycle

THCA: Tetrahydrocannabinolic acid

THCAS: Tetrahydrocannabinolic acid synthase

THCV: Tetrahydrocannabivarin

THCVA: Tetrahydrocannabivarinic acid

THCVAS: Tetrahydrocannabivarinic acid synthase

UDP-G: Uridine diphosphate glucose

UHPLC-UV: Ultra high-performance liquid chromatography with an ultraviolet detector

Δ 8-THC: delta-8-tetrahydrocannabinol

Δ 9-THC: delta-9-tetrahydrocannabinol

Chapter 1 Introduction

1.1 Cannabis

Cannabis, an erect annual, flowering herb, belongs to the family of Cannabaceae; the genus is generally recognized as consisting of *C. sativa*, *C. indica* and *C. ruderalis*, which are differentiated by key physical characteristics (Atakan, 2012; Hillig, 2005; Rana and Choudhary, 2010). Cannabis has a long social and medicinal history, extending back several millennia (Li, 1973; Ren et al., 2021; Zlas et al., 1993). The leaves, flowers, seeds, stalks and resin glands of the cannabis plant can be used as for food, fuel, fiber or medicine (Andre et al., 2016; Ryz et al., 2017). Recently, with the relatively widespread acceptance of cannabis use as a medicine, medical cannabis production has been legalized or authorized in 47 countries around the world, including Canada (Skypala et al., 2022; Wang et al., 2023). In 2018, Canada also became the second country to legalize the recreational use of cannabis, after Uruguay. In the past four years, five more countries have legalized the recreational use of cannabis. Increased cannabis production is not only due to renewed consumer demand, but also an increased requirement for producers to develop varieties for various specific end-use applications (Welling et al., 2016).

The well-known pharmacological and recreational effects of cannabis are because of a set of secondary metabolites in cannabis plants. Thus, cannabis production at high yields and with abundant levels of key secondary metabolites, mainly cannabinoids and terpenes, is a priority. An important challenge in this regard is the need for cannabis producers to achieve high quality and concentrations of bioactive compounds (cannabinoid and terpene), with reduced inputs. While traditional strategies can be used to select genotypes with high cannabinoid/terpene levels, a novel approach, based on exploitation of the phytomicrobiome, could also be used. Phytomicrobiome members have the ability to increase plant growth through a wide range of mechanisms, some of

which are almost certainly not yet discovered. Phytomicrobiome-based technologies have been developed, for use in agriculture, and have the potential to elicit increased cannabis yields and improved quality in *Cannabis sativa* production.

1.2 Plant growth-promoting rhizobacteria (PGPR)

Plant growth-promoting rhizobacteria (PGPR), are associated with the plant rhizosphere and affect plant growth in direct and indirect ways (Ahemad and Kibret, 2014; Beneduzi et al., 2012). PGPR directly contribute to plant growth by producing auxins, cytokinins and gibberellins to stimulate growth, and also produce siderophores and enzymes that enhance plant nutrient absorption, decrease ethylene levels and induce plant systemic resistance (Ahemad and Kibret, 2014; Bhattacharyya and Jha, 2012; Nandal and Hooda, 2013; Ortízcastro et al., 2009; Vacheron et al., 2013). Treatment with PGPR increases seed germination rate and final germination percentage (Parveen et al., 2018; Shah et al., 2022), root and shoot growth (Lyu et al., 2022) and total biomass production of many plant species. Specific strains of PGPR can stimulate growth of important agricultural species, including *Zea mays* L. (maize) (Fan and Smith, 2021, 2022), *Triticum aestivum* L. (wheat) (Danish and Zafar-ul-Hye, 2019), *Brassica napus* L. (canola) (de Aquino et al., 2022) and *Solanum lycopersicum* (tomato) (Takishita et al., 2021). PGPR indirectly contribute to plant growth by controlling deleterious microorganisms or pathogens that inhibit plant growth (Takishita et al., 2021; Wilkes et al., 2021). For instance, *Bacillus* sp. strain KFP-5 protects against *Pyricularia oryzae* by enhancing the activity of antioxidant defense enzymes in rice (Rais et al., 2017), and rhizospheric bacterial isolate SBP-9 increases the level of defense enzymes, protecting wheat plants from pathogen infection (Singh and Jha, 2017) .

Previous research has shown that PGPR-mediated plant growth promotion can occur by altering the entire rhizosphere microbial community, through the production of various substances

by specific microbial species, but this remains virtually unexplored for cannabis, with only one report that examines the microbiome of cannabis in relation to cultivar, soil type and growth stage (Winston et al., 2014). Our laboratory has already illustrated that bacteria isolated from one plant species can trigger growth promotion and induce stress responses in other plant species (Fan and Smith, 2021, 2022; Fan et al., 2017; Ricci, 2015; Smith et al., 2015; Takishita et al., 2021). In the case of cannabis production, there is a lack of data regarding the use of PGPR due to restrictions on production of this crop that were in place until recently in Canada and remain in place throughout much of the world. At this time there are only few publications on the effects of PGPR inoculation on growth and yield of cannabis (Conant et al., 2017; Pagnani et al., 2018); one of them showed positive effects of PGPR on secondary metabolite production and cannabinoid accumulation in cannabis plants. Therefore, it is necessary to study the effects of those potential PGPR on the growth of cannabis and accumulation of key secondary metabolites, which can provide substantial benefits for cannabis production.

Strains from three PGPR genera, *Bacillus*, and *Mucilaginibacter*, and *Pseudomonas*, previously isolated from a range of non-cannabis plant species have shown promising growth promotion effects on other crops (Fan and Smith, 2018, 2021, 2022). Based on 16S rDNA analysis, the three strains were tentatively identified to the species level; these were *Bacillus mobilis* (KJ812449), *Pseudomonas koreensis* (AF468452), and *Mucilaginibacter lappiensis* (jgi.1095764), respectively. However, these species identifications remain uncertain and will eventually require confirmation by full genome sequencing. In this study, these three PGPR are used to elucidate their potential on cannabis.

1.3 Objectives

A comprehensive understanding of the cannabis growth and development mediated by a

range of PGPR genera (*Bacillus*, *Mucilaginibacter*, and *Pseudomonas*) is not available and this study attempts to address that gap. The main **objectives** of the study were:

1. To determine the effect of inoculation with each of two common phytomicrobiome genera (*Bacillus*, *Pseudomonas*) and one more novel phytomicrobiome member (from the genus *Mucilaginibacter*) on the rooting of cannabis cuttings cannabis plant development and production;
2. To investigate the effects of the same three phytomicrobiome bacterial strains on cannabis yield, cannabinoid concentrations and terpene profile;
3. To elucidate the plant growth and development responses elicited by the inoculation of *Bacillus* sp., *Mucilaginibacter* sp., and *Pseudomonas* sp. through proteomic analysis of cannabis flowers;

Chapter 2 Literature Review

Plant Growth-Promoting Rhizobacteria for *Cannabis sativa* Production: Yield, Cannabinoid and Terpene Profile

Authors: Dongmei Lyu¹, Rachel Backer¹, George Robinson², Donald L. Smith¹

Affiliations:

¹Department of Plant Science, McGill University, Montréal, QC, Canada

²Ravenquest Biomed, Inc., Vancouver, British Columbia, Canada

This manuscript was originally published in *Frontiers in Microbiology* journal and shared in the thesis via the Creative Commons Attribution 4.0 International Public License.

Lyu, D., Backer, R. G., Robinson, W. G., and Smith, D. L. (2019). Plant-growth promoting rhizobacteria for cannabis production: Yield, cannabinoid profile and disease resistance.

Frontiers in Microbiology **10**, 1761. <https://doi.org/10.3389/fmicb.2019.01761>

2.1 Abstract

Cannabis production is now experiencing renewed consumer demand due to changing legislation around the world. Due to heavy restrictions on cannabis cultivation over the past century, little scientific research has been conducted on this crop, in particular research regarding the use of members of the phytomicrobiome to improve crop yields. Recent developments in the field of plant science have demonstrated that application of microbes, isolated from the rhizosphere, have enormous potential to improve yields, especially under stressful growing conditions. This review begins with a summary of knowledge about cannabis from taxonomic classification to the biosynthesis of key secondary metabolites (cannabinoids and terpenes) in cannabis plants. It then illustrates the potential for utilization of plant-growth promoting rhizobacteria (PGPR) to improve

cannabis production. Finally, three PGPR were selected as case studies: two PGPR in genera frequently associated with higher plants (*Bacillus* and *Pseudomonas*) and one in a genus less commonly found in this relationship (*Mucilaginibacter*).

2.2 Introduction

Cannabis production is drawing widespread attention due to the multi-purpose use of the crop as food, fiber, medicine and a recreational drug (Jiang et al., 2006; Kostic et al., 2008). The specific application and value is based, in meaningful part, on the concentration and composition of cannabinoids in the cannabis plant (Sawler et al., 2015). The demand for cannabis will increase with expanded social and legal acceptance, especially for medical use.

In medical and recreational cannabis production, the female plant is more desirable than the male for production of cannabinoids, due to much greater flower (where a large proportion of cannabinoids are produced) biomass and overall cannabinoid levels. In commercial production, plants are often propagated as cuttings from mother plants, to produce genetically identical daughter plants, to maintain genotypes that have the greatest yield and cannabinoid levels, and the best cannabinoid composition. Some studies have attempted to determine how much various aspects of cultivation and genetics contribute to cannabis yield and cannabinoid levels/composition. Toonen et al. (2006) and Vanhove et al. (2012) found that cannabis yield was influenced by light intensity and plant density. Results from Vanhove et al. (2011) showed that differences in tetrahydrocannabinol (THC) concentration and cannabinoid composition are predominantly linked with genotypic variation, rather than with cultivation factors. However, little research has been conducted on the response of yield and cannabinoid concentration/composition to application of plant-growth promoting rhizobacteria (PGPR), although research has already indicated the importance of the phytomicrobiome regarding production of many other crop species

(Mabood et al., 2014; Smith et al., 2015). Research has demonstrated that the application of PGPR to plant roots can be an effective strategy for stimulating crop growth by enhancing plant mineral nutrition absorption; PGPR can also improve crop tolerance to abiotic stresses (e.g., drought and salinity) and biotic stresses, such as plant pathogens (Lyu et al., 2020; Takishita et al., 2021; Yan et al., 2016).

The exploitation of PGPR from the phytomicrobiome could play an important role in industrial cannabis production, and there is a clear need to better understand the relationship between the phytomicrobiome and cannabis yield and quality (cannabinoid/terpenes composition). This review focuses on examining the potential role of PGPR, strains of three specific genera (*Bacillus*, *Mucilaginibacter* and *Pseudomonas*) in achieving high yields and desirable cannabinoid (and/or terpenes) profiles.

2.3 Secondary metabolites

2.3.1 Cannabinoids

Cannabinoids are a class of secondary metabolites, produced by the cannabis plant (Atakan, 2012), that have various effects on humans (Aizpurua-Olaizola et al., 2016). At this time, it is reported that cannabis plants produce at least 113 different cannabinoids including cannabidiol (CBD), cannabichromene (CBC), cannabinol (CBN) and Δ^9 -tetrahydrocannabinol (THC) (Aizpurua-Olaizola et al., 2016). For medicinal effects, the key constituents of the cannabinoid profile are THC and CBD (Fine and Rosenfeld, 2013).

THC is well-known as the primary psychoactive ingredient in cannabis; it has therapeutic effects for various illnesses, in part through providing analgesia and appetite stimulation (Chandra et al., 2010; Fishedick et al., 2010; Giroud, 2002; Hazekamp, 2007; Kowal et al., 2016). CBD is the major non-psychoactive cannabinoid found in both industrial hemp and drug-type cannabis

cultivars, with reported positive effects on depression, anxiety and addiction (Benjamin et al., 2012; Russo and Guy, 2006; Zuardi et al., 2012). Drug-type plants have a high THCA/CBDA ratio (>1.0), while typical fiber-type plants have low THCA/CBDA ratios (<1.0) (Aizpurua-Olaizola et al., 2016). However, even though the THC/CBD ratio varies among cannabis cultivars/genotypes, the sum of CBD and THC tends to be roughly constant (Alger, 2013). The criteria for the classification of phenotypes according to cannabinoid content are shown in **Table 2.1**.

Table 2.1 The determination of drug-, intermediate- and fiber phenotypes (Benjamin et al., 2012; Russo and Guy, 2006; Zuardi et al., 2012)

Phenotype	Common name	[THC] (%)	[CBD] (%)	[THC(A)]/[CBD(A)]
I (drug)	Marijuana	≥ 0.3	< 0.5	>1
II (intermediate)	Marijuana	≥ 0.5	≥ 0.5	-
III (fiber)	Hemp	< 0.3	≥ 0.5	<1

2.3.1.1 Biosynthesis of Cannabinoids

With the use of cannabinoids in pharmaceutical formulations for medical application, the biosynthesis of cannabinoids has recently experienced a surge in research interest and the process is now beginning to be elucidated. It mainly occurs in the secretory head cells of the glandular trichomes of cannabis plants (Happyana et al., 2013). The first experiments regarding biosynthesis of cannabinoids were conducted in the 1970s using radiolabeling, and demonstrated that the biosynthesis originates from polyketides (PKS) (Shoyama et al., 1975). Subsequently, data from Fellermeier et al. (2001) showed two pathways leading to biosynthesis of cannabinoids: one is the deoxyxylulose phosphate (DOXP/MEP) pathway, which occurs in plastids, and the other is the mevalonate (MEV) pathway, which occurs in the cytoplasm. A polyketide synthase catalyzes the biosynthesis of olivetolic acid (OLA), one of the precursors for cannabinoid biosynthesis (Raharjo

et al., 2004). Following from the enzymatic prenylation of olivetolic acid with geranyl diphosphate (GPP) or neryl pyrophosphate (NPP), there are two terpenophenolic compounds formed: cannabigerolic acid (CBGA) and cannabimerolic acid (CBNRA) (Fellermeier and Zenk, 1998; Taura et al., 1995a). CBGA is the precursor of tetrahydrocannabinolic acid (THCA) (Taura et al., 1995b), cannabidiolic acid (CBDA) (Taura et al., 1996) and cannabichromenic acid (CBCA) (Morimoto et al., 1997, 1998) which are formed from CBGA by redox enzymes involved in the biosynthetic process. The corresponding cannabinoids, THC, CBD and CBC, are derived from their acid forms by decarboxylation (Chen et al., 2013).

2.3.1.2 Classification of Cannabis

Generally, cannabis is classified into drug (marijuana) and fiber (hemp) types (**Table 2.1**). The classification of cannabis is affected by genetics and growing conditions, and ultimately is based on cannabinoid content and composition (Sawler et al., 2015). Hemp is a high yield, multi-purpose crop that serves as a source of fiber, seed oil and animal feedstuff, with lower THC content than marijuana (Amaducci et al., 2014; Salentijn et al., 2015). CBD can provide medical benefits without the psychoactive side effects related to THC, such as cognitive impacts and abuse potential (Borgelt et al., 2013). By law, the content of THC in industrial hemp biomass must be below 0.3% in Canada, and 0.2% in Europe (Sawler et al., 2015); cannabis plants with higher THC levels are considered to be marijuana. In contrast, the concentration of THC in a marijuana cultivar can range from 2 to 12%, or even higher (ElSohly et al., 2016). Although marijuana, as a source of medical and recreational products, is now legal in Canada, Canadian regulations for marijuana production are more stringent than for hemp production, related to the higher cannabinoid levels in marijuana, and therefore greater potential psychoactive effects. It seems certain that with increased legalization of cannabis production globally, cannabis will be a most promising crop,

due to its multiple uses, and especially due to its potential medical value.

As the indicated by the importance of cannabinoids in the classification of cannabis, levels of each cannabinoid component can dramatically affect medicinal and therapeutic properties related to a range of diseases/disorders. However, our understanding of the effects of cannabinoid ratios, including CBD:THC ratios, is very limited. As we now know, the ratio of CBD to THC is mainly determined by “strain” (genotype/chemotype) genetics. Distinct forms of the same gene control the conversion from CBGA to THCA and CBDA (Lavery et al., 2019), which are precursors of THC and CBD, respectively. However, more research exploration regarding how other factors affect the ratio of these two key cannabinoid components is needed. This will guide thinking around medicinal use of cannabis material with various CBD:THC ratios.

THC and CBD are concentrated in different parts of the cannabis plant with content varying among tissues. Fetterman (1971) and Hemphill (1980) showed the relative concentration of THC in cannabis plant organs is flowers > leaves > stem > roots. In addition to the distribution of cannabinoids among plant tissues, there are several crucial factors that influence the concentration of cannabinoids, including plant genotype and environmental conditions during growth, such as temperature and water availability, and also the development stage of the plant (Backer et al., 2019; Tipparat et al., 2012). Tipparat et al. (2012) demonstrated that a longer vegetative stage and a longer photoperiod led to greater cannabinoid accumulation. In addition, it has been reported that some plant growth regulators affect accumulation of cannabinoids. Mansouri et al. (2011) found that applying of 100 μM gibberellic acid (GA_3) increased the accumulation of THC and CBD in cannabis leaves. Mansouri et al. (2011) and Singh et al. (2011) indicated that specific elicitors can enhance cannabinoid concentration; abscisic acid (ABA) and cycocel increased THC content, while GA_3 decreased THC content. Currently, the relationship(s) among mechanisms leading to

these effects are not understood. One hypothesis is that application of GA₃ contributes to an increase in 1-aminocyclopropane-1-carboxylate (ACC) which subsequently increases ethylene levels in the plant. According to this hypothesis, higher levels of ethylene result in increased THC and CBD contents (Mansouri et al., 2011). There is substantially less knowledge regarding the role of inoculation with microbes on the accumulation of cannabinoids in cannabis plants. However, secondary metabolite accumulation is often responsive to microbial inoculation in other plant species (Braga et al., 2016; Kim et al., 2011; Vacheron et al., 2013). Thus, it is a high priority to determine the effect of microbes on the biosynthesis of cannabinoids and evaluate the resulting THC and CBD contents.

2.3.2 Terpenes

2.3.2.1 Biosynthesis of terpenes

Terpenes are another major secondary metabolite in the Cannabaceae family, found in the glandular trichomes, which can cause unique flavor and aroma qualities (Booth et al., 2017; Lange and Turner, 2013). Terpenes in cannabis do not draw as much attention as cannabinoids in cannabis, whereas terpenes, as typical aroma-related compounds in hops, are well studied because of their value in the brewing industry (Almaguer et al., 2014; Sharpe and Laws, 1981). The classification of terpenes is based on the number of carbons including monoterpene (C₁₀), sesquiterpene (C₁₅), diterpene (C₂₀), sesterpene (C₂₅), triterpene (C₃₀) and tetraterpene (C₄₀) (Ashour et al., 2010; Cseke et al., 2016). About 120 terpenes have been identified in cannabis plants, including 61 monoterpenes, 52 sesquiterpenes, 2 triterpenes, one diterpene, and 4 terpene derivatives (ElSohly and Slade, 2005).

The composition and abundance of terpenes vary among cannabis species (Booth et al., 2017). In general, the most abundant terpenes are caryophyllene (sesquiterpene), and α -pinene and

d-limonene (monoterpenes) in cannabis plants (Russo and Guy, 2006). Terpenes are not as uncommon as cannabinoids; they are present in many plants, but it is thought that the presence of terpenes in cannabis can enhance the effects of CBD and THC, through entourage effects. Individual terpenes and their derivatives can also be used as antibiotic drugs, antioxidants, and a through its effects on reducing anxiety and depression in humans (Aizpurua-Olaizola et al., 2016; Jin et al., 2020).

Like the cannabinoids, the biosynthesis of terpenes is also affected by a range of factors, including genetic, environmental and developmental (Ross and ElSohly, 1996; Hillig and Mahlberg, 2004; Hazekamp, 2007; Fishedick et al., 2010). Both plastidial methylerythritol phosphate and cytosolic mevalonate pathways are involved in terpene biosynthesis, by producing the general 5-carbon isoprenoid diphosphate precursors used in synthesis of terpenes (Booth et al., 2017). During what is a complex biosynthesis process, GPP plays an important role in the biosynthesis of cannabinoids, controlling the substrate pools available for terpene synthases (Fellermeier et al., 2001; Gagne et al., 2012). Therefore, factors affecting cannabinoid biosynthesis are likely to also do so for terpene biosynthesis in cannabis.

2.4 Case studies: *Bacillus*, *Pseudomonas*, and *Mucilaginibacter* as PGPR

Plant growth-promoting rhizobacteria (PGPR) are microbes associated with plant roots, that enhance plant growth by: 1) providing mineral nutrition to plants, 2) producing plant hormones or other molecules that prime plant defenses against biotic and abiotic stresses, 3) producing signal compounds specific to plant-microbe interactions and through these regulating aspects of plant physiology, development and growth and 4) protecting plants against pathogens by affecting survival and virulence of pathogenic microorganisms (Ahemad and Kibret, 2014; Backer et al., 2018; Rosier et al., 2018; Yan et al., 2016). PGPR are well-recognized as promising inputs for

sustainable agricultural production systems (Bhattacharyya and Jha, 2012; Gupta et al., 2015).

2.4.1 *Bacillus*

Bacillus is a spore-forming bacterium, which contributes to its survival in the environment (Brooks et al., 2013). Some *Bacillus* species, *B. subtilis*, *B. licheniformis* and *B. pumilis*, have been isolated as endophytes and have been shown to be beneficial to growth for a range of plant species, such as rice (*Oryza sativa* L.) (Chung et al., 2015) and sugar beet (*Beta vulgaris* L.) (Shi et al., 2010). Those studies have shown that the impact of *Bacillus* spp. varies among crop species and that the application of *Bacillus* can improve agronomic traits of crop plants (Choudhary, 2011; Lyngwi and Joshi, 2014). Like *Pseudomonas*, *Bacillus* species are known to be able to promote plant growth by: 1) excreting cytokinins into the rhizosphere and 2) stimulating the synthesis of phytohormones, such as gibberellins (GA) (Bottini et al., 2004; Idris et al., 2007) and indole-3-acetic acid (IAA) (Shao et al., 2015).

2.4.2 *Pseudomonas*

Pseudomonas is a non-spore-forming, gram-negative, rod-shaped bacterial genus that occurs commonly in disease-suppressive soils (Compant et al., 2005; Santoyo et al., 2012). *Pseudomonas* strains use a range of substrates as nutrients and survive in a wide range of conditions; this adaptability could contribute to their generally rapid growth. *Pseudomonas* strains show good colonization in numerous ecological niches including in soil and water, and on plant surfaces (Humphris et al., 2005; Parret et al., 2003; Schreiter et al., 2018). *Pseudomonas* strains can also enhance plant growth through, for instance, releasing siderophores to sequester rhizosphere iron (O'sullivan and O'Gara, 1992) and producing plant hormones such as IAA and other plant hormone effectors, e.g. ACC deaminase (Khan et al., 2016), also producing antifungal compounds, phloroglucinol, phenazines (Pascale et al., 1997; Raaijmakers et al., 2009; Shahnaz et

al., 2020).

2.4.3 *Mucilaginibacter*

Mucilaginibacter is a member of the family Sphingobacteriaceae, which was described by Pankratov et al. (2007). It is gram-negative, non-spore-forming, non-motile rod and is strictly aerobic or facultatively anaerobic (Pankratov et al., 2007). The genus *Mucilaginibacter* has generally been isolated from moist environments, such as peat bogs, tidal flat sediments and lichens (Madhaiyan et al., 2010; Pankratov et al., 2007).

Bacillus and *Pseudomonas* are well-known as plant growth promoters, however, there are few descriptions of *Mucilaginibacter* as a PGPR, particularly for commercial use. Madhaiyan et al. (2010) reported that the root length of tomato seedlings (*Lycopersicon esculentum* L. cv Mairokuand) and canola (*Brassica campestris*) inoculated with *Mucilaginibacter* strains Gh-67^T and Gh-48^T was greater than the control. Kim et al. (2012) found that *Mucilaginibacter* strain 56 promotes growth when added into the rhizosphere of plants and lichens (Kim et al., 2012). The mechanism of plant growth promotion is unclear; some studies have shown that *Mucilaginibacter* strains produce ACC deaminase (Madhaiyan et al., 2010). Moreover, *Mucilaginibacter* strains can produce exopolysaccharides (EPS) (Lee et al., 2013), which are macromolecular electrolyte compounds that are excreted as mucus, contributing to better soil aggregation, caused by bacterial cells (Subair, 2015). It has been reported that many bacteria isolated from EPS can produce IAA (Subair, 2015), which plays an important role in regulating plant growth and development. In addition, EPS protects bacteria from various environmental stresses, such as heavy metals, drought and salinity stresses, by functioning as biofloculants, bio-absorbents and heavy metal removal agents (Iqbal et al., 2002; Zajšek et al., 2013). Madhaiyan et al. (2010) showed that tomato and canola seeds treated with *Mucilaginibacter* strains Gh-67^T and Gh-48^T can tolerate a 1 mM

NiCl₂/CdCl₂ metal solution. EPS produced by PGPR strains increased root and shoot length, leaf area and plant biomass of maize (*Zea mays* cv. Agaiti-2002) under drought stress conditions (Naseem and Bano, 2014). Some reported studies related to growth promoting substances released by PGPR of the three genera of interest, on other crops, are listed in **Table 2.2**. To date, the potential effects, and underlying mechanisms, of *Mucilaginibacter* effects on cannabis production and cannabinoid content/composition have not been studied.

Evaluating effects of the genera *Bacillus*, *Mucilaginibacter* and *Pseudomonas* on cannabis growth promotion is based on results from Fan et al. (2018). Fan et al. (2018) found that treatment of seeds or root tips of *Arabidopsis* with *Bacillus*, *Mucilaginibacter* and *Pseudomonas* sp. significantly increased seedling growth relative to controls after 21 d of incubation. For instance, the rosette fresh weight of root-tip treated seedlings was significantly increased, by approximately 43, 30, and 20%, by strains of *Bacillus*, *Mucilaginibacter*, and *Pseudomonas* sp., respectively, compared to uninoculated control plants. This study also showed that the *Mucilaginibacter* sp. produced an average of 0.83 µg mL⁻¹ of IAA when grown with 500 mg mL⁻¹ of L-tryptophan in KB liquid medium, while *Bacillus* sp. produced significantly lower amounts of IAA (0.1 µg mL⁻¹). In the same time, P solubilization, siderophore production, nitrogen fixation or ammonia production were detected for the *Bacillus* sp., *Mucilaginibacter* sp. and *Pseudomonas* sp. (Fan et al., 2018; Fan et al., 2020). Compared with other PGPR strains isolated from various plants the selected *Bacillus* sp., *Mucilaginibacter* sp. and *Pseudomonas* sp., showed the most pronounced abilities to promote growth of the tested plant species (Fan et al., 2018). Therefore, it is possible that these PGPR have potential to enhance the growth and quality of cannabis, and may result high quality plants with high utility in the medicinal area.

Table 2.2 Growth-promoting substances released by PGPR (*Bacillus* sp., *Pseudomonas* sp. and *Mucilaginibacter* sp.)

PGPR	Plant growth promoting traits	References
<i>Bacillus</i> sp.	P solubilization, IAA, siderophores, hydrogen cyanide (HCN) production, ammonia.	Canbolat et al. (2006); Rajkumar et al. (2006); Wani et al. (2007); Wani and Khan (2010); Ahmad et al. (2014); Fan and Smith (2021).
<i>Pseudomonas</i> sp.	ACC deaminase, IAA, siderophore, P solubilization, HCN, biocontrol potentials, heavy metal solubilization Antifungal compounds. (phloroglucinol, phenazines)	Pascale et al. (1997); Poonguzhali et al. (2008); Rajkumar and Freitas (2008); Raaijmakers et al. (2009); Tank and Saraf (2009); Ma et al. (2011); Shahnaz et al (2020); Fan and Smith (2021).
<i>Mucilaginibacter</i> sp.	IAA, ACC deaminase, exopolysaccharides (EPS).	Madhaiyan et al. (2010); Fan and Smith (2022).

2.5 Conclusions

Cannabis is a globally important crop, and its importance is increasing with the number of countries legalizing the use of cannabis both for fiber and medical applications. It is now important to investigate how to improve cannabis yields and alter cannabinoid concentration and composition as these attributes affect the crop's value. However, because cannabis use for medical or recreational purposes has been illegal in most of the world, there is a shortage of good research data in this area. As an important part of most ecosystems, the phytomicrobiome helps crop plants in a wide range of ways, such as nutrient mobilization, hormone production, disease control and improved stress tolerance. Thus, study on the responses of cannabis plants to PGPR inoculation could provide an efficient approach to improving cannabis yield and quality for medical use. Overall, elements of the phytomicrobiome have the potential to increase the yield and quality of cannabis.

2.6 References

- Ahemad, M., and Kibret, M. (2014). Mechanisms and applications of plant growth promoting rhizobacteria: current perspective. *Journal of King saud University-Science* **26**, 1-20.
- Aizpurua-Olaizola, O., Soydaner, U., Öztürk, E., Schibano, D., Simsir, Y., Navarro, P., Etxebarria, N., and Usobiaga, A. (2016). Evolution of the cannabinoid and terpene content during the growth of *Cannabis sativa* plants from different chemotypes. *Journal of Natural Products* **79**, 324-331.
- Alger, B. E. (2013). Getting high on the endocannabinoid system. In "Cerebrum: the Dana forum on brain science", Vol. 2013. Dana Foundation.
- Almaguer, C., Schönberger, C., Gastl, M., Arendt, E. K., and Becker, T. (2014). *Humulus lupulus*—a story that begs to be told. A review. *Journal of the Institute of Brewing* **120**, 289-314.
- Amaducci, S., Scordia, D., Liu, F. H., Zhang, Q., Guo, H., Testa, G., and Cosentino, S. L. (2014). Key cultivation techniques for hemp in Europe and China. *Industrial Crops & Products* **68**, 2-16.
- Ashour, M., Wink, M., and Gershenzon, J. (2010). Biochemistry of terpenoids: monoterpenes, sesquiterpenes and diterpenes. *Annual Plant Reviews* 258-303.
- Atakan, Z. (2012). Cannabis, a complex plant: different compounds and different effects on individuals. *Therapeutic Advances in Psychopharmacology* **2**, 241-254.
- Backer, R., Rokem, J. S., Ilangumaran, G., Lamont, J., Praslickova, D., Ricci, E., Subramanian, S., and Smith, D. L. (2018). Plant growth-promoting rhizobacteria: context, mechanisms of action, and roadmap to commercialization of biostimulants for sustainable agriculture. *Frontiers in Plant Science* **9**, 1473.

- Backer, R. G., Rosenbaum, P., McCarty, V., Eichhorn Bilodeau, S., Lyu, D., Ahmed, M. B., Robinson, W. G., Lefsrud, M., Wilkins, O., and Smith, D. L. (2019). Closing the yield gap for cannabis: a meta-analysis of factors determining cannabis yield. *Frontiers in Plant Science* **10**, 495.
- Benjamin, D. B., Kevin, M., G., V. A., and Corinne, C. (2012). Evolution of the content of THC and other major cannabinoids in drug - type cannabis cuttings and seedlings during growth of plants. *Journal of Forensic Sciences* **57**, 918-922.
- Bhattacharyya, P. N., and Jha, D. K. (2012). Plant growth-promoting rhizobacteria (PGPR): emergence in agriculture. *World Journal of Microbiology & Biotechnology* **28**, 1327-1350.
- Booth, J. K., Page, J. E., and Bohlmann, J. (2017). Terpene synthases from *Cannabis sativa*. *PLoS One* **12**, e0173911.
- Borgelt, L. M., Franson, K. L., Nussbaum, A. M., and Wang, G. S. (2013). The pharmacologic and clinical effects of medical cannabis. *The Journal of Human Pharmacology and Drug Therapy* **33**, 195-209.
- Bottini, R., Cassán, F., and Piccoli, P. (2004). Gibberellin production by bacteria and its involvement in plant growth promotion and yield increase. *Applied Microbiology & Biotechnology* **65**, 497-503.
- Braga, R. M., Dourado, M. N., and Araújo, W. L. (2016). Microbial interactions: ecology in a molecular perspective. *Brazilian Journal of Microbiology* **47**, 86-98.
- Brooks, G., Carroll, K., Butel, J., Morse, S., and Mietzner, T. (2013). Chapter 11. Spore-forming gram-positive Bacilli: *Bacillus* and *Clostridium* species. In "Jawetz, Melnick, and Adelberg's medical microbiology. "

- Canbolat, M. Y., Bilen, S., Çakmakçı, R., Şahin, F., and Aydın, A. (2006). Effect of plant growth-promoting bacteria and soil compaction on barley seedling growth, nutrient uptake, soil properties and rhizosphere microflora. *Biology and Fertility of Soils* **42**, 350-357.
- Chandra, S., Lata, H., Mehmedic, Z., Khan, I. A., and Elsohly, M. A. (2010). Assessment of cannabinoids content in micropropagated plants of *Cannabis sativa* and their comparison with conventionally propagated plants and mother plant during developmental stages of growth. *Planta Medica* **76**, 743.
- Chen, X., Guo, M., Zhang, Q., Xu, Y., Guo, H., Yang, M., and Yang, Q. (2013). Chemotype and genotype of Cannabinoids in hemp landrace from southern Yunnan. *Acta Botanica Boreali-Occidentalia Sinica* **33**, 1817-1822.
- Choudhary, D. (2011). Plant growth-promotion (PGP) activities and molecular characterization of rhizobacterial strains isolated from soybean (*Glycine max* L. Merrill) plants against charcoal rot pathogen, *Macrophomina phaseolina*. *Biotechnology Letters* **33**, 2287.
- Chung, E. J., Hossain, M. T., Khan, A., Kim, K. H., Jeon, C. O., and Chung, Y. R. (2015). *Bacillus oryzicola* sp. nov., an endophytic bacterium isolated from the roots of rice with antimicrobial, plant growth promoting, and systemic resistance inducing activities in rice. *The Plant Pathology Journal* **31**, 152.
- Compant, S., Duffy, B., Nowak, J., Clément, C., and Barka, E. A. (2005). Use of plant growth-promoting bacteria for biocontrol of plant diseases: principles, mechanisms of action, and future prospects. *Applied and Environmental Microbiology* **71**, 4951-4959.
- Cseke, L. J., Kirakosyan, A., Kaufman, P. B., Warber, S., Duke, J. A., and Brielmann, H. L. (2016). "Natural products from plants," CRC press.

- ElSohly, M. A., Mehmedic, Z., Foster, S., Gon, C., Chandra, S., and Church, J. C. (2016). Changes in cannabis potency over the last 2 decades (1995–2014): analysis of current data in the United States. *Biological Psychiatry* **79**, 613-619.
- ElSohly, M. A., and Slade, D. (2005). Chemical constituents of marijuana: the complex mixture of natural cannabinoids. *Life Sciences* **78**, 539-548.
- Fan, D., Schwinghamer, T., and Smith, D. L. (2018). Isolation and diversity of culturable rhizobacteria associated with economically important crops and uncultivated plants in Québec, Canada. *Systematic Applied Microbiology* **41**, 629-640.
- Fan, D., and Smith, D. L. (2021). Characterization of selected plant growth-promoting rhizobacteria and their non-host growth promotion effects. *Microbiology Spectrum* **9**, e00279-21.
- Fan, D., and Smith, D. L. (2022). *Mucilaginibacter* sp. K improves growth and induces salt tolerance in nonhost plants via multilevel mechanisms. *Frontiers in Plant Science* **13**.
- Fan, D., Subramanian, S., and Smith, D. L. (2020). Plant endophytes promote growth and alleviate salt stress in *Arabidopsis thaliana*. *Scientific Reports* **10**, 1-18.
- Fellermeier, M., Eisenreich, W., Bacher, A., and Zenk, M. H. (2001). Biosynthesis of cannabinoids: Incorporation experiments with ¹³C - labeled glucoses. *European Journal of Biochemistry* **268**, 1596-1604.
- Fellermeier, M., and Zenk, M. H. (1998). Prenylation of olivetolate by a hemp transferase yields cannabigerolic acid, the precursor of tetrahydrocannabinol. *FEBS Letters* **427**, 283-285.
- Fetterman, P. S., Keith, E. S., Waller, C. W., Guerrero, O., Doorenbos, N. J., and Quimby, M. W. (1971). Mississippi - grown *cannabis sativa* L.: Preliminary observation on chemical

- definition of phenotype and variations in tetrahydrocannabinol content versus age, sex, and plant part. *Journal of Pharmaceutical Sciences* **60**, 1246-1249.
- Fine, P. G., and Rosenfeld, M. J. (2013). The endocannabinoid system, cannabinoids, and pain. *Rambam Maimonides Medical Journal* **4**.
- Fishedick, J. T., Hazekamp, A., Erkelens, T., Choi, Y. H., and Verpoorte, R. (2010). Metabolic fingerprinting of *Cannabis sativa* L., cannabinoids and terpenoids for chemotaxonomic and drug standardization purposes. *Phytochemistry* **71**, 2058-2073.
- Gagne, S. J., Stout, J. M., Liu, E., Boubakir, Z., Clark, S. M., and Page, J. E. (2012). Identification of olivetolic acid cyclase from *Cannabis sativa* reveals a unique catalytic route to plant polyketides. *Proceedings of the National Academy of Sciences* **109**, 12811-12816.
- Giroud, C. (2002). Analysis of cannabinoids in hemp plants. *Chimia International Journal for Chemistry* **56**, 80-83.
- Gupta, G., Parihar, S. S., Ahirwar, N. K., Snehi, S. K., and Singh, V. (2015). Plant growth promoting rhizobacteria (PGPR): current and future prospects for development of sustainable agriculture. *Journal of Microbial & Biochemical Technology* **07**, 1013-1020.
- Happyana, N., Agnolet, S., Muntendam, R., Van Dam, A., Schneider, B., and Kayser, O. (2013). Analysis of cannabinoids in laser-microdissected trichomes of medicinal *Cannabis sativa* using LCMS and cryogenic NMR. *Phytochemistry* **87**, 51-59.
- Hazekamp, A. (2007). *Cannabis; extracting the medicine*. Leiden University.
- Hemphill, J. K., Turner, J. C., and Mahlberg, P. G. (1980). Cannabinoid content of individual plant organs from different geographical strains of *cannabis sativa* L. *Journal of Natural Products* **43**, 112-122.

- Hillig, K. W., and Mahlberg, P. G. (2004). A chemotaxonomic analysis of cannabinoid variation in *Cannabis* (Cannabaceae). *American Journal of Botany* **91**, 966-975.
- Humphris, S. N., Bengough, A. G., Griffiths, B. S., Kilham, K., Rodger, S., Stubbs, V., Valentine, T. A., and Young, I. M. (2005). Root cap influences root colonisation by *Pseudomonas fluorescens* SBW25 on maize. *Fems Microbiology Ecology* **54**, 123-130.
- Idris, E. E., Iglesias, D. J., Talon, M., and Borriss, R. (2007). Tryptophan-dependent production of indole-3-acetic acid (IAA) affects level of plant growth promotion by *Bacillus amyloliquefaciens* FZB42. *Molecular Plant-Microbe Interactions* **20**, 619.
- Iqbal, A., Bhatti, H. N., Nosheen, S., Jamil, A., and Malik, M. A. (2002). Histochemical and physicochemical study of bacterial exopolysaccharides. *Biotechnology* **1**, 28-33.
- Jiang, H. E., Li, X., Zhao, Y. X., Ferguson, D. K., Hueber, F., Bera, S., Wang, Y. F., Zhao, L. C., Liu, C. J., and Li, C. S. (2006). A new insight into *Cannabis sativa* (Cannabaceae) utilization from 2500-year-old Yanghai Tombs, Xinjiang, China. *Journal of Ethnopharmacology* **108**, 414-22.
- Jin, D., Dai, K., Xie, Z., and Chen, J. (2020). Secondary metabolites profiled in cannabis inflorescences, leaves, stem barks, and roots for medicinal purposes. *Scientific Reports* **10**, 1-14.
- Khan, A. L., Halo, B. A., Elyassi, A., Ali, S., Al-Hosni, K., Hussain, J., Al-Harrasi, A., and Lee, I.-J. (2016). Indole acetic acid and ACC deaminase from endophytic bacteria improves the growth of *Solanum lycopersicum*. *Electronic Journal of Biotechnology* **21**, 58-64.
- Kim, B.-C., Poo, H., Lee, K. H., Kim, M. N., Kwon, O.-Y., and Shin, K.-S. (2012). *Mucilaginibacter angelicae* sp. nov., isolated from the rhizosphere of *Angelica polymorpha* Maxim. *International Journal of Systematic and Evolutionary Microbiology* **62**, 55-60.

- Kim, Y. C., Leveau, J., Gardener, B. B. M., Pierson, E. A., Pierson, L. S., and Ryu, C.-M. (2011). The multifactorial basis for plant health promotion by plant-associated bacteria. *Applied and Environmental Microbiology* **77**, 1548-1555.
- Kostic, M., Pejic, B., and Skundric, P. (2008). Quality of chemically modified hemp fibers. *Bioresource Technology* **99**, 94.
- Kowal, M. A., Hazekamp, A., and Grotenhermen, F. (2016). Review on clinical studies with cannabis and cannabinoids 2010-2014. *Multiple Sclerosis* **6**, 1515.
- Lange, B. M., and Turner, G. W. (2013). Terpenoid biosynthesis in trichomes—current status and future opportunities. *Plant Biotechnology Journal* **11**, 2-22.
- Laverty, K. U., Stout, J. M., Sullivan, M. J., Shah, H., Gill, N., Holbrook, L., Deikus, G., Sebra, R., Hughes, T. R., and Page, J. E. (2019). A physical and genetic map of *Cannabis sativa* identifies extensive rearrangements at the THC/CBD acid synthase loci. *Genome Research* **29**, 146-156.
- Lee, H.-R., Han, S.-I., Rhee, K.-H., and Whang, K.-S. (2013). *Mucilaginibacterherbaticus* sp. nov., isolated from the rhizosphere of the medicinal plant *Angelica sinensis*. *International Journal of Systematic and Evolutionary Microbiology* **63**, 2787-2793.
- Lyngwi, N. A., and Joshi, S. (2014). Economically important *Bacillus* and related genera: a mini review. *Biology of Useful Plants and Microbes* **3**, 33-43.
- Lyu, D., Backer, R., and Smith, D. L. (2020). "Chapter 8: Plant growth-promoting rhizobacteria (PGPR) as plant biostimulants in agriculture." in *Biostimulants for sustainable crop production* by Burleigh Dodds Science Publishing.

- Ma, Y., Rajkumar, M., Luo, Y., and Freitas, H. (2011). Inoculation of endophytic bacteria on host and non-host plants—effects on plant growth and Ni uptake. *Journal of Hazardous Materials* **195**, 230-237.
- Mabood, F., Zhou, X., and Smith, D. L. (2014). Microbial signaling and plant growth promotion. *Canadian Journal of Plant Science* **94**, 1051-1063.
- Madhaiyan, M., Poonguzhali, S., Lee, J.-S., Senthilkumar, M., Lee, K. C., and Sundaram, S. (2010). *Mucilaginibacter gossypii* sp. nov. and *Mucilaginibacter gossypicola* sp. nov., plant-growth-promoting bacteria isolated from cotton rhizosphere soils. *International Journal of Systematic and Evolutionary Microbiology* **60**, 2451-2457.
- Mansouri, H., Asrar, Z., and Amarowicz, R. (2011). The response of terpenoids to exogenous gibberellic acid in *Cannabis sativa* L. at vegetative stage. *Acta Physiologiae Plantarum* **33**, 1085-1091.
- Morimoto, S., Komatsu, K., Taura, F., and Shoyama, Y. (1997). Enzymological evidence for cannabichromenic acid biosynthesis. *Journal of Natural Products* **60**, 854-857.
- Morimoto, S., Komatsu, K., Taura, F., and Shoyama, Y. (1998). Purification and characterization of cannabichromenic acid synthase from *Cannabis sativa*. *Phytochemistry* **49**, 1525-1529.
- Naseem, H., and Bano, A. (2014). Role of plant growth-promoting rhizobacteria and their exopolysaccharide in drought tolerance of maize. *Journal of Plant Interactions* **9**, 689-701.
- O'sullivan, D. J., and O'Gara, F. (1992). Traits of fluorescent *Pseudomonas* spp. involved in suppression of plant root pathogens. *Microbiological Reviews* **56**, 662-676.
- Pankratov, T. A., Tindall, B. J., Liesack, W., and Dedysh, S. N. (2007). *Mucilaginibacter paludis* gen. nov., sp. nov. and *Mucilaginibacter gracilis* sp. nov., pectin-, xylan- and laminarin-

- degrading members of the family Sphingobacteriaceae from acidic Sphagnum peat bog. *International Journal of Systematic and Evolutionary Microbiology* **57**, 2349-2354.
- Parret, A. H., Schoofs, G., Proost, P., and De, M. R. (2003). Plant lectin-like bacteriocin from a rhizosphere-colonizing *Pseudomonas* isolate. *Journal of Bacteriology* **185**, 897-908.
- Pascale, G., Sauriol, F., Benhamou, N., Bélanger, R. R., and Paulitz, T. C. (1997). Novel butyrolactones with antifungal activity produced by *Pseudomonas aureofaciens* strain 63-28. *The Journal of Antibiotics* **50**, 742-749.
- Poonguzhali, S., Madhaiyan, M., and Sa, T. (2008). Isolation and identification of phosphate solubilizing bacteria from chinese cabbage and their effect on growth and phosphorus utilization of plants. *Journal of Microbiology and Biotechnology* **18**, 773-777.
- Raaijmakers, J. M., Paulitz, T. C., Steinberg, C., Alabouvette, C., and Moëgne-Loccoz, Y. (2009). The rhizosphere: a playground and battlefield for soilborne pathogens and beneficial microorganisms. Springer.
- Raharjo, T. J., Chang, W.-T., Verberne, M. C., Peltenburg-Looman, A. M., Linthorst, H. J., and Verpoorte, R. (2004). Cloning and over-expression of a cDNA encoding a polyketide synthase from *Cannabis sativa*. *Plant Physiology and Biochemistry* **42**, 291-297.
- Rajkumar, M., and Freitas, H. (2008). Effects of inoculation of plant-growth promoting bacteria on Ni uptake by Indian mustard. *Bioresource Technology* **99**, 3491-3498.
- Rajkumar, M., Nagendran, R., Lee, K. J., Lee, W. H., and Kim, S. Z. (2006). Influence of plant growth promoting bacteria and Cr⁶⁺ on the growth of Indian mustard. *Chemosphere* **62**, 741-748.

- Rosier, A., Medeiros, F. H., and Bais, H. P. (2018). Defining plant growth promoting rhizobacteria molecular and biochemical networks in beneficial plant-microbe interactions. *Plant and Soil*, 1-21.
- Ross, S. A., and ElSohly, M. A. (1996). The volatile oil composition of fresh and air-dried buds of *Cannabis sativa*. *Journal of Natural Products* **59**, 49-51.
- Russo, E., and Guy, G. W. (2006). A tale of two cannabinoids: The therapeutic rationale for combining tetrahydrocannabinol and cannabidiol. *Medical Hypotheses* **66**, 234-46.
- Salentijn, E. M. J., Zhang, Q., Amaducci, S., Yang, M., and Trindade, L. M. (2015). New developments in fiber hemp (*Cannabis sativa* L.) breeding. *Industrial Crops & Products* **68**, 32-41.
- Santoyo, G., Orozco-Mosqueda, M. d. C., and Govindappa, M. (2012). Mechanisms of biocontrol and plant growth-promoting activity in soil bacterial species of *Bacillus* and *Pseudomonas*: a review. *Biocontrol Science & Technology* **22**, 855-872.
- Sawler, J., Stout, J. M., Gardner, K. M., Hudson, D., Vidmar, J., Butler, L., Page, J. E., and Myles, S. (2015). The genetic structure of marijuana and hemp. *PloS One* **10**, e0133292.
- Schreiter, S., Babin, D., Smalla, K., and Grosch, R. (2018). Rhizosphere competence and biocontrol effect of *pseudomonas* sp. RU47 independent from plant species and soil type at the field scale. *Frontiers in Microbiology* **9**.
- Shahnaz, E., Surma, S., Banday, S., Bhat, Z., and Muzaffar, M. (2020). Plant growth promoting rhizobacteria (PGPR): A promising approach for plant disease management. *SKUAST Journal of Research* **22**, 11-20.

- Shao, J., Xu, Z., Zhang, N., Shen, Q., and Zhang, R. (2015). Contribution of indole-3-acetic acid in the plant growth promotion by the rhizospheric strain *Bacillus amyloliquefaciens* SQR9. *Biology & Fertility of Soils* **51**, 321-330.
- Sharpe, F., and Laws, D. (1981). The essential oil of hops a review. *Journal of the Institute of Brewing* **87**, 96-107.
- Shi, Y., Lou, K., and Li, C. (2010). Growth and photosynthetic efficiency promotion of sugar beet (*Beta vulgaris* L.) by endophytic bacteria. *Photosynthesis Research* **105**, 5-13.
- Shoyama, Y., Yagi, M., Nishioka, I., and Yamauchi, T. (1975). Biosynthesis of cannabinoid acids. *Phytochemistry* **14**, 2189-2192.
- Singh, R. K., Ali, S. A., Nath, P., and Sane, V. A. (2011). Activation of ethylene-responsive p-hydroxyphenylpyruvate dioxygenase leads to increased tocopherol levels during ripening in mango. *Journal of Experimental Botany* **62**, 3375-3385.
- Smith, D. L., Subramanian, S., Lamont, J. R., and Bywater-Ekegård, M. (2015). Signaling in the phytomicrobiome: breadth and potential. *Frontiers in Plant Science* **6**, 709.
- Subair, H. (2015). Isolation and screening bacterial exopolysaccharide (EPS) from potato rhizosphere in highland and the potential as a producer indole acetic acid (IAA). *Procedia Food Science* **3**, 74-81.
- Takishita, Y., Souleimanov, A., Bourguet, C., Ohlund, L. B., Arnold, A. A., Sleno, L., and Smith, D. L. (2021). *Pseudomonas* entomophila 23S produces a novel antagonistic compound against *Clavibacter michiganensis* subsp. *michiganensis*, a pathogen of tomato bacterial canker. *Applied Microbiology* **1**, 60-73.
- Tank, N., and Saraf, M. (2009). Enhancement of plant growth and decontamination of nickel - spiked soil using PGPR. *Journal of Basic Microbiology* **49**, 195-204.

- Taura, F., Morimoto, S., and Shoyama, Y. (1995a). Cannabinerolic acid, a cannabinoid from *Cannabis sativa*. *Phytochemistry* **39**, 457-458.
- Taura, F., Morimoto, S., and Shoyama, Y. (1996). Purification and characterization of cannabidiolic-acid synthase from *Cannabis sativa* L. Biochemical analysis of a novel enzyme that catalyzes the oxidocyclization of cannabigerolic acid to cannabidiolic acid. *Journal of Biological Chemistry* **271**, 17411-17416.
- Taura, F., Morimoto, S., Shoyama, Y., and Mechoulam, R. (1995b). First direct evidence for the mechanism of DELTA. 1-tetrahydrocannabinolic acid biosynthesis. *Journal of the American Chemical Society* **117**, 9766-9767.
- Tipparat, P., Natakankitkul, S., Chamnivikaipong, P., and Chutiwat, S. (2012). Characteristics of cannabinoids composition of Cannabis plants grown in Northern Thailand and its forensic application. *Forensic Science International* **215**, 164-170.
- Toonen, M., Ribot, S., and Thissen, J. (2006). Yield of illicit indoor cannabis cultivation in the Netherlands. *Journal of Forensic Sciences* **51**, 1050-4.
- Vacheron, J., Desbrosses, G., Bouffaud, M. L., Touraine, B., Moënne-Loccoz, Y., Muller, D., Legendre, L., Wisniewski-Dyé, F., and Prigent-Combaret, C. (2013). Plant growth-promoting rhizobacteria and root system functioning. *Frontiers in Plant Science* **4**, 356.
- Vanhove, W., Surmont, T., Van, D. P., and De, R. B. (2012). Yield and turnover of illicit indoor cannabis (*Cannabis* spp.) plantations in Belgium. *Forensic Science International* **220**, 265-270.
- Vanhove, W., Van Damme, P., and Meert, N. (2011). Factors determining yield and quality of illicit indoor cannabis (*Cannabis* spp.) production. *Forensic Science International* **212**, 158-163.

- Wani, P. A., and Khan, M. S. (2010). *Bacillus* species enhance growth parameters of chickpea (*Cicer arietinum* L.) in chromium stressed soils. *Food and Chemical Toxicology* **48**, 3262-3267.
- Wani, P. A., Khan, M. S., and Zaidi, A. (2007). Synergistic effects of the inoculation with nitrogen - fixing and phosphate - solubilizing rhizobacteria on the performance of field - grown chickpea. *Journal of Plant Nutrition and Soil Science* **170**, 283-287.
- Yan, H. X., Liu, L., Li, L., Zhang, P. P., Liang, W. H., and Zhao, H. T. (2016). Research progress on agriculture of plant growth promoting rhizobacteria. *Heilongjiang Agricultural Sciences*, 148-151.
- Zajšek, K., Goršek, A., and Kolar, M. (2013). Cultivating conditions effects on kefir production by the mixed culture of lactic acid bacteria imbedded within kefir grains. *Food Chemistry* **139**, 970-977.
- Zuardi, A. W., Crippa, J. A., Hallak, J. E., Moreira, F. A., and Guimarães, F. S. (2012). Cannabidiol, a *Cannabis sativa* constituent, as an antipsychotic drug. *Revista Brasileira De Psiquiatria* **34**, S104-S117.

Connecting text

The previous chapter provided an overview of cannabis and its production, and the current understanding around beneficial members of the phytomicrobiome associated with the rhizosphere. Plant growth-promoting rhizobacteria (PGPR) hold the potential to improve plant growth and development in a sustainable way. PGPR has been used to improve the growth of various plants through direct and indirect mechanisms, including nutrient mobilization, phytohormone production and stress tolerance.

However, there is limited research on cannabis growth, as it was illegal for about a century around the world. More recently, the pharmaceutical potential of the key secondary metabolites (cannabinoids and terpenes) in cannabis plants has been clearly demonstrated. Therefore, cannabis yield and quality improvement will provide improved accessibility to the medicinal area in the future. In the present study, we hypothesize that the selected PGPR strains (*Bacillus* sp., *Mucilaginibacter* sp., and *Pseudomonas* sp.) can be applied to enhance cannabis growth and development. Based on the background information and literature review, the project described below addresses the following research questions: 1) Do the three selected PGPR affect the rate and degree of cannabis cutting rooting at the vegetative stage, and whole plant growth production at harvest? 2) If the PGPR can alter the secondary metabolite accumulations in cannabis flowers? 3) What are the mechanisms/pathways in cannabis that are elicited by PGPR that contribute to improved plant growth and development?

Chapter 3 Three Plant Growth-Promoting Rhizobacteria Alter Morphological Development, Physiology and Flower Yield of *Cannabis sativa* L.

Authors: Dongmei Lyu ^a, Rachel Backer ^a, Donald L. Smith ^a

Affiliations:

^a Department of Plant Science, McGill University, Sainte-Anne-de-Bellevue, Quebec, Canada, H9X3V9

This manuscript was originally published in *Industrial Crop and Products Journal* and shared in the thesis via the Creative Commons Attribution 4.0 International Public License.

Lyu, D., Backer, R., & Smith, D. L. (2022). Three plant growth-promoting rhizobacteria alter morphological development, physiology, and flower yield of *Cannabis sativa* L. *Industrial Crops and Products*, 178, 114583. <https://doi.org/10.1016/j.indcrop.2022.114583>.

3.1 Abstract

The beneficial phytomicrobiome is a sustainable approach with the potential to enhance plant growth; it has been evaluated for a number of crop species, but not for *Cannabis sativa* L. The legalization of cannabis and awareness of its end-use applications has resulted in expanded consumer demand. An important challenge is the achievement of high yield with minimum input for indoor production. This study evaluated three individual plant growth-promoting rhizobacteria (*Bacillus* sp., *Mucilaginibacter* sp. and *Pseudomonas* sp.) on the root development and subsequent plant growth of cannabis (cv. CBD Kush) cuttings. The hypothesis tested was that the application of plant growth-promoting rhizobacteria would improve rooting speed of cuttings, and subsequent physiological variables and yield attributes. When compared with control plants (mock inoculation with MgSO₄), plants inoculated with plant growth-promoting rhizobacteria (PGPR) increased root

length at the vegetative stage. At harvest, the fresh flower weight was increased by 5.13, 6.94 and 11.45%, compared to the control, for plants inoculated with *Bacillus* sp., *Mucilaginibacter* sp. and *Pseudomonas* sp., respectively. However, the plant height, node number, branch number and leaf area of plants treated with plant growth-promoting rhizobacteria were rarely different from the control treatment. Inoculation with *Pseudomonas* sp. resulted in the greatest increase in photosynthetic rate during the vegetative and reproductive growth stages, and final harvest index, while *Bacillus* sp., and *Mucilaginibacter* sp. increased flower number and axillary bud outgrowth rate.

3.2 Introduction

The recreational and medicinal history of *Cannabis sativa* L. (a genus of the Cannabaceae family) extends back thousands of years (Ren et al., 2021). The need for cannabis production has increased dramatically with globally expanding legalization of both medical and recreational utilization during the past decade (Caulkins et al., 2012; Pacula and Smart, 2017); however, industrial hemp (*Cannabis sativa*) has a very long history of utilization, being first used as fiber about 50,000 years ago (Tourangeau, 2015). With expanded understanding of this plant, it is estimated that the global cannabis market will reach USD 90.4 billion by 2026 (GlobeNewswire, 2021). Thus, increasing demand of cannabis is driving research regarding breeding and management agriculture systems to achieve high yield and quality.

The illegal status of this crop, for almost a century, led to limited knowledge and cultivation practices. Similarly, cultivation practices and precise technological configurations used in the production of other crops can also be applied to cannabis production, but considering the attributes of cannabis plants, especially medicinal types, indoor growth is currently the main cultivation system. To date, fertilization and lighting are mostly being investigated as ways to improve

cannabis yield and quality. Caplan et al. (2017) illustrated that the application of 389 mg N L⁻¹, supplied by organic fertilizer, resulted in the highest yield, and data published by Backer et al. (2019) indicates that varying fertilization impacts cannabis yield, although not necessarily single plant yield. However, the improvement in cannabis yield could be affected by fertilizer application time (Backer et al., 2019). In addition, as a short-day plant, cannabis production is predominately linked to photoperiod (Moher et al., 2021; Tipparat et al., 2012), light quality (Danziger and Bernstein, 2021; Magagnini et al., 2018; Wei et al., 2021) and light intensity (Rodriguez-Morrison et al., 2021; Zarei et al., 2021). For instance, plants under 600 W lamps have higher flower bud yield than 400 W lamps (Vanhove et al., 2012), and more yield can be obtained with added sub-canopy lighting (SCL) (Hawley, 2018). Plant density also affected cannabis yield (Deng et al., 2019; Kerckhoffs et al., 2017). The results can be linked to lighting because individual plants can capture more light when grown at lower densities, which results in improved photosynthesis, leading to higher yield production (Van Der Werf, 1997).

It is also important to obtain high levels of cannabinoids, in addition to increased flower yield, since cannabinoids are unique secondary metabolites with various psychoactive and non-psychoactive effects on humans. This class of compounds includes Δ^9 -tetrahydrocannabinol (THC), cannabidiol (CBD) and cannabigerol (CBG) (Aizpurua-Olaizola et al., 2016; Fine and Rosenfeld, 2013) which are mainly concentrated in the trichomes of female cannabis plants. Although the accumulation of key cannabinoids mainly relates to genotypic variation rather than cultivation factors (Vanhove et al., 2011), flower yield improvement could also be an option for obtaining elevated amounts of cannabinoids from the same genotype. Additional fertilizer application and lighting control are widely used and evaluated for all types of crops but can be costly, whereas to achieve more sustainable energy use and minimize inputs, such as plant growth-

promoting rhizobacteria (PGPR) could be a feasible strategy (Backer et al., 2018; Fan et al., 2017; Lyu et al., 2019; Ricci, 2015; Smith et al., 2015).

Plant growth-promoting rhizobacteria are beneficial bacteria, usually isolated from soil associated with host plants or their roots. The PGPR can improve nutrient availability and trigger hormone production (Lyu et al., 2020; Shah et al., 2021), improving root development and increasing plant enzymatic activity (Fan et al., 2020; Lyu et al., 2020); these effects have been verified across various crops. However, there have been only a few research reports regarding application of PGPR resulting in effects on final cannabis yield and chemical profile. A PGPR consortium (*Azospirillum brasilense*, *Gluconacetobacter diazotrophicus*, *Burkholderia ambifaria*, and *Herbaspirillum seropedicae*) inoculation improved *Cannabis sativa* ‘Finola’ (a hemp cultivar) growth and plant physiological status and affected the secondary metabolite accumulation; moreover, those bacteria were found adhering in the surface of plant roots (Pagnani et al., 2018). Another example, from Conant et al. (2017), reported that inoculation with a microbial biostimulant (Mammoth PTM) increased the cannabis plant height and basal stem area as well as leading to a 16.5% increase of flower yield.

In previous work, we suggested the potential of *Bacillus* sp. and *Pseudomonas* sp. to promote cannabis growth as they are the most common species of PGPR (Lyu et al., 2019), however, these ideas have not been directly tested by experimentation. The three PGPR evaluated here (*Bacillus* sp., *Mucilaginibacter* sp. and *Pseudomonas* sp.) have not previously been tested on cannabis plants, but their effects have been explored in other plants species (maize, canola, and *Arabidopsis thaliana*). All three bacteria manifested potential to positively influence plant growth (e.g., phytohormone production, P solubilization and nitrogen fixation) especially under stressful growing conditions (Fan et al., 2020). Thus, two studies were established to investigate the effect

of each PGPR (*Bacillus* sp., *Mucilaginibacter* sp. and *Pseudomonas* sp.), applied individually, onto cannabis cv “CBD Kush”. The first study evaluated early root development of inoculated cuttings, and the second study evaluated plant physiological variables (e.g., photosynthesis rate) and yield variables (e.g., number of flowers per plant, total flower yield) of inoculated plants.

3.3 Materials and methods

3.3.1 Bacterial strains, culture conditions, and inoculum preparation

Plant growth-promoting rhizobacteria strains of *Bacillus mobilis* (KJ812449), *Pseudomonas koreensis* (AF468452), and *Mucilaginibacter lappiensis* (jgi.1095764) were provided by Dr. Fan through work conducted at McGill University; the strains had been stored in glycerol at -80 °C after isolation. Cultures were taken out of storage and streaked onto petri plates containing sterile (30 min, 121 °C) King’s Medium B (KB; 20.0 g L⁻¹ protease peptone, 1.5 g L⁻¹ K₂HPO₄, 10.0 g L⁻¹ glycerol, 0.25 g L⁻¹ MgSO₄•7H₂O, and 15 g L⁻¹ agar). Fresh cultures were prepared by scraping the bacterial colonies grown on KB agar off the surface of the agar, transferring the resulting material to a tube containing 25 mL sterile KB liquid and growing for 24 h (*Bacillus* sp. and *Pseudomonas* sp.) or 72 h (*Mucilaginibacter* sp.) at 28 ± 2 °C on an orbital shaker (150 rev min⁻¹) to reach the exponential phase. The bacterial cell inoculum was obtained by centrifuging (6,000×g, 10 min, 4 °C) the fresh bacterial culture, then washing cell pellets free of growth medium four times with sterile 10 mM MgSO₄ and resuspending the pellet in 10 mM MgSO₄ to achieve a final density of 1 × 10⁸ colony forming units (CFU) mL⁻¹, determined by optical density (OD) at 600 nm. The final bacterial suspension was used as inoculum to assess the effects of each strain on cannabis cutting root development and whole plant growth.

3.3.2 Plant material and growth conditions

Two series of experiments were carried out at the Large Research Animal Unit, Department

of Plant Science, McGill University, Quebec, Canada (latitude 45°24'22" N, longitude 73°56'44" W) in a licensed growth facility (Licence No. LIC-5AZZW7S4GM-2019). A set of young cuttings were taken from a CBD Kush mother plant (Dutch Passion, Amsterdam, Netherlands). Extra foliage, except for the youngest three fully unfurled leaves, was removed from each cutting and the ends of the retained leaves were trimmed. The base of each stem was then cut at a 45° angle, dipped into Stim-Root rooting powder (Plant Products, Laval, QC, Canada) and placed into rooting medium (vermiculite, for the rooting development experiment, or a rockwool cube (3.8 cm × 3.8 cm) for the whole plant growth experiment; both from Plant Products, Laval, QC, Canada) in a plastic tray (53 cm × 28 cm × 6.4 cm) that was pre-treated with water and a dilute nutrient solution (2.11 mL L⁻¹ Velokelp, REMO Nutrients, Maple Ridge, British Columbia, Canada). Trays filled with cuttings were covered with a dome (18 cm high) with vent to retain humidity and were then placed on a growth shelf under LED (light emitting diodes) lights (approximately 150 μmol m⁻² s⁻¹, 24 h photoperiod) for two weeks prior to transplanting.

3.3.3 Root development of cannabis cuttings

The cuttings used in this experiment were rooted in vermiculite so that the intact root structure could be maintained for detailed root structure analysis. Rooted cannabis cuttings were carefully removed from vermiculite and transferred into sterile magenta jars (7.6 cm x 7.6 cm x 10 cm, Fisher scientific) with 50 mL sterile water containing 0.5 mL single bacterial strain cell suspension (strains of *Bacillus* sp., *Mucilaginibacter* sp. or *Pseudomonas* sp., prepared as described in Section 3.3.1) or 0.5 mL 10 mM MgSO₄ as a control. The experiment was arranged following a randomized complete block design, where the cuttings were blocked into five replications according to cutting fresh weight prior to rooting and size of roots developed after two

weeks of rooting. Magenta jars were kept on a growth shelf (22 °C, 60 % relative humidity, 24 h photoperiod) under LED lights (approximately 150 $\mu\text{mol m}^{-2} \text{s}^{-1}$).

Root scanning was conducted two weeks after inoculation. Clear roots from cuttings harvested and placed in a 30 × 40 cm plastic plate and submerged in deionized water. Roots were scanned (Modified Epson Expression 10000XL, Regent Instruments Inc., Québec, QC, Canada) and output images were analyzed using WinRhizo software (Regent Instruments Inc.). The root length (cm), volume (cm^3), mean root diameter (mm), and root surface area (cm^2) were measured. Each variable was adjusted for the initial cutting mass prior to bacterial inoculation; this allowed for comparison of the final root development per initial cutting mass. The whole experiment was repeated twice, thus the mean from ten plants of each treatment was used.

3.3.4 Growth and yield of cannabis plants inoculated with PGPR

For this experiment, cuttings were rooted in rockwool to reduce the occurrence and severity of root damage during transplantation to pots. After two weeks of rooting, the most uniform cuttings were transplanted into 15 cm pots containing 360 g Agro Mix G2 Compost (contains brown peat, fibro moss peat, perlite, compost, limestone, gypsum and micronutrients; Fafard). Plants were grown at an indoor facility for a 3-week vegetative growth period (Day 1 to 21), followed by a 7-week flowering period (Day 22 to 70); the details of growth conditions are provided below (**Table 3.1**). Environmental conditions were monitored throughout the growth cycle using temperature and humidity sensors.

Table 3.1 The growth conditions for cannabis plants. Cannabis plants were growing under 18 h light for three weeks at vegetative stage, then plants were shifted to 12 h light for reproductive stage. During each week, plant received the nutrients and water following the table.

Vegetative stage					Flowering stage						
	Transplanting day	Week 1	Week 2	Week 3	Week 4	Week 5	Week 6	Week 7	Week 8	Week 9	Week 10
Nutrients	1.3 mL L ⁻¹ VeloKelp	1.84 mL L ⁻¹ each of VeloKelp, Micro, Grow, MagNifiCal			2.2 mL L ⁻¹ each of Velokelp, Micro, MagNifiCal, Bloom, AstroFlower					0	
Average Water Quantity	350 mL	150 mL	250 mL	500 mL	600 mL	700 mL	800 mL	1000 mL	1100 mL	1200 mL	1200 mL
Light Duration	18 h light/6 h dark				12 h dark/light						
PAR ^x (mmol·m ⁻² ·s ⁻¹)	300			475	635	715	800				
Temperature (Degree Celsius)	25.3 ± 0.25 °C										
Humidity	59 ± 0.49%				60.7 ± 1.37%					55 ± 1.25%	
CO ₂ concentration (ppm)	485 ± 9.5										

Bacterial cell pellets (strains of *Bacillus* sp., *Mucilaginibacter* sp. and *Pseudomonas* sp.), suspended in 10 mL of 10 mM MgSO₄ or 10 mL of 10 mM MgSO₄ (control) were poured onto the surface of the compost substrate in each pot, at the base of the plant, at the time of transplanting. The experiment was arranged following a completely randomized design with five replications per treatment, and the entire experiment was conducted two times. Pots were hand-watered with nutrient solutions prepared using tap water according to the schedule shown in **Table 3.1**. Remo Nutrients solution (prepared according to growth stage, as detailed in **Table 3.1**) was applied for three consecutive days; on the fourth day plants received only water. The volume of solution (nutrients and water) increased over the course of the growth cycle, to match plant requirements.

3.3.4.1 Physiological measurements and harvest

Non-destructive measurements of plant height, number of nodes, branch number and bud number were taken on days 21, 42 and 70 after transplanting. At the same time, photosynthetic rate was measured on the third-from-the-top fully unfolded leaf of the main stem, to facilitate comparison of tissue of similar physiological age using a LI-COR 6400 (Lincoln, NE, USA). Ten weeks after transplanting (70 days), plants were manually harvested and separated into stems, leaves and flower buds. The leaf area was estimated using a leaf area meter (LI-3100C, Lincoln, NE, USA). Stems, leaves and flower buds were immediately weighed for fresh weight (FW); dry weight (DW) was recorded after freeze drying at -60 °C to a constant weight using a lyophilizer (SNL216V freezing-dryer, Thermo Savant Co. Ltd. USA).

3.3.5 Calculations and statistical analysis

Based on cannabis plant morphology (**Figure 3.1**), the axillary bud outgrowth rate was calculated according to Thomas and Hay (2009):

$$\text{Axillary bud outgrowth rate} = \frac{\text{Total flower numbers}}{\text{Number of nodes}} * 100\% \quad (3.1)$$

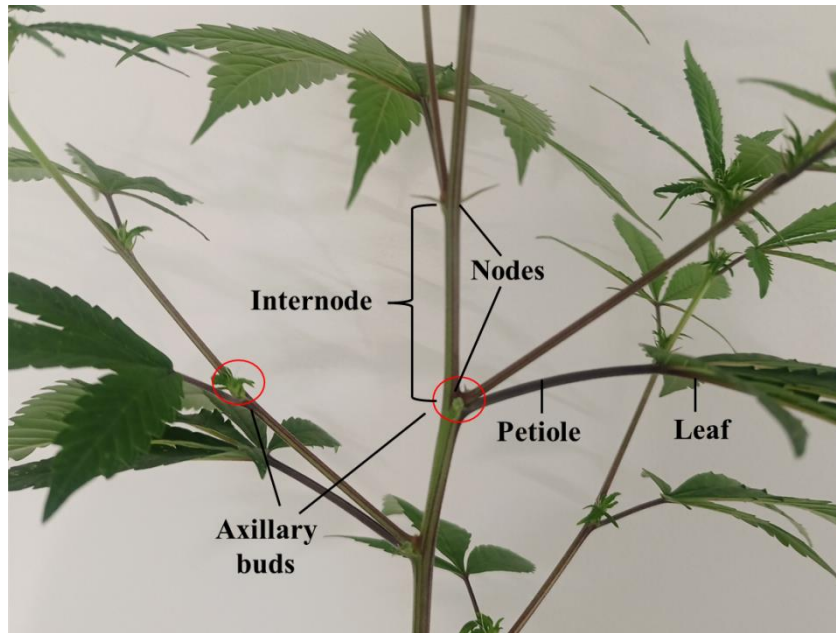


Figure 3.1 Cannabis leaves are attached to the plant stem at nodes. The axillary buds emerged just above the nodes.

Harvest index (HI) was calculated as follows:

$$HI = \frac{\text{Dry weight of flowers}}{\text{Sum of total aboveground dry biomass}} \quad (3.2)$$

Data analysis was performed using SPSS (IBM SPSS Statistics for Citrix, Version 24.0. Armonk, NY: IBM Corp.). Differences between each treatment and the control were evaluated using analysis of variance (ANOVA). The level of significance was set at $p < 0.05$; both significant effects ($p < 0.05$) and/or numerical trends in the data ($0.05 < p < 0.1$) are discussed. The correlations between initial cutting mass and final root length were determined using bivariate Pearson Correlation in SPSS.

3.4 Results

3.4.1 PGPR inoculation improves cannabis early root development

At the vegetative stage, cuttings treated with bacteria showed different levels of root

morphological responses (**Table 3.2**). The highest value of root length/initial cutting (cm g^{-1}) was for cuttings treated with *Pseudomonas* sp. (240.06 cm g^{-1}), which was 32% longer than the control. The presence of *Bacillus* sp., *Mucilaginibacter* sp. and *Pseudomonas* sp. increased root volume/initial cutting ($\text{cm}^3 \text{ g}^{-1}$) by 4.5, 9.1 and 22.7% respectively, but at none statistically level. In addition, for the root surface area, only plants inoculated with *Pseudomonas* sp. inoculation led to the significant change compared to control. Average root diameter/initial cutting (mm g^{-1}) was not affected by PGPR inoculation.

Across treatments, the root length at two weeks after inoculation with PGPR was positively correlated with initial cutting mass, but it was not significantly correlated for the non PGPR treated plants ($p = 0.151$) and plants inoculated with *Mucilaginibacter* sp., though for the latter $p = 0.082$. In comparison, root length increased with the initial cutting mass following *Bacillus* sp. and *Pseudomonas* sp. inoculation, with significant coefficients of determination (r^2) of 0.22 ($p = 0.023$) and 0.35 ($p = 0.020$), respectively.

Table 3.2 Root development (length, diameter, volume and root surface area) as affected by inoculation of individual bacteria onto cannabis cv. CBD Kush. Each parameter was calculated by divided the initial cutting weight. Each column represents the average of ten plants and standard error (SE).

Treatment	Length/ initial cutting weight (cm g ⁻¹)	Average Diameter/ initial cutting weight (mm g ⁻¹)	Root Volume/ initial cutting weight (cm ³ g ⁻¹)	Root surface area/ initial cutting weight (cm ² g ⁻¹)
Control	181.74 ± 18.55	0.27 ± 0.029	0.22 ± 0.022	22.13 ± 2.21
<i>Bacillus</i> sp.	205.29 ± 24.69	0.23 ± 0.025	0.23 ± 0.020	24.42 ± 2.45
<i>Mucilaginibacter</i> sp.	213.50 ± 15.84	0.22 ± 0.018	0.24 ± 0.017	25.25 ± 1.74
<i>Pseudomonas</i> sp.	240.06 ± 18.52 *	0.23 ± 0.026	0.27 ± 0.017	28.36 ± 1.88*

* The mean difference is significant at the 0.05 probability level compared with the control.

3.4.2 Photosynthetic rate

The reproductive stage of the cannabis plants is considered to have started on the day the photoperiod was changed from 18 h to 12 h, which coincides with the first photosynthesis reading (i.e., day 21 after transplanting). **Figure 3.2** shows the mean photosynthetic rates of treated plants at 21, 42 and 70 days after transplanting the cuttings into the pots. On Day 21, the last day the plants were in the vegetative stage, the photosynthetic rate was not statistically different among PGPR-inoculated plants and the control. In contrast, at day 42 (the mid-point of the flowering stage), an important week for flower formation, *Mucilaginibacter* sp. and *Pseudomonas* sp. significantly increased the plant photosynthetic rate, compared with the control.

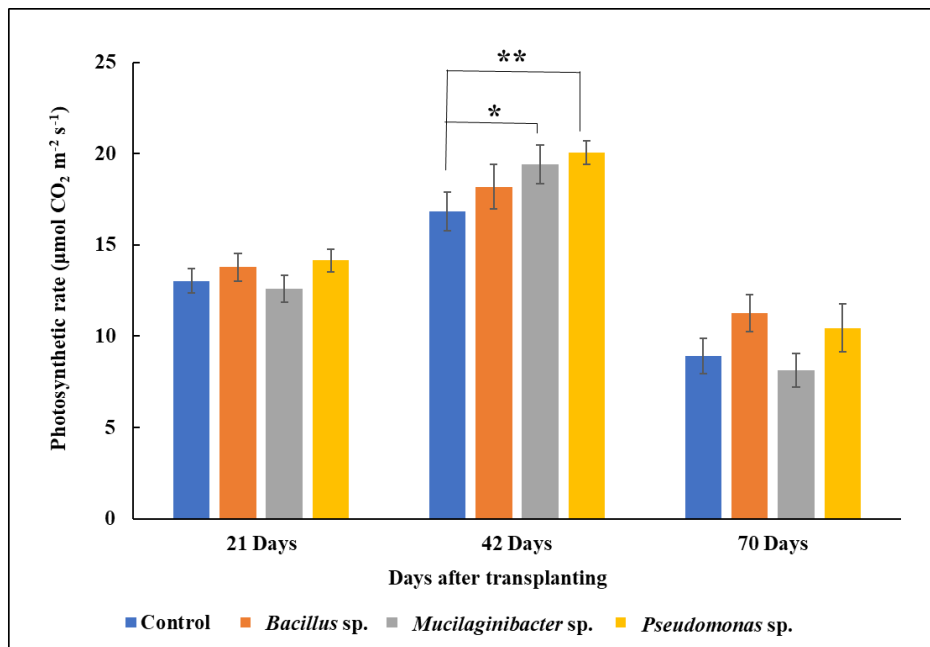


Figure 3.2 Photosynthetic rates of *Cannabis sativa* cv. CBD Kush plants with and without bacterial inoculation. Each bar represents the average of ten plants and standard error (SE).

* The mean difference is significant at the 0.05 probability level compared with the control.

** Indicates the value is significantly different at the 0.01 probability level compared with the control.

3.4.3 PGPR inoculation increases cannabis flower number

All plant agronomic traits were recorded at days 21, 42 and 70 after transplanting the cuttings into the pots, as shown in **Table 3.3**. Inoculation with *Bacillus* sp. and *Mucilaginibacter* sp. significantly increased the final number of flowers buds, but not plant height or numbers of nodes and branches, at days 21, 42 and 70 or final leaf area. The largest increase in number of flowers per plant was observed when plants were inoculated with *Mucilaginibacter* sp. (10.8% compared with the control), while plants inoculated with *Bacillus* sp. had an increase of 9.5% compared with the control. For plants inoculated with *Pseudomonas* sp. flower number did not differ from the control. Total number of nodes per plant was lower for all inoculated plants than the control, however these differences were not statistically significant. The final axillary bud outgrowth rate, calculated based on the number of flowers and nodes according to Equation (3.1), indicated that plants treated with *Bacillus* sp. had a significantly greater axillary bud outgrowth rate at 42 and 70 days after transplanting. Inoculation with *Mucilaginibacter* sp., only caused a significant increase in axillary bud outgrowth at day 70. While plants inoculated with *Pseudomonas* sp. also had a higher bud emergence rate at both the mid-flowering stage and at maturity, neither of these differences were statistically significant when compared with control plants.

Table 3.3 Effects of PGPR treatments on agronomic characteristics of cannabis plants at 21, 42 and 70 days after transplanting.

Each column represents the average of ten plants and standard error (SE).

Traits	Treatment	21 days	42 days	70 days
Height (cm)	Control	26.6 ± 1.13	53.6 ± 1.00	57.9 ± 1.21
	<i>Bacillus</i> sp.	24.6 ± 1.00	52.9 ± 0.53	56.8 ± 0.49
	<i>Mucilaginibacter</i> sp.	25.7 ± 1.41	53.8 ± 0.66	57.9 ± 0.69
	<i>Pseudomonas</i> sp.	25.5 ± 1.13	53.2 ± 0.81	56.5 ± 0.75
Number of nodes	Control	21.2 ± 1.59	62.0 ± 1.14	69.3 ± 2.17
	<i>Bacillus</i> sp.	18.9 ± 1.64	59.2 ± 1.31	66.8 ± 1.91
	<i>Mucilaginibacter</i> sp.	18.9 ± 1.38	60.8 ± 1.58	68.7 ± 1.94
	<i>Pseudomonas</i> sp.	19.4 ± 1.59	59.1 ± 1.62	65.4 ± 0.62
Number of branches	Control	3.1 ± 0.48	13.2 ± 0.39	14.1 ± 0.43
	<i>Bacillus</i> sp.	2.5 ± 0.56	12.4 ± 0.43	13.6 ± 0.43
	<i>Mucilaginibacter</i> sp.	2.3 ± 0.40	13.4 ± 0.40	14.4 ± 0.31
	<i>Pseudomonas</i> sp.	2.6 ± 0.48	12.3 ± 0.33	13.1 ± 0.38
Flower number	Control	-	42.9 ± 1.41	60.6 ± 1.52
	<i>Bacillus</i> sp.	-	44.9 ± 1.29	66.7 ± 1.67**
	<i>Mucilaginibacter</i> sp.	-	45.6 ± 1.34	67.5 ± 1.11**
	<i>Pseudomonas</i> sp.	-	43.6 ± 1.29	61.4 ± 1.76
Axillary bud outgrowth rate (%)	Control	-	69.67 ± 1.84	87.98 ± 2.87
	<i>Bacillus</i> sp.	-	76.03 ± 2.34*	100 ± 1.83**
	<i>Mucilaginibacter</i> sp.	-	75.38 ± 2.75	98.80 ± 2.63**
	<i>Pseudomonas</i> sp.	-	74.13 ± 2.67	93.22 ± 2.72
Leaf area (cm ²)	Control	-	-	1204.72 ± 41.78
	<i>Bacillus</i> sp.	-	-	1208.40 ± 22.46
	<i>Mucilaginibacter</i> sp.	-	-	1243.28 ± 27.48
	<i>Pseudomonas</i> sp.	-	-	1256.18 ± 32.31

* The mean difference is significant at the 0.05 probability level compared with the control.

** The mean difference is significant at the 0.01 probability level compared with the control.

Flower bud yield per plant, was significantly greater than the control for all three bacterial treatments; dry flower yield was significantly increased for plants inoculated with *Mucilaginibacter* sp. and *Pseudomonas* sp., but not for plants inoculated with *Bacillus* sp. (**Table 3.4**). Flower fresh weights were 5.13, 6.94 and 11.45 % higher when treated with *Bacillus* sp., *Mucilaginibacter* sp. and *Pseudomonas* sp., respectively, compared with the control; flower dry weights were 4.87, 7.09 and 11.20 % greater than the control when treated with *Bacillus* sp., *Mucilaginibacter* sp. and *Pseudomonas* sp., respectively. In addition, all inoculation treatments increased total plant aboveground fresh weight, but this difference was only statistically significant for *Mucilaginibacter* sp. and *Pseudomonas* sp. inoculation. Specifically, inoculation with *Bacillus* resulted in a 2.7 % increase, inoculation with *Mucilaginibacter* sp. resulted in a 4.5 % increase, and inoculation with *Pseudomonas* sp. resulted in a 6.6 % increase (**Table 3.4**). The total plant aboveground dry weight increases were 1.96, 4.11, and 5.70 % for *Bacillus* sp., *Mucilaginibacter* sp. and *Pseudomonas* sp., respectively compared with control plants. However, there was no statistically significant difference for leaf and stem fresh or dry weight among PGPR inoculation treatments and the control. Considering the importance of flower biomass, harvest index was calculated following Equation (3.2). There was no statistically significant difference found when comparing the *Bacillus* sp. or *Mucilaginibacter* sp. to the control. In contrast, as was the case for the greatest flower yield enhancement, plants inoculated with *Pseudomonas* sp. significantly increased the harvest index to 0.45, compared with 0.42 for the control (**Table 3.5**). *Pseudomonas* sp. also increased both fresh and dry average weight of single flowers by 9.8 and 9.5%, respectively, however, in this case $0.05 < p < 0.1$.

Table 3.4 The fresh and dry weight of leaves, stems, flowers and total aboveground biomass per cannabis plant as affected by inoculation with single bacterium cell suspensions. Each column represents the average of ten plants and standard error (SE).

Treatment	Leaf biomass		Stem biomass		Flower biomass		Total biomass	
	Fresh weight (g)	Dry weight (g)						
Control	23.69±0.59	9.29±0.18	9.44±0.25	2.68±0.11	44.67±0.52	8.81±0.18	77.79±1.34	20.78±0.37
<i>Bacillus</i> sp.	23.79±0.27	9.32±0.06	9.15±0.22	2.62±0.09	46.96±0.75 *	9.24±0.17	79.89±1.42	21.18±0.29
<i>Mucilaginibacter</i> sp.	24.31±0.39	9.53±0.11	9.24±0.12	2.67±0.07	47.76±0.77 **	9.43±0.17*	81.31±1.42*	21.63±0.27*
<i>Pseudomonas</i> sp.	24.03±0.12	9.42±0.05	9.14±0.12	2.75±0.05	49.78±1.37 **	9.80±0.29 **	82.94±1.50**	21.96±0.35*

* The mean difference is significant at the 0.05 probability level compared with the control.

** The mean difference is significant at the 0.01 probability level compared with the control.

Table 3.5 Effects of PGPR treatments on flower yield characteristics of cannabis plants. Each column represents the average of ten plants (n=10) and standard error (SE).

Traits	Treatment	Mean \pm SE
Harvest Index	Control	0.42 \pm 0.017
	<i>Bacillus</i> sp.	0.44 \pm 0.013
	<i>Mucilaginibacter</i> sp.	0.44 \pm 0.014
	<i>Pseudomonas</i> sp.	0.45 \pm 0.022*
Average flower fresh weight (g)	Control	0.74 \pm 0.033
	<i>Bacillus</i> sp.	0.71 \pm 0.011
	<i>Mucilaginibacter</i> sp.	0.71 \pm 0.016
	<i>Pseudomonas</i> sp.	0.82 \pm 0.019
Average flower dry weight (g)	Control	0.15 \pm 0.007
	<i>Bacillus</i> sp.	0.14 \pm 0.002
	<i>Mucilaginibacter</i> sp.	0.14 \pm 0.004
	<i>Pseudomonas</i> sp.	0.16 \pm 0.003

*The mean difference is significant at the 0.05 probability level compared with the control.

3.5 Discussion

3.5.1 Bacterial inoculation enhances cannabis cutting root development

In cannabis production, vegetative propagation from mother plants with desired traits provides an important mechanism for obtaining high yield and quality and reduces genotype cross-contamination (Frankel and Galun, 2012) and resulting plant-to-plant genetic variability, but it is more costly than growing seedlings (Luna, 2009). Thus, this study examined the hypothesis that inoculation with PGPR, previously verified for other crops (Fan et al., 2020), can be an efficient

and sustainable approach to improving cannabis root development and yield enhancement.

The results of this study indicate that bacterial inoculation contributed to cannabis cutting root development by increasing root length and surface area (**Table 3.2**). Although mechanisms behind these PGPR modifications to cannabis rooting morphology are unknown, PGPR have been shown to regulate gene expression in other plants, leading to increased rooting speed. For instance, *Bacillus altitudinis* (strain FD48) inoculation modified rice (cultivar Co51) root system architecture through regulation of auxin-responsive genes to endogenous (indole-3-acetic acid (IAA)) levels (Ambreetha et al., 2018). Similarly, a recent study from Pace et al. (2020) illustrated that the presence of PGPR influences the rooting stage, and that PGPR inoculation had effects similar to application of synthetic IBA. For the strains used in this study, *Bacillus* sp., *Mucilaginibacter* sp. and *Pseudomonas* sp. produced different levels of IAA, and were shown to increase corn root length (Fan et al., 2018); in addition, the observed increases in root length associated with each strain were significantly correlated with increased N content in corn leaves. In the present study, a positive significant correlation was observed between the final cutting root length and the initial cutting size in the vegetative stage in this study, when plants were treated with the *Bacillus* sp. and the *Pseudomonas* sp. but not the *Mucilaginibacter* sp. (**Supplementary Figure 3.1**). The correlation may not have been significant for the *Mucilaginibacter* sp. because this bacterial strain exhibits a slow growth rate, which may have delayed root colonization. As we described in Section 3.3.1, the *Mucilaginibacter* sp. grows much more slowly in culture, taking three days to achieve the target cell count, compared with the *Bacillus* sp. and the *Pseudomonas* sp., which each took 24 h to achieve the target cell count. Fracchia et al. (2021) found that strains from the genera *Bacteroidota*, *Verrucomicrobiota*, and *Acidobacteriota* can rapidly come to dominate in the roots but show diminishing relative abundances over time, whereas strains from

the genus *Mucilaginibacter* persisted and dominated in roots over time. These findings suggest that the improved rooting speed observed in the presence of PGPR inoculation might also 1) assist in increasing yield, 2) have the potential to shorten the vegetative growth period, therefore shortening the duration of the growth cycle, or 3) reduce the requirements for additional inputs since root morphology is a key variable indicating potential plant nutrient and water uptake capacity (Qin et al., 2006).

3.5.2 PGPR inoculation leads to cannabis yield improvement

The vegetative growth stage duration, which occurs prior to floral induction, is a critical step in optimizing indoor cannabis production (Naim-Feil et al., 2021). Plant growth-promoting rhizobacteria have beneficial effects across the entire life cycle of the plants by accelerating growth rate and shortening the vegetative period (Poupin et al., 2013). These effects are associated with nutrient availability and phytohormone production (Lyu et al., 2020). The results of this study demonstrate that the ability of selected bacteria to promote plant growth and development appears to be present throughout the plant growth cycle following a single inoculation at the time of transplanting. Throughout vegetative and reproductive growth cannabis cuttings inoculated with *Pseudomonas* sp. had improved root development and the greatest yield; the other two bacteria also improved cannabis growth and yield (**Tables 3.3 and 3.4**). Thus, for breeding purposes, these findings suggest that to obtain higher yields, it will be important to evaluate cutting size and rooting speed at the vegetative stage since these traits are directly correlated with final yield.

In addition, PGPR effects on plant morphology in the reproductive growth stage also contribute to final cannabis yield. Previous studies suggested that cannabis vegetative growth ceases three weeks after short day (floral) induction (Chandra et al., 2017). However, in this study, plant height and number of nodes continued to increase until the fifth week after short day

flowering induction. Furthermore, the rate of increase was higher for plants inoculated with PGPR than for control plants. These findings suggested that PGPR inoculation had less effect on plants through the transition into the reproductive stage. In the current study, during the flowering stage, PGPR inoculation was associated with a lower number of nodes at the time of cessation (end of the vegetative stage). Generally, a new branch forms at the axis of a foliage leaf or a bract (Spitzer-Rimon et al., 2019), at the location of flower bud initiation. Usually, the number of flowers is lower than the total number of bracts, because not all initiated axillary buds will develop flowers (Endress, 2010). Therefore, it appears that PGPR inoculation in this study increased the final number of flowers by triggering axillary bud outgrowth and development, as shown in **Table 3.3**, rather than by increasing the number of nodes. The results also showed that application of PGPR enhanced flower yield and final biomass production (the sum of flower, leaf, and stem biomass) although there was no significant difference among treatments for leaf and shoot fresh weights. This finding is consistent with Gryndler et al. (2008) who reported that the application of PGPR (a mixture of 9 strains of *Sinorhizobium* and/or a mixture of 9 strains of *Azotobacter*) to cannabis plants did not increase shoot biomass when compared with the uninoculated control. Final cannabis flower yield is determined by the interactions between physiological traits and plant morphology. Photosynthesis, a physiological process, plays a key role in the determining the rate of cannabis plant growth since it is the primary source of carbon and energy (Chandra et al., 2008). Therefore, higher photosynthetic activity can contribute to increased plant yield (Mia et al., 2010). Moreover, Defez et al. (2019) reported that the IAA produced by *Ensifer meliloti* strain RD64 increased photosynthetic activity and biomass accumulation of *Medicago* (cultivar Legend). The same *Mucilaginibacter* sp. and *Pseudomonas* sp. strains used in this study were previously reported to produce IAA, approximately 0.83 mg L⁻¹ and 0.79 mg L⁻¹, respectively (Fan et al.,

2018). However, in the current study, *Pseudomonas* sp. manifested greater potential to improve cannabis root development and flower yield, which could be associated with other PGPR traits possessed by this strain, namely P-solubilization, siderophore production and nitrogen fixation (Fan et al., 2018). The *Mucilaginibacter* sp. did not possess these PGPR traits (Fan et al., 2018). Since these plant growth promotion traits are commonly reported in a range of PGPR, future research could evaluate plant tissue nutrient content following PGPR application in cannabis, to provide insight into the mechanisms underlying the observed effects on flower yield. In addition, microscopy could be a feasible technique to provide a better understanding of the inoculated PGPR and their interaction with the host plant.

3.6 Conclusions

In the context of cannabis production, PGPR inoculation can be a sustainable and inexpensive (economic) practice to enhance plant growth. There is need for knowledge in this area because the illegal status of cannabis has resulted in a substantial knowledge gap regarding cultivation techniques. In this study, the results clearly indicated that the selected PGPR can improve cannabis growth by enhancing the rate of cannabis cutting rooting in the early vegetative stage; by stimulating axillary bud emergence, by increasing the number of flower buds, and by contributing to flower biomass accumulation and harvest index. Among the three rhizobacteria evaluated in this study, the PGPR strain with the highest potential to promote cannabis growth and yield (*Pseudomonas* sp.), also led to the greatest change in physiological variables, particularly photosynthetic rate. This study provides strong evidence for a clear relationship between plant morphological and physiological variables, and yield of cannabis, all of which are affected by inoculation with beneficial microbes at the vegetative growth stage. Future studies could examine

how inoculation of cannabis cuttings with one of the three PGPR, impacts cannabis secondary metabolite accumulation, mainly cannabinoid and terpene profiles.

3.7 References

- Aizpurua-Olaizola, O., Soydaner, U., Öztürk, E., Schibano, D., Simsir, Y., Navarro, P., Etxebarria, N., and Usobiaga, A. (2016). Evolution of the cannabinoid and terpene content during the growth of *Cannabis sativa* plants from different chemotypes. *Journal of Natural Products* **79**, 324-331.
- Ambreetha, S., Chinnadurai, C., Marimuthu, P., and Balachandar, D. (2018). Plant-associated *Bacillus* modulates the expression of auxin-responsive genes of rice and modifies the root architecture. *Rhizosphere* **5**, 57-66.
- Backer, R., Rokem, J. S., Ilangumaran, G., Lamont, J., Praslickova, D., Ricci, E., Subramanian, S., and Smith, D. L. (2018). Plant growth-promoting rhizobacteria: context, mechanisms of action, and roadmap to commercialization of biostimulants for sustainable agriculture. *Frontiers in Plant Science* **9**.
- Backer, R. G., Rosenbaum, P., McCarty, V., Eichhorn Bilodeau, S., Lyu, D., Ahmed, M. B., Robinson, W. G., Lefsrud, M., Wilkins, O., and Smith, D. L. (2019). Closing the yield gap for cannabis: a meta-analysis of factors determining cannabis yield. *Frontiers in Plant Science* **10**, 495.
- Caplan, D., Dixon, M., and Youbin, Z. (2017). Optimal Rate of Organic Fertilizer during the Vegetative-stage for Cannabis Grown in Two Coir-based Substrates. *HortScience* **52**, 1307-1312.
- Caulkins, J. P., Coulson, C. C., Farber, C., and Vesely, J. V. (2012). Marijuana legalization: Certainty, impossibility, both, or neither? *Journal of Drug Policy Analysis* **5**, 1-27.

- Chandra, S., Lata, H., ElSohly, M. A., Walker, L. A., and Potter, D. (2017). Cannabis cultivation: methodological issues for obtaining medical-grade product. *Epilepsy & Behavior* **70**, 302-312.
- Chandra, S., Lata, H., Khan, I. A., and Elsohly, M. A. (2008). Photosynthetic response of *Cannabis sativa* L. to variations in photosynthetic photon flux densities, temperature and CO₂ conditions. *Physiology and Molecular Biology of Plants* **14**, 299-306.
- Conant, R., Walsh, R., Walsh, M., Bell, C., and Wallenstein, M. (2017). Effects of a microbial biostimulant, Mammoth PTM, on *cannabis sativa* bud yield. *Journal of Horticulture* **4**, 2376-0354.1000191.
- Danziger, N., and Bernstein, N. (2021). Light matters: effect of light spectra on cannabinoid profile and plant development of medical cannabis (*Cannabis sativa* L.). *Industrial Crops and Products* **164**, 113351.
- Defez, R., Andreozzi, A., Romano, S., Pocsfalvi, G., Fiume, I., Esposito, R., Angelini, C., and Bianco, C. (2019). Bacterial IAA-delivery into medicago root nodules triggers a balanced stimulation of C and N metabolism leading to a biomass increase. *Microorganisms* **7**, 403.
- Deng, G., Du, G., Yang, Y., Bao, Y., and Liu, F. (2019). Planting density and fertilization evidently influence the fiber yield of hemp (*Cannabis sativa* L.). *Agronomy* **9**, 368.
- Endress, P. K. (2010). Disentangling confusions in inflorescence morphology: patterns and diversity of reproductive shoot ramification in angiosperms. *Journal of Systematics and Evolution* **48**, 225-239.
- Fan, D., Schwinghamer, T., and Smith, D. L. (2018). Isolation and diversity of culturable rhizobacteria associated with economically important crops and uncultivated plants in Québec, Canada. *Systematic Applied Microbiology* **41**, 629-640.

- Fan, D., Subramanian, S., and Smith, D. L. (2020). Plant endophytes promote growth and alleviate salt stress in *Arabidopsis thaliana*. *Scientific Reports* **10**, 1-18.
- Fan, X., Zhang, S., Mo, X., Li, Y., Fu, Y., and Liu, Z. (2017). Effects of plant growth-promoting rhizobacteria and n source on plant growth and N and P uptake by tomato grown on calcareous soils. *Pedosphere* **27**, 1027-1036.
- Fine, P. G., and Rosenfeld, M. J. (2013). The endocannabinoid system, cannabinoids, and pain. *Rambam Maimonides Medical Journal* **4**.
- Fracchia, F., Mangeot-Peter, L., Jacquot, L., Martin, F., Veneault-Fourrey, C., and Deveau, A. (2021). Colonization of naive roots from *populus tremula* × *alba* involves successive waves of fungi and bacteria with different trophic abilities. *Applied and Environmental Microbiology* **87**, e02541-20.
- Frankel, R., and Galun, E. (2012). "Pollination mechanisms, reproduction and plant breeding," Springer Science & Business Media.
- Global Cannabis Market by Application (Medical, Recreational), Product Type (Flowers, Concentrates), Compound (THC-dominant, CBD-dominant, Balanced THC & CBD), and Region (North America, South America, Europe, RoW) - Forecast to 2026," Research and Markets
- Gryndler, M., Sudová, R., Püschel, D., Rydlová, J., Janoušková, M., and Vosátka, M. (2008). Cultivation of high-biomass crops on coal mine spoil banks: can microbial inoculation compensate for high doses of organic matter? *Bioresource Technology* **99**, 6391-6399.
- Hawley, D. (2018). The influence of spectral quality of light on plant secondary metabolism and photosynthetic acclimation to light quality. (Doctoral dissertation, University of Guelph).

- Kerckhoffs, L., O'Neill, S., Barge, R., and Kawana-Brown, E. (2017). Plant density effects on yield parameters of three industrial hemp cultivars in the Manawatu. *Agronomy New Zealand* **47**, 47-54.
- Luna, T. (2009). Vegetative propagation. *Nursery manual for native plants: A guide for tribal nurseries*, 1, 153-175.
- Lyu, D., Backer, R., and Smith, D. L. (2020). "Chapter 8: Plant growth-promoting rhizobacteria (PGPR) as plant biostimulants in agriculture." in *Biostimulants for sustainable crop production* by Burleigh Dodds Science Publishing.
- Lyu, D., Backer, R. G., Robinson, W. G., and Smith, D. L. (2019). Plant-growth promoting rhizobacteria for cannabis production: Yield, cannabinoid profile and disease resistance. *Frontiers in Microbiology* **10**, 1761.
- Magagnini, G., Grassi, G., and Kotiranta, S. (2018). The effect of light spectrum on the morphology and cannabinoid content of *Cannabis sativa* L. *Medical Cannabis and Cannabinoids* **1**, 19-27.
- Mia, M. B., Shamsuddin, Z., Wahab, Z., and Marziah, M. (2010). Rhizobacteria as bioenhancer and biofertilizer for growth and yield of banana (*Musa* spp. cv. 'Berangan'). *Scientia Horticulturae* **126**, 80-87.
- Moher, M., Jones, M., and Zheng, Y. (2021). Photoperiodic response of in vitro *cannabis sativa* plants. *HortScience* **56**, 108-113.
- Naim-Feil, E., Pembleton, L. W., Spooner, L. E., Malthouse, A. L., Miner, A., Quinn, M., Polotnianka, R. M., Baillie, R. C., Spangenberg, G. C., and Cogan, N. O. (2021). The characterization of key physiological traits of medicinal cannabis (*Cannabis sativa* L.) as a tool for precision breeding. *BMC Plant Biology* **21**, 1-15.

- Pace, L., Pellegrini, M., Palmieri, S., Rocchi, R., Lippa, L., and Del Gallo, M. (2020). Plant growth-promoting rhizobacteria for in vitro and ex vitro performance enhancement of Apennines' Genepì (*Artemisia umbelliformis* subsp. *eriantha*), an endangered phytotherapeutic plant. *In Vitro Cellular & Developmental Biology-Plant* **56**, 134-142.
- Pacula, R. L., and Smart, R. (2017). Medical marijuana and marijuana legalization. *Journal of Annual Review of Clinical Psychology* **13**, 397-419.
- Pagnani, G., Pellegrini, M., Galieni, A., D'Egidio, S., Matteucci, F., Ricci, A., Stagnari, F., Sergi, M., Sterzo, C. L., and Pisante, M. (2018). Plant growth-promoting rhizobacteria (PGPR) in *Cannabis sativa* 'Finola' cultivation: An alternative fertilization strategy to improve plant growth and quality characteristics. *Industrial Crops and Products* **123**, 75-83.
- Poupin, M. J., Timmermann, T., Vega, A., Zuñiga, A., and González, B. (2013). Effects of the plant growth-promoting bacterium *Burkholderia phytofirmans* PsJN throughout the life cycle of *Arabidopsis thaliana*. *PLoS One* **8**, e69435.
- Qin, R., Stamp, P., and Richner, W. (2006). Impact of tillage on maize rooting in a Cambisol and Luvisol in Switzerland. *Soil and Tillage Research* **85**, 50-61.
- Ren, G., Zhang, X., Li, Y., Ridout, K., Serrano-Serrano, M. L., Yang, Y., Liu, A., Ravikanth, G., Nawaz, M. A., and Mumtaz, A. S. (2021). Large-scale whole-genome resequencing unravels the domestication history of *Cannabis sativa*. *Science Advances* **7**, eabg2286.
- Ricci, E. C. (2015). Investigating the role of *Pseudomonas* sp. and *Bacillus* sp. biofilms as plant growth promoting inoculants, Doctoral dissertation, McGill University, Montreal Quebec, Canada.

- Rodriguez-Morrison, V., Llewellyn, D., and Zheng, Y. (2021). Cannabis yield, potency, and leaf photosynthesis respond differently to increasing light levels in an indoor environment. *Frontiers in Plant Science* **12**, 456.
- Shah, A., Nazari, M., Antar, M., Msimbira, L., Naamala, J., Lyu, D., Rabileh, M., Zajonc, J., and Smith, D. (2021). PGPR in Agriculture: A sustainable approach to increasing climate change resilience. *Frontiers in Sustainable Food Systems*.
- Smith, D. L., Subramanian, S., Lamont, J. R., and Bywater-Ekegård, M. (2015). Signaling in the phytomicrobiome: breadth and potential. *Frontiers in Plant Science* **6**, 709.
- Spitzer-Rimon, B., Duchin, S., Bernstein, N., and Kamenetsky, R. (2019). Architecture and florogenesis in female *Cannabis sativa* plants. *Frontiers in Plant Science* **10**, 350.
- Thomas, R., and Hay, M. (2009). Axillary bud outgrowth potential is determined by parent apical bud activity. *Journal of Experimental Botany* **60**, 4275-4285.
- Tipparat, P., Natakankitkul, S., Chamnivikaipong, P., and Chutiwat, S. (2012). Characteristics of cannabinoids composition of Cannabis plants grown in Northern Thailand and its forensic application. *Forensic Science International* **215**, 164-170.
- Tourangeau, W. (2015). Re-defining environmental harms: Green criminology and the state of Canada's hemp industry. *Canadian Journal of Criminology and Criminal Justice* **57**, 528-554.
- Van Der Werf, H. (1997). The effect of plant density on light interception in hemp (*Cannabis sativa* L.). In "The 2nd Int. Bioresources Hemp Symp., Frankfurt am Main, BRD, 1997. Bioresource Hemp 97, Proc. of the Symp. 97, Nova-Institute, Hörth, BRD", pp. 225-235.

- Vanhove, W., Surmont, T., Van, D. P., and De, R. B. (2012). Yield and turnover of illicit indoor cannabis (*Cannabis* spp.) plantations in Belgium. *Forensic Science International* **220**, 265-270.
- Vanhove, W., Van Damme, P., and Meert, N. (2011). Factors determining yield and quality of illicit indoor cannabis (*Cannabis* spp.) production. *Forensic Science International* **212**, 158-163.
- Wei, X., Zhao, X., Long, S., Xiao, Q., Guo, Y., Qiu, C., Qiu, H., and Wang, Y. (2021). Wavelengths of LED light affect the growth and cannabidiol content in *Cannabis sativa* L. *Industrial Crops and Products* **165**, 113433.
- Zarei, A., Behdarvandi, B., Dinani, E. T., and Maccarone, J. (2021). *Cannabis sativa* L. photoautotrophic micropropagation: A powerful tool for industrial scale in vitro propagation. *In Vitro Cellular & Developmental Biology-Plant*, 1-10.

Connecting text

In Chapter 3, cells from pellets (result of cell centrifugation from liquid medium) of three individual pure PGPR were inoculated onto cannabis cuttings and were shown increase rooting speed of cannabis cuttings, subsequent root length, final flower yield, and to cause greater numbers of axillary buds, harvest index and photosynthetic rates. These effects varied among PGPR strains. In cannabis production, key secondary metabolite accumulation is as important as the total biomass and flower yield. In Chapter 4, a subset of cannabis secondary metabolites (cannabinoids and terpenes) was identified and quantified to reveal the response mechanisms, in terms of secondary metabolite production, elicited in cannabis flowers by PGPR treatment.

Chapter 4 Evaluation of PGPR on Cannabinoids and Terpenes Accumulation in Inflorescences of *Cannabis sativa* L.

Authors: Dongmei Lyu ^a, Rachel Backer ^a, Eric Ruan ^b, Donald L. Smith ^a

Affiliations:

^a Department of Plant Science, McGill University, Sainte-Anne-de-Bellevue, Quebec, Canada,
H9X3V9

^b Trace Organic, Air & Gas Analysis Lab, InnoTech Alberta, Vegreville, Alberta, Canada, T9C
1T4

4.1 Abstract

Research regarding secondary metabolites in cannabis is required for the crop's effective medicinal/pharmaceutical use. There are few reports regarding the influence of plant growth-promoting rhizobacteria (PGPR) on cannabis secondary metabolites, despite PGPR being a sustainable approach that has been used with a wide range of other crop species. The effects of inoculation with each of three novel PGPR strains (*Bacillus* sp., *Mucilaginibacter* sp. and *Pseudomonas* sp.) on secondary metabolite profiles was investigated. The levels of 16 cannabinoids and 21 terpenes were determined using ultra high-performance liquid chromatography with an ultraviolet detector (UHPLC-UV), a liquid chromatograph coupled with a tandem mass spectrometer (LC-MS/MS) and gas chromatography-mass spectrometry (GC-MS). *Mucilaginibacter* sp. showed the biggest effects on secondary metabolite accumulation among three PGPR; it caused a 14% increase in tetrahydrocannabinol (THC), cannabidiol (CBD) and 12% in terpenes. *Pseudomonas* sp. was less efficacious resulting in 6% increases in THC, CBD and terpenes, while no secondary metabolite-related benefit was derived from inoculation with

Bacillus sp. Three PGPR inoculation also did not change the CBD/THC ratio. Our results reveal and expand upon the potential of beneficial soil microbes for stimulating the biosynthesis of secondary metabolites in medical cannabis plants.

4.2 Introduction

Cannabis has been used for medicinal purposes for millennia (Backer et al., 2020; Chouvy, 2019; Ren et al., 2021). The pharmaceutical effects are mainly due to the presence of a set of secondary metabolites in cannabis plants. There are more than 500 known secondary metabolites in cannabis plants, including at least 113 cannabinoids and 120 terpenes, with highly variable compositions among cannabis genotypes (Brousseau et al., 2021; ElSohly et al., 2017; Gonçalves et al., 2019). Cannabinoids are the most well-known of the secondary metabolites in cannabis plants (Atakan, 2012). At present, only a few cannabinoids are commonly considered in research investigations, including cannabidiol (CBD), cannabichromene (CBC), Δ^9 -tetrahydrocannabinol (Δ^9 -THC), and cannabigerol (CBG), and their respective acidic forms (CBDA, CBCA, THCA and CBGA, respectively), as these are generally major cannabinoid constituents. Terpenes are another major secondary metabolite class present in the Cannabaceae family; like the cannabinoids, they are largely found in the glandular trichomes (Booth et al., 2017). Terpenes impart unique flavor and aroma qualities to cannabis and are used in some commercial cannabis products as a result (Booth et al., 2017; Lange and Turner, 2013). Terpenes are reasonably well understood as aroma-related compounds in hops and are well-studied in that crop because of the value to the brewing industry (Almaguer et al., 2014; Sharpe and Laws, 1981). Terpenes also show some therapeutic effects of anxiety and depression (Aizpurua-Olaizola et al., 2016; Jin et al., 2020; Yang et al., 2020).

The biochemical and pharmacological properties of cannabinoids and terpenes drive a substantial amount of research focused on expanded exploitation of this plant. As research showed, both the 2-C-methyl-D-erythritol 4-phosphate/1-deoxy-D-xylulose 5-phosphate (MEP/DOXP) and cytosolic mevalonate (MEV) pathways are involved in terpene biosynthesis through production of the general 5-carbon isoprenoid diphosphate precursors prior to synthesis of terpenes (Booth et al., 2017). Monoterpenes and sesquiterpenes are synthesized in different plant cells, however, their biosynthesis share the same precursors - isopentenyl diphosphate (IPP) and dimethylallyl diphosphate (DMAPP); it seems that IPP and DMAPP are interchangeable between the two cell types (Booth et al., 2017). Major cannabinoid biosynthesis is well studied and was described in **Chapter 2**. When exposed to UV or heat, these cannabinoids can also be decarboxylated or oxidized to cannabinolic acid (CBNA), cannabinol (CBN), and cannabicyclol (CBL) (Borille et al., 2017; Ferrer, 2020). In addition, cannabigerovarinic acid (CBGVA) has been confirmed as the precursor of tetrahydrocannabivarinic acid (THCVA), cannabichromevarinic acid (CBDVA), and cannabichromevarinic acid (CBCVA) after CBGA was identified as the precursor of THCA, CBDA and CBCA (Shoyama et al., 1977; Taura et al., 1996). Instead of being synthesized from OLA and GPP, the biosynthesis of CBGVA is from GPP and divarinolic acid. In this complicated biosynthesis process, GPP plays an important role in the biosynthesis of cannabinoids and controls the substrate pools available for terpene synthases (Fellermeier et al., 2001; Gagne et al., 2012). These secondary metabolite biosynthesis pathways of cannabis plants are shown in **Figure 4.1**.

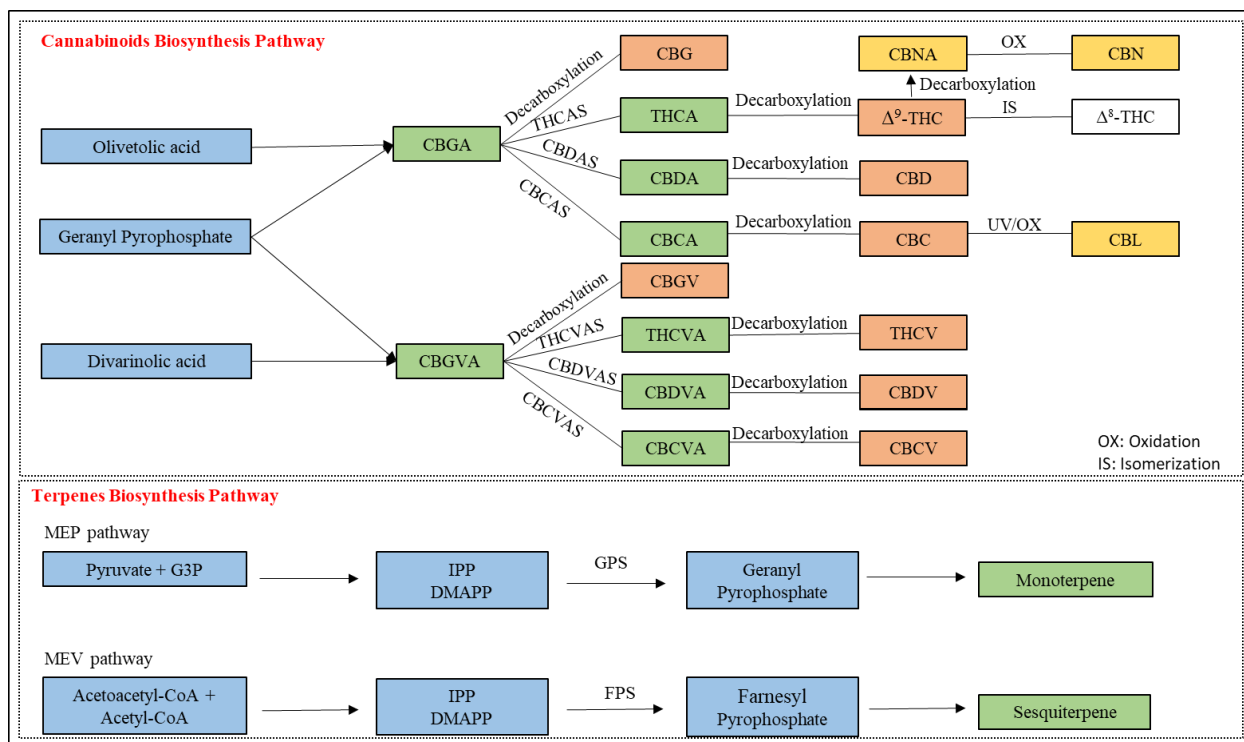


Figure 4.1 Main cannabinoids and terpenes biosynthesis pathway in cannabis flower

Cannabigerolic acid: **CBGA**; Cannabidiolic acid: **CBDA**, Tetrahydrocannabinolic acid: **THCA**; Cannabichromenic acid: **CBCA**; Cannabigerol: **CBG**, Cannabidiol: **CBD**, Δ-9-tetrahydrocannabinol: **d9-THC**, Δ-8-tetrahydrocannabinol: **d8-THC**, Cannabichromene: **CBC**, Cannabinolic acid: **CBNA**; Cannabinol: **CBN**, Cannabicyclol: **CBL**; Cannabigerovarinic acid: **CBGVA**; Cannabidivarinic acid: **CBDVA**; Tetrahydrocannabivarinic acid: **THCVa**; Cannabichromevarinic acid: **CBCVa**; Cannabidivarin: **CBDV**; Tetrahydrocannabivarin: **THCV**; Cannabigerovarin: **CBGV**. Cannabidiolic acid synthase: **CBDAS**; Tetrahydrocannabinolic Acid Synthase: **THCAS**; Cannabichromenic acid Synthase: **CBCAS**; Cannabidivarinic acid synthase: **CBDVAS**; Tetrahydrocannabivarinic acid synthase: **THCVAS**; Cannabichromevarinic acid synthase: **CBCVAS**.

The biosynthesis of secondary metabolites is affected by genetic, environmental, and developmental factors (Fischedick et al., 2010; Hazekamp, 2007; Hillig and Mahlberg, 2004; Ross and ElSohly, 1996). There are some key aspects influencing the concentration of cannabinoids and terpenes, including temperature, water and nutrient availability, light quality and intensity, and photoperiod (Bernstein et al., 2019; Brousseau et al., 2021; Danziger and Bernstein, 2021; Magagnini et al., 2018; Rodriguez-Morrison et al., 2021; Saloner and Bernstein, 2021; Tipparat et al., 2012; Wei et al., 2021). Although there is a shortage of information regarding the effects of PGPR inoculation on the accumulation of cannabinoids and terpenes in cannabis plants, secondary metabolite biosynthesis has been shown to respond to microbial inoculation in other plant species (Braga et al., 2016; Kim et al., 2011; Mishra et al., 2018; Vacheron et al., 2013). In addition, our previous study determined the positive effects of PGPR on cannabis flower yield. This work was focused on the effects of inoculation with specific PGPR on secondary metabolite biosynthesis, altering cannabinoid and terpene biosynthesis in cannabis. This study evaluated the effects of *Bacillus* sp., *Mucilaginibacter* sp. and *Pseudomonas* sp. on the accumulation of cannabinoids and terpenes of cannabis genotype CBD Kush through mass spectrometry. HPLC-UV has been an important technology in quantifying and identifying the metabolites in cannabis plants; however, detecting some of the minor compounds remains a challenge (Berthold et al., 2020; McRae and Melanson, 2020). LC-MS/MS was also used in this study to improve detection and identification of lower abundance cannabinoids. Therefore, a total of 16 cannabinoid compounds were identified and quantified using both UHPLC-UV and LC-MS/MS in the current study. The volatile compounds (terpenes) were analyzed using GC-MS.

4.3 Materials and methods

4.3.1 Plant materials

The flowers from plants treated with *Bacillus mobilis* (KJ812449), *Pseudomonas koreensis* (AF468452), and *Mucilaginibacter lappiensis* (jgi.1095764) (based on the 16S rDNA sequence), and control (MgSO₄) were collected from the same research experiment described in **Chapter 3** (Lyu et al., 2022). After ten weeks (at day 70 after transplanting) under the conditions shown in **Table 3.1 (Chapter 3)**, all flowers, both in the top inflorescence and branches, were manually harvested from the plant. Each treatment with 5 replicates and whole experiment was repeated twice (n=10). All flowers were dried using a lyophilizer (SNL216V freezing-dryer, Thermo Savant Co. Ltd. USA). Dried flower samples were ground using mortar and pestle, then were preserved in a -20 °C freezer until further analysis.

The effect of PGPR on *Cannabis sativa* L. (cv. CBD Kush) plant compositional development was determined by measuring the main secondary metabolite profile: 16 cannabinoid (CBGA, THCA, CBDA, CBCA, Δ^9 -THC, CBD, CBC, CBG, CBNA, CBN, Δ^8 -THC, CBL, THCVA, CBDVA, THCV, CBDV) and 21 terpene compounds (alpha-pinene, camphene, beta-pinene, myrcene, 3-carene, alpha-terpinene, 4-isopropyltoluene, d-limonene, ocimene, gamma-terpinene, alpha-terpinolene, linalool, (-)-isopulegol, terpineol, geraniol, (-)-trans-caryophyllene, alpha-humulene, cis-nerolidol, trans-nerolidol, (-)-guaaiol, (-)-alpha-bisabolol) of flower samples.

4.3.2 Cannabinoid and terpene analysis

4.3.2.1 Chemical materials and reagents

Commercially available standards (purity > 98%) for CBGA, THCA, CBDA, CBCA, Δ^9 -THC, CBD, CBC, CBG, CBNA, CBN, Δ^8 -THC, CBL, THCVA, CBDVA, THCV, CBDV were obtained from Cerilliant (Round Rock, Texas, USA). Alpha-pinene, camphene, beta-pinene,

myrcene, 3-carene, alpha-terpinene, 4-isopropyltoluene, d-limonene, 3,7-dimethyl-1,3,6-octatriene, gamma-terpinene, alpha-terpinolene, linalool, isopulegol, geraniol, trans-caryophyllene, alpha-humulene, cis-nerolidol, trans-nerolidol, guaiol, bisabolol, naphthalene (internal standard (ISD)) were obtained from LGC Group (North Charleston, South Carolina, USA). LC-MS grade water, methanol, formic acid, acetonitrile, acetic acid, and hexane were sourced from Fisher Scientific (Fair Lawn, NJ, USA).

4.3.2.2 Cannabinoid analysis

4.3.2.2.1 Sample extraction

For each sample, about 200 mg of the ground cannabis flowers were placed in a 50 mL centrifuge tube with a ceramic homogenizer to create a homogenous mixture. Then 20 mL methanol was added into the tube and shaken in a SPEX Geno/Grinder for 5 min operating at a rate of 1500 strokes min^{-1} . Subsequently 1 mL of extraction solution was added into each 1.5 mL Eppendorf tube and centrifuged (10,000 g, 5 min) (Thermo-Scientific, Waltham, Massachusetts, USA). The supernatant was serially diluted using methanol to an appropriate final sample concentration and then was transferred into a 2 mL screw-top HPLC vial for analysis by UHPLC-UV and LC-MS/MS. Details of the dilutions and other aspects of the applied method can be found in **Table 4.1**.

Table 4.1 Target cannabinoids detection method and retention time, and linear curve

Method	Compound	Dilution factor	Retention time	Linear curve	R ²
Ultra-High-Performance Liquid Chromatography with ultraviolet detector (UHPLC-UV)	CBDA	20	3.5	Y=40222.73X	0.999
	CBGA	NA	3.8	Y=42709.70X	0.999
	CBG	NA	4.1	Y=35071.04X	0.999
	CBD	NA	4.3	Y=34526.59X	0.999
	THCV	NA	4.6	Y=34924.53X	0.999
	CBN	NA	7.1	Y=61281.92X	0.999
	Δ^9 -THC	NA	9.3	Y=35377.11X	0.999
	Δ^8 -THC	NA	9.7	Y=28550.24X	0.999
	CBC	NA	12.3	Y=46724.26X	0.999
	THCA	20	12.8	Y=38498.64X	0.999
Liquid Chromatograph coupled with tandem mass spectrometer (LC-MS/MS)	CBDV	20	3.7	Y=13760X-238.77	0.996
	CBDVA	20	4.3	Y=5464.54X+99.28	0.999
	CBL	20	9.6	33244.7X-212.69	0.998
	THCVA	20	10.0	Y=26906.6X-187.04	0.997
	CBNA	20	13.2	Y=202121X+3781.07	0.998
	CBCA	100	14.4	Y=32750x+165.99	0.997

Cannabigerolic acid (CBGA), cannabidiolic acid (CBDA), tetrahydrocannabinolic acid (THCA), cannabichromenic acid (CBCA), cannabigerol (CBG), cannabidiol (CBD), Δ^9 -tetrahydrocannabinol (Δ^9 -THC), Δ^8 -tetrahydrocannabinol (Δ^8 -THC), cannabichromene (CBC),

cannabinolic acid (CBNA), cannabinol (CBN), cannabicyclol (CBL), cannabigerovarinic acid (CBGVA), cannabidivarinic acid (CBDVA), tetrahydrocannabivarinic acid (THCVA), cannabichromevarinic acid (CBCVA), cannabidivarin (CBDV), tetrahydrocannabivarin (THCV), cannabigerovarin (CBGV).

4.3.2.2.2 UHPLC-UV

An Agilent 1290 Infinity Ultra High-Performance Liquid Chromatography (UHPLC) system equipped with an ultraviolet DAD detector was used for identification and quantification of 10 compounds at a wavelength of 220 nm. Considering the abundance of each cannabinoid, the extract was analyzed at its original concentration and at a 20 × dilution. Five µL samples were injected into a C18 reverse phase column (2.1 × 150 nm, 1.8 Micron, Agilent Technologies, Santa Clara, USA) heated to 30 °C. The mobile phase consisted of an isocratic flow of 30% water + 0.1% formic acid (A) and 70% acetonitrile + 0.1% formic acid (B) for 15 min. A standard cannabinoid mixture (containing the 10 compounds) was injected into the column under the above-described conditions at the beginning, and end of sample runs for the calculation and standardization of retention time. Linear five-point calibration curves from 1 to 100 µL mL⁻¹ were generated for each targeted compound. The chromatographic data processing was performed using Agilent offline software. Chromatograph details and calibration curves with co-efficient (R²), are shown in **Figure 4.2** and **Table 4.1**.

4.3.2.2.3 LC-MS/MS

The quantification of minor cannabinoids was conducted using a liquid chromatograph coupled with a tandem mass spectrometer (LC-MS/MS) (Waters Quattro micro, MA, US). The analytes were separated on a Cosmosil 2.5C18-MS- II column, 3.0 mm × 100 mm (Nacalai, Japan). The mobile phase was composed of water containing 0.1% acetic acid (solvent A) and methanol

containing 0.1% acetic acid (solvent B) at a flow rate of 0.5 mL min⁻¹. Separation was achieved using the following gradient sequence: 0-10 min, 75-85% B; 10-14 min, 85-95% B. The column temperature was 25°C, the autosampler temperature was maintained at 10°C and the injection volume was 20 µL. MS/MS was conducted with an electrospray ionization (ESI) unit used in negative ion mode for detection of CBDVA, THCVA and CBNA and CBCA and in positive ion mode for CBDV, and CBL, with multiple reaction monitoring (MRM) for quantitative analysis. A standard cannabinoid mixture was injected into the column with optimized-parameter standard curves under the above-mentioned conditions. Linear six-point calibration curves from 0.1 to 2 µg mL⁻¹ were generated for quantifying each target compound. Data processing was performed using QuanLynx (Waters Quattro micro, MA, US).

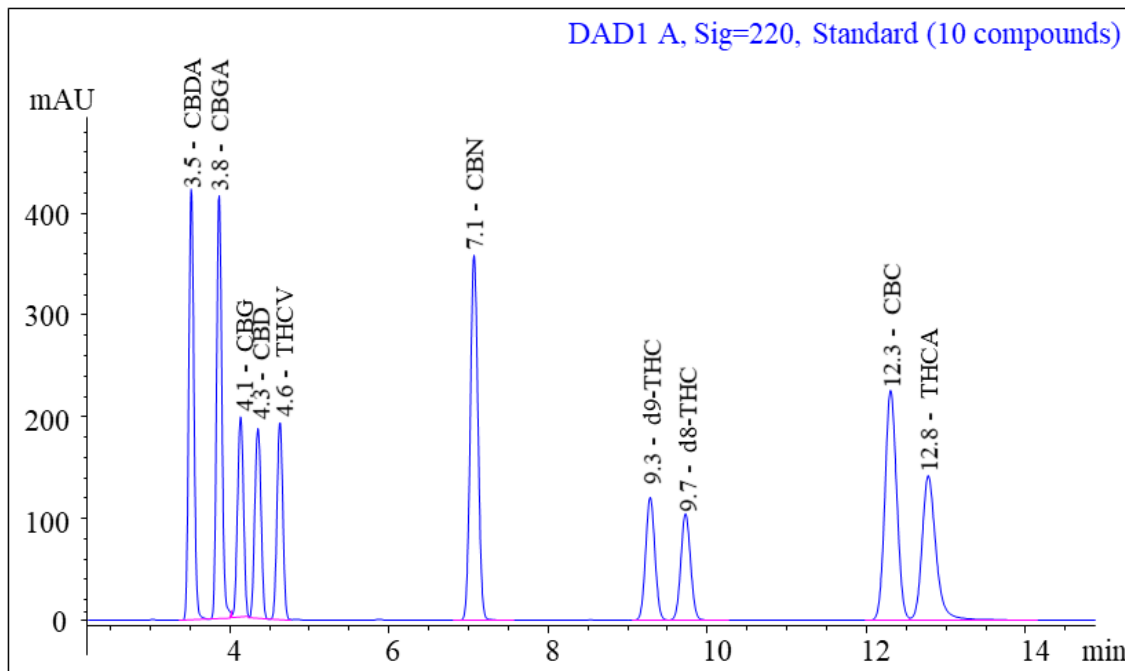


Figure 4.2 Typical chromatograph of 10 compounds by Ultra High-Performance Liquid Chromatography with UV detection at 220 nm

Cannabigerolic acid (CBGA), cannabidiolic acid (CBDA), tetrahydrocannabinolic acid (THCA), cannabigerol (CBG), cannabidiol (CBD), Δ^9 -tetrahydrocannabinol (Δ^9 -THC), Δ^8 -

tetrahydrocannabinol (Δ^8 -THC), cannabichromene (CBC), cannabinol (CBN), tetrahydrocannabivarin (THCV).

4.3.2.3 Terpene analysis

4.3.2.3.1 Sample extraction

Homogenized dried flower material (200 mg) was transferred into a 50 mL centrifuge tube, then 20 mL hexane were added, and the resulting material was shaken for 1 min. The tube was then placed in an ultrasonic bath for 10 min followed by 10-second of vortexing. Next, samples were centrifuged at 3750 g for 5 min. Finally, twenty μ L of supernatant were transferred into an autosampler vial with the associated insert and 180 μ L of hexane was added for terpene analysis.

4.3.2.3.2 GC-MS

A total of 21 terpenes were quantitatively analyzed by using gas chromatography-mass spectrometry (GC-MS) (Agilent Technologies CA, USA), where the instrument was equipped with an HP-5MS column (30 m x 0.25 mm x 0.25 μ m). The injection volume of samples was 1 μ L for GC-MS analysis, after sample extraction. The initial oven temperature was 40 °C for 2 min, followed by a ramp up of 3.5 °C min⁻¹ to 155 °C and then 30 °C min⁻¹ up to 300 °C. The injector temperature was 250 °C and the detector temperature was 280 °C. Helium was used as a carrier gas in the splitless mode.

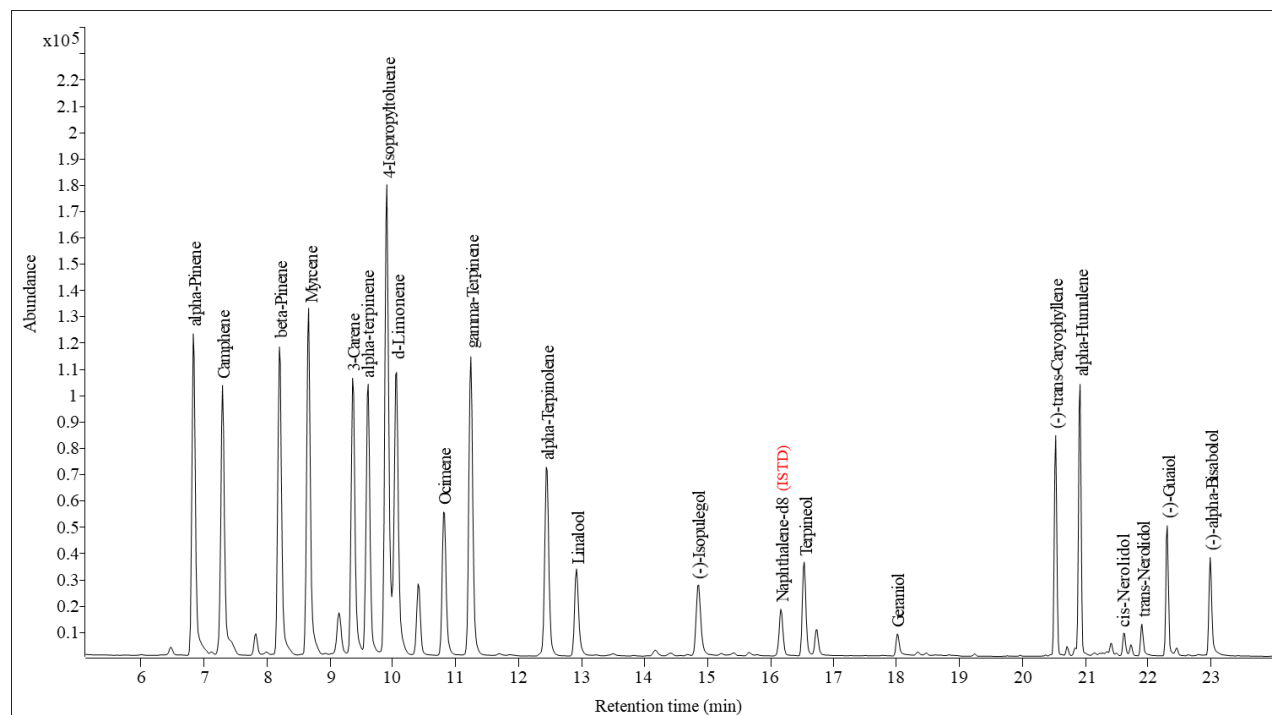


Figure 4.3 Typical chromatograph of the 21 terpenes measured by Gas Chromatography-Mass Spectrometry

The MS data was acquired with a quadrupole mass detector with electron ionization at 70 eV in the range of 41–161 m/z. Identification of the compounds was determined through retention time and mass-to-charge ratio (m/z) with authentic standards. A mixture of standards that included all the target compounds and internal standards was injected into the column with optimized parameters to generate standard curves with a linear range from 0.05 to 5 $\mu\text{g mL}^{-1}$, with a seven-point calibration for each target compound. Chromatographic data processing was performed using MassHunter Workstation Software (Version B.07.01). A typical chromatograph of the 21 terpene compounds of interest is shown in **Figure 4.3** and the calibration linear curve, with co-efficient of correlation (R^2), is shown in **Table 4.2**.

Table 4.2 The retention time and linear calibration parameters for quantification of target terpenes

Type	Name	Retention time (min)	Linear curve	R ²
Monoterpene	Alpha-Pinene	6.83	Y=72.20X-1307.91	0.99
	Camphene	7.30	Y=50.75X-527.83	0.99
	Beta-Pinene	8.20	Y=70.97X-2729.19	0.99
	Myrcene	8.65	Y=52.79X-5355.23	0.99
	3-Carene	9.36	Y=61.01X-2367.10	0.99
	Alpha-Terpinene	9.61	Y=46.09X-6026.32	0.99
	4-Isopropyltoluene	9.90	Y=197.36X+1128.80	0.99
	d-Limonene	10.05	Y=56.55X-3103.77	0.99
	Ocimene	10.80	Y=34.26X-5643.69	0.99
	Gamma-Terpinene	11.24	Y=65.27X-7850.57	0.99
	Alpha-Terpinolene	12.40	Y=35.66X-4783.19	0.99
	Linalool	12.90	Y=17.63X+241.93	0.99
	(-)-Isopulegol	14.80	Y=7.90X-823.51	0.98
	Terpineol	16.53	Y=14.03X-3085.89	0.99
	Geraniol	18.00	Y=5.57X-164.46	0.99

	(-)-trans-Caryophyllene	20.53	Y=25.46X-3746.62	0.99
	Alpha-humulene	20.91	Y=66.83-9250.01	0.99
Sesquiterpene	Cis-Nerolidol	21.60	Y=8.04X-788.24	0.99
	Trans-Nerolidol	21.90	Y=11.79X-3052.48	0.99
	(-)-Guaiol	22.29	Y=16.07X-2024.22	0.98
	(-)-alpha-Bisabolol	23.00	Y=8.92X-543.86	0.98

4.3.3 Data analysis

The chemical structure of all targeted cannabinoids can be found in **Supplementary Figure 4.1**. Total individual cannabinoid concentrations per gram of dry flower (mg g^{-1}) were determined as neutral equivalents as follows:

$$C_{total} = C_{neutral} + C_{acid} \times \left(\frac{MW_{neutral}}{MW_{acid}} \right) \quad (4.1)$$

All measured cannabinoids were illustrated as sum of all cannabinoids per gram of dry flower weight (DFW mg g^{-1}) (**Equation 4.2**) and per plant (mg) (**Equation 4.3**) which were calculated as follows:

$$C_{sum} = C_{neutral} + C_{acid} \quad (4.2)$$

$$CT_{sum} = C_{sum} \times M_{dry\ flower} \quad (4.3)$$

where C_{total} is the concentration of total cannabinoids (neutral cannabinoid equivalent) in the cannabis sample, in mg g^{-1} ; $C_{neutral}$ is the concentration of neutral cannabinoids in the cannabis sample in mg g^{-1} ; C_{acid} is the concentration of acidic cannabinoids in the cannabis sample in mg g^{-1} ; $MW_{neutral}$ is the molecular weight of the neutral cannabinoids; MW_{acid} is the molecular weight of the acidic cannabinoids. C_{sum} is the sum of all measured cannabinoids including neutral and acid

form per gram of dry flower (mg g^{-1}). CT_{sum} is total cannabinoids amount per plant in mg, which also refers to the total dry flower mass ($M_{\text{dry flower}}$) from our previous study in Chapter 3 (Lyu et al., 2022).

The chemical structure of all targeted terpenes can be found in **Supplementary Figure 4.2**. The classification of terpenes was based on the number of carbons, including monoterpene (C10) sesquiterpene (C15), diterpene (C20), sesterpene (C25), triterpene (C30), and tetraterpene (C40) (Ashour et al., 2010). In the current study, total monoterpenes were the sum of the 15 monoterpenes, and total sesquiterpenes were calculated as the sum of the 6 sesquiterpenes. Total terpenes (T_{sum}) per gram of flower (mg g^{-1}) was the sum of total mono- and sesquiterpenes; and total terpenes per plant (TT_{sum}) was calculated as follows:

$$T_{\text{sum}} = T_{\text{monoterpenes}} + T_{\text{sesquiterpenes}} \quad (4.4)$$

$$TT_{\text{sum}} = T_{\text{sum}} \times M_{\text{dry flower}} \quad (4.5)$$

The statistical analysis of cannabinoid and terpene concentration data was performed using SPSS (IBM SPSS Statistics for Citrix, Version 24.0. Armonk, NY: IBM Corp.). Listed data are expressed as the mean ($n=10$) \pm standard error (SE). One-Way Analysis of Variance (ANOVA) was used to test the difference comparison between treatment and control with a probability less than 0.05 indicating significant difference. Pearson correlations were calculated between individual cannabinoids and terpenes to investigate the relation of all targeted cannabis plant metabolites. Principal component analysis (PCA) was used to check within metabolite groups and between PGPR treatment (cluster) variations.

4.4 Results

4.4.1 Cannabinoid accumulation in cannabis flowers

4.4.1.1 Abundance

The targeted cannabinoid profile was obtained from 40 plant samples (4 treatments \times 10 replications). **Figure 4.4** shows the relative abundance of all targeted cannabinoid compounds in cultivar CBD Kush. It can be concluded that the most abundant cannabinoid compound is CBDA, which is about 56% of all measured cannabinoids, followed by THCA which made up 36.5% of the total cannabinoids measured. CBCA is a cannabinoid synthesized from the same precursor as THCA and CBDA, which constitutes about 2.5% of the total cannabinoids measured. As described in Section 4.2, the first cannabinoid precursor-CBGA, accounted for approximately 2.9% of the total cannabinoids measured. CBDA, THCA, CBCA and CBGA can be decarboxylated to neutral forms which are present in cannabis plants in small amounts. In the current study, the neutral CBG, Δ^9 -THC, CBD and CBC are from the decarboxylation of CBGA, CBDA, THCA, and CBCA respectively, and constituted only about 0.13, 0.65, 0.75 and 0.04%, respectively, of the total cannabinoids measured.

The minor cannabinoids, CBN, CBNA and CBL, were also quantified in this study. They are either decarboxylated or oxidized from neutral cannabinoids through oxidation or under UV. As **Figure 4.1** indicates, CBNA, which is decarboxylated from THC, can also be oxidized to CBN. Both CBNA and CBN were detected at low concentrations, of about 0.04 and 0.02%, respectively, of the total cannabinoids measured. Δ^8 -THC as the isomer of Δ^9 -THC, constituted about 0.20% of total measured cannabinoids. CBDVA and THCVA accounted for 0.15 and 0.2% of total cannabinoids measured, respectively, and were derived from CBGVA. In this study, CBL, THCV,

and CBDV were not detected, which indicates that CBC, THCVA, CBDVA were not measurably degraded.

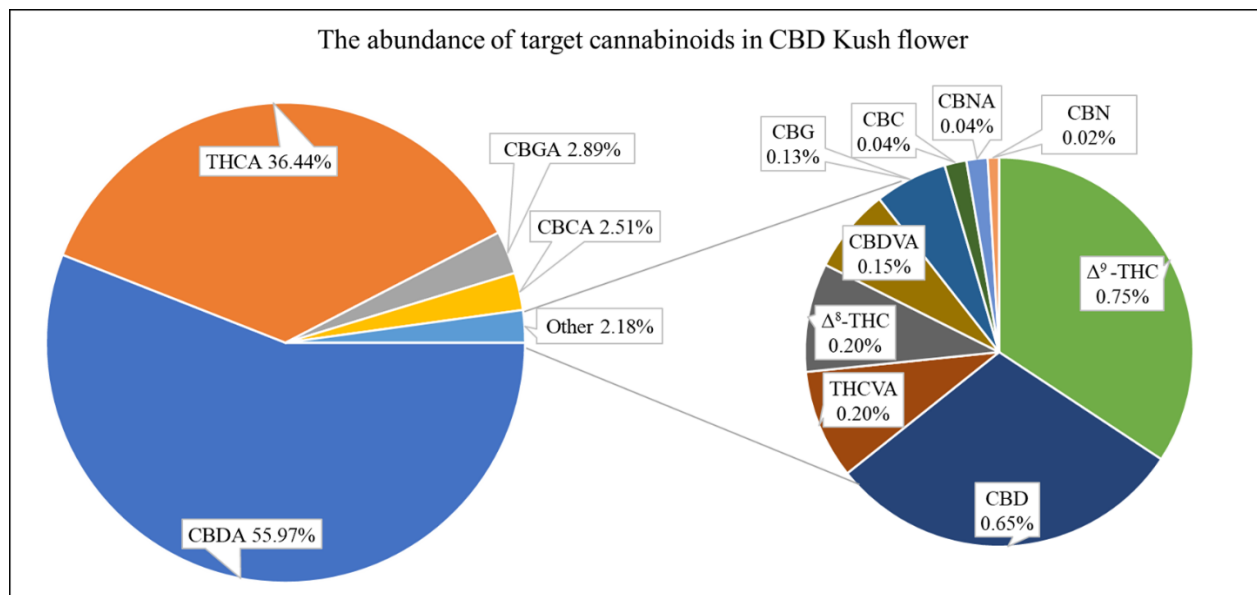


Figure 4.4 The abundance of targeted cannabinoids in CBD Kush flowers averaged across all treatments and replications (total 40 plants)

On the left side are the main key cannabinoid acidic forms (cannabigerolic acid (CBGA), cannabidiolic acid (CBDA), tetrahydrocannabinolic acid (THCA), cannabichromenic acid (CBCA)), and the sum of rest of cannabinoids (cannabigerol (CBG), cannabidiol (CBD), Δ⁹-tetrahydrocannabinol (Δ⁹-THC), Δ⁸-tetrahydrocannabinol (Δ⁸-THC), cannabichromene (CBC), cannabinolic acid (CBNA), cannabinol (CBN), cannabicyclol (CBL), cannabidivarin (CBDV), tetrahydrocannabivarin (THCV), cannabigerovarin (CBGV)), which is individually shown on the pie chart of right side.

4.4.1.2 Cannabinoid accumulation responds to PGPR inoculation

4.4.1.2.1 Major cannabinoids

The accumulation of the major cannabinoids, i.e., neutral THC, CBD, CBC, CBG and their acidic forms THCA, CBDA, CBCA, CBGA in chemotype CBD Kush were affected by PGPR

inoculation (**Figure 4.5**). The totals of THC, CBD, CBC and CBG were calculated following Equation (4.1) and are shown in **Table 4.3**. Several conclusions can be drawn from **Figure 4.5 and Table 4.3**. First, inoculation with *Mucilaginibacter* or *Pseudomonas* sp. caused increases in major acidic cannabinoid concentrations, while inoculation with *Bacillus* sp. did not affect major cannabinoid concentrations. Inoculation with *Mucilaginibacter* sp. led to the greatest increase of major cannabinoid concentrations, including a statistically significant ($p < 0.05$) 14% increase in total THC and CBD, and a 13% increase in total CBC that was not statistically significant ($p = 0.089$), as compared with the control. The second most efficient PGPR for improving cannabinoid concentrations was *Pseudomonas* sp.; application of *Pseudomonas* sp. led to a 6% increase in total THC and CBD but did not affect total CBC accumulation. The *Bacillus* sp. had little effect on the total THC or CBD but decreased CBC levels, although this decreased level was not significantly different from the control treatment level. Interestingly, whether inoculation with a PGPR led to an increase or decrease in the main cannabinoids, the ratio of CBD/THC was consistent across treatments (**Table 4.3**).

In addition, CBGA is one of the first cannabinoids biosynthesized in cannabis plants; it can be converted into THCA, CBDA, and CBCA depending on the specific synthase enzyme involved, and can also be decarboxylated to CBG. In the present study, none of the three PGPR evaluated stimulated CBGA accumulation or total CBG except *Mucilaginibacter* sp. (**Table 4.3**). The neutral CBG in cannabis treated with *Mucilaginibacter* sp. was about 11.5% higher than the control (**Figure 4.5**).

Table 4.3 Accumulation of total main cannabinoids and CBD/THC ratio.

The concentration of cannabinoids is reported as mg g⁻¹ DFW, data are means (n=10) ± standard error (SE). Asterisks indicate statistical significance of numerical differences between PGPR inoculation and control treatment determined (***p* < 0.01 or **p* < 0.05). Cannabigerol (CBG), cannabidiol (CBD), tetrahydrocannabinol (THC), cannabichromene (CBC).

Treatment	Total THC	Total CBD	Total CBC	Total CBG	CBD/THC
Control	61.98±1.03	93.50±1.87	4.49±0.27	5.41±0.26	1.51±0.016
<i>Bacillus</i> sp.	61.59±1.48	92.31±2.25	3.95±0.20	5.20±0.15	1.50±0.009
<i>Mucilaginibacter</i> sp.	70.99±3.64**	106.71±6.42*	5.07±0.39	5.47±0.20	1.50±0.013
<i>Pseudomonas</i> sp.	65.59±0.51**	99.20±1.27*	4.36±0.14	5.00±0.15	1.51±0.022

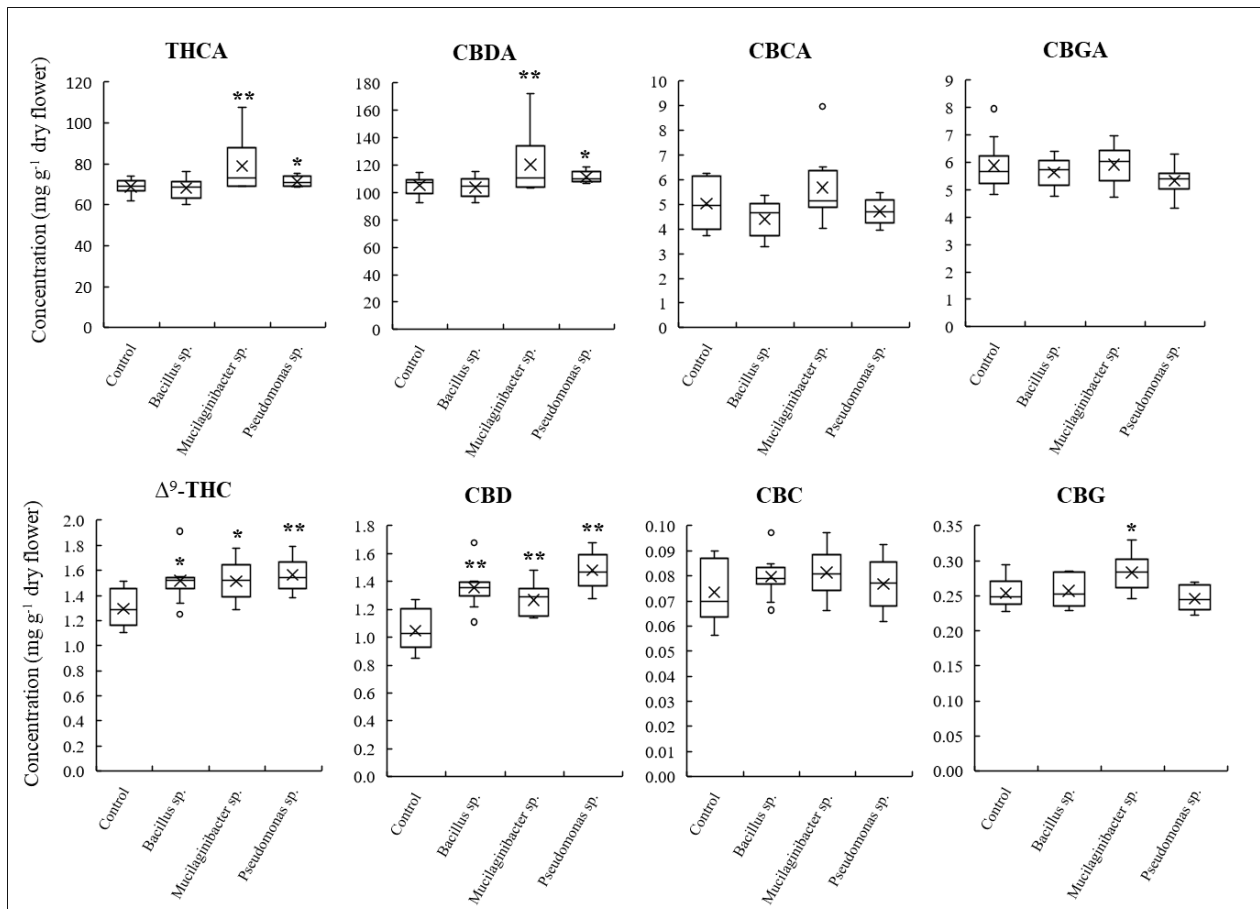


Figure 4.5 Box and whisker plots of the concentrations of the 4 neutral (cannabigerol (CBG), cannabidiol (CBD), tetrahydrocannabinol (THC), cannabichromene (CBC)) and the four acidic cannabinoids (cannabigerolic acid (CBGA), cannabidiolic acid (CBDA), tetrahydrocannabinolic acid (THCA), cannabichromenic acid (CBCA)) in flowers of CBD **Kush**. The cannabis samples were grouped as treated by the control and three bacterial inoculants. The concentration of cannabinoids was reported as mg g⁻¹ DFW. Median and average values are depicted with a horizontal black line and a cross, respectively. Asterisks indicate significant differences between PGPR inoculations and the control treatment (** $p < 0.01$ or * $p < 0.05$).

4.4.1.2.2 Minor cannabinoids

The accumulation of minor cannabinoids Δ^8 -THC, CBN and CBNA, derived from THCA, with and without PGPR treatment are shown in the **Table 4.4**. There were no meaningful differences among treatments for the three cannabinoids. Inoculation with *Mucilaginibacter* sp. and *Pseudomonas* sp. both caused numerical increases in accumulation of CBDVA and THCVA in CBD Kush flower (**Table 4.4**).

Table 4.4 The concentration of minor cannabinoids. Concentration of cannabinoids was reported as mg g⁻¹ DFW, data are means (n=10) \pm SE. Δ^8 -tetrahydrocannabinol (Δ^8 -THC), cannabinol (CBN), cannabichromene (CBC), cannabinolic acid (CBNA), cannabidivarinic acid (CBDVA), tetrahydrocannabivarinic acid (THCVA).

Treatment	Δ^8 -THC	CBN	CBNA	CBDVA	THCVA
Control	0.39 \pm 0.01	0.04 \pm 0.001	0.08 \pm 0.02	0.30 \pm 0.02	0.35 \pm 0.03
<i>Bacillus</i> sp.	0.39 \pm 0.008	0.04 \pm 0.001	0.06 \pm 0.02	0.27 \pm 0.04	0.39 \pm 0.04
<i>Mucilaginibacter</i> sp.	0.40 \pm 0.008	0.04 \pm 0.001	0.08 \pm 0.02	0.35 \pm 0.04	0.43 \pm 0.03
<i>Pseudomonas</i> sp.	0.38 \pm 0.005	0.04 \pm 0.0007	0.08 \pm 0.01	0.37 \pm 0.04	0.43 \pm 0.04

4.4.1.2.3 Total cannabinoid accumulation

The total amount of cannabinoids per gram of dry flower weight (DFW) and per plant were calculated following Equations (4.2) and (4.3) and are shown in **Figure 4.6**. Compared with non-PGPR inoculation (control), there was a significant increase in total cannabinoid contents (C_{sum}) associated with *Mucilaginibacter* sp. ($p < 0.01$) and *Pseudomonas* sp. ($p < 0.05$) inoculations. Specifically, plants treated with *Mucilaginibacter* sp. had 13.8% more total cannabinoids than the control, while they were increased 5.4% by inoculation with *Pseudomonas* sp. On a per plant basis, the total cannabinoids of plants (CT_{sum}) inoculated with *Mucilaginibacter* sp. or

Pseudomonas sp. were greater than the control treatment. Plants treated with *Mucilaginibacter* sp. had 20% CT_{sum} higher than the control. *Pseudomonas* sp. caused a 16.8% increase in CT_{sum} compared to the control. Although *Bacillus* sp. did not affect cannabinoid accumulation per gram of flower, inoculation with this PGPR resulted in an increase in final cannabinoids per plant of about 3.1%.

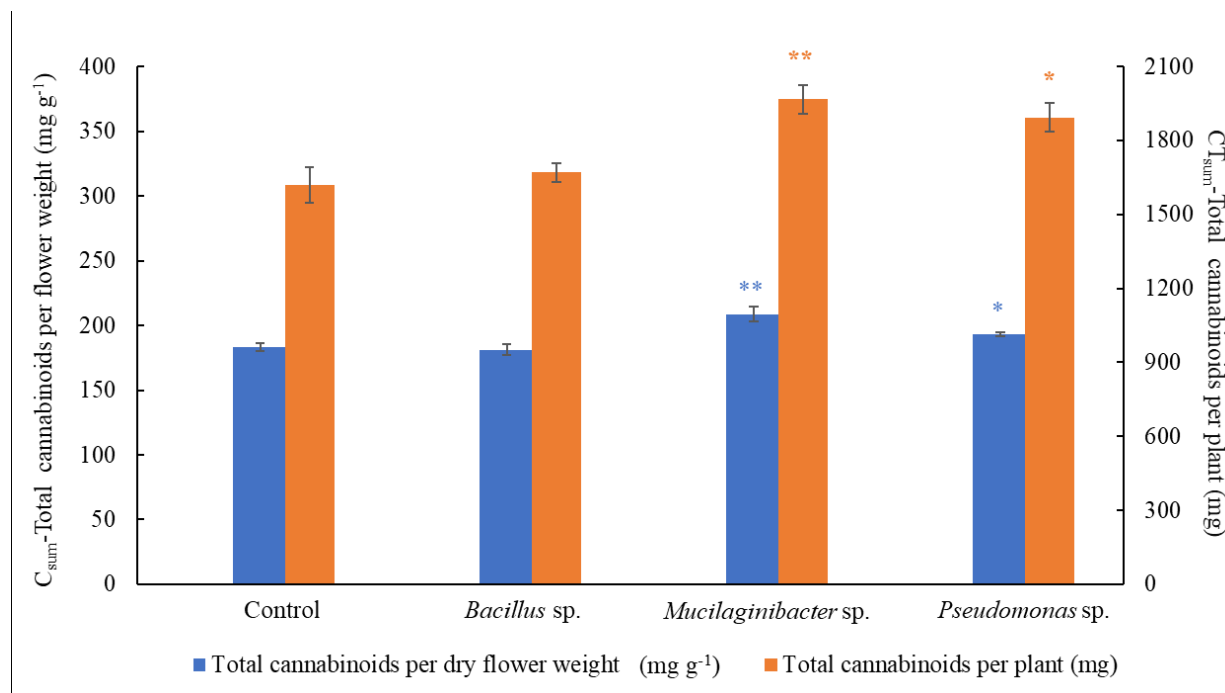


Figure 4.6 Total measured amount of 16 cannabinoids per gram of dry flower (C_{sum} , $mg\ g^{-1}$, blue) and per plant (CT_{sum} , mg, orange) treated with either of the three PGPR.

Asterisks indicate significant differences between PGPR inoculations and the control treatment (** $p < 0.01$ or * $p < 0.05$).

4.4.2 Terpene accumulation in cannabis flowers

4.4.2.1.1 Monoterpenes

In the current study, 15 monoterpenes were identified and quantified. **Table 4.5** shows the content of each monoterpene when plants were treated with one of the three PGPR treatments or with a mock/control inoculation treatment. Alpha-pinene was the most abundant monoterpene in

CBD Kush flowers, followed by myrcene, beta-pinene and d-limonene. Of all the treatments, the enhancement of monoterpenes caused by *Mucilaginibacter* sp. was confined to beta-pinene, linalool and terpineol which were 11, 27 and 23%, respectively, greater than the control.

4.4.2.1.2 Sesquiterpenes

Six sesquiterpenes were analyzed in this study. Caryophyllene, guaiol and trans-nerolidol were the dominant sesquiterpenes, all with contents above 1 mg g⁻¹ DFW. Both *Mucilaginibacter* sp. and *Pseudomonas* sp. showed positive effects on the accumulation of sesquiterpenes. *Mucilaginibacter* sp. significantly increased levels of all six sesquiterpenes. Inoculation with *Pseudomonas* sp. resulted in 63 and 81% increases in cis-nerolidol and trans-nerolidol, respectively, compared with the control treatment. Surprisingly, treating with *Bacillus* sp. also caused increases in levels of both cis- and trans-nerolidol, which is the only terpene positively associated with the application of *Bacillus* sp. Overall, the amount of total sesquiterpenes in plants inoculated with *Mucilaginibacter* sp. ($p < 0.01$) and *Pseudomonas* sp. ($p < 0.01$) were 32.8 and 30.8% significantly higher than control plants (**Figure 4.7**).

Table 4.5 Content of monoterpene (mg g⁻¹ DFW) accumulated in CBD Kush flowers of plants treated with one of the three PGPR. Asterisks indicate significant differences between PGPR inoculation and mock treatment (** $p < 0.01$ or * $p < 0.05$).

	Control	<i>Bacillus sp.</i>	<i>Mucilaginibacter sp.</i>	<i>Pseudomonas sp.</i>
alpha-Pinene	5.51±0.15	4.88±0.13	5.92±0.23	5.47±0.21
Camphene	0.25±0.007	0.23±0.004	0.27±0.009	0.25±0.005
beta-Pinene	2.55±0.07	2.24±0.06	2.82±0.11*	2.58±0.11
Myrcene	4.55±0.12	3.68±0.14	4.69±0.20	4.66±0.23
3-Carene	0.10±0.002	0.10±0.001	0.11±0.002	0.11±0.001
alpha-Terpinene	0.16±0.001	0.15±0.0007	0.16±0.001	0.16±0.0006
4-Isopropyltoluene	0.10±0.003	0.10±0.002	0.10±0.003	0.11±0.008
d-Limonene	2.58±0.06	2.15±0.07	2.66±0.11	2.64±0.11
Ocimene	0.40±0.008	0.35±0.007	0.41±0.01	0.39±0.01
gamma-Terpinene	0.15±0.001	0.15±0.0008	0.15±0.001	0.15±0.001
alpha-Terpinolene	0.20±0.002	0.19±0.002	0.20±0.003	0.20±0.003
Linalool	0.42±0.03	0.31±0.02	0.54±0.03*	0.47±0.06
(-)-Isopulegol	0.22±0.01	0.21±0.006	0.25±0.01	0.24±0.01
Terpineol	1.49±0.05	1.29±0.03	1.84±0.05**	1.57±0.08
Geraniol	0.18±0.007	0.16±0.02	0.19±0.008	0.18±0.01
Total monoterpenes	18.87±0.49	16.18±0.45	20.30±0.75	19.16±1.31

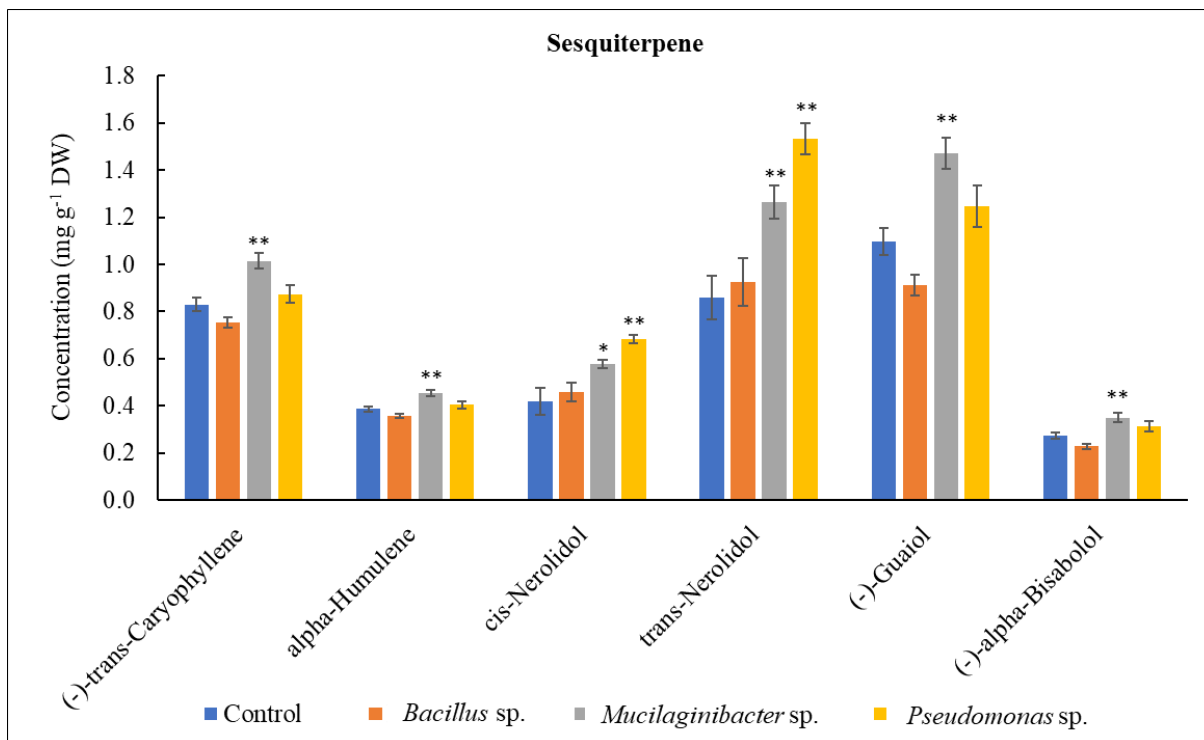


Figure 4.7 Content of sesquiterpene accumulated in CBD Kush flowers treated with each of the PGPR. Asterisks indicate significant differences between PGPR inoculated and the control treatment (** $p < 0.01$ or * $p < 0.05$).

4.4.2.1.3 Total terpene accumulation

Figure 4.8 shows the abundance of 21 terpenes, including monoterpenes and sesquiterpenes, in the flowers of CBD Kush plants treated one of the PGPR. Overall, the most abundant terpene among those measured was alpha-pinene, followed by myrcene, in all treatments. In contrast, the least abundant terpenes were 3-carene and 4-isopropyltoluene, which are monoterpenes. In addition, cannabis plant inoculation with PGPR did change the amount of terpene compounds but did not alter the order of abundance for all measured compounds.

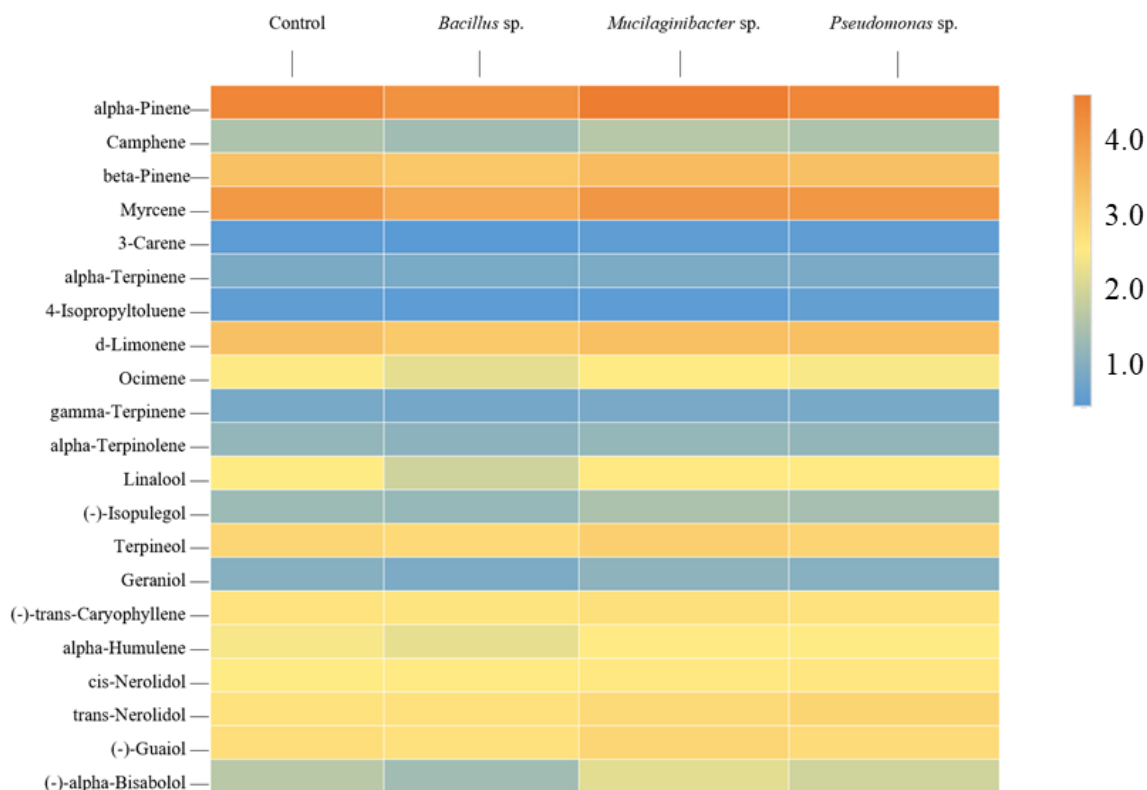


Figure 4.8 The abundance of all 21 measured terpene compounds in CBD Kush treated with PGPR (mg g^{-1} DFW)

The total terpene contents per gram of flower (T_{sum}) were calculated by adding the concentrations (mg g^{-1}) of the 15 monoterpenes and the six sesquiterpenes (Equation 4.4). The same pattern was found for total terpene level as was observed for cannabinoid levels in flowers. Among the three PGPR inoculations, only *Mucilaginibacter* sp. inoculation led to a significant ($p < 0.05$) increase in terpene contents, which was about 11.9% higher than the control (**Figure 4.9**). *Pseudomonas* sp. inoculation led to a 6.5% increment of total terpene per flower weight, but this was not significantly greater than the control (**Figure 4.9**). Considering the whole plant, the total terpene level per plant (TT_{sum}) was calculated based on Equation (4.5). A significant increase in total terpene per plant was associated with *Mucilaginibacter* sp. inoculation, which resulted in a 15.2% enhancement. Surprisingly, there was no influence of *Pseudomonas* sp. inoculation on total

terpene level per flower weight. However, **Figure 4.9** showed the biggest contribution on the total terpene per plant was caused by *Pseudomonas* sp. inoculation, which was 22.3% higher than control.

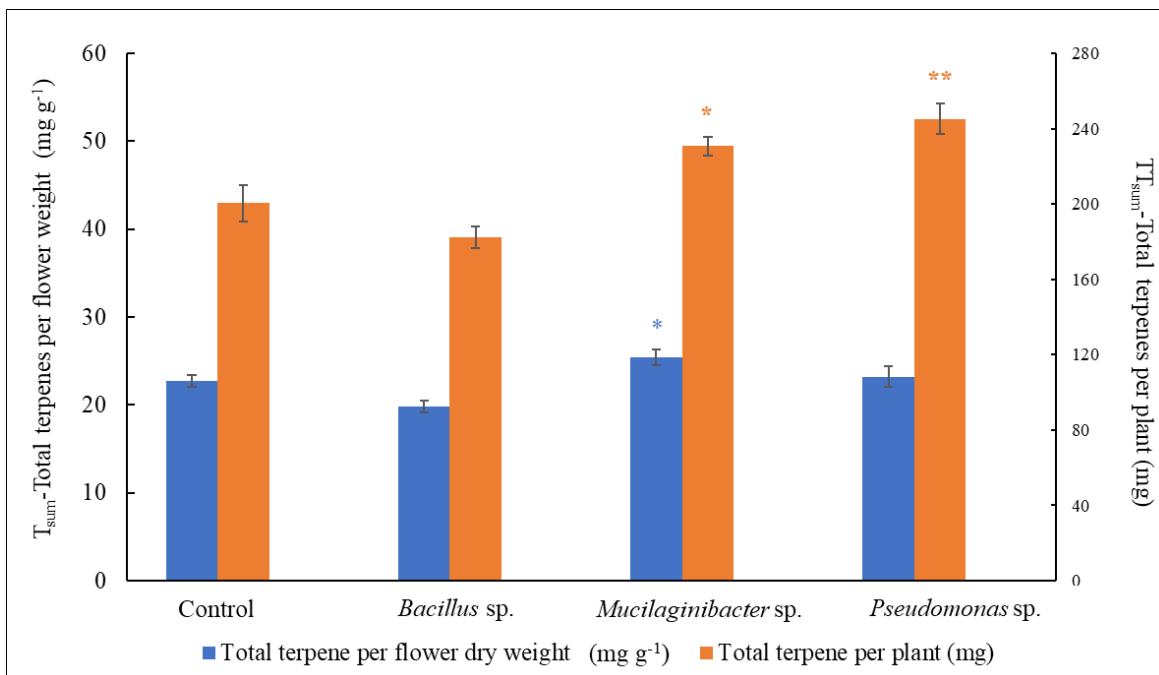


Figure 4.9 The total suite of 21 targeted terpene compounds per gram of dry flower (T_{sum} , mg g⁻¹, blue) and per plant (TT_{sum} , mg, orange) treated with each of the three PGPR.

Asterisks indicate significant differences between PGPR inoculation effects, and the control treatment (** $p < 0.01$ or * $p < 0.05$).

4.4.3 Correlation analysis among secondary metabolites

Correlations between all targeted cannabinoids and terpenes are plotted in **Figure 4.10**. Calculations were performed on quantifiable targeted compounds using the measured concentrations. THCA and CBDA were positively correlated with all cannabinoids, which are also the only cannabinoid compounds strongly correlated with the 21 terpenes. THCA and CBDA were also very strongly ($r = 0.97$) correlated with each other, so compounds that were correlated with THCA were all correlated with CBDA. CBGA was negatively correlated with Δ^9 -THC ($r = -0.16$),

CBD ($r = -0.23$), but moderately positively correlated with CBG ($r = 0.52$) which was accumulated in the plant by decarboxylation of CBGA. Unsurprisingly, CBNA, a natural derivative of Δ^9 -THC, was negatively correlated with Δ^8 -THC (isomers of Δ^9 -THC) and CBN (produced by decarboxylation of CBNA). In the case of terpenes, all targeted terpenes were positively correlated with each other, whereas only 4-Isopropyltoluene was negatively correlated with cis-nerolidol ($r = -0.15$), and trans-nerolidol ($r = -0.04$) and geraniol ($r = -0.30$).

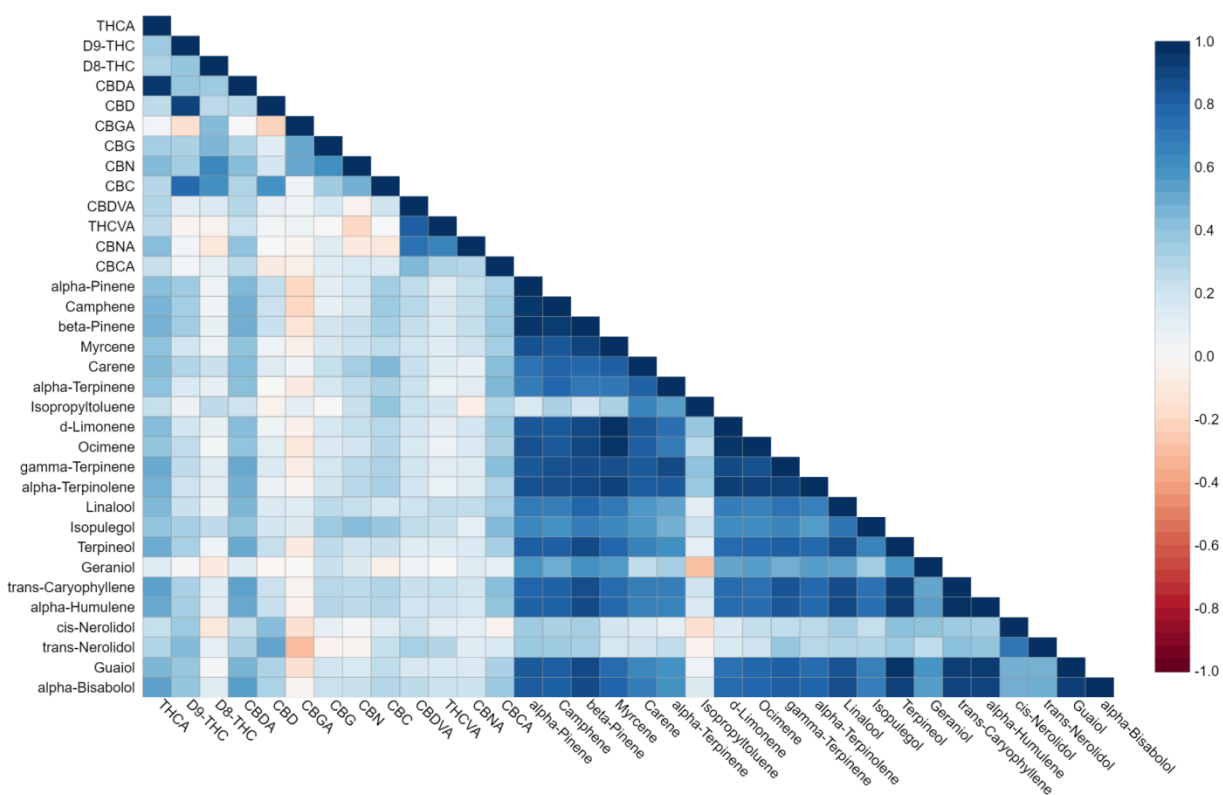


Figure 4.10 Correlation matrix of all analyzed secondary metabolites (13 cannabinoids and 21 terpenes) in cannabis flowers ($r =$ correlation coefficient). Cannabigerolic acid (CBGA), cannabidiolic acid (CBDA), tetrahydrocannabinolic acid (THCA), cannabichromenic acid (CBCA), cannabigerol (CBG), cannabidiol (CBD), Δ^9 -tetrahydrocannabinol (Δ^9 -THC), Δ^8 -tetrahydrocannabinol (Δ^8 -THC), cannabichromene (CBC), cannabinolic acid (CBNA), cannabinol

(CBN), cannabicyclol (CBL), cannabidivarin (CBDV), tetrahydrocannabivarin (THCV), cannabigerovarin (CBGV).

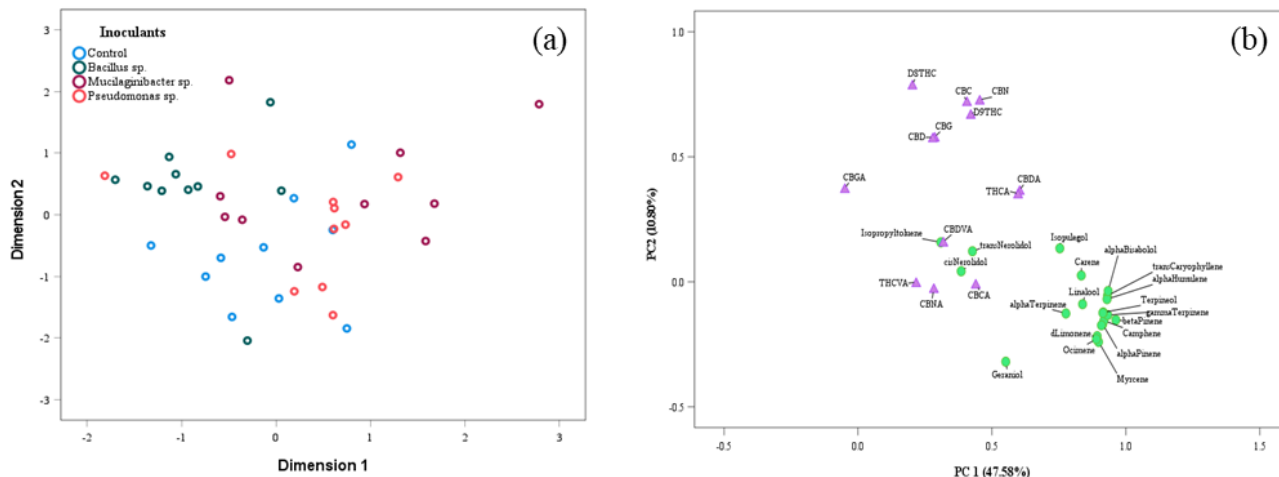


Figure 4.11 Scatterplot and Component Plot (PC1 vs PC2) obtained via Principal Component Analysis (PCA) according to the concentrations of all analyzed compounds of cannabis flowers across the four treatments. For scatterplot analysis, color coding with four treatments was as follows: in component plot, the 3 cannabinoids are colored purple and the 21 terpenes are colored green; the scatterplot color coding is indicated on the graph. Cannabigerolic acid (CBGA), cannabidiolic acid (CBDA), tetrahydrocannabinolic acid (THCA), cannabichromenic acid (CBCA), cannabigerol (CBG), cannabidiol (CBD), Δ 9-tetrahydrocannabinol (Δ 9-THC), Δ 8-tetrahydrocannabinol (Δ 8-THC), cannabichromene (CBC), cannabinolic acid (CBNA), cannabinol (CBN), cannabicyclol (CBL), cannabidivarin (CBDV), tetrahydrocannabivarin (THCV), cannabigerovarin (CBGV).

Principal component analysis (PCA, **Figure 4.11**) demonstrated the relationships among 34 secondary metabolites across all sampled treatments and plants (34 variables \times 40 samples). Although the PCA model requires six PCs to explain the original data structure, the first two main PCs defined 58 % of the total variance (47.58 and 10.80 %) across the examined data. As observed

in the scatter plot (**Figure 4.11a**), there was no distinction among the four treatments. Plants inoculated with *Bacillus* sp. mainly occupied the left side of the plot, while treatment with *Pseudomonas* and *Mucilaginibater* sp. dominated the right side of the plot. From the loadings projection (**Figure 4.11b**), PC1 was positively correlated with all cannabinoids and terpenes, except for CBGA. In contrast, most of analyzed terpene compounds were negatively correlated with the PC2, excluding three monoterpenes (4-isopropyltoluene, carene, isopulegol) and two sesquiterpenes (trans-nerolidol and cis-nerolidol). For cannabinoids, only CBNA was negatively correlated with PC2.

4.5 Discussion

4.5.1 Selection of plant chemotype and reproductive period determination

The cannabis “strain” (genotype) used in current study, was purported to be CBD Kush. Although this has not been verified, we here list the related information about CBD Kush. CBD Kush, created by the prolific Dutch Passion Seeds company, is a strain specifically bred to yield a balance between THC and CBD effects. This CBD Kush variety was produced by crossing the THC rich Kandy Kush selection with the CBD dominant strain. Dutch Passion is reported to have a ratio of CBD: THC about 1:1, but Leafly reported CBD: THC ratios between 1:1 and 4:1 (leafly.com). Nevertheless, 1.5:1 was the CBD:THC ratio determined for the cannabis chemotype type “CBD Kush”, in the present study. Moreover, the variation in final CBD:THC ratio was found to be independent of environmental conditions (Fairbairn and Liebmann, 1974). These results led to some uncertainty regarding the actual identity of the chemotype used in this study, thought to be CBD Kush; the identity needs to be confirmed through genomic analysis. Studies have reported that the main cannabinoids, especially acidic forms, are consistent when plants were harvested in weeks seven, nine and 11 of development (Aizpurua-Olaizola et al., 2016), but there is a significant

difference for neutral cannabinoids caused by long-term exposure to UV light (Hazekamp, 2007) or warmer conditions (Glivar et al., 2020). To minimize the total growing time, our study estimated the cannabinoid concentration at week seven.

4.5.2 Biochemical levels vary in response to PGPR inoculation

The current study evaluated secondary metabolite accumulation in “CBD Kush” plants inoculated with PGPR, to characterize the effects of three novel PGPR of differing genera (*Bacillus*, *Mucilaginibacter* and *Pseudomonas*) on the biochemical composition of *C. sativa*. The results indicate that the level of effects caused by PGPR varies among the three genera evaluated and that THCA, CBDA levels can be significantly enhanced with *Mucilaginibacter* sp. and *Pseudomonas* sp. inoculation. These results indicate that PGPR inoculation influences enzyme activity related to cannabinoid biosynthesis pathways. Cannabis chemotype is defined by the CBD/THC ratio, which is stable during plant growth (Aizpurua-Olaizola et al., 2016). The genes for THCA synthase (THCAS) and CBDA synthase (CBDAS) are considered co-dominant alleles (De Meijer et al., 2003; Onofri et al., 2015) while the gene for CBCA synthase is an independent locus (Richins et al., 2018). Our study found that while PGPR inoculants affected the acidic forms of cannabinoids, the ratio of CBD/THC remained constant across treatments (**Table 4.3**). The lack of response of neutral cannabinoid compounds to PGPR inoculation was notable (**Figure 4.1 and 4.5, Table 4.4**) because these compounds are decarboxylated from the acidic forms of cannabinoids under heat or UV exposure. The plants and plant materials evaluated in the current study were exposed to the same level of heat, and no UV during the flowering stage or during storage. For those cannabinoids which generally get less attention, e.g., CBDVA and THCVA, their accumulation was also affected by inoculation with PGPR (**Table 4.4**). These compounds also show meaningful value in pharmacotherapy (Abioye et al., 2020; Pretzsch et al., 2019),

indicating that there is not only a need for further research into clinically useful medicines related to the rarer cannabinoids but also in improving the accumulation of those compounds in cannabis plants, to provide the basis for clinical research and medical efficacy.

In the case of terpenes, our results revealed that the quantities and relative abundance of monoterpenes were higher than sesquiterpenes for “CBD Kush”. This is consistent with the results reported by Aizpurua-Olaizola et al. (2016) who illustrated that higher monoterpene accumulation during the flowering phase was caused by greater monoterpene synthase expression. In our study, it is also clear that the accumulation of sesquiterpenes responded more strongly to the application of PGPR (**Figure 4.7**). *Mucilaginibacter* sp. significantly increased accumulation of all six measured sesquiterpenes; levels of only three of the 15 measured monoterpenes were significantly increased (**Table 4.5**). Intriguingly, inoculation with *Pseudomonas* sp. resulted in a substantial increase in nerolidol, as compared to all other terpenes measured; the reason for this is unclear. Conversely, the correlation matrix and principal component analysis (**Figure 4.11**) showed that cannabinoid and terpene accumulations in flowers were statistically correlated with THCA and CBDA. Similar results have also been reported across various *C. sativa* strains (Jin et al., 2021; Namdar et al., 2019). However, this correlation has been thought to be due to long-term manipulation or selective breeding or because they are all from same chemical group – secondary metabolites. From the perspective of biosynthesis pathway (**Figure 4.1**), both cannabinoids and terpenes (monoterpenes) share the same precursor - geranyl pyrophosphate (GPP). A recent study determined that a total 22 genes involved in cannabinoid and terpene (terpenoid) biosynthesis are co-expressed with THCA synthase, providing additional evidence for the correlation between both metabolites in cannabis (Zager et al., 2019). There are also some studies indicating the entourage effect, contributed to by terpenes (Blasco-Benito et al., 2018; Santiago et al., 2019), implying that

it is important to understand related mode(s) of action. Combined flower yield (Lyu et al., 2022) and biochemical profile (**Figure 4.6 and Figure 4.9**), following treatment with *Mucilaginibacter* sp. led to improvement of total cannabinoids and terpene content per plant. Interestingly, *Pseudomonas* sp. did not change total terpene content per flower weight, however, performance related to yield enhancement led to a significant increase of total terpene production per plant (**Figure 4.9**). Therefore, it is as important to enhance the concentration of secondary metabolites and to enhance both flower yield, given the potential of cannabinoids and terpenes for pharmaceutical effects and industrial value.

4.5.3 Influence of PGPR inoculation on metabolomics pathways

PGPR can be used to improve the growth of a wide range of plants, including cannabis (Lyu et al., 2022; Pagnani et al., 2018). The influence of PGPR on production of secondary metabolites is much less studied. To date, there is only one publication, examining the effects of a PGPR (a consortium: *Azospirillum brasilense*, *Gluconacetobacter diazotrophicus*, *Herbaspirillum seropedicae*, *Burkholderia ambifaria*) inoculation on THC and CBD accumulation in hemp-type cannabis (Pagnani et al., 2018). There is also no research on the effects of PGPR inoculation on cannabis terpenes; however, these responses have been studied in other plant species. For example, PGPR have been associated with changes to terpene profiles in wine grapes (*Vitis vinifera* L. cv. Malbec), where an increase in terpene accumulation induced by PGPR inoculation protected leaves against molecular reactive oxygen species (Salomon et al., 2016). Terpene profiles of pennyroyal (*Mentha pulegium* L.) also responded to PGPR inoculation under drought conditions (Asghari et al., 2020), while terpene profiles of Italian oregano (*Origanum × majoricum*) responded to PGPR inoculation under optimal growing conditions (Banchio et al., 2010). Activity level in the primary metabolism pathways used for carbon and energy supply, such as photosynthesis, and oxidative

pathways strongly link with the biosynthesis of terpenes (Singh et al., 1990). As such, results presented here are consistent with those of our previous study, which illustrated that cannabis inoculation with *Mucilaginiacter* or *Pseudomonas* sp. led to higher photosynthetic rates at the flower formation stage (Lyu et al., 2022) which may have contributed to the increased total terpene accumulation at harvest reported in the current study. In our previous study, *Pseudomonas* sp. inoculation resulted in the largest increase in total dry flower yield (Lyu et al., 2022), while the current study indicated that *Mucilaginibacter* sp. inoculation resulted in the largest increase in cannabinoid accumulation. Fixed carbon from photosynthesis is partitioned to produce flower biomass and constitutive secondary metabolites in tissues (Kleczewski et al., 2010). Therefore, the two PGPR inoculation treatments that resulted in increased photosynthetic rates had different effects on fixed C partitioning with *Pseudomonas* sp. favouring flower biomass and *Mucilaginibacter* sp. favouring secondary metabolism.

PGPR can affect plant growth and have physiological and metabolic effects through various mechanisms including phytohormone signal production, induced systematic resistance, and antibiotics (Backer et al., 2018; Khan et al., 2019; Lyu et al., 2020). Another mechanism by which PGPR alter metabolic pathways is by acting as elicitors of biosynthetic pathways of secondary metabolites *via* hormone signaling (mainly jasmonate) (Backer et al., 2018; Thakur et al., 2019). For the PGPR used in current study, the three bacteria resulted in different levels of biochemical response related to plant growth promotion, including indole acetic acid (IAA) production, ACC deaminase, P solubilization, siderophore production, nitrogen fixation, ammonia production and antimicrobial activity (Fan et al., 2018). However, the mode(s) of action for enhancement of secondary metabolites caused by PGPR on cannabis should be further investigated.

4.6 Conclusions

Cannabinoids and terpenes have pharmaceutical effects; these are now being investigated widely. Their proportion and concentration in the final cannabis product can determine the end-use and legal status, most notably for THC and THCA levels. The current study provides evidence that cannabis plants inoculated with PGPR at the vegetative stage showed improved secondary metabolite concentrations which builds upon our previous work indicating that inoculation with the same PGPR increased flower yield. However, these effects varied among the three PGPR species studied. Inoculation of cannabis with *Mucilaginibacter* sp. and *Pseudomonas* sp. led to enhanced accumulation of both cannabinoids and terpenes. Inoculation of PGPR did not change the CBD/THC ratio, even when individual cannabinoid levels were positively or negatively affected by the inoculants. In the current study PGPR inoculation had a greater effect on sesquiterpene accumulation than on monoterpene accumulation. Our results demonstrated the ability to improve and expand the ability to regulate medical cannabis secondary metabolite accumulation through application of two out of three previously identified beneficial phytomicrobiome members. The results provide strong support for PGPR inoculation, at least inoculation with those triggering enhancement of important metabolite biosynthesis, thus providing access to more effective medicinal applications, and leading to a need to investigate the potential pharmaceutical properties following PGPR inoculation. Further research should be conducted to investigate possible mechanisms relating to PGPR effects on the biosynthesis of the main cannabinoids and terpenes of cannabis plants using proteomics to evaluate the relevant molecular level changes.

4.7 Reference

- Abioye, A., Ayodele, O., Marinkovic, A., Patidar, R., Akinwekomi, A., and Sanyaolu, A. (2020). Δ^9 -Tetrahydrocannabivarin (THCV): a commentary on potential therapeutic benefit for the management of obesity and diabetes. *Journal of Cannabis Research* **2**, 1-6.
- Aizpurua-Olaizola, O., Soydaner, U., Öztürk, E., Schibano, D., Simsir, Y., Navarro, P., Etxebarria, N., and Usobiaga, A. (2016). Evolution of the cannabinoid and terpene content during the growth of *Cannabis sativa* plants from different chemotypes. *Journal of Natural Products* **79**, 324-331.
- Almaguer, C., Schönberger, C., Gastl, M., Arendt, E. K., and Becker, T. (2014). *Humulus lupulus*—a story that begs to be told. A review. *Journal of the Institute of Brewing* **120**, 289-314.
- Asghari, B., Khademian, R., and Sedaghati, B. (2020). Plant growth promoting rhizobacteria (PGPR) confer drought resistance and stimulate biosynthesis of secondary metabolites in pennyroyal (*Mentha pulegium* L.) under water shortage condition. *Scientia Horticulturae* **263**, 109132.
- Atakan, Z. (2012). Cannabis, a complex plant: different compounds and different effects on individuals. *Therapeutic Advances in Psychopharmacology* **2**, 241-254.
- Backer, R., Mandolino, G., Wilkins, O., ElSohly, M. A., and Smith, D. L. (2020). Cannabis Genomics, Breeding and Production. *Frontiers in Plant Science* **11**.
- Backer, R., Rokem, J. S., Ilangumaran, G., Lamont, J., Praslickova, D., Ricci, E., Subramanian, S., and Smith, D. L. (2018). Plant growth-promoting rhizobacteria: context, mechanisms of action, and roadmap to commercialization of biostimulants for sustainable agriculture. *Frontiers in Plant Science* **9**, 1473.

- Banchio, E., Bogino, P. C., Santoro, M., Torres, L., Zygadlo, J., and Giordano, W. (2010). Systemic induction of monoterpene biosynthesis in *Origanum× majoricum* by soil bacteria. *Journal of Agricultural and Food Chemistry* **58**, 650-654.
- Bernstein, N., Gorelick, J., Zerahia, R., and Koch, S. (2019). Impact of N, P, K, and humic acid supplementation on the chemical profile of medical cannabis (*Cannabis sativa* L.). *Frontiers in Plant Science* **10**, 736.
- Berthold, E. C., Yang, R., Sharma, A., Kamble, S. H., Kanumuri, S. R., King, T. I., Popa, R., Freeman, J. H., Brym, Z. T., and Avery, B. A. (2020). Regulatory sampling of industrial hemp plant samples (*Cannabis sativa* L.) using UPLC-MS/MS method for detection and quantification of twelve cannabinoids. *Journal of Cannabis Research* **2**, 1-11.
- Blasco-Benito, S., Seijo-Vila, M., Caro-Villalobos, M., Tundidor, I., Andradas, C., García-Taboada, E., Wade, J., Smith, S., Guzmán, M., and Pérez-Gómez, E. (2018). Appraising the “entourage effect”: Antitumor action of a pure cannabinoid versus a botanical drug preparation in preclinical models of breast cancer. *Biochemical Pharmacology* **157**, 285-293.
- Booth, J. K., Page, J. E., and Bohlmann, J. (2017). Terpene synthases from *Cannabis sativa*. *PLoS One* **12**, e0173911.
- Borille, B. T., González, M., Steffens, L., Ortiz, R. S., and Limberger, R. P. (2017). *Cannabis sativa*: a systematic review of plant analysis. *Drug Analytical Research* **1**, 1-23.
- Braga, R. M., Dourado, M. N., and Araújo, W. L. (2016). Microbial interactions: ecology in a molecular perspective. *Brazilian Journal of Microbiology* **47**, 86-98.

- Brousseau, V. D., Wu, B.-S., MacPherson, S., Morello, V., and Lefsrud, M. (2021). Cannabinoids and terpenes: how production of photo-protectants can be manipulated to enhance *cannabis sativa* L. *Phytochemistry. Frontiers in Plant Science* **12**.
- Chouvy, P.A. (2019). Cannabis cultivation in the world: heritages, trends and challenges. *EchoGéo*, (48).
- Danziger, N., and Bernstein, N. (2021). Light matters: effect of light spectra on cannabinoid profile and plant development of medical cannabis (*Cannabis sativa* L.). *Industrial Crops and Products* **164**, 113351.
- De Meijer, E. P., Bagatta, M., Carboni, A., Crucitti, P., Moliterni, V. C., Ranalli, P., and Mandolino, G. (2003). The inheritance of chemical phenotype in *Cannabis sativa* L. *Genetics* **163**, 335-346.
- ElSohly, M. A., Radwan, M. M., Gul, W., Chandra, S., and Galal, A. (2017). Phytochemistry of *Cannabis sativa* L. *Progress in the Chemistry of Organic Natural Products* **103**, 1-36.
- Fairbairn, J., and Liebmann, J. (1974). The cannabinoid content of *Cannabis sativa* L grown in England. *Journal of Pharmacy and Pharmacology* **26**, 413-419.
- Fan, D., Schwinghamer, T., and Smith, D. L. (2018). Isolation and diversity of culturable rhizobacteria associated with economically important crops and uncultivated plants in Québec, Canada. *Systematic Applied Microbiology* **41**, 629-640.
- Fellermeier, M., Eisenreich, W., Bacher, A., and Zenk, M. H. (2001). Biosynthesis of cannabinoids: Incorporation experiments with ¹³C-labeled glucoses. *European Journal of Biochemistry* **268**, 1596-1604.
- Ferrer, I. (2020). Analyses of cannabinoids in hemp oils by LC/Q-TOF-MS. In "Comprehensive Analytical Chemistry", Vol. 90, pp. 415-452. Elsevier.

- Fischedick, J. T., Hazekamp, A., Erkelens, T., Choi, Y. H., and Verpoorte, R. (2010). Metabolic fingerprinting of *Cannabis sativa* L., cannabinoids and terpenoids for chemotaxonomic and drug standardization purposes. *Phytochemistry* **71**, 2058-2073.
- Gagne, S. J., Stout, J. M., Liu, E., Boubakir, Z., Clark, S. M., and Page, J. E. (2012). Identification of olivetolic acid cyclase from *Cannabis sativa* reveals a unique catalytic route to plant polyketides. *Proceedings of the National Academy of Sciences* **109**, 12811-12816.
- Glivar, T., Eržen, J., Kreft, S., Zagožen, M., Čerenak, A., Čeh, B., and Benković, E. T. (2020). Cannabinoid content in industrial hemp (*Cannabis sativa* L.) varieties grown in Slovenia. *Industrial Crops and Products* **145**, 112082.
- Gonçalves, J., Rosado, T., Soares, S., Simão, A. Y., Caramelo, D., Luís, Â., Fernández, N., Barroso, M., Gallardo, E., and Duarte, A. P. (2019). Cannabis and its secondary metabolites: their use as therapeutic drugs, toxicological aspects, and analytical Determination. *Medicines (Basel)* **6**.
- Happyana, N., Agnolet, S., Muntendam, R., Van Dam, A., Schneider, B., and Kayser, O. (2013). Analysis of cannabinoids in laser-microdissected trichomes of medicinal *Cannabis sativa* using LCMS and cryogenic NMR. *Phytochemistry* **87**, 51-59.
- Hazekamp, A. (2007). Cannabis; extracting the medicine. Leiden University.
- Hillig, K. W., and Mahlberg, P. G. (2004). A chemotaxonomic analysis of cannabinoid variation in Cannabis (Cannabaceae). *American Journal of Botany* **91**, 966-975.
- Jin, D., Dai, K., Xie, Z., and Chen, J. (2020). Secondary metabolites profiled in cannabis inflorescences, leaves, stem barks, and roots for medicinal purposes. *Scientific Reports* **10**, 1-14.

- Jin, D., Henry, P., Shan, J., and Chen, J. (2021). Identification of chemotypic markers in three chemotype categories of Cannabis using secondary metabolites profiled in inflorescences, leaves, stem bark, and roots. *Frontiers in Plant Science* **12**.
- Khan, N., Bano, A., Rahman, M. A., Guo, J., Kang, Z., and Babar, M. A. (2019). Comparative physiological and metabolic analysis reveals a complex mechanism involved in drought tolerance in chickpea (*Cicer arietinum* L.) induced by PGPR and PGRs. *Scientific Reports* **9**, 1-19.
- Kim, Y. C., Leveau, J., Gardener, B. B. M., Pierson, E. A., Pierson, L. S., and Ryu, C.-M. (2011). The multifactorial basis for plant health promotion by plant-associated bacteria. *Applied and Environmental Microbiology* **77**, 1548-1555.
- Kleczewski, N. M., Herms, D. A., and Bonello, P. (2010). Effects of soil type, fertilization and drought on carbon allocation to root growth and partitioning between secondary metabolism and ectomycorrhizae of *Betula papyrifera*. *Tree Physiology* **30**, 807-817.
- Lange, B. M., and Turner, G. W. (2013). Terpenoid biosynthesis in trichomes—current status and future opportunities. *Plant Biotechnology Journal* **11**, 2-22.
- Lyu, D., Backer, R., and Smith, D. L. (2020). "Chapter 8: Plant growth-promoting rhizobacteria (PGPR) as plant biostimulants in agriculture." in *Biostimulants for sustainable crop production* by Burleigh Dodds Science Publishing.
- Lyu, D., Backer, R., and Smith, D. L. (2022). Three plant growth-promoting rhizobacteria alter morphological development, physiology, and flower yield of *Cannabis sativa* L. *Industrial Crops and Products* **178**, 114583.

- Magagnini, G., Grassi, G., and Kotiranta, S. (2018). The effect of light spectrum on the morphology and cannabinoid content of *Cannabis sativa* L. *Medical Cannabis and Cannabinoids* **1**, 19-27.
- McRae, G., and Melanson, J. E. (2020). Quantitative determination and validation of 17 cannabinoids in cannabis and hemp using liquid chromatography-tandem mass spectrometry. *Analytical and Bioanalytical Chemistry* **412**, 7381-7393.
- Mishra, J., Fatima, T., and Arora, N. K. (2018). Role of secondary metabolites from plant growth-promoting rhizobacteria in combating salinity stress. In "Plant Microbiome: Stress Response", pp. 127-163. Springer.
- Namdar, D., Voet, H., Ajjampura, V., Nadarajan, S., Mayzlish-Gati, E., Mazuz, M., Shalev, N., and Koltai, H. (2019). Terpenoids and phytocannabinoids co-produced in *Cannabis sativa* strains show specific interaction for cell cytotoxic activity. *Molecules* **24**, 3031.
- Onofri, C., de Meijer, E. P., and Mandolino, G. (2015). Sequence heterogeneity of cannabidiolic- and tetrahydrocannabinolic acid-synthase in *Cannabis sativa* L. and its relationship with chemical phenotype. *Phytochemistry* **116**, 57-68.
- Pagnani, G., Pellegrini, M., Galieni, A., D'Egidio, S., Matteucci, F., Ricci, A., Stagnari, F., Sergi, M., Sterzo, C. L., and Pisante, M. (2018). Plant growth-promoting rhizobacteria (PGPR) in *Cannabis sativa* 'Finola' cultivation: An alternative fertilization strategy to improve plant growth and quality characteristics. *Industrial Crops and Products* **123**, 75-83.
- Pretzsch, C. M., Voinescu, B., Lythgoe, D., Horder, J., Mendez, M. A., Wichers, R., Ajram, L., Ivin, G., Heasman, M., and Edden, R. A. (2019). Effects of cannabidivarin (CBDV) on brain excitation and inhibition systems in adults with and without Autism Spectrum

- Disorder (ASD): a single dose trial during magnetic resonance spectroscopy. *Translational Psychiatry* **9**, 1-10.
- Ren, G., Zhang, X., Li, Y., Ridout, K., Serrano-Serrano, M. L., Yang, Y., Liu, A., Ravikanth, G., Nawaz, M. A., and Mumtaz, A. S. (2021). Large-scale whole-genome resequencing unravels the domestication history of *Cannabis sativa*. *Science Advances* **7**, eabg2286.
- Richins, R. D., Rodriguez-Uribe, L., Lowe, K., Ferral, R., and O'Connell, M. A. (2018). Accumulation of bioactive metabolites in cultivated medical Cannabis. *PLoS One* **13**, e0201119.
- Rodriguez-Morrison, V., Llewellyn, D., and Zheng, Y. (2021). Cannabis yield, potency, and leaf photosynthesis respond differently to increasing light levels in an indoor environment. *Frontiers in Plant Science* **12**, 456.
- Ross, S. A., and ElSohly, M. A. (1996). The volatile oil composition of fresh and air-dried buds of *Cannabis sativa*. *Journal of Natural Products* **59**, 49-51.
- Salomon, M. V., Purpora, R., Bottini, R., and Piccoli, P. (2016). Rhizosphere associated bacteria trigger accumulation of terpenes in leaves of *Vitis vinifera* L. cv. Malbec that protect cells against reactive oxygen species. *Plant Physiology and Biochemistry* **106**, 295-304.
- Saloner, A., and Bernstein, N. (2021). Nitrogen supply affects cannabinoid and terpenoid profile in medical cannabis (*Cannabis sativa* L.). *Industrial Crops and Products* **167**, 113516.
- Santiago, M., Sachdev, S., Arnold, J. C., McGregor, I. S., and Connor, M. (2019). Absence of entourage: terpenoids commonly found in *Cannabis sativa* do not modulate the functional activity of Δ^9 -THC at human CB1 and CB2 receptors. *Cannabis and Cannabinoid Research* **4**, 165-176.

- Sharpe, F., and Laws, D. (1981). The essential oil of hops a review. *Journal of the Institute of Brewing* **87**, 96-107.
- Shoyama, Y., Hirano, H., Makino, H., Umekita, N., and Nishioka, I. (1977). Cannabis. X. The isolation and structures of four new propyl cannabinoid acids, tetrahydrocannabivarinic acid, cannabidivarinic acid, cannabichromevarinic acid and cannabigerovarinic acid, from Thai Cannabis, 'Meao variant'. *Chemical and Pharmaceutical Bulletin* **25**, 2306-2311.
- Singh, N., Luthra, R., and Sangwan, R. (1990). Oxidative pathways and essential oil biosynthesis in the developing *Cymbopogon flexuosus* leaf. *Plant Physiology and Biochemistry* **28**, 703-710.
- Taura, F., Morimoto, S., and Shoyama, Y. (1996). Purification and characterization of cannabidiolic-acid synthase from *Cannabis sativa* L. Biochemical analysis of a novel enzyme that catalyzes the oxidocyclization of cannabigerolic acid to cannabidiolic acid. *Journal of Biological Chemistry* **271**, 17411-17416.
- Thakur, M., Bhattacharya, S., Khosla, P. K., and Puri, S. (2019). Improving production of plant secondary metabolites through biotic and abiotic elicitation. *Journal of Applied Research on Medicinal and Aromatic Plants* **12**, 1-12.
- Tipparat, P., Natakankitkul, S., Chamnivikaipong, P., and Chutiwat, S. (2012). Characteristics of cannabinoids composition of Cannabis plants grown in Northern Thailand and its forensic application. *Forensic Science* **215**, 164-170.
- Vacheron, J., Desbrosses, G., Bouffaud, M. L., Touraine, B., Moëgne-Loccoz, Y., Muller, D., Legendre, L., Wisniewski-Dyé, F., and Prigent-Combaret, C. (2013). Plant growth-promoting rhizobacteria and root system functioning. *Frontiers in Plant Science* **4**, 356.

- Wei, X., Zhao, X., Long, S., Xiao, Q., Guo, Y., Qiu, C., Qiu, H., and Wang, Y. (2021). Wavelengths of LED light affect the growth and cannabidiol content in *Cannabis sativa* L. *Industrial Crops and Products* **165**, 113433.
- Yang, W., Chen, X., Li, Y., Guo, S., Wang, Z., and Yu, X. (2020). Advances in pharmacological activities of terpenoids. *Natural Product Communications* **15**, 1934578X20903555.
- Zager, J. J., Lange, I., Srividya, N., Smith, A., and Lange, B. M. (2019). Gene networks underlying cannabinoid and terpenoid accumulation in cannabis. *Plant Physiology* **180**, 1877-1897.

Connecting text

In Chapter 4, a total of 16 cannabinoids and 21 terpenes were identified and quantified with and without PGPR inoculation. The results suggested that two of the selected PGPR (*Mucilaginibacter* sp. and *Pseudomonas* sp.) had positive effects on both cannabinoid and terpene accumulations. These findings led to the understanding that these bacteria can affect secondary metabolite biosynthesis. Associated with the results from Chapters 3 and 4, however, the mode of action through which the strains enhance plant growth and secondary metabolite biosynthesis was not investigated. In Chapter 5, proteomics analysis was conducted to provide some understanding of the mechanisms of plant-microbe interactions, in terms of, cannabis and PGPR interactions, at a molecular level.

Chapter 5 Proteomic Profile of Cannabis Flowers Provides Insights into PGPR Promotion of Cannabis Growth and Development

Authors: Dongmei Lyu ^a, Sowmyalakshmi Subramanian^a, Rachel Backer ^a, Donald L. Smith ^a

Affiliations:

^a Department of Plant Science, McGill University, Sainte-Anne-de-Bellevue, Quebec, Canada, H9X3V9

This manuscript is in preparation for submission.

5.1 Abstract

Higher cannabis yield and quality enhances its value, as it contains various therapeutically effective secondary metabolites in the flowers, including cannabinoids and terpenes. The growth promotion effects contributed by plant growth promoting-rhizobacteria (PGPR) have been confirmed but the mechanism of action is still poorly understood due, in part, to their diversity. In this study, proteomic profiling of flowers of cannabis variety CBD Kush inoculated with PGPR (*Bacillus*, *Mucilaginibacter* and *Pseudomonas* sp.) were performed by LC-MS/MS analysis. Shotgun proteomics of cannabis flower tissue revealed that a number of proteins related to plant growth and stress tolerance were modulated by PGPR inoculation. All three PGPR enhanced levels of a common protein set, but there were also some proteins whose levels were increased by inoculation specific beneficial bacteria. The greatest number of up-regulated proteins were in plants treated with *Pseudomonas* sp. The up-regulated proteins were mainly involved in photosynthesis, glycolysis, the citrate cycle, carbon metabolism and plant defense. *Mucilaginibacter* sp. treatment also led to increased production of proteins involved in cannabinoid biosynthesis. The results provided evidence that inoculation with PGPR enhanced cannabis flower yield and improved secondary metabolite production, which was accompanied by

an increase in the level of proteins involved in key metabolic pathways such as energy and stress management. This work also expanded our more general understanding of PGPR interactions with cannabis plants.

5.2 Introduction

The symbiotic relationship between plants and microbes has evolved over hundreds of millions of years and has been reasonably well studied in recent decades. Beneficial microbes, plant growth-promoting rhizobacteria (PGPR), have been isolated and shown to cause multiple benefits when associated with a plant host. With the improved understanding of PGPR, it is now known that a wide range of plants manifest improved growth when inoculated with a range of phytomicrobiome species that were isolated from different plant species. Previous research conducted in our laboratory showed that *Bacillus* sp., *Mucilaginibacter* sp., and *Pseudomonas* sp. can improve plant growth in *Arabidopsis*, corn, and canola under stress (salt) and optimal conditions and these effects vary with plant species (Fan et al., 2018; Fan and Smith, 2022). By way of extending our understanding of strain function interaction with crop, we have tested their effects on cannabis.

Cannabis sativa L. is a plant with a very long historical use, but its illegal status over much of the last 100 years has led to a knowledge gap regarding this plant. Significant enhancement of final flower yield and photosynthetic rate of cannabis plants, as well as level of some key secondary metabolites (cannabinoids and terpenes) by two of the selected PGPR strains is evaluated and reported by Lyu et al. (2022). In general, the recognized mechanisms of positive effects caused by PGPR through both direct and indirect mechanisms: 1) releasing of phytohormones; 2) nutrient mobilization; 3) biocontrol; and 4) regulation of metabolic pathways through microbe-to-plant signal compounds. To better understand these plant-microbe

interactions, untargeted proteomic analysis was used to reveal effects on metabolic pathways, including those producing key secondary metabolites in cannabis plants. Research conducted by Happyana (2014) explored the full protein profiles of trichomes isolated from cannabis flowers, classified the proteins based on their biological functions and listed the key proteins involved in secondary metabolite biosynthesis. Conneely et al. (2021) demonstrated that the protein profile varied among parts of glandular trichomes and at specific point during flowering. Considering the potency of cannabinoids and terpenes, and their levels in whole flowers, this study focused on the protein profile of the whole flower. This study is the first to investigate the protein profile of cannabis plants as affected by PGPR inoculation. We identified the proteins in cannabis flowers and compared effects among PGPR treatments, to explore mechanisms by which these PGPR alter cannabis plant growth and secondary metabolite biosynthesis.

Based on our previous work, the aim of current work was to 1) identify the proteins likely to be involved in plant growth promotion mechanisms; 2) characterize the features of the three PGPR relevant to changes in secondary metabolite profile; 3) provide insights regarding the precise effects of three taxonomically different PGPR, on the protein profiles of cannabis flowers.

5.3 Materials and methods

5.3.1 Maintenance of bacterial culture

Three PGPR strains, in the genera *Bacillus mobilis* (KJ812449), *Pseudomonas koreensis* (AF468452), and *Mucilaginibacter lappiensis* (jgi.1095764), were isolated by Fan et al. (2018) and were stored in glycerol in a -80°C freezer after initial isolation. Cultures were removed from storage and streaked onto petri plates containing sterile (30 min, 121 °C) King's Medium B (Protease Peptone (20.0 g L⁻¹), K₂HPO₄ (1.5 g L⁻¹), glycerol (10.0 g L⁻¹), MgSO₄•7H₂O (0.25 g L⁻¹) and agar (15 g L⁻¹)). Fresh cultures were prepared by scraping bacterial colonies grown on KB

agar off the surface of the agar, transferring it to a tube containing 25 mL sterile KB liquid followed by incubation at 28 ± 2 °C on an orbital shaker (150 rev min^{-1}) to reach the exponential phase. The suspension was then centrifuged at $6,000 \times g$ for 10 min and the pellet was re-suspended in 10 mM MgSO_4 , until the OD (optical density) (measured at 600 nm) of the culture reached values of 0.1 (about 1×10^8 colony forming units (CFU, mL^{-1})).

5.3.2 Plant material

All plant handling and experimental procedures were carried out at the Large Animal Research Unit, McGill University within a licensed cannabis growth facility (License No. LIC-5AZZW7S4GM-2021). Well rooted cannabis cuttings were individually transplanted into plastic pots containing 360 g of Agromix G2 Compost soil mix containing brown peat, fibre moss peat, perlite, compost, limestone, gypsum and micronutrients. Ten milliliters of bacterial suspension were applied in each pot, just after transplanting, by soil drenching. Inoculated cannabis seedlings were grown indoors under standardized conditions with long day-length conditions (18 h day^{-1}) for three-weeks at the vegetative growth phase. Subsequently, flowering was induced under a shorter (12 h day^{-1}) light regime for 7 weeks. Plants were irrigated regularly with nutrients. The whole experiment was repeated three times, each with three technical replicates. The temperature, nutrients and water supply followed **Chapter 3** (Lyu et al., 2022).

5.3.2.1 Protein Extraction

The protein was extracted using a plant total protein extraction kit (Sigma-Aldrich, St. Louis, MO, USA). The top three centimeters of apical fresh flowers of cannabis plants were harvested at day 70 after transplanting and the flowers were flash frozen in liquid nitrogen. The three technical replicates from each experiment were pooled to represent a biological replicate. Sampled flowers were ground to a fine powder in liquid nitrogen using a sterilized mortar and

pestle. About 100 mg the resulting fine powder was transferred into 2 mL sterilized tubes, was incubated with 1 mL of 80% ice-cold methanol protease inhibitor cocktail for 2 h at -20 °C and centrifuged (10,000 g, 10 min) at 4 °C. The supernatant was discarded, and the procedure was repeated thrice. The sample was then incubated in acetone and washed twice following a similar procedure, to remove pigments and other secondary metabolites. The RW4 (Protein extraction Reagent Type 4) solution was added to the pellet, vortexed for 30s and incubated for 10 min at room temperature (22 °C). After centrifugation at room temperature, the supernatant was collected in a new tube, and this constituted the total protein isolates of the flowers. The protein content was quantified spectrophotometrically following the Lowry method (Waterborg and Matthews, 1984) with modification. After quantification, 20 µg protein in each sample was pipetted into 20 µL of 1M urea. The samples were subjected to shotgun proteomic analysis using LC-MS/MS at the Institut de recherches cliniques de Montréal (IRCM).

5.3.2.2 Proteome profiling

Total extracted proteins from cannabis flowers were tryptic digested before being subjected to LC-MS/MS using a Velos Orbitrap instrument (Thermo Fisher Scientific, Waltham, MA, USA). The method of LC-MS analysis follows Subramanian et al. (2016a; 2016b). All mass spectra obtained from LC-MS were analyzed using Mascot (Matrix Science, London, UK; Mascot in Proteome Discoverer 2.4.0.305). MS/MS spectra were searched based on the Refseq database for *Cannabis sativa*, against the taxonomy of Uniprot Cannabaceae. Carbamidomethylation of cysteines was set as a fixed modification, oxidation of methionine and acetylation on protein N-termini as variable. Mascot was searched with a fragment ion mass tolerance of 0.020 Da and a parent ion tolerance of 10.0 PPM. Identification of peptides and proteins was through validation of MS/MS spectra using Scaffold (version Scaffold 5.1). Results/peptides with discovery rates of

greater than 95.0% probability and a minimum of two matches were considered as significant and real.

5.3.3 Data interpretation and analysis

The FASTA files generated from Scaffold were used to classify the functional annotation of proteins using the integrated Blast2GO-Pro and InterProScan web services of OmicsBox (BioBam, Bioinformatics Solutions) to determine functions of biological processes (BP), molecular functions (MF) and cellular components (CC). In the current study, only those proteins present in all three biological replicates were considered and analyzed. To compare the relative protein abundance between control and treatment, Scaffold 5 was used to compute fold-change and Fisher's exact test of the identified proteins with the recommended Benjamini-Hochberg for multiple test correction at $p < 0.05$ significance level. Only those proteins with fold-changes greater than 1.2 were regarded as differentially expressed proteins. Only comparisons different at $p < 0.05$ are discussed. The differentially affected proteins were grouped using Venn diagrams, to explore the shared and unique proteins in plants treated with each of the three PGPR. All protein accession numbers were subjected to Brenda enzyme database (<https://www.brenda-enzymes.org>) (Chang et al., 2020) to classify the metabolic pathways which the identified proteins are involved in, in cannabis flowers.

5.4 Results

5.4.1 Identification of expressed proteins among treatments

To understand the effect of the three individual PGPR on cannabis growth, total proteins were extracted from the samples and subjected to LC-MS based proteome profiling. The Uniprot database was used for protein identification. Overall, 1203 proteins could be identified in 659 clusters with a total of 39732 spectra based on the quantitative value of the identified spectra, and

at 99% protein probability, with two minimum peptides and 95% peptide probability. The spectral data for each treatment with the number of proteins identified are listed in **Table 5.1**.

Table 5.1 Total number of proteins identified at 99% protein probability and total spectra at 95% peptide probability, with two minimum peptides

Treatment	Protein	Spectra	Cluster
Control	639	7744	419
<i>Bacillus</i> sp.	751	9095	507
<i>Mucilaginibacter</i> sp.	702	9616	475
<i>Pseudomonas</i> sp.	861	12003	599

5.4.2 GO functional annotation and analysis

Gene ontology (GO) enrichment analysis generated three major functional clusters including cellular component (CC), molecular function (MF) and biological process (BP) aspects. GO analysis indicated that the expressed proteins were involved in 11 subgroups of BP (Supplementary **Figure 5.1**), nine subgroups of CC (Supplementary **Figure 5.2**), and seven subgroups of MF (Supplementary **Figure 5.3**) between the PGPR (*Bacillus*, *Mucilaginibacter*, *Pseudomonas* sp.) and control. Overall, the numbers of sequences involved in the cellular components of the cannabis flower proteome altered under specific PGPR treatments were in following the order: *Pseudomonas*, *Mucilaginibacter*, *Bacillus* sp. and control.

5.4.3 Up-regulated differentially expressed proteins (DEPs)

Proteins with fold change (FC) values ≥ 1.2 between the treatment (*Bacillus*, *Mucilaginibacter* and *Pseudomonas* sp.) and control group were grouped as differentially

expressed proteins (DEPs). The treatment contrasts were analyzed for Fisher's Exact test after normalization and were used to narrow the up-regulated proteins, to predict their probable functions. Proteins with fold change (FC) values ≥ 1.2 at the $p \leq 0.05$ level between the treatments (*Bacillus* sp., *Mucilaginibacter* sp., *Pseudomonas* sp.), in comparison with control groups, were regarded as up-regulated DEPs (**Figure 5.1**).

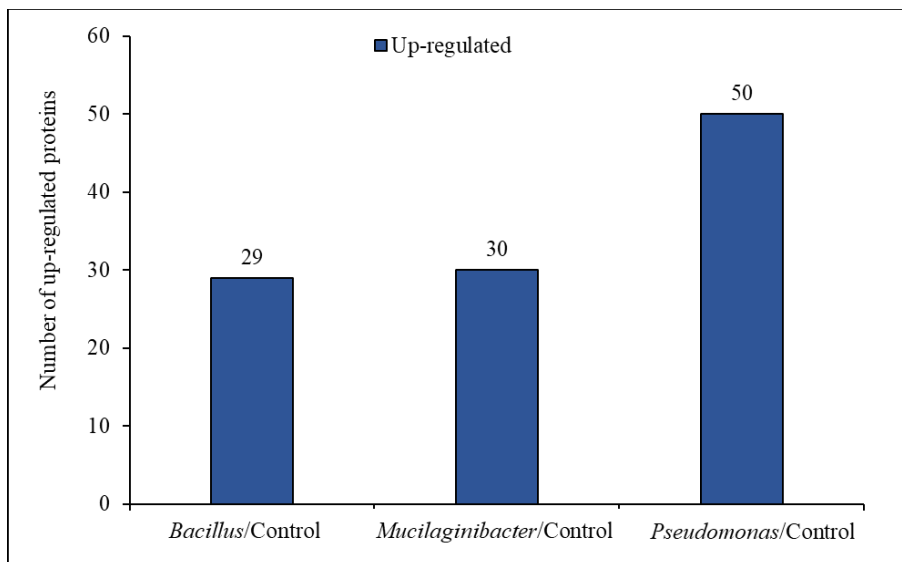


Figure 5.1 Summary of up-regulated ($p \leq 0.05$, Fold change ≥ 1.2) of DEPs between the PGPR treatment groups (*Bacillus*, *Mucilaginibacter*, *Pseudomonas*) and the control.

The up-regulated DEPs among treatment versus control are listed in **Table 5.2**. Proteins involved in amino acid, nucleic acid, sugar and starch biosynthesis, regulation of plant growth and developmental processes such as aconitate hydratase, sucrose synthase, phosphopyruvate hydratase, 5-methyltetrahydropteroyltriglutamate--homocysteine S-methyltransferase were up-regulated by inoculation with PGPR. In addition, a set of proteins related to the photosynthesis was also up-regulated by the application of PGPR, including Photosystem I reaction center subunit V in plants treated with *Bacillus*, Photosystem II D2 protein, PSI subunit V in the plants treated with *Mucilaginibacter* sp., and chloroplast envelope membrane proteins and chloroplastic proteins

in plants treated with *Pseudomonas* sp. There were also four proteins up-regulated by PGPR treatment related to the citrate cycle (TCA), which plays a central role in both the process of energy production and biosynthesis, including isocitrate dehydrogenase (NADP (+)) (plants treated with *Bacillus* sp.); oxoglutarate dehydrogenase (succinyl-transferring) and malate dehydrogenase (plants treated with *Pseudomonas* sp.) and aconitate hydratase (plants treated with *Mucilaginibacter* sp.). In addition, some of the other up-regulated proteins among all three PGPR treatments included dihydrolipoyl dehydrogenase, epimerase domain-containing protein, glycine cleavage system P protein, glucan endo-1,3-beta-D-glucosidase, and xylose isomerase. Some unique proteins were exclusively expressed in the bacterial treatments listed in **Table 5.2**, with fold-change and p value and biological function indicated.

Table 5.2 Proteins that were specifically up-regulated by treatment with *Bacillus*, *Mucilaginibacter*, or *Pseudomonas* relative to the control treatment (Fold change ≥ 1.2 ($p \leq 0.05$; $n=3$)).

INF represents the proteins exclusively expressed in cannabis flowers as a result of the inoculation of PGPR onto the plant roots.

Treatment	Proteins	Accession Number	Fisher's Test (p-value)	Fold Change	Biological function
Control vs. <i>Bacillus</i> sp.	5-methyltetrahydropteroyltriglutamate-homocysteine S-methyltransferase	A0A7J6DX96_CANSA	0.012	INF	Biosynthesis of amino acids, Methionine biosynthetic process; methylation
	GH18 domain-containing protein	A0A803NV35_CANSA	0.043	INF	Carbohydrate metabolic process
	Glucan endo-1,3-beta-D-glucosidase (EC 3.2.1.39) ((1->3)-beta-glucan endohydrolase) (Beta-1,3-endoglucanase)	A0A803PWV8_CANSA	0.03	3.5	Carbohydrate metabolic process
	Isocitrate dehydrogenase (NADP (+))	A0A7J6DS32_CANSA	0.043	INF	Carbon metabolism, isocitrate metabolic process, protein phosphorylation
	Xylose isomerase	A0A7J6GNJ1_CANSA	0.043	INF	D-xylose metabolic process
	Lipoxygenase	A0A7J6FCS8_CANSA	0.0015	2.4	Fatty acid biosynthetic process
	Glycine cleavage system P protein	A0A803QTP3_CANSA	0.012	2.3	Glycine catabolic process

Dihydrolipoyl dehydrogenase	A0A7J6FLE3_CANSA	0.04	2.5	Glycine, serine and threonine metabolism and cell redox homeostasis
Phosphopyruvate hydratase	A0A7J6IBZ8_CANSA	0.033	5	Glycolytic process
Protein kinase domain-containing protein	A0A803NKR5_CANSA	0.023	2.5	MAPK signaling pathway
Photosystem I reaction center subunit V, chloroplastic	A0A7J6EQK0_CANSA	0.043	INF	Photosynthesis
40S ribosomal protein S4	A0A7J6GB14_CANSA	0.013	6	Protein synthesis, translation
Annexin	A0A803NUE6_CANSA	0.031	8	Response to stress
60S ribosomal protein L7a	A0A7J6E0V9_CANSA	0.043	INF	Ribosome
Ribosomal_L19e domain-containing protein	A0A7J6I8T4_CANSA	0.043	INF	Translation
Ribosomal protein L15	A0A7J6IAS2_CANSA	0.021	5.5	Ribosome, translation
Ribos_L4_asso_C domain-containing protein	A0A7J6H117_CANSA	0.049	1.9	Ribosome, translation
Sucrose synthase	A0A7J6GJ42_CANSA	0.045	3.2	Sucrose metabolic process
Uncharacterized protein	A0A803P0E6_CANSA	< 0.00010	INF	
Purple acid phosphatase	A0A7J6HKG5_CANSA	0.0066	INF	
MBD domain-containing protein	A0A7J6FRC9_CANSA	0.0035	INF	
Uncharacterized protein	A0A7J6E7E2_CANSA	0.033	5	
Uncharacterized protein	A0A803R7E0_CANSA	0.05	3.7	
Uncharacterized protein	A0A7J6DSL3_CANSA	0.05	3.7	
Uncharacterized protein	A0A7J6FR79_CANSA	0.03	3.5	

	Epimerase domain-containing protein	A0A7J6DMC9_CANSA	0.025	3	
	Protein disulfide-isomerase	A0A7J6FGV5_CANSA	0.037	2.8	
	Uncharacterized protein	A0A7J6FXX6_CANSA	0.019	2.3	
	NAC-A/B domain-containing protein	A0A7J6HY42_CANSA	0.05	2.1	
Control vs. <i>Mucilaginibacter</i> sp.	Glucan endo-1,3-beta-D-glucosidase	A0A7J6HX51_CANSA	0.0048	12	Carbohydrate metabolic process
	Xylose isomerase	A0A7J6GNJ1_CANSA	0.015	INF	D-xylose metabolic process
	Cluster of Glycine cleavage system P protein	A0A803QTP3_CANSA	0.00075	3.1	Glycine catabolic process
	Dihydrolipoyl dehydrogenase	A0A7J6FLE3_CANSA	0.0079	3.2	Glycine, serine and threonine metabolism and cell redox homeostasis
	Aminomethyltransferase	A0A7J6FPI6_CANSA	0.031	2.5	Glycine catabolic process
	Adenosylhomocysteinase	A0A7J6FVA2_CANSA	0.047	1.7	One-carbon metabolic process
	PSI subunit V	A0A7J6FS73_CANSA	0.05	INF	photosynthesis
	PSII_BNR domain-containing protein	A0A803P0F8_CANSA	0.042	5	Photosynthesis
	Photosystem II D2 protein	A0A0C5ARY2_CANSA	0.017	6	Photosynthetic electron transport in photosystem II

Peroxidase	A0A7J6F7P1_CANSA	0.027	3.8	hydrogen peroxide catabolic process; response to oxidative stress
Cluster of Thioredoxin domain-containing protein	A0A7J6GEH8_CANSA	0.0014	INF	Redox
Bet_v_1 domain-containing protein	A0A7J6F1K3_CANSA	0.014	10	Secondary metabolism
Sucrose synthase	A0A7J6GJ42_CANSA	0.012	4.2	sucrose metabolic process
Aconitate hydratase	A0A7J6GJY5_CANSA	0.034	2.3	Citrate cycle (TCA cycle)
40S ribosomal protein S3a	A0A7J6F5K2_CANSA	0.015	INF	Translation
Ribosomal_L2_C domain-containing protein	A0A7J6I145_CANSA	0.05	INF	Translation
50S ribosomal protein L2, chloroplastic	A0A0C5AS13_CANSA	0.027	INF	Translation
Epimerase domain-containing protein	A0A7J6DPV6_CANSA	0.05	INF	
MBD domain-containing protein	A0A7J6FRC9_CANSA	0.0025	INF	
Purple acid phosphatase	A0A7J6HKG5_CANSA	0.0083	INF	
TRASH domain-containing protein	A0A7J6I6Q3_CANSA	0.05	INF	
Uncharacterized protein	A0A7J6HXN1_CANSA	0.027	INF	
Uncharacterized protein	A0A7J6E157_CANSA	0.003	6	
Uncharacterized protein	A0A7J6DSL3_CANSA	0.0048	5.7	
Uncharacterized protein	A0A803R7E0_CANSA	0.0048	5.7	
Uncharacterized protein	A0A7J6GXD7_CANSA	0.042	5	
Cluster of Uncharacterized protein	A0A7J6FR79_CANSA	0.012	4.2	

	Epimerase domain-containing protein	A0A7J6DMC9_CANSA	0.018	3.3	
	Histone H4	A0A7J6H3M1_CANSA	0.017	2.6	
	Transmembrane 9 superfamily member	A0A7J6E1S1_CANSA	0.0027	2.1	
Control vs. <i>Pseudomonas</i> sp.	Annexin	A0A803NUE6_CANSA	0.013	12	Response to stress
	UDP-glucuronate decarboxylase	A0A7J6EHR5_CANSA	0.04	6	Amino sugar and nucleotide sugar metabolism
	Cluster of GH18 domain-containing protein	A0A7J6I0L9_CANSA	0.046	9	Carbohydrate metabolic process
	Glucan endo-1,3-beta-D-glucosidase	A0A7J6HX51_CANSA	0.046	9	Carbohydrate metabolic process
	Phosphoenolpyruvate carboxylase	A0A7J6EZ97_CANSA	0.035	3	Carbon fixation; tricarboxylic acid cycle
	Phosphogluconate dehydrogenase (NADP (+)-dependent, decarboxylating)	A0A7J6E0B3_CANSA	0.03	10	Carbon metabolism
	Cytochrome f	A0A7J6DRG2_CANSA	0.0021	1.2	Carbon metabolism, Fatty acid biosynthetic process; photorespiration; reductive pentose-phosphate cycle
	Aminomethyltransferase	A0A7J6FPI6_CANSA	0.045	2.8	Carbon metabolism, glycine catabolic process

Pectin acetyltransferase	A0A7J6EEX6_CANSA	0.017	INF	Cell wall modification; pectin catabolic process
Pectinesterase	A0A7J6GRM1_CANSA	0.047	INF	Cell wall modification; pectin catabolic process
Pyruvate dehydrogenase E1 component subunit alpha	A0A7J6HZI1_CANSA	0.046	9	Pyruvate metabolism
Acetyltransferase component of pyruvate dehydrogenase complex	A0A7J6EWH0_CANSA	0.047	INF	Citrate cycle (TCA cycle), Pyruvate metabolic process
6-phosphogluconate dehydrogenase, decarboxylating	A0A7J6E1L7_CANSA	0.033	5	D-gluconate metabolic process; pentose-phosphate shunt, Glycine catabolic process
Xylose isomerase	A0A7J6GNJ1_CANSA	0.01	INF	D-xylose metabolic process
Lipoyl-binding domain-containing protein	A0A7J6HQN3_CANSA	0.0087	3.7	Fatty acid biosynthetic process
Ribonuclease	A0A7J6GP72_CANSA	0.017	INF	Gene silencing by RNA
Glutamate decarboxylase	A0A803PJC6_CANSA	0.046	9	Glutamate metabolic process
Glycine cleavage system P protein	A0A803QTP3_CANSA	0.042	2.6	Glycine catabolic process
Dihydrolipoyl dehydrogenase	A0A7J6FLE3_CANSA	0.0044	4.1	Glycine, serine and threonine metabolism and cell redox homeostasis

Malic enzyme	A0A7J6GZ23_CANSA	0.04	6	malate metabolic process
Oxoglutarate dehydrogenase (succinyl-transferring)	A0A7J6EBT7_CANSA	0.028	INF	Metabolic pathways, Tricarboxylic acid cycle
Phospholipase D	A0A803P039_CANSA	0.029	2.4	Phospholipase D signaling pathway, Lipid catabolic process; phosphatidylcholine metabolic process
Chloroplast envelope membrane protein	A0A7J6I1E6_CANSA	0.0036	INF	Ion transport; photosynthesis
ATP synthase subunit beta, chloroplastic	A0A0U2DTF2_CANSA	0.02	1.2	Photosynthesis
AAA domain-containing protein	A0A7J6DR43_CANSA	0.022	1.2	Photosynthesis
HATPase_c domain-containing protein	A0A803Q3Y6_CANSA	0.021	2.6	Protein folding
Sucrose synthase	A0A7J6GJ42_CANSA	0.0066	5.5	Sucrose metabolic process
40S ribosomal protein S3a	A0A7J6F5K2_CANSA	0.0001	INF	Translation
60S ribosomal protein L7a	A0A7J6E0V9_CANSA	0.047	INF	Translation
40S ribosomal protein S4	A0A7J6GB14_CANSA	0.012	7.5	Translation
Epimerase domain-containing protein	A0A7J6DPV6_CANSA	0.028	INF	
TRASH domain-containing protein	A0A7J6I6Q3_CANSA	0.028	INF	
Uncharacterized protein	A0A7J6GYT5_CANSA	0.047	INF	
Uncharacterized protein	A0A7J6DSH1_CANSA	0.028	INF	
Uncharacterized protein	A0A7J6HW96_CANSA	0.0036	INF	
Uncharacterized protein	A0A803P0E6_CANSA	0.0013	INF	

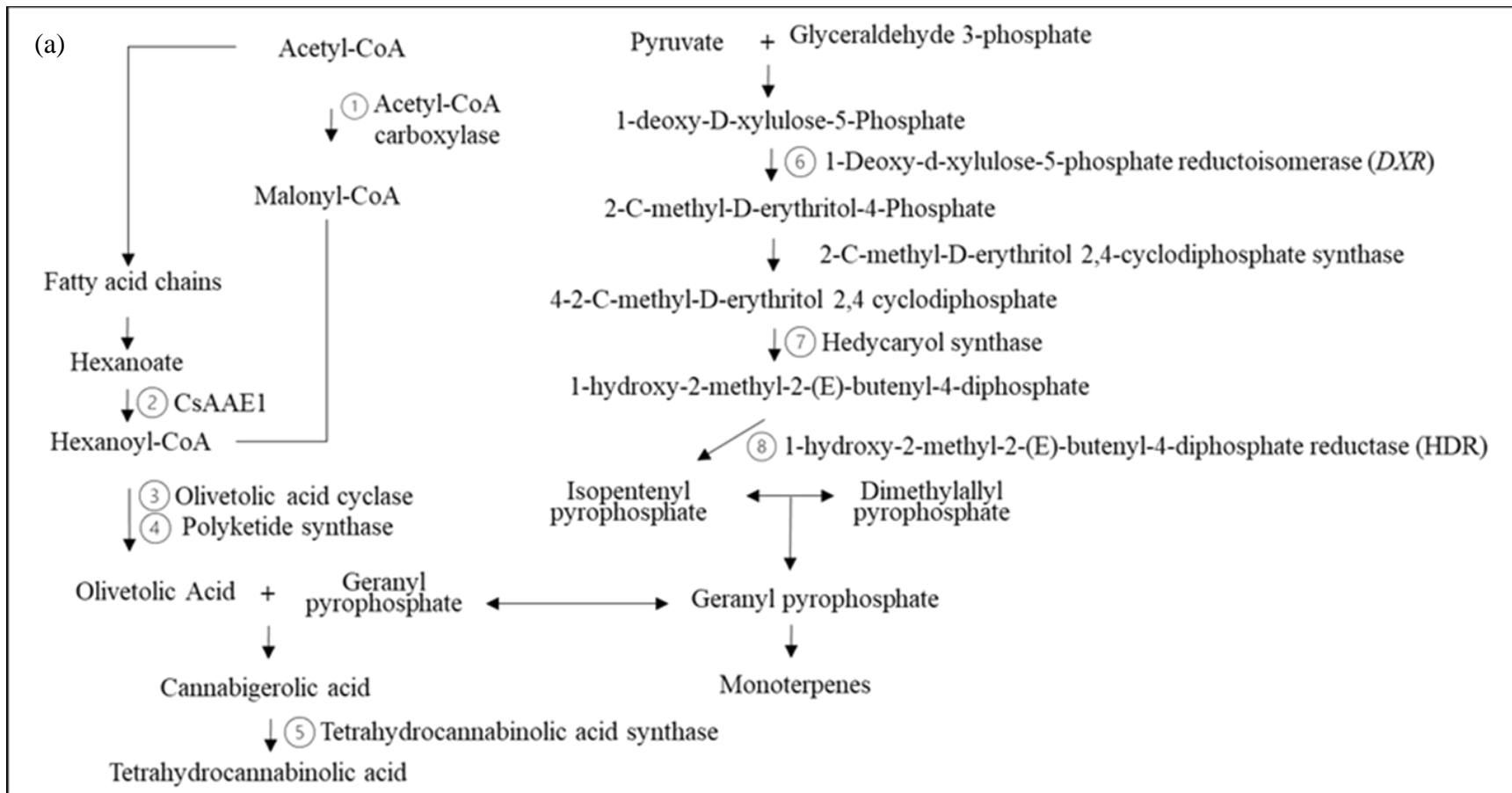
Uncharacterized protein	A0A7J6DNT0_CANSA	0.02	11	
Uncharacterized protein	A0A7J6E157_CANSA	< 0.00010	11	
HIT domain-containing protein	A0A7J6HP21_CANSA	0.03	10	
RNA helicase	A0A7J6I498_CANSA	0.03	10	
Uncharacterized protein	A0A7J6GXD7_CANSA	0.04	6	
Uncharacterized protein	A0A7J6DSL3_CANSA	0.033	5	
Uncharacterized protein	A0A803R7E0_CANSA	0.033	5	
Uncharacterized protein	A0A7J6HMA9_CANSA	0.002	4.7	
Cluster of Uncharacterized protein	A0A7J6E157_CANSA	0.00074	4.6	
Uncharacterized protein	A0A803PIY5_CANSA	0.04	3.8	
Epimerase domain-containing protein	A0A7J6DMC9_CANSA	0.031	3.7	
Cluster of Uncharacterized protein	A0A7J6FXX6_CANSA	0.0064	3.2	
Uncharacterized protein	A0A7J6FXX6_CANSA	0.0064	3.2	
Cluster of MFS domain-containing protein	A0A7J6DKF6_CANSA	0.04	1.2	

5.4.4 Proteins involved in cannabis secondary metabolite biosynthesis

In this study, proteins participating in the biosynthesis of cannabinoids and terpenes were also identified (**Table 5.3**). Although the name of proteins was not uniform, all identified proteins related in biosynthesis of cannabinoids and terpenes were determined by searching the name and sequences in the Uniprot (<https://www.uniprot.org/>). The proteins related to cannabinoid and terpene biosynthesis are well described by Happyana (2014). In current study, the detailed biosynthesis pathway of cannabinoids and terpenes is described in **Figure 5.2 (a)** and the quantitative spectra of those proteins are given in **Figure 5.2 (b)**. There is only one protein (Bet_v_1 domain-containing protein) significantly up-regulated by *Mucilaginibacter* sp. (FC=10) (**Table 5.2 & 5.3**), which is responsible for the production of olivetolic acid, the precursor of cannabinoids in cannabis flowers. The remaining proteins related to cannabinoid and terpene biosynthesis were not significantly up-regulated but the quantitative total spectra of the proteins in plants treated with PGPR were greater than in the control treatment (**Figure 5.2(b)**).

Table 5.3 The identified proteins responding to PGPR inoculation and involved in cannabinoid and terpene biosynthesis in cannabis flowers

Identified Proteins	Precursors proteins	Secondary metabolite
Very-long-chain 3-oxoacyl-CoA synthase	Hexanoyl CoA	Cannabinoids
Naringenin-chalcone synthase	Hexanoyl CoA	
Cluster of Acetyl-CoA carboxytransferase	Malonyl-CoA	
Cluster of Biotin carboxylase	Malonyl-CoA	
Bet_v_1 domain-containing protein	Olivetolic acid	
Chalcone isomerase	Olivetolic acid	
Polyketide synthase 2	Polyketide synthase	
Cannabidiolic acid synthase	Cannabidiolic acid	
Tetrahydrocannabinolic acid synthase	Tetrahydrocannabinolic acid	
Cluster of HDR	Isopentenyl diphosphate and dimethylallyl pyrophosphate	
2-C-methyl-D-erythritol 2,4-cyclodiphosphate synthase	Isopentenyl diphosphate and dimethylallyl pyrophosphate	
4-(cytidine 5'-diphospho)-2-C-methyl-D-erythritol kinase	Isopentenyl diphosphate and dimethylallyl pyrophosphate	
Cluster of Hedycaryol synthase	Monoterpene	
Cluster of (-)-limonene synthase	Monoterpene	



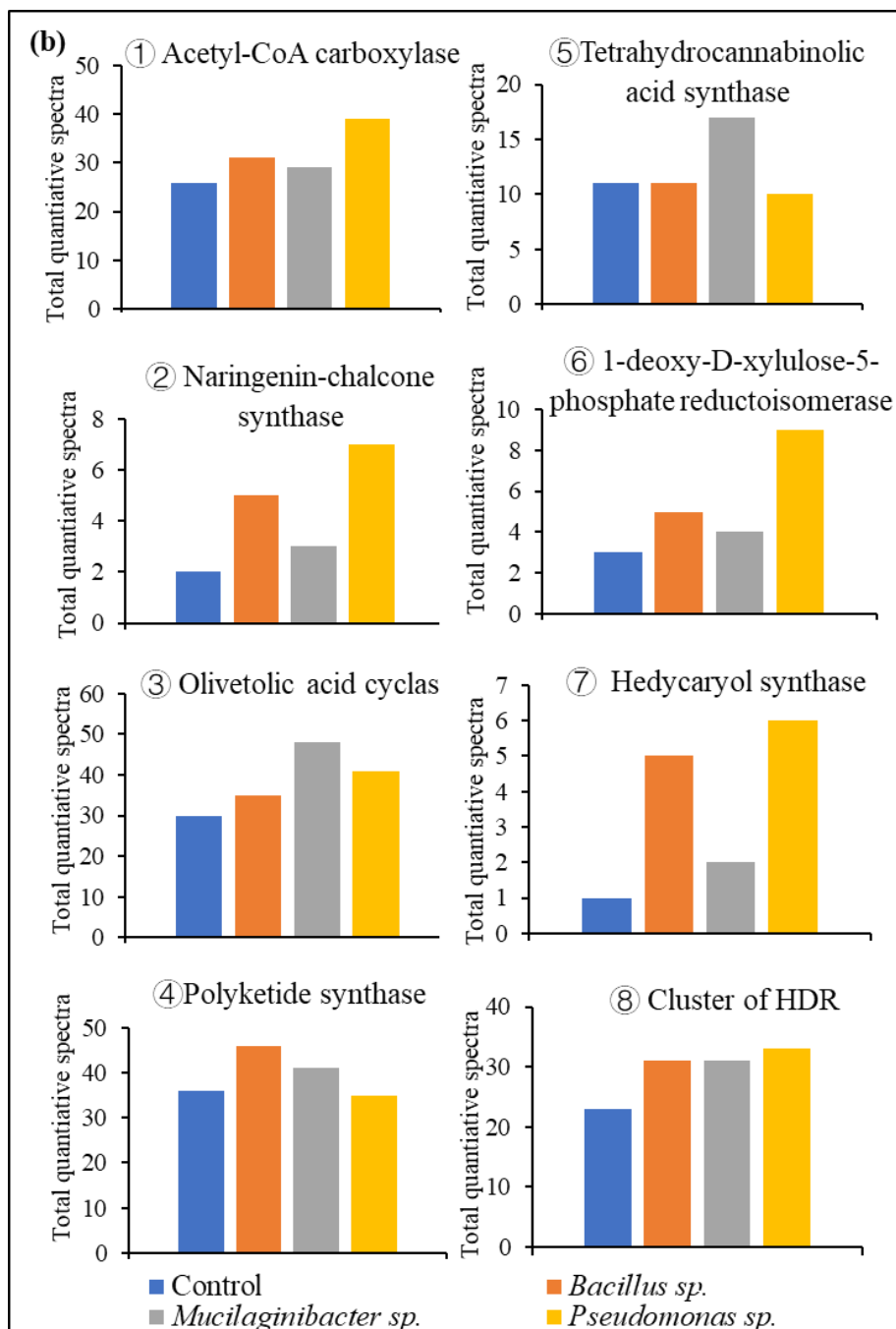


Figure 5.2 The quantitative spectra of proteins which respond to PGPR inoculation and are involved in cannabinoid and terpene biosynthesis in cannabis flowers. (a) The detailed cannabinoids and terpene biosynthesis pathway, (b) Quantitative spectra of proteins involved in cannabinoids and terpene biosynthesis.

5.5 Discussion

Cannabis growth and development is affected by a range of factors. Our previous study demonstrated the effects of *Bacillus*, *Mucilaginibacter* and *Pseudomonas* sp. on cannabis growth. Investigating the protein expression pattern can play a vital role in understanding the effects of PGPR on the metabolic status of cannabis plants. The roles of plant proteins are enzymatic, structural and functional; they are involved in all aspects of a plant's life (Bontinck et al., 2018; Rasheed et al., 2020). This study of the cannabis proteome showed PGPR effects on the metabolic pathways listed in **Figure 5.3**, using the Brenda enzyme database (<https://www.brenda-enzymes.org>) (Chang et al., 2020). A set of pathways were significantly up-regulated in plants due to bacterial inoculation, as highlighted in **Figure 5.3**, including photosynthesis, glycolysis, citrate cycle (TCA), pentose phosphate pathway, glycine metabolism, acetyl-CoA biosynthesis, *etc.* Photosynthesis, TCA, glycine metabolism, and acetyl-CoA biosynthesis were all markedly increased in activity by the *Bacillus* sp., *Mucilaginibacter* sp., and *Pseudomonas* sp.. A few key examples found in this study are discussed below, categorized by the type of protein.

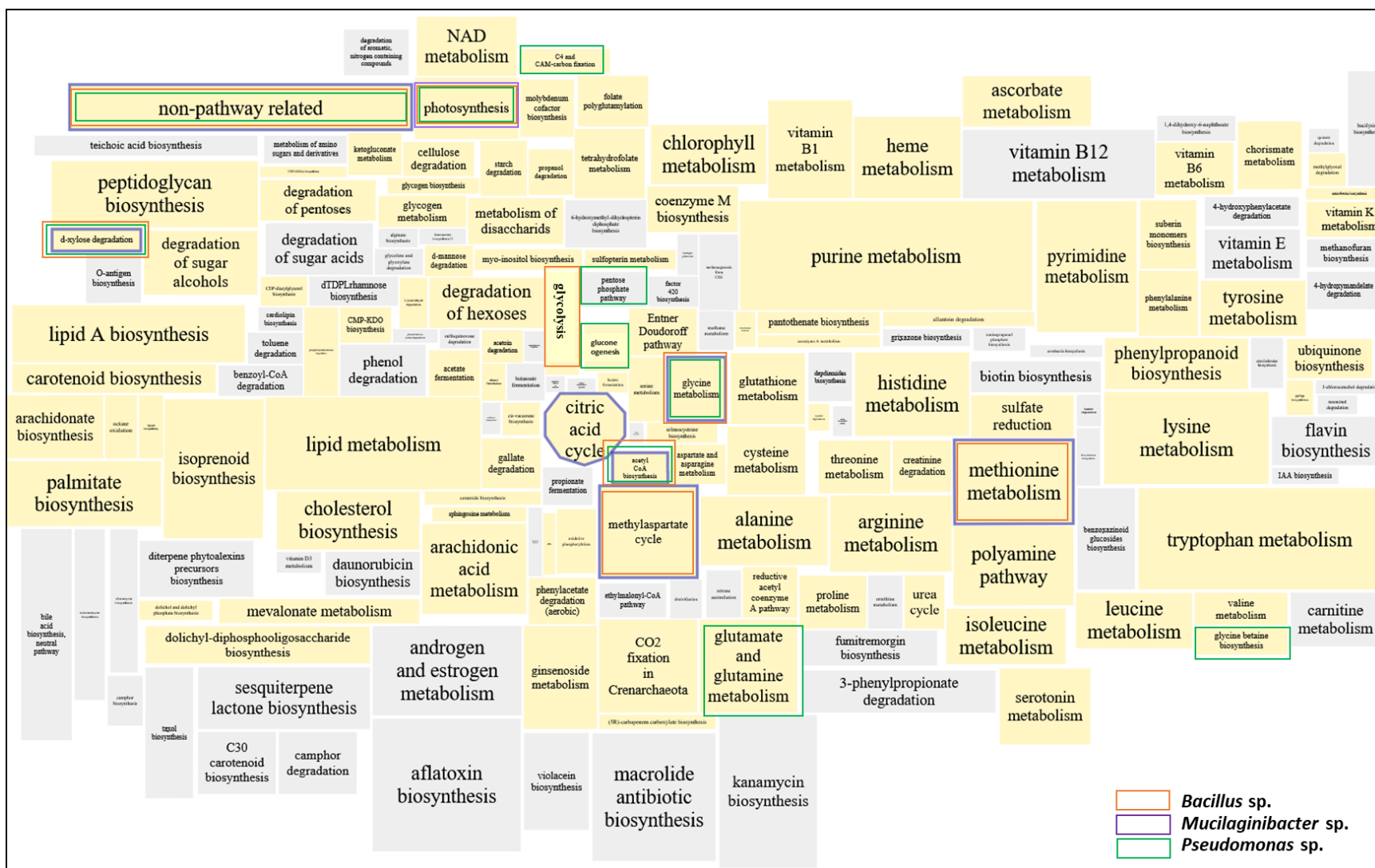


Figure 5.3 The metabolic pathways identified in cannabis flowers. The metabolic pathway with the yellow background are those, with respect to metabolic roles of cannabis flowers, identified in this study. Color (orange, purple and green) and shape indicate the metabolic pathways up-regulated by treatment with *Bacillus* sp., *Mucilaginibacter* sp. and *Pseudomonas* sp., respectively.

5.5.1 Protein synthesis

Several proteins related to protein synthesis were shown to be up-regulated and identified, from cannabis flowers treated with one of the three PGPR. The proteins expressed in flowers of cannabis plants treated with PGPR are the 40S subunit ribosome protein which decodes the genetic messages and the 60S subunit ribosome protein used to catalyze peptide bond formation (Gregory et al., 2019). Both *Bacillus* and *Pseudomonas* sp. treated plants overexpressed 40S and 60S ribosomal proteins. These proteins are involved in mRNA translation, or protein synthesis, and can contribute to the metabolic activity level of trichomes, the location for key secondary metabolite biosynthesis (Wu et al., 2012). In addition, these ribosomal proteins are critical for plant growth and adaptation (Hang et al., 2018).

5.5.2 Photosynthesis

Photosynthesis is a critical pathway for plants to acquire energy from sunlight and its end products play a key role in other metabolic pathways. In our previous study, we found that inoculation with PGPR can improve the photosynthetic rate of cannabis plants, especially during the flowering stage. Therefore, proteome profiling identification could provide evidence for possible mechanisms of PGPR effects leading to the elevated photosynthetic rate. In this study, we identified some energy proteins related to plant photosynthesis that were up-regulated by the evaluated PGPR. The up-regulated proteins in plants treated with the PGPR varied among the applied species of bacteria. For instance, in plants treated with *Bacillus* sp., the photosystem I reaction center subunit V was up-regulated, while the chloroplast envelope membrane protein, and cytochrome f were regulated in plants inoculated with *Pseudomonas* sp., and photosystem II D2 protein, PSI subunit V, PSII_BNR domain-containing protein were regulated by *Mucilaginibacter* sp.. PGPR treatment has been shown to be associated with increases in photosynthetic capacity by

regulating the relative protein profiles in various plant species including *Arabidopsis thaliana* (Kwon et al., 2016) and wheat (Yildiztugay et al., 2022). The ATP synthase complex (beta), involved in electron transport, was also identified in cannabis flowers and was up-regulated by *Pseudomonas* sp. This protein has been identified in cannabis trichomes and verified for its importance in energy production, which can be used in metabolic pathways such as those involved in carbon fixation and secondary metabolite biosynthesis in glandular trichomes (Wu et al., 2012). The increased photosynthetic rate following PGPR treatment is because those beneficial microbes regulate expression of the related photosynthesis proteins, which validates our previous results (Lyu et al., 2022).

5.5.3 Carbohydrate metabolism

5.5.3.1 Primary metabolism

Plant growth and development occur through regulating and allocating available nutrients and energy (Sakr et al., 2018). As the main energy source, sugars, in the form of sucrose as the critical product of plant photosynthesis, can manipulate biological processes involved in growth and development of plants and is the key carbohydrate for systemic source-to-sink transport in plants (Sakr et al., 2018; Wingler, 2018). In the current study, all three PGPR inoculants caused up-regulation of sucrose synthase, which is the key enzyme catalyzing the reversible cleavage of sucrose into fructose and uridine diphosphate glucose (UDP-G) which both participate in many key metabolic pathways, including energy production, carbohydrate catabolism and primary-metabolite synthesis (Stein and Granot, 2019). Sucrose synthase has been studied in cannabis plants, but mostly as related to the abiotic stress (Gao et al., 2018; Sardoei et al., 2014). However, the overexpression of sucrose synthase has been reported for other plants including strawberry, cotton and potato and *Arabidopsis*, which suggested that it can lead to early flowering (Xu and

Joshi, 2010), increased vegetative growth (Xu et al., 2012) and plant biomass, and regulate fruit ripening (Zhao et al., 2017).

5.5.3.2 The central carbohydrate metabolism pathways (glycolysis-, redox-, and tricarboxylic acid-related proteins)

The present proteomic analysis revealed that several proteins related to glycolysis and the TCA cycle were increased substantially in the flowers of PGPR inoculated cannabis plants. In the current study, the level of phosphopyruvate hydratase (enolase), which is responsible for the production of phosphoenolpyruvate in the glycolysis pathway, was only significantly expressed in the flowers of cannabis plants treated with *Bacillus* sp.. Although, the application of *Pseudomonas* sp. did not lead to changes in the levels of proteins involved in the glycolysis pathway, 6-phosphogluconate dehydrogenase levels, in the pentose phosphate pathway, was increased; it plays an important role in plant growth and development (Chen et al., 2020).

In the central glycolysis metabolic pathway, the intermediate pyruvate can be catalyzed by the pyruvate dehydrogenase into acetyl-CoA which then enters the TCA cycle and other metabolic pathways. Pyruvate oxidation was only up-regulated by *Pseudomonas* sp. treatment; it is involved in the production of NADH. The TCA cycle generates energy which serves as the main energy source for a range of biological activities and supply precursors for many biosynthetic pathways (Gupta and Gupta, 2021). The abundance of proteins involved in the TCA cycle were also increased in the cannabis flowers, such as isocitrate dehydrogenase (**Figure 5.4**). A protein overexpressed following treatment with *Bacillus* sp. is NADP-dependent isocitrate dehydrogenase, which can be found in the cytosol, chloroplasts, peroxisomes, and mitochondria. It is involved in nitrogen assimilation (Lemaitre et al., 2007), and not only leads to increased levels of nitrate in tomato (Sienkiewicz-Porzucek et al., 2010), but also plays an important role in

Arabidopsis plants under salt stress (Leterrier et al., 2012) and in the resilience of corn in the face of water stress (Aliyeva and Mamedov, 2021).

The abundance of aconitate hydratase was higher in plants treated with *Mucilaginibacter* sp.. In addition to the enzymatic activity in citrate metabolism, it is also a multifunctional protein in amino acid synthesis and lipid metabolism (Borek and Nuc, 2011). Carrari et al. (2003) verified that aconitase can regulate sucrose synthetic pathways of tomato plants. Moeder et al. (2007) indicated that aconitase is also an important enzyme in mediating oxidative stress and regulating cell death in *Arabidopsis*.

Following inoculation with *Pseudomonas* sp., overexpression of two key enzymes in TCA cycle, including oxoglutarate dehydrogenase and malic enzyme was observed. 2-oxoglutarate can be converted into succinyl CoA and degraded by 2-oxoglutarate dehydrogenase releasing CO₂ and NADH (Bunik and Fernie, 2009). It has been reported that 2-oxoglutarate dehydrogenase plays an important role in nitrogen assimilation through the alteration in levels of organic (TCA intermediates) and amino acids crucial to nitrate assimilation (Araujo et al., 2008). Although we could not conclude that the overexpression of 2-oxoglutarate, caused by *Pseudomonas* sp. treatment led to enhanced accumulation of cannabinoids and terpenes, the intermediate 2-oxoglutarate of TCA cycle is reported to link amino acids, glucosinolate, flavonoids, alkaloids and gibberellin biosynthesis (Araújo et al., 2014). The level of glutamate decarboxylase was increased by the inoculation with *Pseudomonas* sp., catalyzing the conversion of glutamate into GABA. Eventually, it re-enters the TCA cycle as succinate (**Figure 5.4**). Another enzyme up-regulated by *Pseudomonas* sp. in the TCA cycle is malic enzyme, which is responsible for the production of pyruvate, CO₂, and NADPH as well as plant growth (Sun et al., 2019).

Both pyruvate and acetyl-CoA also involve in the cellular reactions in the cannabis flowers including fatty acid, and some secondary metabolites biosynthesis pathways including cannabinoids and monoterpene and sesquiterpene biosynthesis (**Figure 5.3 & 5.5**). The application of PGPR up-regulated proteins that were involved in glycolysis, the TCA cycle and the respiratory electron transport chain, which implied that that energy generation was enhanced in cannabis flowers, thereby ensuring an adequate source to promote cannabis plant growth. Similar results were also found for the overexpressed proteins involved in carbohydrate and amino acid metabolism in canola (cv. Hyola308) under severe osmotic stress (Oskuei et al., 2018). *Pseudomonas fluorescens* FY32 inoculation onto canola increased salt tolerance by inducing an increase in the abundance of proteins related to glycolysis, the tricarboxylic acid cycle, and amino acid metabolism (Banaei-Asl et al., 2016). Overexpressed proteins in plant glycolysis and the TCA cycle caused by PGPR were also often associated with stress condition responses; bacterial inoculation has been shown to increase the abundance of TCA-related proteins (Du et al., 2016).

5.5.3.3 Glycine cleavage (GCV) system

Among the identified proteins, some are involved in one carbon metabolism and are also overexpressed by PGPR inoculants in cannabis flowers, including the glycine cleavage system P protein and 5-methyltetrahydropteroyltriglutamate-homocysteine S-methyltransferase. Some of these proteins overexpressed following inoculation of PGPR are key components of the glycine cleavage (GCV) system. As reported, there are four key proteins in the GCV system including the P protein (glycine dehydrogenase (aminomethyl-transferring)), T protein (aminomethyltransferase), L protein (dihydrolipoyl dehydrogenase) and the non-enzyme H protein (lipoyl-carrier protein) (Hasse et al., 2013). These four proteins were all up-regulated by the

inoculation with *Pseudomonas* sp., while P protein, L protein and T protein were also identified as up-regulated by *Mucilaginiabcter* sp.; *Bacillus* sp. inoculation only led to increases in the level of P protein and L protein in the cannabis flowers. Overexpression of the H-protein increased the biomass yield of tobacco plants (López-Calcano et al., 2019), which is consistent with the findings of Timm et al. (2012), who found higher level of the H-protein enhanced *Arabidopsis thaliana* growth and increased photosynthetic activity. They also found that elevated L-protein activity led to significantly higher rates of CO₂ assimilation and photorespiration, and alters cellular reactions to improve the growth of *Arabidopsis thaliana* (Timm et al., 2015). T-protein is also a storage protein. Storage proteins can be used as reservoirs to support plant growth and development and accumulates in both vegetative and reproductive tissues (Fujiwara et al., 2002). In addition, in the reaction cycle of P-, T-, L-proteins with H-protein, methylene tetrahydrofolate (CH₂-THF), CO₂, ammonia, and NADH are produced (Bauwe et al., 2010; Hasse et al., 2013; Timm et al., 2012).

5.5.4 Defense proteins

The benefits plants acquired from PGPR inoculation are from multiple aspects of metabolism and plant growth including enhanced overall production and increased stress resistance/tolerance. Some stress related proteins were overexpressed following PGPR inoculation. For instance, annexin was up-regulated by both *Bacillus* sp. and *Pseudomonas* sp. Plant annexin is a calcium-dependent phospholipid-binding protein from a superfamily of proteins which are linked to membrane lipid components (Clark et al., 2012). Annexin has multiple functions related to improving plant growth and acting in response to various abiotic stresses (Clark et al., 2012; Saad et al., 2020). In the superfamily of thioredoxin oxidoreductases, protein disulfide-isomerase and thioredoxin are the key members, which are responsible for the reversal of diverse redox-based modifications (Mata-Pérez and Spoel, 2019). Inoculation with *Bacillus* sp. also up-regulated protein disulfide-isomerase, which is involved in protein folding and assembly (Du et al., 2016). (Gruber et al., 2007) Li et al. (2013) reported that the application of PGPR recovered the expression of this protein under stress conditions. Thioredoxin domain-containing protein and peroxidase were also up-regulated in plants treated with *Mucilaginibacter* sp.. Peroxidase production in maize plants, induced by *Mucilaginibacter* sp. treatment has been reported as a key enzyme involved in oxidative mechanisms to protect plant growth under oxidative toxicity and osmotic stress (Fan and Smith, 2022).

In the case of *Pseudomonas* sp. application, plant phospholipase D (PLDs) was up-regulated. Takáč et al. (2019) and Deepika and Singh (2022) reported PLDs are important membrane lipid-modifying enzymes, which play key roles in plant growth as well as being a defense protein involved in responses to environmental stress conditions. Although the conditions used in the current study were well controlled, the application of PGPR led to the up-regulation of

stress related proteins. It seems that the selected PGPR improved plant growth not only through regulation of key metabolic pathways but also enhancing the levels of stress resistance proteins. PGPR were used to protect and promote plant growth via producing defense-related metabolites, such as flavonoids (Mhlongo et al., 2020). In the case of cannabis, trichomes, which is the major site for production of cannabinoids and terpenes, the defense-related proteins were reported to protect plants against attack from insects (Romero et al., 2008).

5.5.5 Other proteins

5.5.5.1 Cell wall

Proteins related to cell wall synthesis, such as UDP-glucuronate decarboxylase were up-regulated exclusively by *Pseudomonas* sp. in our study. UDP-glucuronate decarboxylase catalyzes the biosynthesis of UDP-xylose, which is important in cell wall synthesis (Kuang et al., 2016). *Pseudomonas* sp. also exclusively contributed to overexpression of proteins involved in the cell wall organization and modification including pectin acetyltransferase and pectinesterase. It provided a possible explanation as to why *Pseudomonas* sp. showed the best performance with regard to increases in the stem biomass accumulation in our previous study; pectin is the main component of the cannabis stem (Pejic et al., 2009). *Pseudomonas fluorescens* has also been reported to be an effective biostimulant, to regulate the biosynthesis of some secondary metabolites including pectin in citrus fruit peel (Wang et al., 2021).

5.5.5.2 Purple acid phosphatases

Purple acid phosphatase (PAP) was only up-regulated by *Bacillus* sp. and *Mucilaginibacter* sp.. Fan and Smith (2021) reported that *Bacillus* sp. showed efficient phosphate solubilization, while they did not detect any phosphate solubilization activity from *Mucilaginibacter* sp. (Fan et al., 2018). Beneficial bacteria with phosphate solubilizing activity could increase plant growth, at

least in part because PAP catalyzes the hydrolysis of inorganic phosphorus (Antonyuk et al., 2014) in the agricultural soils, thereby affecting cellular metabolism and bioenergetics (Tran et al., 2010). Some studies also demonstrated that the higher level of acid phosphatases detected in plants were related to effects on plant biomass accumulation, and played the key role in photosynthesis and respiration (Richardson, 2009; Tran et al., 2010). The overexpression of secreted PAPs, such as GmPAP14 in soybean plants, caused enhanced APase and phytase activities thereby taking full advantage of phytate in the surroundings to help contribute phosphorus for the growth of plant shoots (Kong et al., 2018).

In summary, enriched levels of key proteins caused by PGPR inoculation, as identified in this study, provide strong evidence that the presence of PGPR can regulate the proteins in cannabis flowers that are involved in metabolism and plant development. The proteins overexpressed in glycolysis and the TCA cycle in current study also play a significant role in biosynthesis of secondary metabolites. Key proteins participating in cannabinoid and terpene biosynthesis were all identified as having higher quantitative spectra.

5.6 Conclusions

Previous studies elucidated the effects of PGPR inoculation on cannabis growth and development. The current study focused on differential expression of proteins following inoculation of cannabis plants with beneficial microbes, which is important for understanding the biological process and in turn narrowing the knowledge gap regarding how these PGPR enhance cannabis growth. Based on the results of mature cannabis flower proteomic profiles, we conclude that PGPR inoculants alter a multi-protein regulatory mechanism to enhance cannabis growth and development and key cannabinoid and terpene biosynthesis. These overexpressed proteins are involved in photosynthesis, metabolic regulation, secondary metabolite biosynthesis and defense

which are key pathways in plant growth and development. These results provide insights into molecular-level mechanisms underlying positive effects of the selected PGPR strains on cannabis growth.

5.7 Reference

- Aliyeva, N., and Mamedov, Z. (2021). The Effects of water stress on the growth of corn and the activity dynamics of NADP-Dependent isocitrate dehydrogenase enzyme in the leaf and root tissues. Khazar University.
- Antonyuk, S. V., Olczak, M., Olczak, T., Ciuraszkiewicz, J., and Strange, R. W. (2014). The structure of a purple acid phosphatase involved in plant growth and pathogen defence exhibits a novel immunoglobulin-like fold. *International Union of Crystallography Journal* **1**, 101-9.
- Araújo, W. L., Martins, A. O., Fernie, A. R., and Tohge, T. (2014). 2-Oxoglutarate: linking TCA cycle function with amino acid, glucosinolate, flavonoid, alkaloid, and gibberellin biosynthesis. *Frontiers in Plant Science* **5**.
- Araujo, W. L., Nunes-Nesi, A., Trenkamp, S., Bunik, V. I., and Fernie, A. R. (2008). Inhibition of 2-oxoglutarate dehydrogenase in potato tuber suggests the enzyme is limiting for respiration and confirms its importance in nitrogen assimilation. *Plant Physiology* **148**, 1782-1796.
- Banaei-Asl, F., Farajzadeh, D., Bandehagh, A., and Komatsu, S. (2016). Comprehensive proteomic analysis of canola leaf inoculated with a plant growth-promoting bacterium, *Pseudomonas fluorescens*, under salt stress. *Biochimica et Biophysica Acta (BBA)-Proteins and Proteomics* **1864**, 1222-1236.
- Bauwe, H., Hagemann, M., and Fernie, A. R. (2010). Photorespiration: players, partners and origin. *Trends in Plant Science* **15**, 330-336.

- Bontinck, M., Van Leene, J., Gadeyne, A., De Rybel, B., Eeckhout, D., Nelissen, H., and De Jaeger, G. (2018). Recent trends in plant protein complex analysis in a developmental context. *Frontiers in Plant Science* **9**, 640.
- Borek, S., and Nuc, K. (2011). Sucrose controls storage lipid breakdown on gene expression level in germinating yellow lupine (*Lupinus luteus* L.) seeds. *Journal of Plant Physiology* **168**, 1795-1803.
- Bunik, V. I., and Fernie, A. R. (2009). Metabolic control exerted by the 2-oxoglutarate dehydrogenase reaction: a cross-kingdom comparison of the crossroad between energy production and nitrogen assimilation. *Biochemical Journal* **422**, 405-421.
- Carrari, F., Nunes-Nesi, A., Gibon, Y., Lytovchenko, A., Loureiro, M. E., and Fernie, A. R. (2003). Reduced expression of aconitase results in an enhanced rate of photosynthesis and marked shifts in carbon partitioning in illuminated leaves of wild species tomato. *Plant Physiology* **133**, 1322-1335.
- Chang, A., Jeske, L., Ulbrich, S., Hofmann, J., Koblitz, J., Schomburg, I., Neumann-Schaal, M., Jahn, D., and Schomburg, D. (2020). BRENDA, the ELIXIR core data resource in 2021: new developments and updates. *Nucleic Acids Research* **49**, D498-D508.
- Chen, L., Kuai, P., Ye, M., Zhou, S., Lu, J., and Lou, Y. (2020). Overexpression of a Cytosolic 6-Phosphogluconate Dehydrogenase Gene Enhances the Resistance of Rice to *Nilaparvata lugens*. *Plants (Basel)* **9**.
- Clark, G. B., Morgan, R. O., Fernandez, M. P., and Roux, S. J. (2012). Evolutionary adaptation of plant annexins has diversified their molecular structures, interactions and functional roles. *New Phytologist* **196**, 695-712.

- Conneely, L. J., Mauleon, R., Mieog, J., Barkla, B. J., and Kretzschmar, T. (2021). Characterization of the *Cannabis sativa* glandular trichome proteome. *PLoS One* **16**, e0242633.
- Deepika, D., and Singh, A. (2022). Plant phospholipase D: novel structure, regulatory mechanism, and multifaceted functions with biotechnological application. *Critical Reviews in Biotechnology* **42**, 106-124.
- Du, N., Shi, L., Yuan, Y., Li, B., Shu, S., Sun, J., and Guo, S. (2016). Proteomic analysis reveals the positive roles of the plant-growth-promoting rhizobacterium NSY50 in the response of cucumber roots to *Fusarium oxysporum* f. sp. *cucumerinum* inoculation. *Frontiers in Plant Science* **7**, 1859.
- Fan, D., Schwinghamer, T., and Smith, D. L. (2018). Isolation and diversity of culturable rhizobacteria associated with economically important crops and uncultivated plants in Québec, Canada.
- Fan, D., and Smith, D. L. (2021). Characterization of selected plant growth-promoting rhizobacteria and their non-host growth promotion effects. *Microbiology Spectrum* **9**, e00279-21.
- Fan, D., and Smith, D. L. (2022). *Mucilaginibacter* sp. K improves growth and induces salt tolerance in nonhost plants via multilevel mechanisms. *Frontiers in Plant Science* **13**.
- Fujiwara, T., Nambara, E., Yamagishi, K., Goto, D. B., and Naito, S. (2002). Storage proteins. *Arabidopsis Book* **1**, e0020.
- Gao, C., Cheng, C., Zhao, L., Yu, Y., Tang, Q., Xin, P., Liu, T., Yan, Z., Guo, Y., and Zang, G. (2018). Genome-wide expression profiles of hemp (*Cannabis sativa* L.) in response to drought stress. *International Journal of Genomics* **2018**.

- Gregory, B., Rahman, N., Bommakanti, A., Shamsuzzaman, M., Thapa, M., Lescure, A., Zengel, J. M., and Lindahl, L. (2019). The small and large ribosomal subunits depend on each other for stability and accumulation. *Life Science Alliance* **2**.
- Gruber, C. W., Cemazar, M., Clark, R. J., Horibe, T., Renda, R. F., Anderson, M. A., and Craik, D. J. (2007). A novel plant protein-disulfide isomerase involved in the oxidative folding of cystine knot defense proteins. *Journal of Biological Chemistry* **282**, 20435-20446.
- Gupta, R., and Gupta, N. (2021). Tricarboxylic Acid Cycle. In "Fundamentals of Bacterial Physiology and Metabolism", pp. 327-346. Springer.
- Hang, R., Wang, Z., Deng, X., Liu, C., Yan, B., Yang, C., Song, X., Mo, B., and Cao, X. (2018). Ribosomal RNA biogenesis and its response to chilling stress in *Oryza sativa*. *Plant Physiology* **177**, 381-397.
- Happyana, N. (2014). Metabolomics, proteomics, and transcriptomics of *Cannabis sativa* L. trichomes, Universitätsbibliothek Dortmund.
- Hasse, D., Andersson, E., Carlsson, G., Masloboy, A., Hagemann, M., Bauwe, H., and Andersson, I. (2013). Structure of the homodimeric glycine decarboxylase P-protein from *Synechocystis* sp. PCC 6803 suggests a mechanism for redox regulation. *Journal of Biological Chemistry* **288**, 35333-45.
- Kong, Y., Li, X., Wang, B., Li, W., Du, H., and Zhang, C. (2018). The soybean purple acid phosphatase GmPAP14 predominantly enhances external phytate utilization in plants. *Frontiers in Plant Science* **9**.
- Kuang, B., Zhao, X., Zhou, C., Zeng, W., Ren, J., Ebert, B., Beahan, C. T., Deng, X., Zeng, Q., and Zhou, G. (2016). Role of UDP-glucuronic acid decarboxylase in xylan biosynthesis in *Arabidopsis*. *Molecular Plant* **9**, 1119-1131.

- Kwon, Y. S., Lee, D. Y., Rakwal, R., Baek, S. B., Lee, J. H., Kwak, Y. S., Seo, J. S., Chung, W. S., Bae, D. W., and Kim, S. G. (2016). Proteomic analyses of the interaction between the plant-growth promoting rhizobacterium *Paenibacillus polymyxa* E681 and *Arabidopsis thaliana*. *Proteomics* **16**, 122-135.
- Lemaitre, T., Urbanczyk-Wochniak, E., Flesch, V., Bismuth, E., Fernie, A. R., and Hodges, M. (2007). NAD-dependent isocitrate dehydrogenase mutants of *Arabidopsis* suggest the enzyme is not limiting for nitrogen assimilation. *Plant Physiology* **144**, 1546-1558.
- Leterrier, M., Barroso, J. B., Valderrama, R., Palma, J. M., and Corpas, F. J. (2012). NADP-dependent isocitrate dehydrogenase from *Arabidopsis* roots contributes in the mechanism of defence against the nitro-oxidative stress induced by salinity. *The Scientific World Journal* **2012**.
- Li, J., McConkey, B. J., Cheng, Z., Guo, S., and Glick, B. R. (2013). Identification of plant growth-promoting bacteria-responsive proteins in cucumber roots under hypoxic stress using a proteomic approach. *Journal of Proteomics* **84**, 119-131.
- López-Calcagno, P. E., Fisk, S., Brown, K. L., Bull, S. E., South, P. F., and Raines, C. A. (2019). Overexpressing the H-protein of the glycine cleavage system increases biomass yield in glasshouse and field-grown transgenic tobacco plants. *Plant Biotechnology Journal* **17**, 141-151.
- Lyu, D., Backer, R., and Smith, D. L. (2022). Three plant growth-promoting rhizobacteria alter morphological development, physiology, and flower yield of *Cannabis sativa* L. *Industrial Crops and Products* **178**, 114583.
- Mata-Pérez, C., and Spoel, S. H. (2019). Thioredoxin-mediated redox signalling in plant immunity. *Plant Science* **279**, 27-33.

- Mhlongo, M. I., Piater, L. A., Steenkamp, P. A., Labuschagne, N., and Dubery, I. A. (2020). Metabolic profiling of PGPR-treated tomato plants reveal priming-related adaptations of secondary metabolites and aromatic amino acids. *Metabolites* **10**.
- Moeder, W., del Pozo, O., Navarre, D. A., Martin, G. B., and Klessig, D. F. (2007). Aconitase plays a role in regulating resistance to oxidative stress and cell death in *Arabidopsis* and *Nicotiana benthamiana*. *Plant Molecular Biology* **63**, 273-287.
- Oskuei, B. K., Bandehagh, A., Sarikhani, M. R., and Komatsu, S. (2018). Protein profiles underlying the effect of plant growth-promoting rhizobacteria on canola under osmotic stress. *Journal of Plant Growth Regulation* **37**, 560-574.
- Pejic, B., Vukcevic, M., Kostic, M., and Skundric, P. (2009). Biosorption of heavy metal ions from aqueous solutions by short hemp fibers: effect of chemical composition. *Journal of Hazardous Materials* **164**, 146-153.
- Rasheed, F., Markgren, J., Hedenqvist, M., and Johansson, E. (2020). Modeling to understand plant protein structure-function relationships—implications for seed storage proteins. *Molecules* **25**, 873.
- Richardson, A. E. (2009). Regulating the phosphorus nutrition of plants: molecular biology meeting agronomic needs. *Plant and Soil* **322**, 17-24.
- Romero, G. Q., Souza, J. C., and Vasconcellos-Neto, J. (2008). Anti-herbivore protection by mutualistic spiders and the role of plant glandular trichomes. *Ecology* **89**, 3105-3115.
- Saad, R. B., Ben Romdhane, W., Ben Hsouna, A., Mihoubi, W., Harbaoui, M., and Brini, F. (2020). Insights into plant annexins function in abiotic and biotic stress tolerance. *Plant Signaling & Behavior* **15**, 1699264.

- Sakr, S., Wang, M., Dédaldéchamp, F., Perez-Garcia, M. D., Ogé, L., Hamama, L., and Atanassova, R. (2018). The sugar-signaling hub: overview of regulators and interaction with the hormonal and metabolic network. *International Journal of Molecular Sciences* **19**.
- Sardoei, A. S., Yazdi, M. R., and Shshdadneghad, M. (2014). Effect of cycocel on growth retardant cycocel on reducing sugar, malondialdehyde and other aldehydes of *Cannabis sativa* L. *International Journal of Biosciences* **4**, 127-133.
- Sienkiewicz-Porzucek, A., Sulpice, R., Osorio, S., Krahnert, I., Leisse, A., Urbanczyk-Wochniak, E., Hodges, M., Fernie, A. R., and Nunes-Nesi, A. (2010). Mild reductions in mitochondrial NAD-dependent isocitrate dehydrogenase activity result in altered nitrate assimilation and pigmentation but do not impact growth. *Molecular Plant* **3**, 156-173.
- Stein, O., and Granot, D. (2019). An overview of sucrose synthases in plants. *Frontiers in Plant Science* **10**, 95.
- Subramanian, S., Ricci, E., Souleimanov, A., and Smith, D. L. (2016a). A proteomic approach to lipo-chitooligosaccharide and thuricin 17 effects on soybean germination unstressed and salt stress. *PloS One* **11**.
- Subramanian, S., Souleimanov, A., and Smith, D. L. (2016b). Proteomic studies on the effects of lipo-chitooligosaccharide and thuricin 17 under unstressed and salt stressed conditions in *Arabidopsis thaliana*. *Frontiers in Plant Science* **7**, 1314.
- Sun, X., Han, G., Meng, Z., Lin, L., and Sui, N. (2019). Roles of malic enzymes in plant development and stress responses. *Plant Signaling & Behavior* **14**, e1644596.
- Takáč, T., Novák, D., and Šamaj, J. (2019). Recent advances in the cellular and developmental biology of phospholipases in plants. *Frontiers in Plant Science* **10**, 362.

- Timm, S., Florian, A., Arrivault, S., Stitt, M., Fernie, A. R., and Bauwe, H. (2012). Glycine decarboxylase controls photosynthesis and plant growth. *FEBS Letters* **586**, 3692-7.
- Timm, S., Wittmiß, M., Gamlien, S., Ewald, R., Florian, A., Frank, M., Wirtz, M., Hell, R., Fernie, A. R., and Bauwe, H. (2015). Mitochondrial dihydrolipoyl dehydrogenase activity shapes photosynthesis and photorespiration of *Arabidopsis thaliana*. *The Plant Cell* **27**, 1968-1984.
- Tran, H. T., Hurley, B. A., and Plaxton, W. C. (2010). Feeding hungry plants: the role of purple acid phosphatases in phosphate nutrition. *Plant Science* **179**, 14-27.
- Wang, Z., Chen, X., Zhong, T., Li, B., Yang, Q., Du, M., Zalán, Z., and Kan, J. (2021). Bioeffector *Pseudomonas fluorescens ZX* elicits biosynthesis and accumulation of functional ingredients in citrus fruit peel: a promising strategy for a more sustainable crop. *Journal of Agricultural and Food Chemistry* **69**, 13810-13820.
- Waterborg, J. H., and Matthews, H. R. (1984). The lowry method for protein quantitation. In "Proteins" (J. M. Walker, ed.), pp. 1-3. Humana Press, Totowa, NJ.
- Wingler, A. (2018). Transitioning to the next phase: the role of sugar signaling throughout the plant life cycle. *Plant Physiology* **176**, 1075-1084.
- Wu, T., Wang, Y., and Guo, D. (2012). Investigation of glandular trichome proteins in *Artemisia annua* L. using comparative proteomics. *PloS One*.
- Xu, F., and Joshi, C. P. (2010). Overexpression of aspen sucrose synthase gene promotes growth and development of transgenic *Arabidopsis* plants. *Advances in Bioscience and Biotechnology* **1**, 426.

- Xu, S.-M., Brill, E., Llewellyn, D. J., Furbank, R. T., and Ruan, Y.-L. (2012). Overexpression of a potato sucrose synthase gene in cotton accelerates leaf expansion, reduces seed abortion, and enhances fiber production. *Molecular Plant* **5**, 430-441.
- Yildiztugay, E., Ozfidan-Konakci, C., Cavusoglu, H., Arikan, B., Alp, F. N., Elbasan, F., Kucukoduk, M., and Turkan, I. (2022). Nanomaterial sulfonated graphene oxide advances the tolerance against nitrate and ammonium toxicity by regulating chloroplastic redox balance, photochemistry of photosystems and antioxidant capacity in *Triticum aestivum*. *Journal of Hazardous Materials* **424**, 127310.
- Zhao, C., Hua, L.-N., Liu, X.-F., Li, Y.-Z., Shen, Y.-Y., and Guo, J.-X. (2017). Sucrose synthase FaSS1 plays an important role in the regulation of strawberry fruit ripening. *Plant Growth Regulation* **81**, 175-181.

Chapter 6 General Discussion

Cannabis production is increasing worldwide, as a result of legalization, to varying degrees, in many countries, including both as industrial hemp and medicinal marijuana. Therapeutic use of cannabis has focused production on flower yield and quality, as the key behavior-modifying secondary metabolites are biosynthesized in flowers, specifically in flower-associated trichomes. Improved understanding of agricultural practices that enhance cannabis plant growth and development are needed. Application of plant growth enhancing microbes is a sustainable strategy to enhance plant growth and improve plant stress resistance. However, the effects of applying these beneficial microbes on cannabis growth are not well studied. Hence, this research effort was focused on the examination of the interaction between PGPR and cannabis plants, to fill the gap.

The PGPR selected was based on Fan et al. (2018), who isolated a set of microbes from the local Quebec area and identified them as PGPR on the corn and canola grown under optimum and stressful conditions. In this study, three PGPR (*Bacillus* sp., *Mucilaginibacter* sp. and *Pseudomonas* sp.) were initially tested rigorously through an experiment using Magenta Jars to monitor the influence of PGPR inoculation on cannabis root structure, by measuring root length, volume, density and surface area. In addition, a set of greenhouse trials were conducted to determine the effects of PGPR application on cannabis plant growth throughout the entire growth period, from initial vegetative to final reproduction, by measuring agronomic traits, physiological variables and biomass production. Thirdly, metabolomics analysis was applied to identify and quantify the key cannabinoid and terpene contents in cannabis flowers, to demonstrate the effects of PGPR inoculation on the biosynthesis of secondary metabolites. Finally, proteomics techniques were used to illustrate at least some of the mechanisms underlying how PGPR interact with cannabis plants, and how this leads to the observed effects on yield and quality.

Cannabis production is mainly divided into seed and cloning propagation. Seed cultivation is easy but leads to possible genotype cross contamination and a lack of genetic uniformity. Cloning is time consuming but provides consistent genetics from the selected mother plant(s). Thus, shortening the time required for cutting rooting and development provides an important approach for obtaining high yield and optimal quality more quickly and at reduced cost. Rooting morphology, is a key element in the potential of plants to absorb nutrients and water (Qin et al., 2006). As our results demonstrated (**Chapter 3**), the cutting size at the vegetative stage was significantly ($p = 0.01$) related to the root development, and inoculation with microbes was shown to affect root morphology, for example, root diameter, root volume and root length (**Supplementary Figure 6.1**). For the inoculation with PGPR, during cannabis plant propagation, *Pseudomonas* sp. inoculation most enhances root length; it was also the most efficient PGPR, causing the greatest increases in photosynthesis and flower yield. Therefore, our results further provided evidence that cutting growth during early plant propagation provided the basis for subsequent plant growth; growth of cannabis during the vegetative stage is strongly correlated with reproductive growth and final biomass.

In the case of *Mucilaginibacter* sp., inoculation had the greatest effects on the axillary bud formation at the stage of cannabis flowering. The physiological state/activity of apical buds plays a pivotal role in bud formation; in a similar way, axillary buds also determine the developmental maturity of stem and branching hierarchy (Thomas and Hay, 2009). As Schneider et al. (2019) reported, the regulation of bud outgrowth could be the result of competition for carbohydrates among branches. In the current study, fewer buds were initiated in plants treated with *Pseudomonas* sp., but this inoculation resulted in taller and heavier cannabis plant stems. In addition, IAA production induced by PGPR has been shown to affect axillary bud production

(Rawat et al., 2020). The PGPR used in this study have been reported to affect phytohormone production (Fan et al., 2018). The growth promotion traits of *Mucilaginibacter* sp. have been reported by Fan and Smith (2022), who found it promotes corn growth through inducing ion transportation, photosynthesis, ABA biosynthesis, and carbon metabolism, and enhances *Arabidopsis* growth by releasing auxin, gibberellin, and MPK6 signaling. Fan et al. (2018) found that inoculation of *Bacillus* sp. led to increased chlorophyll content of maize, which was associated with plant growth stimulation. In addition, our study also demonstrated that cannabis yield is related to all measured variables, including photosynthesis, height, flower bud number and fresh weight. Interestingly, all above variables correlated with each other. The above ground biomass yield significantly relates to plant height, node number, number of flower buds and flower fresh weight. While the number of flower buds relates to plant height and node number. Therefore, plant growth enhancement should be considered from all aspects of plant morphology.

The content of specific cannabinoids and terpenes affects the therapeutic and recreational value of cannabis flowers. Secondary metabolite biosynthesis meaningfully affects the final application/utility of cannabis plants. Thus, the key cannabinoids and terpenes were quantified and identified. We also quantified the precursors and derivatives of both THC and CBD to understand the pathways of cannabinoid biosynthesis. To analyze these crucial biochemical compounds, the cannabis flowers were extracted, and the extracts injected into LC-MS/MS, UHPLC, and GC-MS. A total of 16 key cannabinoids and 21 terpenes were identified and quantified in this study (**Chapter 4**). In cannabis production, the chemotype is defined based on the abundance of THC(A) and/or CBD(A). For the cultivar CBD Kush, used in this study, the ratio of CBD(A): THC(A) is about 1.5, which indicated that CBD Kush is dominated by CBD. The total CBD(A) plus THC(A)

constituted about 94% of total quantified of cannabinoids. The sum of all targeted cannabinoids was about 18-26%, while there is only 2-4% of 21 terpenes in every gram dried cannabis flower.

The biosynthesis of secondary metabolites in plants is affected by inoculation with PGPR, but variation occurred depending on the beneficial microbe and the crop. We assessed several studies in the Review Section (**Chapter 2**), which reported the effects of PGPR on accumulation of key cannabinoids in cannabis plant (Conant et al., 2017; Pagnani et al., 2018). There are numerous studies illustrating the effects of inoculation with PGPR on secondary metabolite biosynthesis for other plant species. For instance, the application of a consortium of *Chitinophaga* sp., *Allorhizobium* sp., *Duganella* sp., and *Micromonospora* sp., resulted in significantly more alkannin and shikonin in the hairy roots than the uninoculated control of *Alkanna tinctoria* plants (Rat et al., 2021). De Leo et al. (2017) found a group of 37 endophytic bacterial strains that enhanced alkamide biosynthesis when inoculated onto *Echinacea purpurea* (L.) Moench (Asteraceae). Pagnani et al. (2018) found that inoculation with a microbial consortium led to THC, CBD and CBN increases in cannabis cultivar “Finola”, which was potentially attributed to enhanced nutrient availability provided by PGPR. For the PGPR strains used in current study, two of the selected strains showed positive effects on the accumulation of cannabinoids and terpenes. Unlike the performance PGPR on the cannabis flower yield, *Mucilaginibacter* sp. surprisingly resulted in the greatest effects on the accumulation of THC and CBD (14% increase), followed by *Pseudomonas* sp., while there was no benefit associated with *Bacillus* sp. Same trends were also observed for the set of quantified terpenes (**Chapter 4**).

To understand how these PGPR inoculations led to the described results, another omics technology was used; it helped elucidate the promotion of growth and secondary metabolite biosynthesis mechanisms at the molecular level. Thus, whole cannabis flower proteome profile

was analyzed to provide enhanced understanding of the function of *Bacillus* sp., *Mucilaginibacter* sp. and *Pseudomonas* sp. in the enhancing plant growth and key secondary metabolite biosynthesis. Results of the proteomics analysis (**Chapter 5**) indicated that the selected PGPR led to better yield and photosynthetic rates, which was related to more presence of specific proteins involved in energy production, primary metabolism and photosynthesis pathways in cannabis flowers. For instance, up-regulated proteins expressed in cannabis flowers following *Pseudomonas* sp. treatment included ATP synthase subunit beta, cytochrome f, phospholipase D, pectin esterase, pyruvate dehydrogenase, annexin (functions in photosynthesis), lipid metabolism, primary metabolism and defense. The important proteins, photosystem II D2 protein, aconitate hydratase, ribosomal protein, and peroxidase, were differentially expressed in the plants treated with *Mucilaginibacter* sp.. The PGPR strain which provided the best enhancement of root length of vegetative cuttings, yield enhancement, photosynthetic rate and harvest index (**Chapter 3**), also up-regulated the greatest number of proteins involved in multiple-function pathways. In addition, that strain caused the most abundant levels of cannabinoids and terpenes accumulated in cannabis plants (**Chapter 4**) and also led to the overexpression of Bet_v_1 domain-containing protein, related to the biosynthesis of olivetolic acid, which is the precursor of cannabinoids (**Chapter 5**).

Proteomics analysis allows improved global understanding of processes modulated through levels of proteins, providing a window on understanding the complex molecular mechanisms involved in plant-bacteria associations (Alberton et al., 2020). There is limited research on the interactions between PGPR and cannabis plants at the proteomic level. However, some studies have illustrated differential proteomic response patterns of other crops inoculated with PGPR leading to enhanced production of proteins involved in metabolism/energy and plant resistance. For example, increased production of 22 proteins were identified in rice inoculated with

Bacillus cereus NMSL88; these were involved in plant growth and development and plant defense and included xyloglucan endotransglycosylase, peroxidases, glutathione S-transferases and kinases (Wang et al., 2013). Inoculation of *Herbaspirillum frisingense* GSF 30 onto the grass *Miscanthus sinensis* suggested that *H. frisingense* improves plant growth by modulating protein expression in plant hormone signaling pathways that affect biomass production by grass plants (Straub et al., 2013). Lade et al. (2019) reported improved abundance of proteins involved in photosynthesis, plastid functions, and self-defense proteins (NADP-dependent malic enzyme) in maize seedlings treated with *Azospirillum brasilense* (Sp7). The protein levels in our study were increased by the three PGPR, and these increased various aspects of plant growth, including elements of key metabolism pathways. Therefore, we can conclude that the three PGPR investigated affect cannabis growth and development by altering the abundance of key metabolic proteins. Proteomic analysis has provided an in-depth understanding of plant mechanisms and the modes of action elicited by PGPR involved in plant growth promotion and biochemical compound accumulations, which appear to be manipulated through intricate signaling pathways within the context of plant-microbe interaction.

Chapter 7 Final Conclusions and Future Directions

Cannabis sativa L. is a multi-functional plant with medical, recreational, fibre and biofuel value. Its medicinal and recreational use is contributed to by unique biochemical compounds in cannabis plants. Cannabinoids, of which THC and CBD are the key components, are largely responsible for the therapeutic properties of this plant. However, cannabis was made illegitimate for about a century, which has led to its not being well understood with regard to the production to the biosynthesis of secondary metabolites at this time. PGPR have been used as sustainable technologies in agricultural production for the last two decades. PGPR are isolated from the plant rhizosphere and are often associated with host growth and development. Yet, there is almost no research constituting in depth exploration of the relationship between cannabis and PGPR isolated from non-cannabis plants. Therefore, this study focused on three PGPR, which have been reported to show growth promotion potential on corn and canola (and Arabidopsis) under both optimum and stress conditions. Strains of *Bacillus* sp., *Mucilaginibacter* sp., *Pseudomonas* sp. were applied on to cannabis (CBD Kush) cuttings at the vegetative stage; rooting speed, flower yield and formation during the reproductive stage of development were evaluated. Metabolomics and proteomics were applied as analytical approaches in order to study secondary metabolites and proteins that are synthesized in the cannabis flowers. Furthermore, the effectiveness of PGPR applied in liquid King's B bacterial growth medium on the growth of cannabis also was investigated to provide a more efficacious technology for efficient industrial production.

The findings of the study on plant growth from the vegetative to flowering stage, and also on secondary metabolites biosynthesis and proteome profiling in cannabis flowers implied that at least some PGPR can alter cannabis plant growth via: 1) enhancing rooting of cannabis cuttings at the vegetative stage, 2) improving plant photosynthesis, 3) regulating the expression of the relevant

proteins in cannabis flowers, 4) increasing the flower numbers and axillary bud outgrowth and final flower biomass, and 5) altering the accumulation of key cannabinoids and terpenes.

Overall, this study is the first to provide a comprehensive understanding of the potential role of phytomicrobiome members in cannabis production through work on the responses of cannabis plants to PGPR at the levels of cannabis growth and development, phytochemical compound biosynthesis, and the effects of PGPR on plants on the proteome. In addition, this study also contributed to development of potential production techniques leading to higher quality cannabis flowers through changes to yield of cannabinoids/terpenes, which could lead improved medicinal utility. Moreover, the knowledge of plant responses influenced by the phytomicrobiome has also been extended to a new crop species and could be a feasible application to sustainable cannabis production systems, and possibly for other crops as well.

Results of the current study highlight in-depth research in the critical role of PGPR on cannabis production, however, there are still many gaps; future studies are needed to expand the work and detail new findings associated with the above results. Future research directions could be: 1) metabolomics analysis of the cannabinoids: only several targeted key cannabinoids being focused on and analyzed from among the 113 cannabinoids in cannabis flowers; some untargeted cannabinoids should also be explored, 2) investigation of possible approaches to change the ratio of CBD/THC in cannabis plants, which will benefit both medicinal cannabis and industrial hemp producers, 3) examination of the possible mechanisms that underpin the effects of PGPR on sesquiterpenes but not monoterpenes, 4) microbe-to-plant signaling: the efficiency of pure cells and cells with growth medium were evaluated in this study, and suggest that microbial signal molecule(s) might be responsible for some part of observed plant growth promotion, 5) development of potentially commercializable bioinoculants: three PGPR have been tested on a set

of crops for growth enhancement, including corn, canola, and now cannabis, and show promising effects on all of these crops. It is important to consider deploying these, and similar PGPR, as bioinoculants to support crop production worldwide.

Bibliography

- Ahemad, M., and Kibret, M. (2014). Mechanisms and applications of plant growth promoting rhizobacteria: current perspective. *Journal of King Saud University-science* **26**, 1-20.
- Alberton, D., Valdameri, G., Moure, V. R., Monteiro, R. A., Pedrosa, F. d. O., Müller-Santos, M., and de Souza, E. M. (2020). What did we learn from plant growth-promoting rhizobacteria (PGPR)-grass associations studies through proteomic and metabolomic approaches? *Frontiers in Sustainable Food Systems* **4**, 607343.
- Andre, C. M., Hausman, J.-F., and Guerriero, G. (2016). *Cannabis sativa*: the plant of the thousand and one molecules. *Frontiers in Plant Science* **7**, 19.
- Atakan, Z. (2012). Cannabis, a complex plant: different compounds and different effects on individuals. *Therapeutic Advances in Psychopharmacology* **2**, 241-254.
- Beneduzi, A., Ambrosini, A., and Passaglia, L. M. (2012). Plant growth-promoting rhizobacteria (PGPR): their potential as antagonists and biocontrol agents. *Genetics Molecular Biology* **35**, 1044-1051.
- Bhattacharyya, P. N., and Jha, D. K. (2012). Plant growth-promoting rhizobacteria (PGPR): emergence in agriculture. *World Journal of Microbiology & Biotechnology* **28**, 1327-1350.
- Conant, R., Walsh, R., Walsh, M., Bell, C., and Wallenstein, M. (2017). Effects of a microbial biostimulant, Mammoth PTM, on *Cannabis sativa* bud yield. *Journal of Horticulture and Forestry* **4**, 2376-0354.1000191.
- Danish, S., and Zafar-ul-Hye, M. (2019). Co-application of ACC-deaminase producing PGPR and timber-waste biochar improves pigments formation, growth and yield of wheat under drought stress. *Scientific Reports* **9**, 1-13.

- de Aquino, G. S., Shahab, M., Moraes, L. A., and Moreira, A. (2022). Plant growth promoting rhizobacteria increased canola yield and root system. *Journal of Plant Nutrition*, 1-7.
- De Leo, M., Maggini, V., Mengoni, A., Rosaria, G. E., Miceli, E., Bandeira Reidel, R. V., Biffi, S., Pistelli, L., Fani, R., and Firenzuoli, F. (2017). Chemical profile of alkamides in *Echinacea purpurea* axenic in vitro plants infected with their endophytic bacteria. In "International PSE Symposium New & Old Phytochemicals: Their Role in Ecology, Veterinary, & Welfare", pp. 32-32. Congresso PSE 2017.
- Fan, D., Schwinghamer, T., and Smith, D. L. (2018). Isolation and diversity of culturable rhizobacteria associated with economically important crops and uncultivated plants in Québec, Canada. *Systematic Applied Microbiology* **41**, 629-640.
- Fan, D., and Smith, D. L. (2021). Characterization of selected plant growth-promoting rhizobacteria and their non-host growth promotion effects. *Microbiology Spectrum* **9**, e00279-21.
- Fan, D., and Smith, D. L. (2022). *Mucilaginibacter* sp. K improves growth and induces salt tolerance in nonhost plants via multilevel mechanisms. *Frontiers in Plant Science* **13**.
- Fan, X., Zhang, S., Mo, X., Li, Y., Fu, Y., and Liu, Z. (2017). Effects of plant growth-promoting rhizobacteria and N source on plant growth and N and P uptake by tomato grown on calcareous soils. *Pedosphere* **27**, 1027-1036.
- Hillig, K. W. (2005). Genetic evidence for speciation in *Cannabis* (Cannabaceae). *Genetic Resources and Crop Evolution* **52**, 161-180.
- Lade, S. B., Román, C., del Cueto-Ginzo, A. I., Serrano, L., Sin, E., Achón, M. A., and Medina, V. (2019). Differential proteomics analysis reveals that *Azospirillum brasilense* (Sp7)

- promotes virus tolerance in maize and tomato seedlings. *European Journal of Plant Pathology* **155**, 1241-1263.
- Li, H. L. (1973). An archaeological and historical account of cannabis in China. *Economic Botany* **28**, 437-448.
- Lyu, D., Backer, R., and Smith, D. L. (2022). Three plant growth-promoting rhizobacteria alter morphological development, physiology, and flower yield of *Cannabis sativa* L. *Industrial Crops and Products* **178**, 114583.
- Nandal, M., and hooda, R. (2013). Plant growth promoting rhizobacteria: a review article *International Journal of Current Research* **5**, 3863-3871.
- Ortízcastro, R., Contrerascornejo, H. A., Macíasrodríguez, L., and Lópezbucio, J. (2009). The role of microbial signals in plant growth and development. *Plant Signaling & Behavior* **4**, 701-712.
- Pagnani, G., Pellegrini, M., Galieni, A., D'Egidio, S., Matteucci, F., Ricci, A., Stagnari, F., Sergi, M., Sterzo, C. L., and Pisante, M. (2018). Plant growth-promoting rhizobacteria (PGPR) in *Cannabis sativa* 'Finola'cultivation: An alternative fertilization strategy to improve plant growth and quality characteristics. *Industrial Crops and Products* **123**, 75-83.
- Parveen, H., Singh, A. V., Khan, A., Prasad, B., and Pareek, N. (2018). Influence of plant growth promoting rhizobacteria on seed germination and seedling vigour of green gram. *International Journal of Chemical Studies* **6**, 611-618.
- Qin, R., Stamp, P., and Richner, W. (2006). Impact of tillage on maize rooting in a Cambisol and Luvisol in Switzerland. *Soil and Tillage Research* **85**, 50-61.

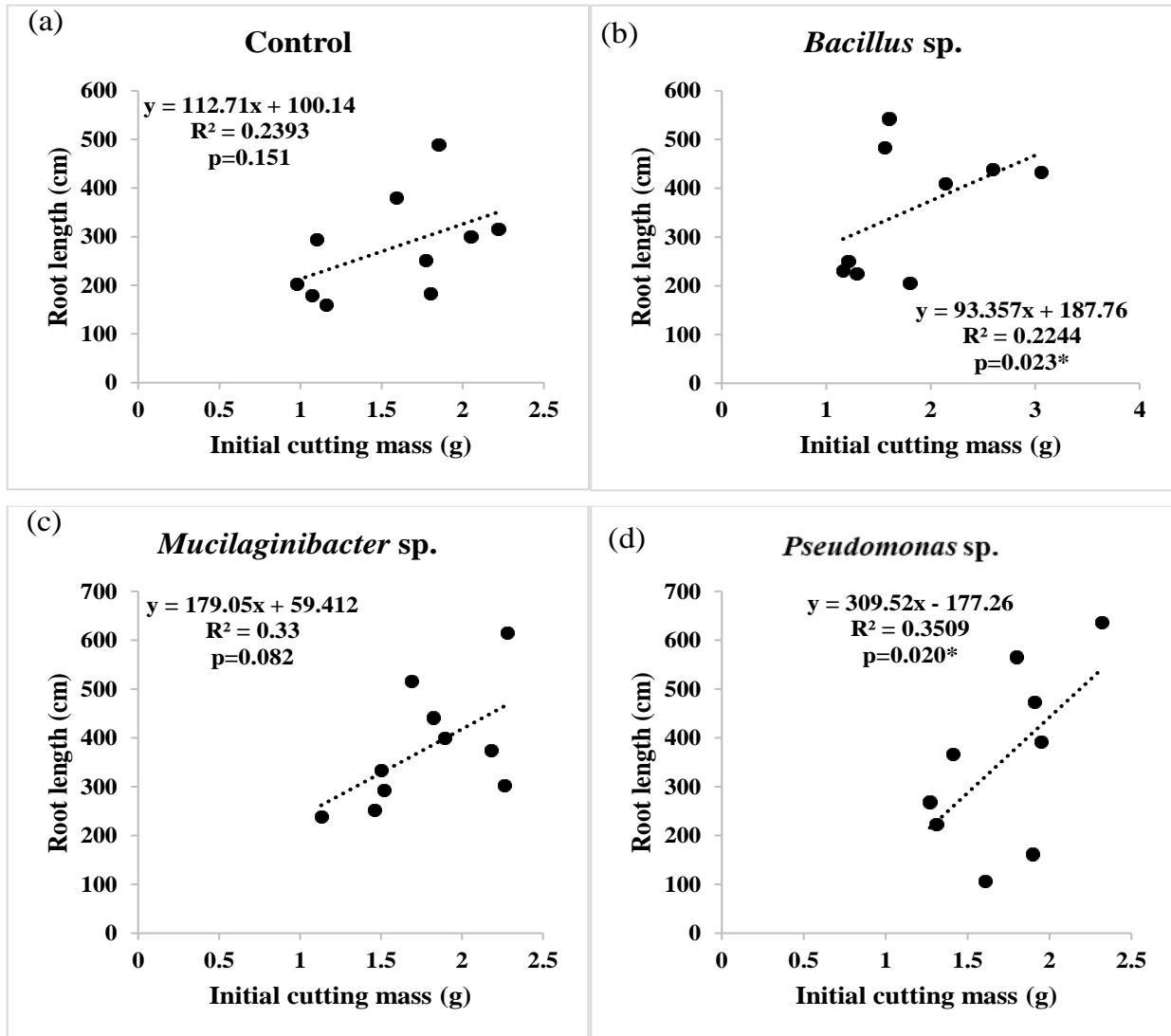
- Rais, A., Jabeen, Z., Shair, F., Hafeez, F. Y., and Hassan, M. N. (2017). *Bacillus* spp., a bio-control agent enhances the activity of antioxidant defense enzymes in rice against *Pyricularia oryzae*. *PLoS One* **12**, e0187412.
- Rana, A., and Choudhary, N. (2010). Floral Biology and Pollination Biology of *Cannabis sativa* L. *The International Journal of Plant Reproductive Biology* **2**, 191-195.
- Rat, A., Naranjo, H. D., Krigas, N., Grigoriadou, K., Maloupa, E., Alonso, A. V., Schneider, C., Papageorgiou, V. P., Assimopoulou, A. N., Tsafantakis, N., Fokialakis, N., and Willems, A. (2021). Endophytic bacteria from the roots of the medicinal plant *Alkanna tinctoria* Tausch (Boraginaceae): Exploration of plant growth promoting properties and potential role in the production of plant secondary metabolites. *Frontiers in Microbiology* **12**.
- Rawat, P., Shankhdhar, D., and Shankhdhar, S. (2020). Plant growth-promoting rhizobacteria: a booster for ameliorating soil health and agriculture production. In "Soil Health", pp. 47-68. Springer.
- Ren, G., Zhang, X., Li, Y., Ridout, K., Serrano-Serrano, M. L., Yang, Y., Liu, A., Ravikanth, G., Nawaz, M. A., and Mumtaz, A. S. (2021). Large-scale whole-genome resequencing unravels the domestication history of *Cannabis sativa*. *Science Advances* **7**, eabg2286.
- Ricci, E. C. (2015). Investigating the role of *Pseudomonas* sp. and *Bacillus* sp. biofilms as plant growth promoting inoculants, Doctoral dissertation, McGill University, Montreal Quebec, Canada.
- Ryz, N. R., Remillard, D. J., and Russo, E. B. (2017). Cannabis roots: a traditional therapy with future potential for treating inflammation and pain. *Cannabis and Cannabinoid Research* **2**, 210-216.

- Schneider, A., Godin, C., Boudon, F., Demotes-Mainard, S., Sakr, S., and Bertheloot, J. (2019). Light regulation of axillary bud outgrowth along plant axes: an overview of the roles of sugars and hormones. *Frontiers in Plant Science* **10**, 1296.
- Shah, A., Subramanian, S., and Smith, D. L. (2022). Seed priming with *Devosia* sp. cell-free supernatant (CFS) and citrus bioflavonoids enhance canola and soybean seed germination. *Molecules* **27**, 3410.
- Singh, R. P., and Jha, P. N. (2017). The PGPR *Stenotrophomonas maltophilia* SBP-9 augments resistance against biotic and abiotic stress in wheat plants. *Frontiers in Microbiology* **8**, 1945.
- Skypala, I. J., Jeimy, S., Brucker, H., Nayak, A. P., Decuyper, I. I., Bernstein, J. A. (2022). International Cannabis Allergy Collaboration. Cannabis-related allergies: An international overview and consensus recommendations. *Allergy*, *77*(7), 2038-2052.
- Smith, D. L., Subramanian, S., Lamont, J. R., and Bywater-Ekegård, M. (2015). Signaling in the phytomicrobiome: breadth and potential. *Frontiers in Plant Science* **6**, 709.
- Straub, D., Yang, H., Liu, Y., Tsap, T., and Ludewig, U. (2013). Root ethylene signalling is involved in *Miscanthus sinensis* growth promotion by the bacterial endophyte *Herbaspirillum frisingense* GSF30T. *Journal of Experimental Botany* **64**, 4603-4615.
- Takishita, Y., Souleimanov, A., Bourguet, C., Ohlund, L. B., Arnold, A. A., Sleno, L., and Smith, D. L. (2021). *Pseudomonas entomophila* 23S produces a novel antagonistic compound against *Clavibacter michiganensis* subsp. *michiganensis*, a pathogen of tomato bacterial canker. *Applied Microbiology* **1**, 60-73.
- Thomas, R., and Hay, M. (2009). Axillary bud outgrowth potential is determined by parent apical bud activity. *Journal of Experimental Botany* **60**, 4275-4285.

- Vacheron, J., Desbrosses, G., Bouffaud, M. L., Touraine, B., Moënne-Loccoz, Y., Muller, D., Legendre, L., Wisniewski-Dyé, F., and Prigent-Combaret, C. (2013). Plant growth-promoting rhizobacteria and root system functioning. *Frontiers in Plant Science* **4**, 356.
- Wang, L. X., & Chan, N. (2023). Is Grass Greener in the Gray Zone? Legalization and Innovation in the Cannabis Market. *Legalization and Innovation in the Cannabis Market (February 28, 2023)*.
- Wang, W., Chen, L. N., Wu, H., Zang, H., Gao, S., Yang, Y., Xie, S., and Gao, X. (2013). Comparative proteomic analysis of rice seedlings in response to inoculation with *Bacillus cereus*. *Letters in Applied Microbiology* **56**, 208-215.
- Welling, M. T., Shapter, T., Rose, T. J., Liu, L., Stanger, R., and King, G. J. (2016). A belated green revolution for cannabis: virtual genetic resources to fast-track cultivar development. *Frontiers in Plant Science* **7**.
- Wilkes, T. I., Warner, D. J., Edmonds-Brown, V., Davies, K. G., and Denholm, I. (2021). The tripartite Rhizobacteria-AM fungal-host plant relationship in winter wheat: impact of multi-species inoculation, tillage regime and naturally occurring Rhizobacteria species. *Plants* **10**, 1357.
- Winston, M. E., Hampton-Marcell, J., Zarraindia, I., Owens, S. M., Moreau, C. S., Gilbert, J. A., Hartsel, J., Kennedy, S. J., and Gibbons, S. M. (2014). Understanding cultivar-specificity and soil determinants of the cannabis microbiome. *PLoS One* **9**, e99641.
- Zlas, J., Stark, H., Seligman, J., Levy, R., Werker, E., Breuer, A., and Mechoulam, R. (1993). Early medical use of cannabis. *Nature* **363**, 215.

Appendix A

Chapter 3



Supplementary Figure 3.1. Linear regression relationships between initial cuttings mass and final root length with PGPR inoculation: (a) MgSO₄ (control); (b) *Bacillus* sp. (c) *Mucilaginibacter* sp. (d) *Pseudomonas* sp. after two weeks of growth in magenta jars following PGPR inoculation

*Correlation is significant at the 0.05 level.



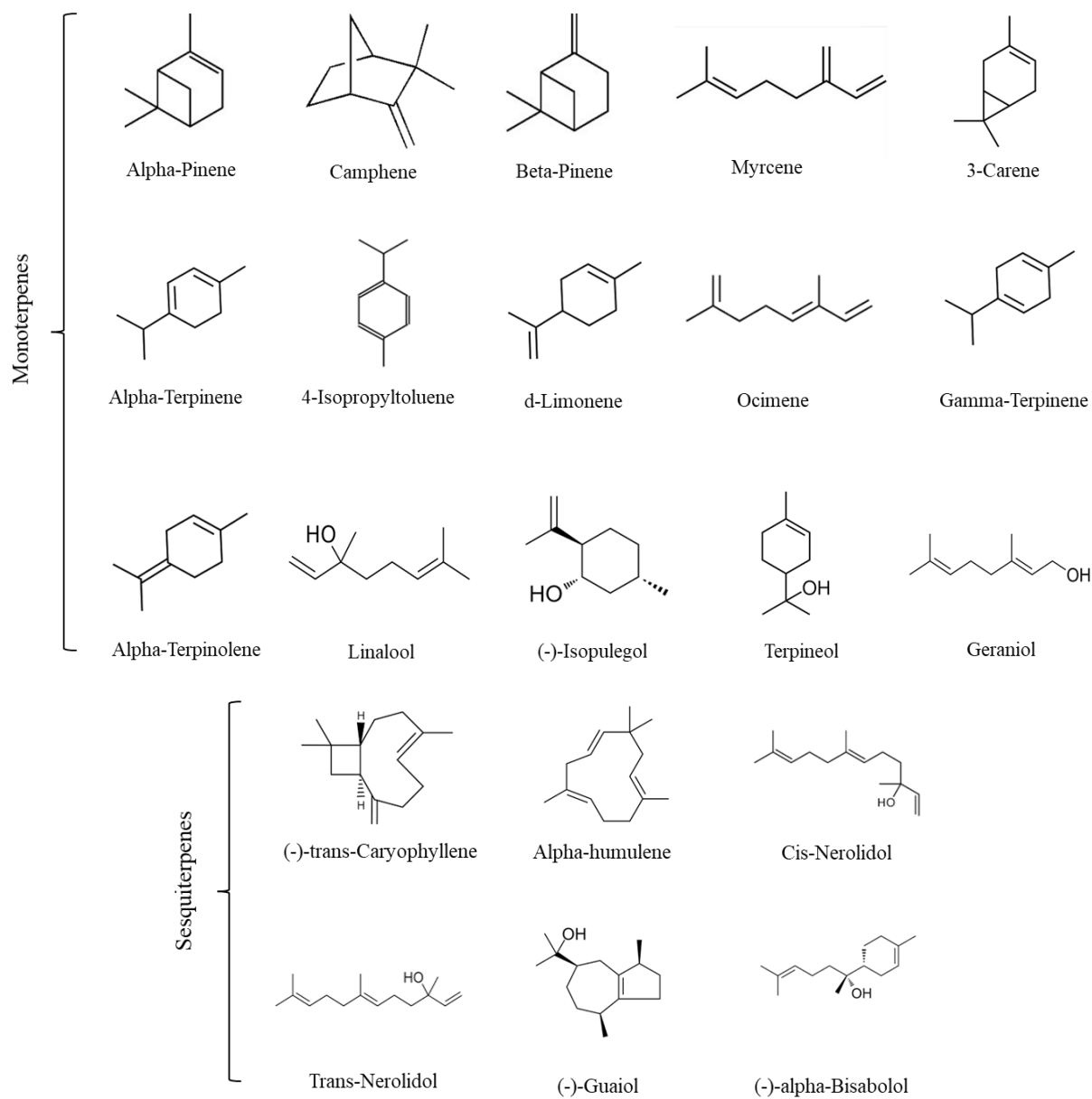
Supplementary Figure 3.2. The flowering cannabis plant treated with pure PGPR suspension (control, *Mucilaginibacter* sp., *Bacillus* sp., and *Pseudomonas* sp.)

Appendix B

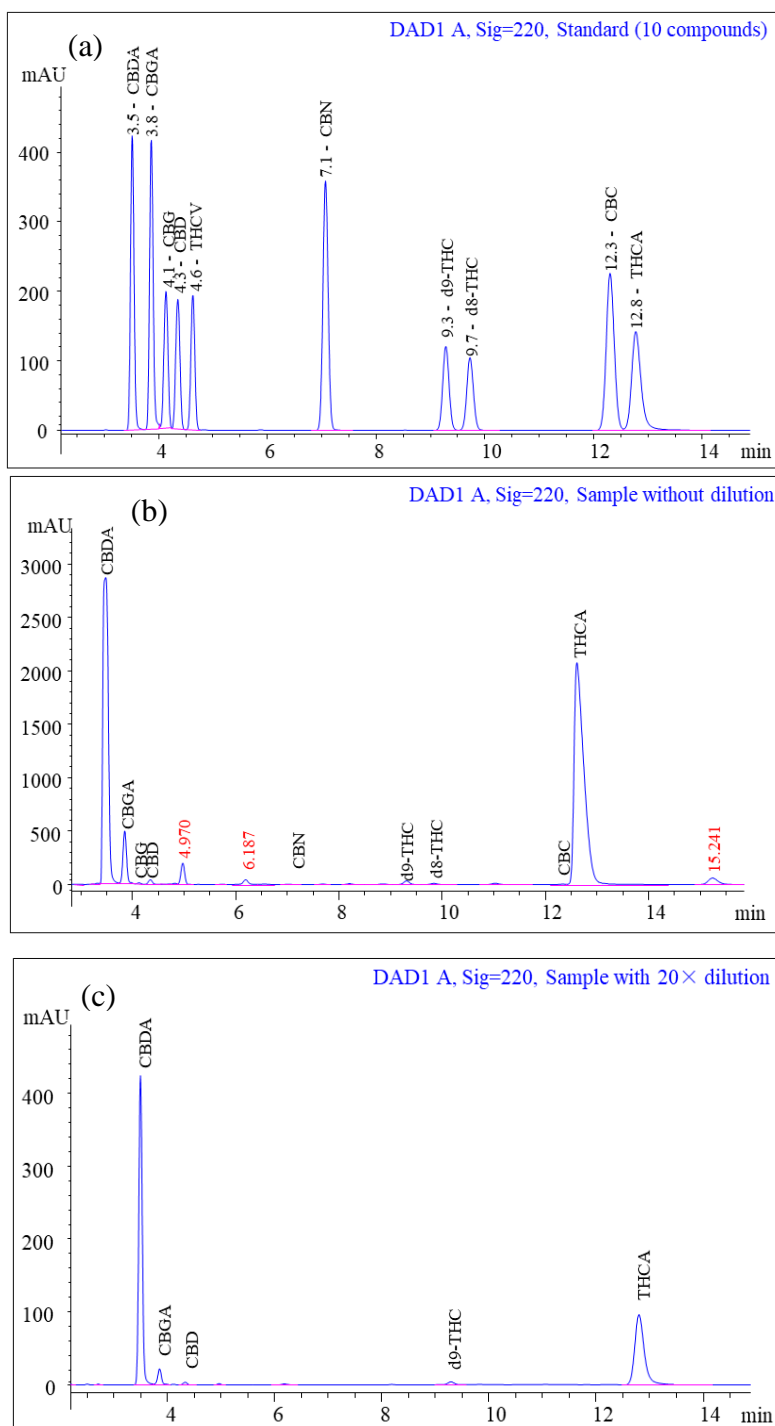
Chapter 4

<p>Cannabigerolic acid (CBGA)</p>	<p>Cannabidiolic acid (CBDA)</p>	<p>Tetrahydrocannabinolic acid (THCA)</p>	<p>Cannabichromenic acid (CBCA)</p>
<p>Cannabidivarinic acid (CBDVA)</p>	<p>Tetrahydrocannabivarinic acid (THCVA)</p>	<p>Cannabinolic acid (CBNA)</p>	<p>Cannabigerol (CBG)</p>
<p>Cannabidiol (CBD)</p>	<p>Δ9-Tetrahydrocannabinol (Δ9-THC)</p>	<p>Δ8-Tetrahydrocannabinol (Δ8-THC)</p>	<p>Cannabichromene (CBC)</p>
<p>Cannabicyclol (CBL)</p>	<p>Cannabinol (CBN)</p>	<p>Tetrahydrocannabivarin (THCV)</p>	<p>Cannabidivarin (CBDV)</p>

Supplementary Figure 4.1 The chemical structure of all targeted cannabinoids in cannabis flowers



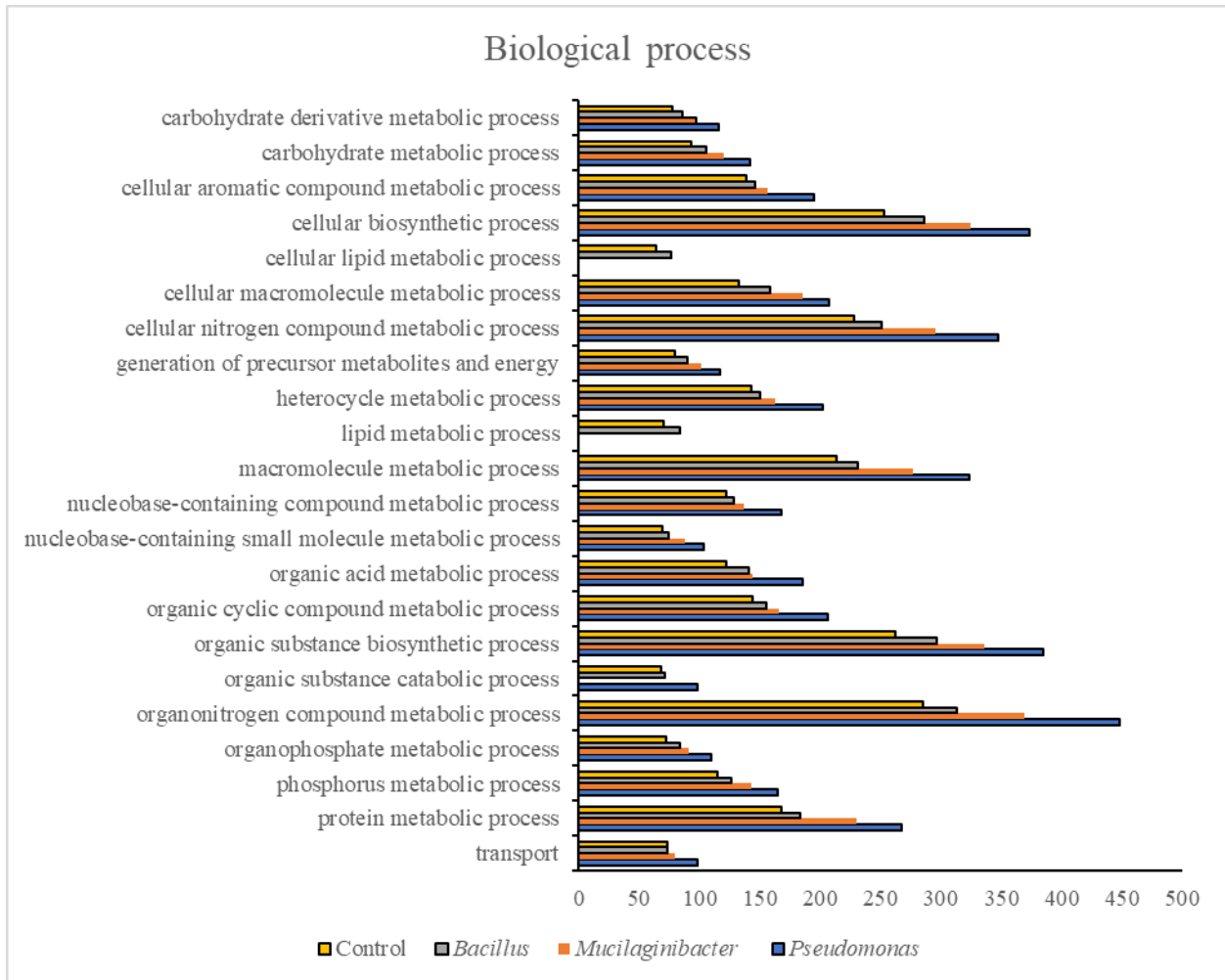
Supplementary Figure 4.2 The chemical structure of terpenes (monoterpenes and sesquiterpenes) identified and quantified in cannabis flowers



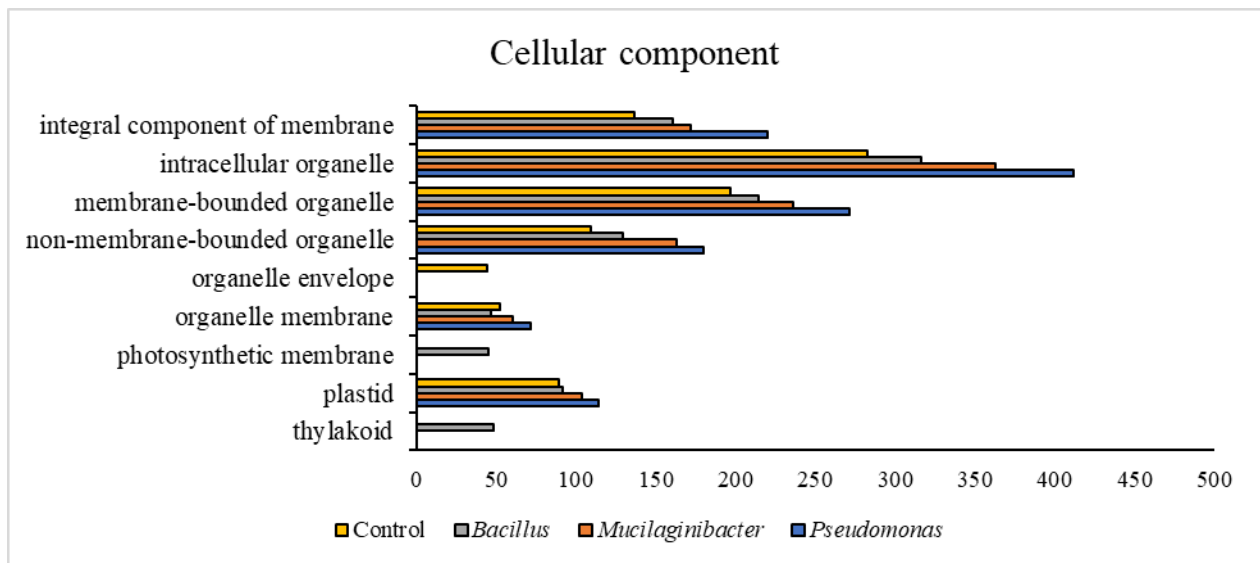
Supplementary Figure 4.3. The chromatograph of cannabinoids for (a) standard and samples with (b) original concentration, and (c) dilution in UHPLC.

Appendix C

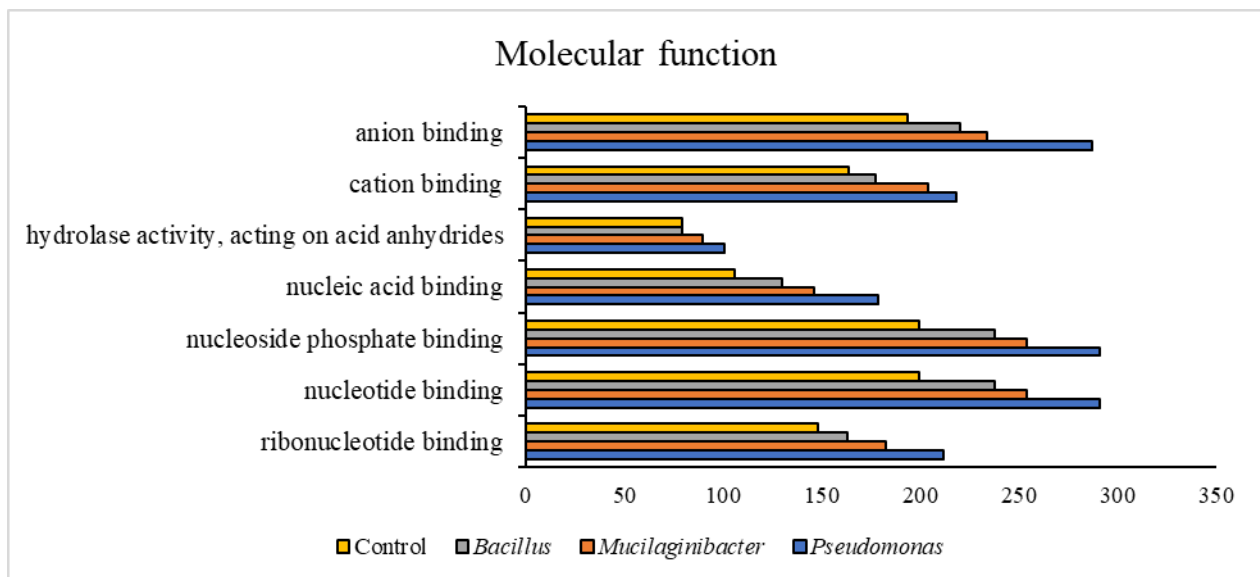
Chapter 5



Supplement Figure 5.1. Number of sequences involved in the cellular and metabolic processes of the cannabis flower proteome under different PGPR treatment.



Supplement Figure 5.2. Number of sequences involved in the cellular components – membranes and organelles of the cannabis flower proteome under different PGPR treatment.



Supplement Figure 5.3. Number of sequences involved in the molecular function – binding of the cannabis flower proteome under different PGPR treatment.

Supplementary Table 5.1. Differential expressed proteins with fold change ≥ 1.2 in the treatment *Bacillus* sp., relative to control in cannabis flower

Identified Proteins (1203)	Molecular Weight	Fisher's Exact Test (p-value)	Fold Change	Control	<i>Bacillus</i> sp.
Cluster of ATP synthase subunit beta, chloroplastic	54 kDa	0.35	1.2	166	199
Cluster of MFS domain-containing protein	109 kDa	0.47	1.2	109	127
Fructose-bisphosphate aldolase	43 kDa	0.42	1.2	83	99
Glyceraldehyde-3-phosphate dehydrogenase	43 kDa	0.16	1.4	59	81
Cluster of Tubulin beta chain	50 kDa	0.3	1.3	63	80
Transketolase	80 kDa	0.29	1.3	62	79
Cluster of ATP synthase subunit alpha, chloroplastic	55 kDa	0.39	1.2	59	72
Cluster of 5-methyltetrahydropteroyltriglutamate--homocysteine S-methyltransferase	85 kDa	0.42	1.2	58	70
Cluster of Lipoxygenase	98 kDa	0.0044	2	34	68
Cluster of Polyketide synthase	43 kDa	0.49	1.2	53	62
Cluster of Transmembrane 9 superfamily member	104 kDa	0.15	1.4	41	59
Cluster of Bet_v_1 domain-containing protein	18 kDa	0.49	1.2	45	53
Cluster of Adenosylhomocysteinase	53 kDa	0.34	1.3	40	51
Cluster of GH18 domain-containing protein	35 kDa	0.22	1.4	36	50
Cluster of Plastocyanin	18 kDa	0.5	1.2	41	48
Cluster of LRRNT_2 domain-containing protein	37 kDa	0.23	1.4	34	47
Cluster of HATPase_c domain-containing protein	80 kDa	0.23	1.4	33	46
Cluster of Phosphopyruvate hydratase	46 kDa	0.017	2	23	46
Photosystem I reaction center subunit II, chloroplastic	24 kDa	0.35	1.3	31	40
Calreticulin	48 kDa	0.13	1.6	24	38
Cluster of Glycine cleavage system P protein	114 kDa	0.012	2.3	15	35
Cluster of Ubiquitin-like domain-containing protein	18 kDa	0.11	1.7	21	35

Cluster of Isocitrate dehydrogenase [NADP]	46 kDa	0.17	1.5	22	34
Ribos_L4_asso_C domain-containing protein	45 kDa	0.049	1.9	17	33
Cluster of 14_3_3 domain-containing protein	31 kDa	0.33	1.3	24	32
Cluster of EF1_GNE domain-containing protein	25 kDa	0.15	1.6	20	32
Cluster of Phospholipase D	93 kDa	0.33	1.3	24	32
Cluster of HDR (Fragment)	46 kDa	0.33	1.3	23	31
Cluster of Ferredoxin-NADP reductase, chloroplastic	41 kDa	0.54	1.2	25	29
Cluster of Lysine-tRNA ligase	81 kDa	0.12	1.7	17	29
HATPase_c domain-containing protein	123 kDa	0.2	1.5	19	29
Aconitate hydratase	98 kDa	0.24	1.5	19	28
Cluster of Non-specific lipid-transfer protein	12 kDa	0.53	1.2	24	28
Cluster of Catalase	57 kDa	0.52	1.2	23	27
Cluster of Glutamine synthetase	39 kDa	0.4	1.3	21	27
NAC-A/B domain-containing protein	22 kDa	0.05	2.1	13	27
40S ribosomal protein S8	26 kDa	0.22	1.5	17	26
ATP citrate synthase	68 kDa	0.17	1.6	16	26
60S acidic ribosomal protein P0	34 kDa	0.44	1.2	20	25
L-ascorbate peroxidase 0GN=G4B88_005358	27 kDa	0.38	1.3	19	25
Protein kinase domain-containing protein	58 kDa	0.023	2.5	10	25
Phosphoglycerate mutase (2,3-diphosphoglycerate-independent)	61 kDa	0.36	1.4	17	23
Aminomethyltransferase	46 kDa	0.087	2	11	22
Cluster of (S)-2-hydroxy-acid oxidase	41 kDa	0.22	1.6	14	22
Cluster of 40S ribosomal protein S7	29 kDa	0.28	1.5	15	22
Formate dehydrogenase, mitochondrial	42 kDa	0.35	1.4	16	22
PfkB domain-containing protein	36 kDa	0.55	1.2	19	22
Phosphoribulokinase	46 kDa	0.48	1.2	18	22
Ribosomal_L2_C domain-containing protein	84 kDa	0.057	2.2	10	22
Cluster of Dihydrolipoyl dehydrogenase	54 kDa	0.029	2.6	8	21
Cluster of Plastoquinol--plastocyanin reductase	24 kDa	0.34	1.4	15	21

Cluster of UDP-arabinopyranose mutase	41 kDa	0.27	1.5	14	21
Germin-like protein	22 kDa	0.27	1.5	14	21
GTP-binding nuclear protein	51 kDa	0.34	1.4	15	21
Cluster of Aldedh domain-containing protein	61 kDa	0.32	1.4	14	20
Lactoylglutathione lyase	33 kDa	0.53	1.2	17	20
Lipoyl-binding domain-containing protein	86 kDa	0.066	2.2	9	20
Peptidase A1 domain-containing protein	47 kDa	0.14	1.8	11	20
Pyr_redox_2 domain-containing protein	47 kDa	0.39	1.3	15	20
Aconitate hydratase	108 kDa	0.31	1.5	13	19
Cluster of 40S ribosomal protein S3a	30 kDa	0.38	1.4	14	19
Cluster of NADPH-protochlorophyllide oxidoreductase (Fragment)	157 kDa	0.31	1.5	13	19
ATP synthase subunit d, mitochondrial	23 kDa	0.29	1.5	12	18
Cluster of Cytochrome b559 subunit alpha	19 kDa	0.44	1.3	14	18
Cluster of Multifunctional fusion protein	94 kDa	0.52	1.2	15	18
Epimerase domain-containing protein	43 kDa	0.025	3	6	18
Glycine cleavage system H protein	19 kDa	0.52	1.2	15	18
Proteasome subunit alpha type	27 kDa	0.12	2	9	18
Cluster of 40S ribosomal protein	33 kDa	0.1	2.1	8	17
Cluster of LRRNT_2 domain-containing protein	39 kDa	0.51	1.2	14	17
Cluster of Protein disulfide-isomerase	68 kDa	0.037	2.8	6	17
Cluster of Ribosomal_L18_c domain-containing protein	34 kDa	0.15	1.9	9	17
Cluster of PKS_ER domain-containing protein	34 kDa	0.34	1.5	11	16
Cluster of Ribosomal_L16 domain-containing protein	25 kDa	0.052	2.7	6	16
Glutamate-1-semialdehyde 2,1-aminomutase	51 kDa	0.42	1.3	12	16
Cluster of 50S ribosomal protein L23, chloroplastic	71 kDa	0.073	2.5	6	15

Cluster of Glucan endo-1,3-beta-D-glucosidase	113 kDa	0.00065	15	1	15
Cluster of Histone H4	20 kDa	0.41	1.4	11	15
Cluster of Ribosomal_L6e_N domain-containing protein (Fragment)	31 kDa	0.32	1.5	10	15
Formate--tetrahydrofolate ligase	68 kDa	0.12	2.1	7	15
Glutaredoxin-dependent peroxiredoxin	78 kDa	0.49	1.2	12	15
NAD(P)H dehydrogenase (quinone)	22 kDa	0.49	1.2	12	15
Proteasome subunit alpha type	27 kDa	0.18	1.9	8	15
S-adenosylmethionine synthase	47 kDa	0.49	1.2	12	15
Chlorophyll a-b binding protein, chloroplastic	26 kDa	0.39	1.4	10	14
Cluster of Adenosine kinase	37 kDa	0.16	2	7	14
Cluster of CYTB_NTER domain-containing protein	95 kDa	0.16	2	7	14
Cluster of Glucan endo-1,3-beta-D-glucosidase	80 kDa	0.03	3.5	4	14
Cluster of Histone H2B	16 kDa	0.1	2.3	6	14
Epimerase domain-containing protein	42 kDa	0.48	1.3	11	14
Glutaredoxin-dependent peroxiredoxin	24 kDa	0.48	1.3	11	14
Proteasome subunit alpha type	27 kDa	0.48	1.3	11	14
40S ribosomal protein S8	26 kDa	0.47	1.3	10	13
Cluster of Glucose-6-phosphate isomerase	67 kDa	0.21	1.9	7	13
Cluster of Phosphoenolpyruvate carboxylase	109 kDa	0.55	1.2	11	13
Cluster of Ribosomal protein L19	24 kDa	0.38	1.4	9	13
Sucrose synthase	93 kDa	0.045	3.2	4	13
60S ribosomal protein L13	39 kDa	0.45	1.3	9	12
AAA domain-containing protein	76 kDa	0.45	1.3	9	12
Cluster of Eukaryotic translation initiation factor	17 kDa	0.19	2	6	12
Glutamine amidotransferase type-2 domain-containing protein	177 kDa	0.27	1.7	7	12
Thioredoxin-dependent peroxiredoxin (Fragment)	135 kDa	0.067	3	4	12
Aldedh domain-containing protein	59 kDa	0.44	1.4	8	11
Cluster of PSII_BNR domain-containing protein	46 kDa	0.097	2.8	4	11
Ribose-5-phosphate isomerase _	36 kDa	0.25	1.8	6	11
Ribosomal protein L15	28 kDa	0.021	5.5	2	11

Succinate-CoA ligase [ADP-forming] subunit beta, mitochondrial	45 kDa	0.34	1.6	7	11
Transaldolase	48 kDa	0.25	1.8	6	11
UDP-glucose 6-dehydrogenase	53 kDa	0.44	1.4	8	11
ATP-dependent Clp protease proteolytic subunit	34 kDa	0.52	1.2	8	10
Cluster of 60S ribosomal protein L27	16 kDa	0.42	1.4	7	10
Cluster of Glycerophosphodiester phosphodiesterase	83 kDa	0.42	1.4	7	10
Cluster of Photosystem II D2 protein	40 kDa	0.52	1.2	8	10
Dihydrolipoamide acetyltransferase component of pyruvate dehydrogenase complex	56 kDa	0.32	1.7	6	10
Alanine--glyoxylate transaminase	44 kDa	0.4	1.5	6	9
Alpha-1,4 glucan phosphorylase	103 kDa	0.053	4.5	2	9
Cluster of Aspartate aminotransferase	50 kDa	0.51	1.3	7	9
Cluster of Peroxidase	37 kDa	0.4	1.5	6	9
Cluster of Proteasome subunit beta	25 kDa	0.4	1.5	6	9
Cluster of Pyrophosphate--fructose 6-phosphate 1-phosphotransferase subunit alpha	67 kDa	0.4	1.5	6	9
Cluster of STI1 domain-containing protein	38 kDa	0.4	1.5	6	9
Dihydrolipoyl dehydrogenase	60 kDa	0.19	2.2	4	9
Uroporphyrinogen decarboxylase	45 kDa	0.4	1.5	6	9
AAI domain-containing protein	14 kDa	0.5	1.3	6	8
CCT-beta	54 kDa	0.16	2.7	3	8
Cluster of Annexin	31 kDa	0.031	8	1	8
Cluster of Cysteine synthase _	34 kDa	0.16	2.7	3	8
Cluster of Cysteine synthase	78 kDa	0.38	1.6	5	8
Cluster of Glutaredoxin domain-containing protein	17 kDa	0.16	2.7	3	8
Cluster of Peptidylprolyl isomerase	64 kDa	0.16	2.7	3	8
Cluster of S5 DRBM domain-containing protein	30 kDa	0.27	2	4	8
Ferredoxin-NADP reductase, chloroplastic	42 kDa	0.27	2	4	8
Glycine-tRNA ligase	81 kDa	0.083	4	2	8
Isocitrate dehydrogenase [NAD] subunit, mitochondrial	66 kDa	0.16	2.7	3	8

Adenylosuccinate synthetase, chloroplastic	54 kDa	0.053	7	1	7
Cluster of (-)-limonene synthase, chloroplastic	72 kDa	0.48	1.4	5	7
Cluster of Abhydrolase_3 domain-containing protein	41 kDa	0.48	1.4	5	7
Cluster of Alpha-mannosidase	233 kDa	0.23	2.3	3	7
Cluster of Fumarylacetoacetase	128 kDa	0.23	2.3	3	7
Cluster of PKS_ER domain-containing protein	39 kDa	0.6	1.2	6	7
Cluster of Proteasome subunit alpha type	27 kDa	0.36	1.8	4	7
Cluster of Proteasome subunit alpha type	25 kDa	0.6	1.2	6	7
Cluster of Pyruvate dehydrogenase E1 component subunit beta	36 kDa	0.6	1.2	6	7
Cluster of Ribosomal_S10 domain-containing protein	14 kDa	0.48	1.4	5	7
Cluster of rRNA N-glycosylase	29 kDa	0.48	1.4	5	7
Dihydrolipoamide acetyltransferase component of pyruvate dehydrogenase complex _018793	49 kDa	0.23	2.3	3	7
Glutathione reductase	54 kDa	0.23	2.3	3	7
KOW domain-containing protein	17 kDa	0.36	1.8	4	7
Photolyase/cryptochrome alpha/beta domain-containing protein	119 kDa	0.23	2.3	3	7
S-(hydroxymethyl)glutathione dehydrogenase	99 kDa	0.48	1.4	5	7
Bet_v_1 domain-containing protein	19 kDa	0.088	6	1	6
Cluster of 60S ribosomal protein L18a	21 kDa	0.46	1.5	4	6
Cluster of 6-phosphogluconate dehydrogenase, decarboxylating	59 kDa	0.32	2	3	6
Cluster of Carbamoyl-phosphate synthase (glutamine-hydrolyzing)	132 kDa	0.088	6	1	6
Importin subunit alpha	65 kDa	0.088	6	1	6
Thioredoxin domain-containing protein	19 kDa	0.46	1.5	4	6
40S ribosomal protein S24	16 kDa	0.29	2.5	2	5
60S ribosomal protein L7a	29 kDa	0.043	INF	0	5
Cluster of 1-deoxy-D-xylulose-5-phosphate reductoisomerase	51 kDa	0.44	1.7	3	5
Cluster of 60S ribosomal protein L36	13 kDa	0.44	1.7	3	5

Cluster of Acetyl-CoA carboxytransferase	84 kDa	0.14	5	1	5
Cluster of Aspartate-tRNA ligase	62 kDa	0.29	2.5	2	5
Cluster of GH18 domain-containing protein	101 kDa	0.14	5	1	5
Cluster of Hedycaryol synthase	65 kDa	0.14	5	1	5
Cluster of Malic enzyme	70 kDa	0.29	2.5	2	5
Coproporphyrinogen oxidase	45 kDa	0.29	2.5	2	5
Epimerase domain-containing protein	52 kDa	0.043	INF	0	5
GST N-terminal domain-containing protein	35 kDa	0.44	1.7	3	5
Iso_dh domain-containing protein	41 kDa	0.29	2.5	2	5
Naringenin-chalcone synthase	43 kDa	0.29	2.5	2	5
NmrA domain-containing protein	34 kDa	0.29	2.5	2	5
Peptidase_M24 domain-containing protein	88 kDa	0.29	2.5	2	5
Peptidylprolyl isomerase	50 kDa	0.29	2.5	2	5
Phosphoserine aminotransferase	47 kDa	0.29	2.5	2	5
Photosystem I reaction center subunit V, chloroplastic	18 kDa	0.043	INF	0	5
PKS_ER domain-containing protein (Fragment)	47 kDa	0.44	1.7	3	5
RRM domain-containing protein	22 kDa	0.14	5	1	5
UDP-glucuronate decarboxylase	73 kDa	0.29	2.5	2	5
Xylose isomerase	56 kDa	0.043	INF	0	5
40S ribosomal protein S24	31 kDa	0.57	1.3	3	4
40S ribosomal protein S25	12 kDa	0.23	4	1	4
AAA domain-containing protein	48 kDa	0.081	INF	0	4
Cluster of 6-phosphogluconate dehydrogenase, decarboxylating	54 kDa	0.57	1.3	3	4
Cluster of Alpha-galactosidase	76 kDa	0.41	2	2	4
Cluster of Glutamate decarboxylase	56 kDa	0.23	4	1	4
Cluster of Ribosomal_L2_C domain-containing protein	34 kDa	0.23	4	1	4
Cluster of RNA helicase	67 kDa	0.23	4	1	4
Cluster of Semialdehyde_dh domain-containing protein	38 kDa	0.23	4	1	4
E1 ubiquitin-activating enzyme	247 kDa	0.081	INF	0	4
Epimerase domain-containing protein	40 kDa	0.081	INF	0	4
Glucose-1-phosphate adenylyltransferase	57 kDa	0.081	INF	0	4
H (+)-exporting diphosphatase	80 kDa	0.41	2	2	4
Lactoylglutathione lyase	42 kDa	0.41	2	2	4

Proteasome subunit alpha type	27 kDa	0.41	2	2	4
Proteasome subunit beta	27 kDa	0.081	INF	0	4
Pterin-binding domain-containing protein	41 kDa	0.081	INF	0	4
Pyrophosphate-fructose 6-phosphate 1-phosphotransferase subunit beta	142 kDa	0.57	1.3	3	4
Ribosomal_L18e/L15P domain-containing protein	21 kDa	0.57	1.3	3	4
Uridine 5'-monophosphate synthase	53 kDa	0.081	INF	0	4
30S ribosomal protein S17, chloroplastic	18 kDa	0.36	3	1	3
Aspartate aminotransferase	47 kDa	0.56	1.5	2	3
Chalcone isomerase	24 kDa	0.36	3	1	3
Cluster of AB hydrolase-1 domain-containing protein	36 kDa	0.56	1.5	2	3
Cluster of Asparagine synthetase [glutamine-hydrolyzing]	73 kDa	0.15	INF	0	3
Cluster of CS domain-containing protein	24 kDa	0.56	1.5	2	3
Cluster of Eukaryotic translation initiation factor 3 subunit I	36 kDa	0.56	1.5	2	3
Cluster of Peroxidase_4 domain-containing protein	38 kDa	0.36	3	1	3
Cluster of Pyruvate kinase	55 kDa	0.56	1.5	2	3
Elongation factor Ts, mitochondrial	117 kDa	0.15	INF	0	3
Eukaryotic translation initiation factor 3 subunit B	83 kDa	0.15	INF	0	3
Ferredoxin	16 kDa	0.36	3	1	3
HIT domain-containing protein _	19 kDa	0.36	3	1	3
NAD(P)-bd_dom domain-containing protein	55 kDa	0.15	INF	0	3
Nascent polypeptide-associated complex subunit beta	17 kDa	0.36	3	1	3
NTF2 domain-containing protein	13 kDa	0.15	INF	0	3
Prohibitin	32 kDa	0.56	1.5	2	3
Proliferating cell nuclear antigen	29 kDa	0.15	INF	0	3
Pyruvate dehydrogenase E1 component subunit alpha	48 kDa	0.36	3	1	3
Pyruvate dehydrogenase E1 component subunit alpha	44 kDa	0.36	3	1	3
Pyruvate kinase	63 kDa	0.15	INF	0	3
Ribonuclease	109 kDa	0.15	INF	0	3
Ribosomal_L14e domain-containing protein	15 kDa	0.36	3	1	3

Ribosomal_L18e/L15P domain-containing protein	22 kDa	0.15	INF	0	3
Ribosomal_L18e/L15P domain-containing protein	16 kDa	0.36	3	1	3
TRASH domain-containing protein	18 kDa	0.15	INF	0	3
3-oxoacyl-[acyl-carrier-protein] reductase	33 kDa	0.55	2	1	2
Acetyltransferase component of pyruvate dehydrogenase complex	59 kDa	0.28	INF	0	2
Amine oxidase	79 kDa	0.55	2	1	2
ATP-dependent Clp protease proteolytic subunit	27 kDa	0.55	2	1	2
CCT-theta (Fragment)	122 kDa	0.55	2	1	2
Cluster of Aspartate carbamoyltransferase	46 kDa	0.28	INF	0	2
Cluster of Citrate synthase	68 kDa	0.55	2	1	2
Cluster of Epimerase domain-containing protein	45 kDa	0.28	INF	0	2
Cluster of Glutamate dehydrogenase	43 kDa	0.28	INF	0	2
Cluster of Methylthioribose-1-phosphate isomerase	39 kDa	0.28	INF	0	2
Cluster of Pyruvate kinase	57 kDa	0.28	INF	0	2
Cluster of SCP domain-containing protein	51 kDa	0.55	2	1	2
Cluster of Thioredoxin domain-containing protein	20 kDa	0.28	INF	0	2
Epimerase domain-containing protein	46 kDa	0.55	2	1	2
Malic enzyme	67 kDa	0.55	2	1	2
Oxoglutarate dehydrogenase (succinyl-transferring)	116 kDa	0.28	INF	0	2
Peptidylprolyl isomerase	12 kDa	0.55	2	1	2
RRM domain-containing protein	28 kDa	0.28	INF	0	2
RRM domain-containing protein	49 kDa	0.28	INF	0	2
SAP domain-containing protein	86 kDa	0.28	INF	0	2
T-complex protein 1 subunit alpha	63 kDa	0.28	INF	0	2
4-(cytidine 5'-diphospho)-2-C-methyl-D-erythritol kinase	45 kDa	0.53	INF	0	1
Chalcone-flavonone isomerase family protein	38 kDa	0.53	INF	0	1
Cluster of Glutamate decarboxylase	57 kDa	0.53	INF	0	1
Cluster of Sec16_C domain-containing protein	120 kDa	0.53	INF	0	1
Pectin acetyltransferase	31 kDa	0.53	INF	0	1
Pept_C1 domain-containing protein	41 kDa	0.53	INF	0	1

Probable bifunctional methylthioribulose-1-phosphate dehydratase/enolase-phosphatase E1	59 kDa	0.53	INF	0	1
PSI subunit V	23 kDa	0.53	INF	0	1
STI1 domain-containing protein	48 kDa	0.53	INF	0	1

Supplementary Table 5.1. Differential expressed proteins with fold change ≥ 1.2 in the treatment *Mucilaginibacter* sp., relative to control in cannabis flower

Identified Proteins (1203)	Molecular Weight	Fisher's Exact Test (p-value)	Fold Change	Control	<i>Mucilaginibacter</i> sp.
14_3_3 domain-containing protein	28 kDa	0.39	1.4	25	34
30S ribosomal protein S17, chloroplastic	18 kDa	0.57	2	1	2
3-oxoacyl-[acyl-carrier-protein] reductase	34 kDa	0.62	1.2	4	5
4-(cytidine 5'-diphospho)-2-C-methyl-D-erythritol kinase	45 kDa	0.55	INF	0	1
40S ribosomal protein S12	15 kDa	0.62	1.2	4	5
40S ribosomal protein S24	16 kDa	0.22	3	2	6
40S ribosomal protein S24	31 kDa	0.36	2	3	6
40S ribosomal protein S25	12 kDa	0.57	2	1	2
40S ribosomal protein S8	26 kDa	0.38	1.5	10	15
40S ribosomal protein S8	26 kDa	0.43	1.4	17	23
60S ribosomal protein L13	39 kDa	0.3	1.7	9	15
60S ribosomal protein L7a	29 kDa	0.17	INF	0	3
AAA domain-containing protein	48 kDa	0.17	INF	0	3
AAI domain-containing protein	20 kDa	0.39	3	1	3
Acetyltransferase component of pyruvate dehydrogenase complex	59 kDa	0.17	INF	0	3
Aconitate hydratase	108 kDa	0.034	2.3	13	30
Aconitate hydratase	98 kDa	0.27	1.5	19	29
Adenylosuccinate synthetase, chloroplastic	54 kDa	0.063	7	1	7
Alanine transaminase	53 kDa	0.092	3.3	3	10
Alanine--glyoxylate transaminase	44 kDa	0.17	2.2	6	13
Aldedh domain-containing protein	59 kDa	0.17	2	8	16
Allene-oxide cyclase	27 kDa	0.52	1.4	5	7
Alpha-1,4 glucan phosphorylase	103 kDa	0.31	2.5	2	5
Amine oxidase	79 kDa	0.063	7	1	7
Aminomethyltransferase	46 kDa	0.031	2.5	11	27
Aminotran_1_2 domain-containing protein	52 kDa	0.46	1.3	15	20
ATP citrate synthase	68 kDa	0.54	1.2	16	19
ATP synthase subunit d, mitochondrial	23 kDa	0.48	1.3	12	16
ATP-dependent Clp protease proteolytic subunit	27 kDa	0.39	3	1	3

ATP-synt_DE_N domain-containing protein	22 kDa	0.44	2	2	4
Bet_v_1 domain-containing protein	19 kDa	0.014	10	1	10
Bet_v_1 domain-containing protein	18 kDa	0.43	1.3	29	38
Beta-fructofuranosidase	74 kDa	0.59	1.5	2	3
Beta-galactosidase	90 kDa	0.61	1.3	3	4
Beta-ketoacyl-[acyl-carrier-protein] synthase I	55 kDa	0.47	1.7	3	5
Calreticulin	48 kDa	0.52	1.2	24	30
Carbonic anhydrase	104 kDa	0.31	1.4	47	64
CCT-theta (Fragment)	122 kDa	0.1	6	1	6
Chalcone isomerase	24 kDa	0.39	3	1	3
Chlorophyll a-b binding protein, chloroplastic	26 kDa	0.17	1.9	10	19
Cluster of (-)-limonene synthase, chloroplastic	72 kDa	0.42	1.6	5	8
Cluster of (S)-2-hydroxy-acid oxidase	41 kDa	0.28	1.6	14	22
Cluster of 14_3_3 domain-containing protein_019064	31 kDa	0.079	1.8	24	43
Cluster of 1-deoxy-D-xylulose-5-phosphate reductoisomerase	51 kDa	0.61	1.3	3	4
Cluster of 26S proteasome non-ATPase regulatory subunit 1 homolog_	109 kDa	0.36	2	3	6
Cluster of 40S ribosomal protein S3a_021799 \	30 kDa	0.28	1.6	14	22
Cluster of 40S ribosomal protein S7	29 kDa	0.46	1.3	15	20
Cluster of 40S ribosomal protein SA	33 kDa	0.13	2.1	8	17
Cluster of 50S ribosomal protein L23, chloroplastic	71 kDa	0.36	1.7	6	10
Cluster of 5-methyltetrahydropteroyltriglutamate--homocysteine S-methyltransferase	85 kDa	0.51	1.2	58	70
Cluster of 60S ribosomal protein L18a	21 kDa	0.084	3	4	12
Cluster of 60S ribosomal protein L27	16 kDa	0.085	2.4	7	17
Cluster of 60S ribosomal protein L36	13 kDa	0.47	1.7	3	5
Cluster of 6-phosphogluconate dehydrogenase, decarboxylating	59 kDa	0.26	2.3	3	7

Cluster of AAA domain-containing protein	101 kDa	0.43	1.4	9	13
Cluster of Abhydrolase_3 domain-containing protein	41 kDa	0.52	1.4	5	7
Cluster of Acetyl-CoA carboxytransferase	84 kDa	0.57	2	1	2
Cluster of Adenosine kinase	37 kDa	0.15	2.1	7	15
Cluster of Adenosylhomocysteinase	53 kDa	0.047	1.7	40	69
Cluster of Adenylate kinase	27 kDa	0.42	1.4	12	17
Cluster of Agglutinin domain-containing protein	19 kDa	0.55	1.2	27	33
Cluster of Aldedh domain-containing protein	61 kDa	0.51	1.3	14	18
Cluster of Aldehyde dehydrogenase (NAD (+))	54 kDa	0.55	1.2	27	33
Cluster of Alpha-galactosidase	45 kDa	0.47	1.4	7	10
Cluster of Alpha-mannosidase	233 kDa	0.61	1.3	3	4
Cluster of Annexin	31 kDa	0.063	7	1	7
Cluster of Argininosuccinate synthase	54 kDa	0.59	1.2	9	11
Cluster of Asparagine synthetase [glutamine-hydrolyzing]	73 kDa	0.55	INF	0	1
Cluster of Aspartate carbamoyltransferase	46 kDa	0.55	INF	0	1
Cluster of Aspartate-tRNA ligase	62 kDa	0.44	2	2	4
Cluster of ATP synthase subunit beta, chloroplastic	54 kDa	0.5	1.2	166	201
Cluster of Carbamoyl-phosphate synthase (glutamine-hydrolyzing)	132 kDa	0.25	4	1	4
Cluster of Chitinase	31 kDa	0.57	1.2	8	10
Cluster of Chlorophyll a-b binding protein, chloroplastic	28 kDa	0.54	1.2	16	20
Cluster of Citrate synthase	68 kDa	0.57	2	1	2
Cluster of CS domain-containing protein	24 kDa	0.59	1.5	2	3
Cluster of Cysteine synthase	34 kDa	0.19	2.7	3	8
Cluster of Cysteine synthase	78 kDa	0.61	1.2	5	6
Cluster of Cytochrome b559 subunit alpha	19 kDa	0.57	1.2	14	17
Cluster of Cytochrome f	127 kDa	0.31	1.2	268	312
Cluster of Cytosol_AP domain-containing protein	60 kDa	0.3	1.5	15	23
Cluster of Dihydrolipoyl dehydrogenase	54 kDa	0.0079	3.2	8	26

Cluster of Dihydrolipoyllysine-residue succinyltransferase (Fragment)	66 kDa	0.33	1.8	5	9
Cluster of DNA-directed RNA polymerase subunit beta	171 kDa	0.3	INF	0	2
Cluster of EF1_GNE domain-containing protein	24 kDa	0.54	1.2	16	20
Cluster of Elongation factor Tu	53 kDa	0.53	1.2	38	46
Cluster of Epimerase domain-containing protein	45 kDa	0.55	INF	0	1
Cluster of Eukaryotic translation initiation factor 3 subunit G	32 kDa	0.22	2	6	12
Cluster of Eukaryotic translation initiation factor 5A	17 kDa	0.29	1.8	6	11
Cluster of Ferredoxin-NADP reductase, chloroplastic	41 kDa	0.53	1.2	25	31
Cluster of Fumarate hydratase	82 kDa	0.57	2	1	2
Cluster of Fumarylacetoacetase	128 kDa	0.092	3.3	3	10
Cluster of GH18 domain-containing protein	101 kDa	0.25	4	1	4
Cluster of Glucan endo-1,3-beta-D-glucosidase	113 kDa	0.0017	14	1	14
Cluster of Glucan endo-1,3-beta-D-glucosidase	80 kDa	0.059	3.2	4	13
Cluster of Glucose-6-phosphate isomerase	67 kDa	0.25	1.9	7	13
Cluster of Glutamate decarboxylase	57 kDa	0.17	INF	0	3
Cluster of Glutamate decarboxylase	56 kDa	0.063	7	1	7
Cluster of Glutamine synthetase	39 kDa	0.16	1.7	21	35
Cluster of Glutaredoxin domain-containing protein	17 kDa	0.47	1.7	3	5
Cluster of Glutathione peroxidase	27 kDa	0.61	1.3	3	4
Cluster of Glycerophosphodiester phosphodiesterase	83 kDa	0.47	1.4	7	10
Cluster of Glycine cleavage system P protein	114 kDa	0.00075	3.1	15	46
Cluster of HATPase_c domain-containing protein	80 kDa	0.43	1.3	33	43
Cluster of HDR (Fragment)	46 kDa	0.41	1.3	23	31
Cluster of Hedycaryol synthase	65 kDa	0.57	2	1	2
Cluster of Histone H2A	32 kDa	0.59	1.2	9	11
Cluster of Histone H2B	16 kDa	0.095	2.5	6	15
Cluster of Histone H4	20 kDa	0.017	2.6	11	29
Cluster of Isocitrate dehydrogenase [NADP]	46 kDa	0.4	1.4	22	30

Cluster of Lipoygenase	98 kDa	0.2	1.5	34	51
Cluster of LRRNT_2 domain-containing protein	37 kDa	0.098	1.6	34	56
Cluster of LRRNT_2 domain-containing protein	39 kDa	0.45	1.4	14	19
Cluster of Lysine-tRNA ligase	81 kDa	0.28	1.5	17	26
Cluster of Malate dehydrogenase	36 kDa	0.29	1.4	44	61
Cluster of Malic enzyme	70 kDa	0.31	2.5	2	5
Cluster of MFS domain-containing protein	109 kDa	0.51	1.2	109	132
Cluster of Multifunctional fusion protein	94 kDa	0.25	1.6	15	24
Cluster of NADH dehydrogenase [ubiquinone] 1 beta subcomplex subunit 9	35 kDa	0.39	3	1	3
Cluster of NADPH-protochlorophyllide oxidoreductase (Fragment)	157 kDa	0.52	1.2	13	15
Cluster of NTP_transf_2 domain-containing protein	84 kDa	0.42	1.6	5	8
Cluster of Peptidylprolyl isomerase	64 kDa	0.36	2	3	6
Cluster of Peroxidase	30 kDa	0.61	1.3	3	4
Cluster of Phosphoenolpyruvate carboxylase	109 kDa	0.47	1.4	11	15
Cluster of Phosphoglycerate kinase	92 kDa	0.26	1.3	93	125
Cluster of Phospholipase D	93 kDa	0.16	1.6	24	39
Cluster of Phosphopyruvate hydratase	46 kDa	0.28	1.5	23	34
Cluster of Photosystem I P700 chlorophyll an apoprotein A1	170 kDa	0.26	2.3	3	7
Cluster of Photosystem I reaction center subunit III	25 kDa	0.15	3.5	2	7
Cluster of Photosystem II D2 protein	40 kDa	0.057	2.5	8	20
Cluster of Plastoquinol--plastocyanin reductase	24 kDa	0.46	1.3	15	20
Cluster of Proteasome subunit alpha type	27 kDa	0.62	1.2	4	5
Cluster of Proteasome subunit alpha type	25 kDa	0.45	1.5	6	9
Cluster of Proteasome subunit beta	25 kDa	0.29	1.8	6	11
Cluster of Protein disulfide-isomerase	68 kDa	0.29	1.8	6	11
Cluster of PsbP domain-containing protein	29 kDa	0.47	1.2	36	42

Cluster of PSII_BNR domain-containing protein	46 kDa	0.17	2.5	4	10
Cluster of Purple acid phosphatase	55 kDa	0.3	2	4	8
Cluster of Pyruvate dehydrogenase E1 component subunit beta	36 kDa	0.22	2	6	12
Cluster of Pyruvate kinase	57 kDa	0.3	INF	0	2
Cluster of Pyruvate kinase	55 kDa	0.59	1.5	2	3
Cluster of Ribosomal protein	25 kDa	0.2	2.2	5	11
Cluster of Ribosomal_L16 domain-containing protein	25 kDa	0.36	1.7	6	10
Cluster of Ribosomal_L18_c domain-containing protein	34 kDa	0.09	2.2	9	20
Cluster of Ribosomal_L2_C domain-containing protein	34 kDa	0.1	6	1	6
Cluster of Ribosomal_L6e_N domain-containing protein (Fragment)	31 kDa	0.45	1.4	10	14
Cluster of Ribosomal_S10 domain-containing protein	14 kDa	0.42	1.6	5	8
Cluster of RNA helicase	67 kDa	0.39	3	1	3
Cluster of rRNA N-glycosylase	29 kDa	0.61	1.2	5	6
Cluster of S5 DRBM domain-containing protein_010941	30 kDa	0.3	2	4	8
Cluster of SCP domain-containing protein	51 kDa	0.39	3	1	3
Cluster of Sec16_C domain-containing protein	120 kDa	0.55	INF	0	1
Cluster of Semialdehyde_dh domain-containing protein	38 kDa	0.39	3	1	3
Cluster of STI1 domain-containing protein	38 kDa	0.54	1.3	6	8
Cluster of Superoxide dismutase	26 kDa	0.45	1.5	6	9
Cluster of Thioredoxin domain-containing protein	20 kDa	0.0014	INF	0	11
Cluster of Transmembrane 9 superfamily member	104 kDa	0.0027	2.1	41	85
Cluster of Tubulin beta chain	50 kDa	0.48	1.2	63	75
Cluster of Ubiquitin_4 domain-containing protein	59 kDa	0.26	1.7	10	17
CP12 domain-containing protein	14 kDa	0.31	2.5	2	5
Cytochrome b5 heme-binding domain-containing protein	61 kDa	0.59	1.5	2	3
Cytochrome c domain-containing protein	12 kDa	0.45	1.5	6	9

Dihydrolipoamide acetyltransferase component of pyruvate dehydrogenase complex _018793	49 kDa	0.36	2	3	6
Dihydrolipoamide acetyltransferase component of pyruvate dehydrogenase complex	56 kDa	0.22	2	6	12
Dihydrolipoyl dehydrogenase	60 kDa	0.17	2.5	4	10
E1 ubiquitin-activating enzyme	247 kDa	0.55	INF	0	1
Elongation factor Ts, mitochondrial	117 kDa	0.3	INF	0	2
Epimerase domain-containing protein	42 kDa	0.23	1.7	11	19
Epimerase domain-containing protein	44 kDa	0.071	2.2	11	24
Epimerase domain-containing protein	40 kDa	0.55	INF	0	1
Epimerase domain-containing protein	43 kDa	0.018	3.3	6	20
Epimerase domain-containing protein	52 kDa	0.05	INF	0	5
Eukaryotic translation initiation factor 3 subunit B	83 kDa	0.55	INF	0	1
Ferredoxin	16 kDa	0.25	4	1	4
Ferredoxin-NADP reductase, chloroplastic	42 kDa	0.5	1.5	4	6
Ferritin	31 kDa	0.54	1.3	6	8
Fn3_like domain-containing protein	85 kDa	0.59	1.5	2	3
Formate--tetrahydrofolate ligase	68 kDa	0.39	1.6	7	11
Fructose-bisphosphatase	45 kDa	0.57	1.2	8	10
Fructose-bisphosphate aldolase	43 kDa	0.22	1.4	83	114
Germin-like protein	22 kDa	0.39	1.4	14	20
GH18 domain-containing protein	153 kDa	0.25	4	1	4
Glucose-1-phosphate adenylyltransferase	57 kDa	0.55	INF	0	1
Glutamate-1-semialdehyde 2,1-aminomutase	51 kDa	0.53	1.2	12	14
Glutamine amidotransferase type-2 domain-containing protein	177 kDa	0.19	2	7	14
Glutamine synthetase	48 kDa	0.53	1.2	29	35
Glutaredoxin-dependent peroxiredoxin	24 kDa	0.47	1.4	11	15
Glutaredoxin-dependent peroxiredoxin	78 kDa	0.16	1.8	12	22
Glutathione reductase	54 kDa	0.36	2	3	6
Glyceraldehyde-3-phosphate dehydrogenase	43 kDa	0.18	1.4	59	85

Glyceraldehyde-3-phosphate dehydrogenase	47 kDa	0.5	1.2	33	39
Glycine cleavage system H protein	19 kDa	0.17	1.7	15	26
Glycine-tRNA ligase	81 kDa	0.099	4	2	8
GST N-terminal domain-containing protein	35 kDa	0.61	1.3	3	4
GTP-binding nuclear protein	51 kDa	0.41	1.4	15	21
H (+)-exporting diphosphatase	80 kDa	0.44	2	2	4
HATPase_c domain-containing protein	123 kDa	0.11	1.8	19	34
HIT domain-containing protein	19 kDa	0.25	4	1	4
Importin subunit alpha	65 kDa	0.16	5	1	5
Iso_dh domain-containing protein	41 kDa	0.59	1.5	2	3
Isocitrate dehydrogenase [NAD] subunit, mitochondrial	66 kDa	0.19	2.7	3	8
Ketol-acid reductoisomerase	63 kDa	0.35	1.4	29	40
Lactoylglutathione lyase	42 kDa	0.44	2	2	4
L-ascorbate peroxidase	47 kDa	0.39	1.8	4	7
Lipoyl-binding domain-containing protein	86 kDa	0.3	1.7	9	15
Malate dehydrogenase	51 kDa	0.43	1.4	17	23
Mg-protoporphyrin IX chelatase	46 kDa	0.3	2	4	8
NAC-A/B domain-containing protein	22 kDa	0.32	1.5	13	20
NAD(P)-bd_dom domain-containing protein	55 kDa	0.091	INF	0	4
Naringenin-chalcone synthase	43 kDa	0.59	1.5	2	3
NmrA domain-containing protein	34 kDa	0.59	1.5	2	3
NTF2 domain-containing protein	13 kDa	0.55	INF	0	1
Nucleoside diphosphate kinase	26 kDa	0.47	1.7	3	5
Nucleoside-diphosphate kinase	16 kDa	0.5	1.2	23	27
Oxoglutarate dehydrogenase (succinyl-transferring)	116 kDa	0.3	INF	0	2
Pectinesterase	58 kDa	0.55	INF	0	1
Pept_C1 domain-containing protein	41 kDa	0.091	INF	0	4
Peptidase A1 domain-containing protein	47 kDa	0.47	1.4	11	15
Peptidyl-prolyl cis-trans isomerase (Fragment)	23 kDa	0.59	1.5	2	3
Peptidyl-prolyl cis-trans isomerase	28 kDa	0.17	2.2	6	13
Peptidylprolyl isomerase	50 kDa	0.099	4	2	8
Peroxidase	35 kDa	0.45	1.4	10	14
Peroxidase	37 kDa	0.027	3.8	4	15
PfkB domain-containing protein	40 kDa	0.3	1.6	12	19

PfkB domain-containing protein	36 kDa	0.36	1.4	19	27
Phosphoglucosmutase (alpha-D-glucose-1,6-bisphosphate-dependent)	63 kDa	0.31	1.7	7	12
Phosphoglycerate mutase (2,3-diphosphoglycerate-independent)	61 kDa	0.49	1.3	17	22
Phosphoribulokinase	46 kDa	0.1	1.8	18	33
Phosphoserine aminotransferase	47 kDa	0.31	2.5	2	5
Photolyase/cryptochrome alpha/beta domain-containing protein	119 kDa	0.61	1.3	3	4
Photosystem I reaction center subunit II, chloroplastic	24 kDa	0.11	1.6	31	51
PNP_UDP_1 domain-containing protein	32 kDa	0.53	1.2	12	14
Polyadenylate-binding protein	71 kDa	0.37	1.5	13	19
Probable bifunctional methylthioribulose-1-phosphate dehydratase/enolase-phosphatase E1	59 kDa	0.55	INF	0	1
Prohibitin	32 kDa	0.59	1.5	2	3
Proteasome subunit alpha type	27 kDa	0.59	1.5	2	3
Proteasome subunit alpha type	27 kDa	0.13	2.1	8	17
Proteasome subunit alpha type	27 kDa	0.51	1.3	9	12
Proteasome subunit beta	27 kDa	0.3	INF	0	2
Protein kinase domain-containing protein	58 kDa	0.13	2	10	20
PSI subunit V	23 kDa	0.05	INF	0	5
Pyr_redox_2 domain-containing protein	47 kDa	0.55	1.2	15	18
Pyrophosphate-fructose 6-phosphate 1-phosphotransferase subunit beta	142 kDa	0.26	2.3	3	7
Pyruvate dehydrogenase E1 component subunit alpha	44 kDa	0.39	3	1	3
Pyruvate kinase	63 kDa	0.55	INF	0	1
Ribos_L4_asso_C domain-containing protein	45 kDa	0.092	1.9	17	32
Ribose-5-phosphate isomerase	36 kDa	0.29	1.8	6	11
Ribosomal protein L15	28 kDa	0.064	4.5	2	9
Ribosomal_L14e domain-containing protein	15 kDa	0.16	5	1	5
Ribosomal_L18e/L15P domain-containing protein	29 kDa	0.17	INF	0	3

Ribosomal_L18e/L15P domain-containing protein	21 kDa	0.61	1.3	3	4
Ribosomal_L2_C domain-containing protein	84 kDa	0.21	1.8	10	18
Ribosomal_S13_N domain-containing protein	17 kDa	0.41	1.5	8	12
RRM domain-containing protein	22 kDa	0.57	2	1	2
RRM domain-containing protein	49 kDa	0.17	INF	0	3
S-(hydroxymethyl)glutathione dehydrogenase	99 kDa	0.2	2.2	5	11
S1 motif domain-containing protein	106 kDa	0.091	INF	0	4
S-adenosylmethionine synthase	47 kDa	0.36	1.5	12	18
S-adenosylmethionine synthase	50 kDa	0.43	1.4	17	23
Smr domain-containing protein	115 kDa	0.5	1.2	55	66
Succinate dehydrogenase [ubiquinone] iron-sulfur subunit, mitochondrial	31 kDa	0.5	1.5	4	6
Succinate-CoA ligase [ADP-forming] subunit beta, mitochondrial	45 kDa	0.25	1.9	7	13
Sucrose synthase	93 kDa	0.012	4.2	4	17
Sucrose synthase	93 kDa	0.25	4	1	4
Superoxide dismutase [Cu-Zn]	15 kDa	0.51	1.3	14	18
Superoxide dismutase	21 kDa	0.54	1.3	6	8
T-complex protein 1 subunit alpha	63 kDa	0.55	INF	0	1
TCTP domain-containing protein	19 kDa	0.61	1.2	5	6
Thioredoxin domain-containing protein	20 kDa	0.5	1.3	13	17
Thioredoxin domain-containing protein	19 kDa	0.39	1.8	4	7
Thioredoxin-dependent peroxiredoxin (Fragment)	135 kDa	0.39	1.8	4	7
Thioredoxin-dependent peroxiredoxin	29 kDa	0.5	1.3	22	28
Transaldolase	48 kDa	0.58	1.2	6	7
Transketolase	80 kDa	0.24	1.4	62	86
TRASH domain-containing protein	18 kDa	0.05	INF	0	5
UDP-glucose 6-dehydrogenase	53 kDa	0.34	1.6	8	13
UDP-glucuronate decarboxylase	73 kDa	0.31	2.5	2	5
Uroporphyrinogen decarboxylase	45 kDa	0.45	1.5	6	9
Usp domain-containing protein	18 kDa	0.39	1.6	7	11
UTP--glucose-1-phosphate uridylyltransferase	52 kDa	0.27	1.5	19	29
Xylose isomerase	56 kDa	0.015	INF	0	7

Supplementary Table 5.3. Differential expressed proteins with fold change ≥ 1.2 in the treatment *Pseudomonas* sp., relative to control in cannabis flower

Identified Proteins (1203)	Molecular Weight	Fisher's Exact Test (p-value)	Fold Change	Control	<i>Pseudomonas</i> sp.
Cluster of Cytochrome f	127 kDa	0.002	1.2	268	316
Cluster of Purple acid phosphatase	70 kDa	0.38	1.5	184	267
Cluster of ATP synthase subunit beta, chloroplastic	54 kDa	0.019	1.2	166	199
Cluster of Lipoxygenase	301 kDa	0.21	1.7	88	148
Cluster of MFS domain-containing protein	109 kDa	0.04	1.2	109	129
Cluster of Gp_dh_N domain-containing protein	79 kDa	0.11	1.3	96	121
Cluster of Phosphoglycerate kinase	92 kDa	0.1	1.2	93	116
Fructose-bisphosphate aldolase	43 kDa	0.26	1.3	83	112
Cluster of 5-methyltetrahydropteroyltriglutamate--homocysteine S-methyltransferase	85 kDa	0.3	1.7	58	96
Cluster of Tubulin beta chain	50 kDa	0.52	1.5	63	94
Transketolase	80 kDa	0.48	1.5	62	91
Cluster of Patatin	178 kDa	0.27	1.3	67	90
zf-RVT domain-containing protein	69 kDa	0.058	1.2	76	88
Glyceraldehyde-3-phosphate dehydrogenase	43 kDa	0.47	1.5	59	86
Cluster of Transmembrane 9 superfamily member	104 kDa	0.058	2	41	84
Cluster of Fructose-bisphosphate aldolase_000689	38 kDa	0.16	1.2	64	80
Cluster of Lipoxygenase	98 kDa	0.056	2.1	34	72
Cluster of Tubulin alpha chain	50 kDa	0.38	1.4	51	71
Cluster of ATP synthase subunit alpha, chloroplastic	55 kDa	0.11	1.2	59	70
Cluster of Annexin	36 kDa	0.25	1.3	53	69
Cluster of Tr-type G domain-containing protein	94 kDa	0.35	1.6	40	66
Cluster of LRRNT_2 domain-containing protein	37 kDa	0.16	1.9	34	64
Cluster of Adenosylhomocysteinase	53 kDa	0.41	1.6	40	64
Carbonic anhydrase	104 kDa	0.26	1.3	47	61
Malate dehydrogenase	37 kDa	0.094	1.2	53	61
Serine hydroxymethyltransferase	156 kDa	0.49	1.5	39	60

Cluster of Malate dehydrogenase	36 kDa	0.32	1.3	44	59
Cluster of Chlorophyll a-b binding protein, chloroplastic	28 kDa	0.1	1.2	51	59
Cluster of Phospholipase D	93 kDa	0.029	2.4	24	58
ATP synthase subunit alpha	55 kDa	0.16	1.2	47	57
Cluster of GH18 domain-containing protein	35 kDa	0.54	1.5	36	54
Cluster of Peroxidase	40 kDa	0.11	1.2	46	53
Cluster of Bet_v_1 domain-containing protein	18 kDa	0.14	1.2	45	53
Photosystem I reaction center subunit II, chloroplastic	24 kDa	0.35	1.7	31	52
Cluster of Catalase	57 kDa	0.51	1.5	34	52
HATPase_c domain-containing protein	123 kDa	0.021	2.6	19	50
Cluster of HATPase_c domain-containing protein	80 kDa	0.53	1.5	33	50
V-type proton ATPase catalytic subunit A	69 kDa	0.37	1.4	36	49
Cluster of Elongation factor Tu	53 kDa	0.28	1.3	38	49
Fructose-bisphosphate aldolase	43 kDa	0.15	1.2	40	47
Aconitate hydratase	98 kDa	0.069	2.3	19	44
Cluster of 14_3_3 domain-containing protein	31 kDa	0.25	1.8	24	44
Ketol-acid reductoisomerase	63 kDa	0.53	1.5	29	43
Cluster of Phosphopyruvate hydratase	46 kDa	0.26	1.8	23	42
Calreticulin	48 kDa	0.32	1.8	24	42
Cluster of RRM domain-containing protein	17 kDa	0.28	1.3	33	42
Cluster of Glycine cleavage system P protein	114 kDa	0.042	2.6	15	39
Phosphoglycerate mutase (2,3-diphosphoglycerate-independent)	61 kDa	0.088	2.3	17	39
Glyceraldehyde-3-phosphate dehydrogenase	47 kDa	0.19	1.2	33	39
Cluster of Glutamine synthetase	39 kDa	0.29	1.8	21	38
Cluster of Catalase	57 kDa	0.45	1.6	23	37
Ribos_L4_asso_C domain-containing protein	45 kDa	0.15	2.1	17	36
Cluster of Isocitrate dehydrogenase [NADP]	46 kDa	0.43	1.6	22	36
Vacuolar proton pump subunit B	54 kDa	0.31	1.3	28	36
Phosphoribulokinase	46 kDa	0.22	1.9	18	35
Cluster of Biotin carboxylase	58 kDa	0.45	1.4	25	35

Cluster of Ferredoxin-NADP reductase, chloroplastic	41 kDa	0.45	1.4	25	35
Aconitate hydratase	108 kDa	0.055	2.6	13	34
Cluster of Dihydrolipoyl dehydrogenase	54 kDa	0.0044	4.1	8	33
Lipoyl-binding domain-containing protein	86 kDa	0.0087	3.7	9	33
Cluster of Phosphoenolpyruvate carboxylase	109 kDa	0.027	3	11	33
Cluster of EF1_GNE domain-containing protein	25 kDa	0.42	1.6	20	33
Cluster of HDR (Fragment)	46 kDa	0.49	1.4	23	33
Ribulose biphosphate carboxylase small subunit, chloroplastic	20 kDa	0.25	1.2	27	33
Cluster of Serine hydroxymethyltransferase	52 kDa	0.47	1.6	20	32
Cluster of Aldehyde dehydrogenase (NAD (+))	54 kDa	0.22	1.2	27	32
Aminomethyltransferase	46 kDa	0.045	2.8	11	31
40S ribosomal protein S8	26 kDa	0.31	1.8	17	31
Cluster of Non-specific lipid-transfer protein	12 kDa	0.34	1.3	24	31
Elongation factor Tu	49 kDa	0.4	1.3	23	31
Cluster of Lysine-tRNA ligase	81 kDa	0.35	1.8	17	30
UTP--glucose-1-phosphate uridylyltransferase	52 kDa	0.49	1.6	19	30
Cluster of VWFA domain-containing protein	58 kDa	0.55	1.5	20	30
14_3_3 domain-containing protein	28 kDa	0.24	1.2	25	30
Cluster of VOC domain-containing protein	17 kDa	0.3	1.2	24	30
S-adenosylmethionine synthase	50 kDa	0.4	1.7	17	29
Cluster of Aldedh domain-containing protein	61 kDa	0.24	2	14	28
GTP-binding nuclear protein	51 kDa	0.3	1.9	15	28
Formate dehydrogenase, mitochondrial	42 kDa	0.37	1.8	16	28
Cluster of Multifunctional fusion protein	94 kDa	0.34	1.8	15	27
Glycine cleavage system H protein	19 kDa	0.34	1.8	15	27
ATP citrate synthase	68 kDa	0.42	1.7	16	27
Thioredoxin-dependent peroxiredoxin	29 kDa	0.29	1.2	22	27
Cluster of Ribosomal_L18_c domain-containing protein	34 kDa	0.057	2.9	9	26

Cluster of EF1_GNE domain-containing protein	24 kDa	0.47	1.6	16	26
Peptidase A1 domain-containing protein	47 kDa	0.16	2.3	11	25
Cluster of NADPH-protochlorophyllide oxidoreductase (Fragment)	157 kDa	0.29	1.9	13	25
Cluster of KH type-2 domain-containing protein	29 kDa	0.36	1.8	14	25
Cluster of LRRNT_2 domain-containing protein	39 kDa	0.36	1.8	14	25
Aminotran_1_2 domain-containing protein	52 kDa	0.44	1.7	15	25
Cluster of 40S ribosomal protein S7	29 kDa	0.44	1.7	15	25
Cluster of Cytosol_AP domain-containing protein	60 kDa	0.44	1.7	15	25
PfkB domain-containing protein	36 kDa	0.39	1.3	19	25
S-adenosylmethionine synthase	47 kDa	0.26	2	12	24
Cluster of (S)-2-hydroxy-acid oxidase	41 kDa	0.41	1.7	14	24
Cluster of 40S ribosomal protein S3a	30 kDa	0.41	1.7	14	24
Pyr_redox_2 domain-containing protein	47 kDa	0.49	1.6	15	24
Cluster of ADP-ribosylation factor	21 kDa	0.28	1.2	20	24
UDP-glucose 6-dehydrogenase	53 kDa	0.073	2.9	8	23
Polyadenylate-binding protein	71 kDa	0.38	1.8	13	23
V-type proton ATPase subunit G	12 kDa	0.29	1.2	19	23
Sucrose synthase	93 kDa	0.0066	5.5	4	22
Epimerase domain-containing protein	43 kDa	0.031	3.7	6	22
Protein kinase domain-containing protein	58 kDa	0.2	2.2	10	22
Epimerase domain-containing protein	42 kDa	0.27	2	11	22
ATP synthase subunit d, mitochondrial	23 kDa	0.35	1.8	12	22
NAC-A/B domain-containing protein 0	22 kDa	0.44	1.7	13	22
Aminotran_1_2 domain-containing protein	51 kDa	0.52	1.6	14	22
Cluster of UDP-arabinopyranose mutase	41 kDa	0.52	1.6	14	22
Cluster of Peroxidase	93 kDa	0.074	3	7	21

Glutamine amidotransferase type-2 domain-containing protein	177 kDa	0.074	3	7	21
NAD(P)H dehydrogenase (quinone)	22 kDa	0.41	1.8	12	21
Cluster of Plastocyanin--plastocyanin reductase	24 kDa	0.48	1.4	15	21
Lactoylglutathione lyase	33 kDa	0.33	1.2	17	21
Cluster of Glucan endo-1,3-beta-D-glucosidase	80 kDa	0.013	5	4	20
Cluster of Ribosomal_L16 domain-containing protein	25 kDa	0.056	3.3	6	20
Proteasome subunit alpha type	27 kDa	0.15	2.5	8	20
Germin-like protein	22 kDa	0.51	1.4	14	20
Malate dehydrogenase	51 kDa	0.28	1.2	17	20
Cluster of Adenosine kinase	37 kDa	0.12	2.7	7	19
Cluster of Glucose-6-phosphate isomerase	67 kDa	0.12	2.7	7	19
Peroxidase	35 kDa	0.34	1.9	10	19
Cluster of Histone H4	20 kDa	0.43	1.7	11	19
Cluster of Peroxidase	93 kDa	0.54	1.5	13	19
Cluster of AAA domain-containing protein	101 kDa	0.31	2	9	18
40S ribosomal protein S8	26 kDa	0.4	1.8	10	18
Cluster of PKS_ER domain-containing protein	34 kDa	0.49	1.6	11	18
PfkB domain-containing protein	40 kDa	0.57	1.5	12	18
Inorganic diphosphatase	120 kDa	0.12	2.8	6	17
Cluster of Glycerophosphodiester phosphodiesterase	83 kDa	0.19	2.4	7	17
Aldedh domain-containing protein	59 kDa	0.27	2.1	8	17
Cluster of Argininosuccinate synthase	54 kDa	0.36	1.9	9	17
Proteasome subunit alpha type	27 kDa	0.36	1.9	9	17
Cluster of Ribosomal_L6e_N domain-containing protein (Fragment)	31 kDa	0.46	1.7	10	17
Alanine transaminase	58 kDa	0.55	1.5	11	17
Glutaredoxin-dependent peroxiredoxin	24 kDa	0.55	1.5	11	17
PAP_fibrillin domain-containing protein	27 kDa	0.55	1.5	11	17
Prohibitin	31 kDa	0.55	1.5	11	17
Glutamate-1-semialdehyde 2,1-aminomutase	51 kDa	0.51	1.4	12	17
Glutaredoxin-dependent peroxiredoxin	78 kDa	0.51	1.4	12	17

Cluster of HABP4_PA1-RBP1 domain-containing protein	39 kDa	0.42	1.3	13	17
Formate--tetrahydrofolate ligase	68 kDa	0.24	2.3	7	16
Cluster of 40S ribosomal protein SA	33 kDa	0.33	2	8	16
Ribosomal_L2_C domain-containing protein	84 kDa	0.52	1.6	10	16
Cluster of 6-phosphogluconate dehydrogenase, decarboxylating	59 kDa	0.033	5	3	15
Dihydrolipoyl dehydrogenase	60 kDa	0.069	3.8	4	15
S-(hydroxymethyl)glutathione dehydrogenase	99 kDa	0.13	3	5	15
Cluster of Eukaryotic translation initiation factor 3 subunit G	32 kDa	0.2	2.5	6	15
Cluster of Histone H2B	16 kDa	0.2	2.5	6	15
Cluster of 60S ribosomal protein L27	16 kDa	0.29	2.1	7	15
Ribosomal_S13_N domain-containing protein	17 kDa	0.39	1.9	8	15
Cluster of Ribosomal protein L19	24 kDa	0.49	1.7	9	15
Non-reducing end alpha-L-arabinofuranosidase	74 kDa	0.49	1.7	9	15
Xyloglucan endotransglucosylase/hydrolase	34 kDa	0.58	1.5	10	15
Cluster of Ribosomal_S7 domain-containing protein	22 kDa	0.31	1.2	13	15
Cluster of Succinate-CoA ligase [ADP-forming] subunit alpha, mitochondrial	35 kDa	0.31	1.2	13	15
Cluster of Ribosomal protein	25 kDa	0.16	2.8	5	14
Cluster of Eukaryotic translation initiation factor 5A	17 kDa	0.25	2.3	6	14
60S ribosomal protein L13	39 kDa	0.56	1.6	9	14
AAA domain-containing protein	76 kDa	0.56	1.6	9	14
Chlorophyll a-b binding protein, chloroplastic	26 kDa	0.51	1.4	10	14
Cluster of Annexin	31 kDa	0.0081	13	1	13
Alanine transaminase	53 kDa	0.065	4.3	3	13
Cluster of Fumarylacetoacetase	128 kDa	0.065	4.3	3	13
Cluster of Peptidylprolyl isomerase	64 kDa	0.065	4.3	3	13
Cluster of 60S ribosomal protein L18a	21 kDa	0.13	3.2	4	13
Ferredoxin-NADP reductase, chloroplastic	42 kDa	0.13	3.2	4	13

Cluster of Pyrophosphate-fructose 6-phosphate 1-phosphotransferase subunit alpha 0GN=PPF-ALPHA	67 kDa	0.31	2.2	6	13
Dihydrolipoamide acetyltransferase component of pyruvate dehydrogenase complex	56 kDa	0.31	2.2	6	13
Peptidyl-prolyl cis-trans isomerase	28 kDa	0.31	2.2	6	13
Phosphoglucosmutase (alpha-D-glucose-1,6-bisphosphate-dependent)	63 kDa	0.42	1.9	7	13
Cluster of S-formylglutathione hydrolase	37 kDa	0.44	1.3	10	13
Cluster of Ubiquitin_4 domain-containing protein	59 kDa	0.44	1.3	10	13
Proteasome subunit alpha type	27 kDa	0.35	1.2	11	13
Cluster of Malic enzyme	70 kDa	0.04	6	2	12
UDP-glucuronate decarboxylase	73 kDa	0.04	6	2	12
Cluster of Ribosomal_S10 domain-containing protein	14 kDa	0.26	2.4	5	12
Alanine--glyoxylate transaminase	44 kDa	0.37	2	6	12
Uroporphyrinogen decarboxylase	45 kDa	0.37	2	6	12
ATP-dependent Clp protease proteolytic subunit	34 kDa	0.58	1.5	8	12
Cluster of ATP citrate synthase	47 kDa	0.58	1.5	8	12
Cluster of Photosystem II D2 protein	40 kDa	0.58	1.5	8	12
Cluster of Histone H2A	32 kDa	0.48	1.3	9	12
Cluster of Chlorophyll a-b binding protein, chloroplastic	28 kDa	0.38	1.2	10	12
Cluster of Fn3_like domain-containing protein	83 kDa	0.38	1.2	10	12
Alpha-1,4 glucan phosphorylase	103 kDa	0.058	5.5	2	11
Cluster of Aspartate-tRNA ligase	62 kDa	0.058	5.5	2	11
Cluster of PSII_BNR domain-containing protein	46 kDa	0.22	2.8	4	11
Cluster of S5 DRBM domain-containing protein	30 kDa	0.22	2.8	4	11
Cluster of Cysteine synthase	78 kDa	0.33	2.2	5	11
Cluster of Dihydrolipoyllysine-residue succinyltransferase (Fragment)	66 kDa	0.33	2.2	5	11
Cluster of 50S ribosomal protein L23, chloroplastic	71 kDa	0.45	1.8	6	11
Cluster of PKS_ER domain-containing protein	76 kDa	0.45	1.8	6	11

Cluster of Proteasome subunit alpha type	25 kDa	0.45	1.8	6	11
Cluster of Protein disulfide-isomerase	68 kDa	0.45	1.8	6	11
Ribose-5-phosphate isomerase	36 kDa	0.45	1.8	6	11
Cluster of Alpha-galactosidase	45 kDa	0.56	1.6	7	11
Cluster of CYTB_NTER domain-containing protein	95 kDa	0.56	1.6	7	11
Cluster of Glutamate decarboxylase	56 kDa	0.03	10	1	10
Cluster of RNA helicase	67 kDa	0.03	10	1	10
HIT domain-containing protein	19 kDa	0.03	10	1	10
Ribosomal protein L15	28 kDa	0.083	5	2	10
Cluster of Cysteine synthase	34 kDa	0.17	3.3	3	10
Nucleoside diphosphate kinase	26 kDa	0.17	3.3	3	10
40S ribosomal protein S12	15 kDa	0.28	2.5	4	10
ACB domain-containing protein	10 kDa	0.28	2.5	4	10
Thioredoxin-dependent peroxiredoxin (Fragment)	135 kDa	0.28	2.5	4	10
Cluster of NTP_transf_2 domain-containing protein	84 kDa	0.4	2	5	10
Cluster of rRNA N-glycosylase	29 kDa	0.4	2	5	10
Cluster of Isocitrate lyase	33 kDa	0.53	1.7	6	10
Cluster of STI1 domain-containing protein	38 kDa	0.53	1.7	6	10
Cytochrome c domain-containing protein	12 kDa	0.53	1.7	6	10
Superoxide dismutase	21 kDa	0.53	1.7	6	10
Cluster of HATPase_c domain-containing protein	83 kDa	0.55	1.4	7	10
Peroxidase	35 kDa	0.55	1.4	7	10
Succinate-CoA ligase [ADP-forming] subunit beta, mitochondrial	45 kDa	0.55	1.4	7	10
Fructose-bisphosphatase	45 kDa	0.44	1.2	8	10
Cluster of Glutamate decarboxylase	57 kDa	0.01	INF	0	9
Xylose isomerase	56 kDa	0.01	INF	0	9
Cluster of GH18 domain-containing protein	101 kDa	0.046	9	1	9
Cluster of Glucan endo-1,3-beta-D-glucosidase	113 kDa	0.046	9	1	9
Pyruvate dehydrogenase E1 component subunit alpha	44 kDa	0.046	9	1	9
H (+)-exporting diphosphatase	80 kDa	0.12	4.5	2	9
40S ribosomal protein S24	31 kDa	0.22	3	3	9
Beta-galactosidase	90 kDa	0.22	3	3	9

Cluster of 1-deoxy-D-xylulose-5-phosphate reductoisomerase	51 kDa	0.22	3	3	9
Cluster of 60S ribosomal protein L36	13 kDa	0.22	3	3	9
Cluster of Glutathione peroxidase	27 kDa	0.22	3	3	9
Isocitrate dehydrogenase [NAD] subunit, mitochondrial	66 kDa	0.22	3	3	9
VWFA domain-containing protein	43 kDa	0.22	3	3	9
SWIB/MDM2 domain-containing protein	15 kDa	0.35	2.2	4	9
Cluster of Abhydrolase_3 domain-containing protein	41 kDa	0.49	1.8	5	9
AAI domain-containing protein	14 kDa	0.6	1.5	6	9
Cluster of H15 domain-containing protein	20 kDa	0.6	1.5	6	9
Cluster of Proteasome subunit beta	25 kDa	0.6	1.5	6	9
Ferritin	31 kDa	0.6	1.5	6	9
Transaldolase	48 kDa	0.6	1.5	6	9
Cluster of Aspartate aminotransferase	50 kDa	0.47	1.3	7	9
Pectin acetyltransferase	31 kDa	0.017	INF	0	8
Ribonuclease	109 kDa	0.017	INF	0	8
Bet_v_1 domain-containing protein	19 kDa	0.07	8	1	8
Importin subunit alpha	65 kDa	0.07	8	1	8
Cytochrome b5 heme-binding domain-containing protein OGN=G4B88	61 kDa	0.17	4	2	8
Peptidylprolyl isomerase	50 kDa	0.17	4	2	8
Cluster of Alpha-mannosidase	233 kDa	0.3	2.7	3	8
Photolyase/cryptochrome alpha/beta domain-containing protein	119 kDa	0.3	2.7	3	8
Pyrophosphate-fructose 6-phosphate 1-phosphotransferase subunit beta	142 kDa	0.3	2.7	3	8
Cluster of Proteasome subunit alpha type	27 kDa	0.44	2	4	8
L-ascorbate peroxidase	47 kDa	0.44	2	4	8
Tryptophan synthase (Fragment)	103 kDa	0.44	2	4	8
Allene-oxide cyclase	27 kDa	0.57	1.6	5	8
Cluster of Peptidyl-prolyl cis-trans isomerase	22 kDa	0.51	1.3	6	8
Cluster of Peroxidase	37 kDa	0.51	1.3	6	8
Cluster of Pyruvate dehydrogenase E1 component subunit beta	36 kDa	0.51	1.3	6	8
PAP_fibrillin domain-containing protein	28 kDa	0.51	1.3	6	8

Epimerase domain-containing protein	52 kDa	0.028	INF	0	7
Oxoglutarate dehydrogenase (succinyl-transferring)	116 kDa	0.028	INF	0	7
TRASH domain-containing protein	18 kDa	0.028	INF	0	7
Amine oxidase	79 kDa	0.11	7	1	7
Cluster of NADH dehydrogenase [ubiquinone] 1 beta subcomplex subunit	35 kDa	0.11	7	1	7
Cluster of Alpha-galactosidase	76 kDa	0.23	3.5	2	7
Cluster of Eukaryotic translation initiation factor 3 subunit I	36 kDa	0.23	3.5	2	7
Cluster of Photosystem I reaction center subunit III	25 kDa	0.23	3.5	2	7
D-3-phosphoglycerate dehydrogenase	63 kDa	0.23	3.5	2	7
Glycine-tRNA ligase	81 kDa	0.23	3.5	2	7
Naringenin-chalcone synthase	43 kDa	0.23	3.5	2	7
Prohibitin	32 kDa	0.23	3.5	2	7
Proteasome subunit beta	25 kDa	0.23	3.5	2	7
CCT-beta	54 kDa	0.38	2.3	3	7
Cluster of 26S proteasome non-ATPase regulatory subunit 1 homolog	109 kDa	0.38	2.3	3	7
Cluster of Glutaredoxin domain-containing protein	17 kDa	0.38	2.3	3	7
Cluster of Peroxidase	30 kDa	0.38	2.3	3	7
Cluster of Ubiquitin receptor RAD23	41 kDa	0.38	2.3	3	7
Cysteine proteinase inhibitor	25 kDa	0.38	2.3	3	7
GST N-terminal domain-containing protein	35 kDa	0.38	2.3	3	7
MBD domain-containing protein	50 kDa	0.38	2.3	3	7
Ribosomal_L18e/L15P domain-containing protein	21 kDa	0.38	2.3	3	7
Cluster of Phycocyanin domain-containing protein	20 kDa	0.53	1.8	4	7
Succinate dehydrogenase [ubiquinone] iron-sulfur subunit, mitochondrial	31 kDa	0.53	1.8	4	7
Thioredoxin domain-containing protein	19 kDa	0.53	1.8	4	7
Cluster of (-)-limonene synthase, chloroplastic	72 kDa	0.56	1.4	5	7

Cluster of RNase H type-1 domain-containing protein	54 kDa	0.43	1.2	6	7
Cluster of Superoxide dismutase	26 kDa	0.43	1.2	6	7
DUF3700 domain-containing protein	29 kDa	0.43	1.2	6	7
60S ribosomal protein L7a	29 kDa	0.047	INF	0	6
Acetyltransferase component of pyruvate dehydrogenase complex	59 kDa	0.047	INF	0	6
Pectinesterase	58 kDa	0.047	INF	0	6
AAI domain-containing protein	20 kDa	0.16	6	1	6
Cluster of Fumarate hydratase	82 kDa	0.16	6	1	6
Cluster of Hedycaryol synthase	65 kDa	0.16	6	1	6
Pyruvate dehydrogenase E1 component subunit alpha	48 kDa	0.16	6	1	6
Coproporphyrinogen oxidase	45 kDa	0.31	3	2	6
Iso_dh domain-containing protein	41 kDa	0.31	3	2	6
NmrA domain-containing protein	34 kDa	0.31	3	2	6
40S ribosomal protein S27	10 kDa	0.48	2	3	6
Cluster of tRNA-binding domain-containing protein	79 kDa	0.48	2	3	6
Cluster of UBC core domain-containing protein	17 kDa	0.48	2	3	6
Glutathione reductase	54 kDa	0.48	2	3	6
Mg-protoporphyrin IX chelatase	46 kDa	0.62	1.5	4	6
Peroxidase	37 kDa	0.62	1.5	4	6
PHB domain-containing protein	46 kDa	0.62	1.5	4	6
Transaldolase	91 kDa	0.62	1.5	4	6
TCTP domain-containing protein	19 kDa	0.47	1.2	5	6
Cluster of Methylthioribose-1-phosphate isomerase	39 kDa	0.078	INF	0	5
Cluster of Thioredoxin domain-containing protein	20 kDa	0.078	INF	0	5
Lipoxygenase	94 kDa	0.078	INF	0	5
Ribosomal_L18e/L15P domain-containing protein	29 kDa	0.078	INF	0	5
CCT-theta (Fragment)	122 kDa	0.23	5	1	5
Cluster of Carbamoyl-phosphate synthase (glutamine-hydrolyzing)	132 kDa	0.23	5	1	5
Cluster of Citrate synthase	68 kDa	0.23	5	1	5
Cluster of Ribosomal_L2_C domain-containing protein	34 kDa	0.23	5	1	5
Cluster of SCP domain-containing protein	51 kDa	0.23	5	1	5
Ferredoxin	16 kDa	0.23	5	1	5

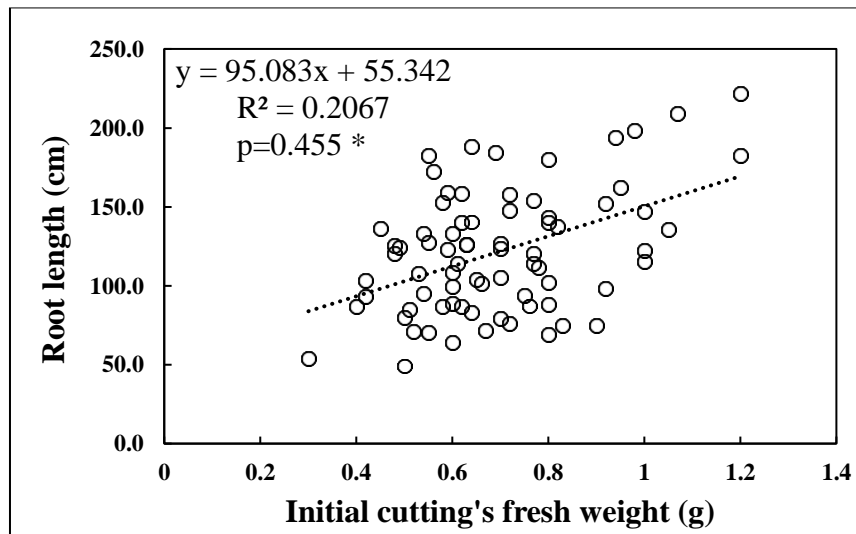
Ribosomal_L14e domain-containing protein	15 kDa	0.23	5	1	5
RRM domain-containing protein	22 kDa	0.23	5	1	5
S5 DRBM domain-containing protein	34 kDa	0.23	5	1	5
Cluster of Pyruvate kinase	55 kDa	0.42	2.5	2	5
S10_pectin domain-containing protein	20 kDa	0.42	2.5	2	5
Threonine-tRNA ligase	80 kDa	0.42	2.5	2	5
Beta-ketoacyl-[acyl-carrier-protein] synthase I	55 kDa	0.59	1.7	3	5
Cluster of 6-phosphogluconate dehydrogenase, decarboxylating	54 kDa	0.59	1.7	3	5
Cluster of CN hydrolase domain-containing protein	39 kDa	0.59	1.7	3	5
Dihydrolipoamide acetyltransferase component of pyruvate dehydrogenase complex	49 kDa	0.59	1.7	3	5
Glutaredoxin-dependent peroxiredoxin	22 kDa	0.59	1.7	3	5
Cluster of Purple acid phosphatase	55 kDa	0.52	1.2	4	5
KOW domain-containing protein	17 kDa	0.52	1.2	4	5
Chalcone-flavonone isomerase family protein	38 kDa	0.13	INF	0	4
Cluster of Aspartate carbamoyltransferase	46 kDa	0.13	INF	0	4
Cluster of Epimerase domain-containing protein	45 kDa	0.13	INF	0	4
NAD(P)-bd_dom domain-containing protein	55 kDa	0.13	INF	0	4
NTF2 domain-containing protein	13 kDa	0.13	INF	0	4
Peroxidase	22 kDa	0.13	INF	0	4
Photosystem I reaction center subunit V, chloroplastic	18 kDa	0.13	INF	0	4
Proteasome subunit beta	27 kDa	0.13	INF	0	4
30S ribosomal protein S17, chloroplastic	18 kDa	0.34	4	1	4
Adenylosuccinate synthetase, chloroplastic 0GN=PURA	54 kDa	0.34	4	1	4
Chalcone isomerase	24 kDa	0.34	4	1	4
Cluster of Acetyl-CoA carboxytransferase	84 kDa	0.34	4	1	4
Cluster of Peroxidase_4 domain-containing protein	38 kDa	0.34	4	1	4
GH18 domain-containing protein	153 kDa	0.34	4	1	4

Malic enzyme	67 kDa	0.34	4	1	4
PCI domain-containing protein	47 kDa	0.34	4	1	4
Ribosomal_L18e/L15P domain-containing protein	16 kDa	0.34	4	1	4
40S ribosomal protein S24	16 kDa	0.54	2	2	4
Aspartate aminotransferase	47 kDa	0.54	2	2	4
ATP-synt_DE_N domain-containing protein	22 kDa	0.54	2	2	4
Cluster of 50S ribosomal protein L14, chloroplastic	14 kDa	0.54	2	2	4
Cluster of AB hydrolase-1 domain-containing protein	36 kDa	0.54	2	2	4
CP12 domain-containing protein	14 kDa	0.54	2	2	4
Peptidyl-prolyl cis-trans isomerase (Fragment)	23 kDa	0.54	2	2	4
Proteasome subunit alpha type	27 kDa	0.54	2	2	4
RanBD1 domain-containing protein	285 kDa	0.54	2	2	4
Cluster of 3-isopropylmalate dehydrogenase	44 kDa	0.58	1.3	3	4
Cluster of Lysine-tRNA ligase	67 kDa	0.58	1.3	3	4
Cluster of Non-specific lipid-transfer protein	12 kDa	0.58	1.3	3	4
AAA domain-containing protein	48 kDa	0.22	INF	0	3
Cluster of Dynamin GTPase	73 kDa	0.22	INF	0	3
E1 ubiquitin-activating enzyme	247 kDa	0.22	INF	0	3
Glucose-1-phosphate adenylyltransferase	57 kDa	0.22	INF	0	3
PSI subunit V	23 kDa	0.22	INF	0	3
Pyruvate kinase	63 kDa	0.22	INF	0	3
STI1 domain-containing protein	48 kDa	0.22	INF	0	3
T-complex protein 1 subunit alpha	63 kDa	0.22	INF	0	3
ATP-dependent Clp protease proteolytic subunit	27 kDa	0.47	3	1	3
Cluster of Beta-galactosidase	80 kDa	0.47	3	1	3
Epimerase domain-containing protein	46 kDa	0.47	3	1	3
Sucrose synthase	93 kDa	0.47	3	1	3
Cluster of CS domain-containing protein	24 kDa	0.66	1.5	2	3
Fn3_like domain-containing protein	85 kDa	0.66	1.5	2	3
4-(cytidine 5'-diphospho)-2-C-methyl-D-erythritol kinase	45 kDa	0.36	INF	0	2
AB hydrolase-1 domain-containing protein	36 kDa	0.36	INF	0	2

Cluster of Asparagine synthetase [glutamine-hydrolyzing]	73 kDa	0.36	INF	0	2
Cluster of Pyruvate kinase	57 kDa	0.36	INF	0	2
Cluster of Sec16_C domain-containing protein	120 kDa	0.36	INF	0	2
Eukaryotic translation initiation factor 3 subunit B	83 kDa	0.36	INF	0	2
Pept_C1 domain-containing protein	41 kDa	0.36	INF	0	2
Probable bifunctional methylthioribulose-1-phosphate dehydratase/enolase-phosphatase E1	59 kDa	0.36	INF	0	2
RRM domain-containing protein	49 kDa	0.36	INF	0	2
S1 motif domain-containing protein	106 kDa	0.36	INF	0	2
Biotin carboxyl carrier protein of acetyl-CoA carboxylase	33 kDa	0.65	2	1	2
Cluster of NAD(P)H dehydrogenase (quinone)	43 kDa	0.65	2	1	2
Cluster of Semialdehyde_dh domain-containing protein	38 kDa	0.65	2	1	2
Uracil phosphoribosyltransferase	32 kDa	0.65	2	1	2
Cluster of Glutamate dehydrogenase	43 kDa	0.6	INF	0	1
Epimerase domain-containing protein	40 kDa	0.6	INF	0	1
Proliferating cell nuclear antigen	29 kDa	0.6	INF	0	1
Pterin-binding domain-containing protein	41 kDa	0.6	INF	0	1
Ribosomal_L18e/L15P domain-containing protein	22 kDa	0.6	INF	0	1
SAP domain-containing protein	86 kDa	0.6	INF	0	1

Appendix D

Chapter 6



Supplementary Figure 6.1. Correlation between original cutting's fresh weight and root length after inoculated with PGPR

Note: Correlation is significant at the $p = 0.01$ level